ISSN 2307-8960 (online)

World Journal of *Clinical Cases*

World J Clin Cases 2024 September 16; 12(26): 5839-6003

Published by Baishideng Publishing Group Inc

World Journal of Clinical Cases

Contents

Thrice Monthly Volume 12 Number 26 September 16, 2024

EDITORIAL

ORIGINAL ARTICLE

Case Control Study

Retrospective Cohort Study

Retrospective Study

World Journal of Clinical Cases

Thrice Monthly Volume 12 Number 26 September 16, 2024

Contents

World Journal of Clinical Cases

Thrice Monthly Volume 12 Number 26 September 16, 2024

Contents

LETTER TO THE EDITOR

World Journal of Clinical Cases

Thrice Monthly Volume 12 Number 26 September 16, 2024

Contents

ABOUT COVER

Peer Reviewer of *World Journal of Clinical Cases*, Ralph Victor Yap, MD, RN, Assistant Professor, Surgeon, Department of Surgery, Cebu Doctors' University Hospital, Cebu 6000, Philippines. rvyapmd@gmail.com

AIMS AND SCOPE

The primary aim of *World Journal of Clinical Cases* (*WJCC*, *World J Clin Cases*) is to provide scholars and readers from various fields of clinical medicine with a platform to publish high-quality clinical research articles and communicate their research findings online.

WJCC mainly publishes articles reporting research results and findings obtained in the field of clinical medicine and covering a wide range of topics, including case control studies, retrospective cohort studies, retrospective studies, clinical trials studies, observational studies, prospective studies, randomized controlled trials, randomized clinical trials, systematic reviews, meta-analysis, and case reports.

INDEXING/ABSTRACTING

The *WJCC* is now abstracted and indexed in PubMed, PubMed Central, *Reference Citation Analysis*, China Science and Technology Journal Database, and Superstar Journals Database. The 2024 Edition of Journal Citation Reports® cites the 2023 journal impact factor (JIF) for *WJCC* as 1.0; JIF without journal self cites: 0.9; 5-year JIF: 1.1; JIF Rank: 168/325 in medicine, general and internal; JIF Quartile: Q3; and 5-year JIF Quartile: Q3.

RESPONSIBLE EDITORS FOR THIS ISSUE

NAME OF JOURNAL
World Journal of Clinical Cases

ISSN
ISSN 2307-8960 (online)

LAUNCH DATE
April 16, 2013

FREQUENCY
Thrice Monthly

PUBLICATION DATE
September 16, 2024

World Journal of Clinical Cases

Submit a Manuscript: https://www.f6publishing.com

World J Clin Cases 2024 September 16; 12(26): 5839-5844

DOI: 10.12998/wjcc.v12.i26.5839

ISSN 2307-8960 (online)

EDITORIAL

Orthopedic manifestations of Li-Fraumeni syndrome: Prevention and treatment of a polymorphic spectrum of malignancies

Giulia Cenci, Valerio Pace

Specialty type: Medicine, research and experimental

Provenance and peer review: Invited article; Externally peer reviewed.

Peer-review model: Single blind

Peer-review report's classification
Scientific Quality: Grade C, Grade D
Novelty: Grade B, Grade C
Creativity or Innovation: Grade C, Grade C
Scientific Significance: Grade B, Grade C

P-Reviewer: Yang LY, China

Received: March 15, 2024
Revised: April 25, 2024
Accepted: May 22, 2024
Published online: September 16, 2024
Processing time: 129 Days and 5.6 Hours

Giulia Cenci, Department of Trauma and Orthopedics, Azienda Ospedaliera Santa Maria Hospital, Terni 05100, Italy

Valerio Pace, Department of Trauma and Orthopedics, AOSP Terni, Terni 05100, Italy

Corresponding author: Valerio Pace, MBBS, MSc, Researcher, Senior Research Fellow, Surgeon, Department of Trauma and Orthopedics, AOSP Terni, Via Joannuccio, Terni 05100, Italy. valeriopace@doctors.org.uk

Abstract

Li-Fraumeni syndrome (LFS) is a rare hereditary cancer predisposition syndrome characterized by a heightened risk of developing various malignancies at an early age. Emerging evidence suggests a correlation between LFS and orthopedic manifestations, underscoring the importance of orthopedic screening in individuals with this syndrome. Pediatric cancer is rare. It is estimated that more than 10%-15% of tumors are secondary to a pathogenic variant in a cancer predisposition gene. More than 100 cancer predisposition genes and their association with syndromes or isolated tumors have been identified. LFS is one of those who have been most widely described. Patients with this syndrome present a high risk of developing one or more tumors. Its knowledge enables the establishment of a follow-up protocol for the patient and affected family members, facilitating early detection of new tumors and reducing tumor and treatment-related morbidity and mortality. The primary objective of this invited editorial article is to provide a thorough review of the existing knowledge of LFS and its polymorphic spectrum of related malignancies, with a focus on aspects directly linked to orthopedic manifestations. Another objective is to offer an update on the most modern prevention, treatment and follow up guidelines that could be useful for the physicians dealing with this cohort of patients.

Key Words: Li-Fraumeni syndrome; Tumor protein P53; Orthopedic diseases; Osteosarcoma; Chondrosarcoma; Screening; Prevention

Core Tip: Modern screening approaches, including comprehensive genetic testing and advanced imaging modalities, offer promising avenues for early detection and intervention, ultimately improving outcomes in individuals with Li-Fraumeni syndrome (LFS). We advocate the need for internationally recognized and standardized guidelines for diagnosis, treatment and follow up of LFS and the need to form an international multidisciplinary network able to provide the highest level of expertise.

Citation: Cenci G, Pace V. Orthopedic manifestations of Li-Fraumeni syndrome: Prevention and treatment of a polymorphic spectrum of malignancies. *World J Clin Cases* 2024; 12(26): 5839-5844
URL: https://www.wjgnet.com/2307-8960/full/v12/i26/5839.htm
DOI: https://dx.doi.org/10.12998/wjcc.v12.i26.5839

INTRODUCTION

Li-Fraumeni syndrome (LFS) is an autosomal dominant cancer predisposition syndrome first described by Frederick and Joseph in 1969. It is primarily caused by germline mutations in the tumor protein P53 (TP53), leading to an increased susceptibility to a broad spectrum of cancers, including sarcomas, breast cancer, brain tumors, adrenocortical carcinomas, and leukemia. While cancer is the hallmark of LFS, emerging evidence suggests a potential association between this syndrome and orthopedic manifestations, which necessitates further investigation and specialized screening approaches [1-3].

LFS is associated with an early onset in life, with the majority of cases occurring prior to the age of 46. The incidence of LFS is reported to range from 0.05% to 0.2% globally. These percentages make LFS as a truly rare condition[1-3].

Chompret criteria have been developed in order to make the LFS diagnosis. Patients should match at least one of the following criteria for the LFS diagnosis: (1) LFS diagnosis and associated malignancy before the age of 46; (2) Having 1 or more 1st or 2nd-degree relatives with LFS-associated malignancy before the age of 56; and (3) Having 1 or more 1st or 2nd-degree relatives with multiple tumors, independent from the age of onset[1]. These criteria are essential for identifying individuals who may have an inherited predisposition to LFS. It is thought that the most appropriate screening and application of preventive measures and treatments for LFS patients and their families could be allowed by the use of the above mentioned criteria, diagnosis strategies and genetic testing[1-3].

The primary objective of this invited editorial article is to provide a thorough review of the existing knowledge of LFS and its polymorphic spectrum of related malignancies, with a focus on aspects directly linked to orthopedic manifestations. Another objective is to offer an update on the most modern prevention, treatment and follow up guidelines that could be useful for the physicians dealing with this cohort of patients.

Pathogenesis of LFS

LFS is predominantly attributed to germline mutations in the *TP53* gene, encoding the P53 protein, a critical regulator of cell cycle arrest, DNA repair, and apoptosis. The loss or dysfunction of P53 function disrupts cellular homeostasis, facilitating the accumulation of genetic alterations and predisposing individuals to cancer development[4].

During the past few years, a huge progress has been achieved with regards to new information. In fact, numerous genes that were associated with osteosarcoma and its clinical disease progression have been further studied and identified. These genes can be divided into subgroups: Self-sufficiency in growth signals, insensitivity to growth inhibitory signals, evasion of apoptosis, limitless replicative potential, sustained angiogenesis, and tissue evasion and metastasis. Despite the fact that the full understanding of the process of osteosarcoma is still not fully clear, this new information might have the potential to improve the care for this cohort of patients in the future[5].

Clinical variability is commonly seen in LFS. Phenotypic heterogeneity is present among different families affected by the same pathogenic variant in the *TP53* gene and among members of the same family. However, causes of this huge clinical spectrum have not been studied in depth. The real causes for this clinical heterogeneity are not clearly known yet; possible reasons should be sought among the different types of TP53 mutations that are involved in LFS[6].

Few studies have concluded that the general sex-specific P53 effect model was the most plausible model and that sex is not a predisposing factor for malignant cancer development in subjects carrying mutations.

However, the exact mechanisms underlying the diverse cancer spectrum observed in LFS remain incompletely understood, highlighting the complexity of this syndrome's pathogenesis and the need for further high levels of evidence in research[7,8].

Correlation between LFS and orthopedic diseases

Recent studies have elucidated a potential association between LFS and orthopedic manifestations, particularly osteosarcoma and chondrosarcoma. Osteosarcoma, a primary malignant bone tumor arising from osteoblasts, has been reported at an increased frequency in individuals with LFS, suggesting a predisposition to skeletal neoplasms.

Although the prognosis, diagnostic process, treatments and quality of life of patients with osteosarcoma were improved significantly during the past few years, the pathogenesis and etiology of this disease is still unclear. However, several etiologic agents have already been identified due to intense research and interest in the field.

Several chemical agents such as beryllium, viruses such as Finkel-Biskis-Jenkins murine osteosarcoma virus, a virus-induced osteosarcoma named after its discoverers (Finkel, Biskis, and Jinkins), subsequently found to contain the src-oncogene, and radiation were found to be among possible significant inducers of osteosarcoma. Less significant factors may include: Paget's disease, electrical burn and trauma. In the last few years, researchers have shown that an increased risk of osteosarcoma is carried by patients with hereditary diseases such as Rothmund-Thomson syndrome, Bloom syndrome, and LFS[5,9,10].

Recent studies have demonstrated the familial association of osteosarcoma. A higher-than-expected frequency of pathogenic or likely pathogenic variants has been observed in the LFS-associated gene, *TP53*, as well as in genes not traditionally associated with osteosarcoma, such as *CDKN2A*, *MEN1*, *VHL*, *POT1*, *APC*, *MSH2*, and *ATRX*[5,9,10].

The above concepts and considerations should drive the clinicians towards the belief that it is not just essential to search and identify genetic mutations in patients affected by osteosarcoma (osteosarcoma is a sentinel cancer in LFS), but it is paramount to prioritize early sarcoma detection in individuals with a family history of LFS or those diagnosed with LFS.

Similarly, to osteosarcoma, chondrosarcoma (characterized by the malignant transformation of cartilaginous tissue) has been documented in LFS cohorts, albeit with less frequency[11,12].

Approximately 27% of TP53 mutation carriers develop soft-tissue sarcomas (frequently rhabdomyosarcomas, but also liposarcomas or pleiomorphic sarcomas have been diagnosed)[13]. Studies have shown that greater than 5% of pediatric patients with rhabdomyosarcomas may have germline TP53 mutations. This discovery may help to increase suspicion of LFS among patients with these tumors[14-16].

These tumors of mesenchymal origin may arise from the skeletal muscle and can invade the adjacent neurovascular bundles. Although iso- to hypointense on T1-weighted imaging, they are either homogeneously or heterogeneously hyperintense on T2-weighted imaging with areas of necrosis and intrinsic soft-tissue signal intensity. Prominent flow voids and areas of hemorrhage have also been typically reported. Moreover, marked enhancement on contrast-enhanced T1-weighted imaging is considered among the radiological characteristics of these tumors[16-19].

These findings emphasize the importance of vigilant orthopedic monitoring in individuals with LFS. This proactive approach aims to enable early detection and intervention for diagnosing sarcomas at the earliest stage possible, and potentially implementing preventive strategies for patients with a family history or diagnosis of LFS.

MODERN SCREENING APPROACHES FOR PREVENTION

The autosomal dominant inherited LFS increases the lifetime risk of developing a malignancy to almost 100%. Although breast cancer, central nervous system tumors and sarcomas are particularly common, tumors can ultimately occur almost anywhere in the body. As causal therapy is not available, it seems that the only strategy able to improve prognosis is early cancer detection. In fact, current cancer surveillance recommendations include a series of examinations including genetic analysis and regular imaging that must be planned and carried out since birth[20].

Advancements in genomic technologies have revolutionized the screening and management of hereditary cancer syndromes, including LFS. Comprehensive genetic testing for TP53 mutations enables early identification of at-risk individuals, facilitating personalized risk assessment and tailored surveillance strategies. However, little information is available about TP53 pathogenic variants or phenotypes for LFS patients, making it difficult to provide precise genetic counseling with regard to long-term cancer risk[21-24].

It has been reported that significant factors able to influence the providers' decision to offer TP53 testing are linked to the list of potential implications for other family members and the possibility that surveillance imaging would detect new malignancies at an earlier stage[25].

Because of variability in familial presentation and the largely unexplained genetic basis of sarcomas, it could be very difficult to identify the patients that would require a genetics evaluation. The sarcoma clinic genetic screening questionnaire proved to be an efficient tool for identifying patients who would benefit most from a genetic evaluation. The tool allowed us to identify high-risk families fitting the criteria for Li-Fraumeni-like syndrome and, surprisingly, other hereditary cancer syndromes. Similar questionnaires could be used in other cancer-specific clinics to increase awareness of the genetic component of these cancers[26].

Furthermore, advanced imaging modalities such as whole-body magnetic resonance imaging (MRI) and positron emission tomography-computed tomography (PET-CT) offer sensitive methods for detecting occult tumors and monitoring disease progression in LFS patients. The most recent internationally accepted guidelines include an annual whole-body MRI among their recommendations in order to provide the most adequate screening for cancer patients carrying germline TP53[27].

Due to the wide range of tumor entities that can occur in individuals affected by LFS, a sensitive detection requires imaging of various tissue contrasts; however, because life-long screening is potentially initiated at a young age, this requirement for comprehensiveness must be balanced against the presumed high psychological burden associated with frequent or invasive examinations. It is well known that an increased radiation exposure could lead to a secondary increased risk of secondary tumors. Therefore, the need and use of CT and X-ray exams should be avoided as long as possible[28].

The use of annual whole-body MRI, given as propriety of not causing any radiation to the patients, is the exam of choice for this cohort of patients. However, due to the rarity of the syndrome, expertise is sometimes lacking and whole-body MRI examinations are performed heterogeneously and sometimes with limited diagnostic quality. Optimization and standardization of MRI protocols should therefore be studied and implemented. Moreover, the need for an

intravenously administered contrast agent has not been conclusively clarified despite its high relevance[27,28].

After reviewing the most up to date literature and having discussed the above aspects, we believe that it is of utmost importance to form an international multidisciplinary network able to provide the highest level of expertise and integrate the studied modalities (genetic and radiological aspects) into routine screening protocols in order to achieve the earliest possible diagnosis and plan the most appropriate treatment course for all LFS patients. These future prospective holds promise for mitigating the morbidity and mortality associated with LFS-associated malignancies, including orthopedic tumors. To close the loop, we advocate the need for internationally recognized and standardized guidelines for diagnosis, treatment and follow up of LFS.

TREATMENT CHALLENGES

LFS is a rare inherited disease characterized by the early onset of multiple primary malignant tumors. Sarcomas account for more than 30% of all malignant tumors occurring at pediatric ages. Furthermore, it was shown that the rates of second cancer were higher in childhood cancer survivors[27,29,30].

The most difficult aspects with regards to orthopedic diseases related to LFS are related to the fact that LFS is a rare inherited disease characterized by the early onset of multiple primary malignant tumors. Unfortunately, it can happen that a patient is referred to a specialist center when they already have synchronous skeletal tumors. This situation has led to difficulties for the medical team in diagnosing malignancy and determining suitable surgical treatments, ultimately resulting in a poor prognosis for this group of patients[25,27,28-30].

It has been clearly shown that a multidisciplinary approach for diagnosis and treatment in reference centers improves survival of sarcoma patients. Therefore, early referral to a reference center is always advocated as soon as the suspicion of LFS is raised, possibly without having made any surgical intervention and prognosis[26-30].

Appropriate imaging screening is essential to plan the best treatment algorithm. The frequent discovery of multiple lesions after radiological follow up appointments with MRI scans highlights the importance of performing whole-body MRIs for the patients with germline TP53 mutations[26-30].

The discovery of multiple lesions whilst performing investigations on suspected LFS cases raises the problem of the surveillance of patients with germline TP53 mutations. Performing an appropriate cancer screening for these patients is truly challenging, mainly because of the very wide spectrum of cancer linked to TP53 mutations[1].

The treatment of the orthopedic diseases related to TP53 mutations is strictly related to the type of pathology. Malignant sarcomas should be treated in specialized centers according to the latest international guidelines. Consequently, a summary or algorithm with regards to LFS treatment cannot be drawn as every sarcoma has specific characteristics (particularly anatomical), and the surgical management strictly depends on these aspects. At the same time, radiotherapy, chemotherapy and any other cancer treatments are specifically planned on the basis of the type, stage, location of sarcoma and all other specific characteristics.

CONCLUSION

LFS represents a complex hereditary cancer predisposition syndrome characterized by a heightened risk of developing diverse malignancies, including those with orthopedic manifestations.

Emerging evidence suggests a potential correlation between LFS and skeletal neoplasms, emphasizing the importance of specialized orthopedic screening in affected individuals. Modern screening approaches, including comprehensive genetic testing and advanced imaging modalities, offer promising avenues for early detection and intervention, ultimately improving outcomes in individuals with LFS.

We advocate for internationally recognized and standardized guidelines for the diagnosis, treatment, and follow-up of LFS, emphasizing the importance of establishing an international, multidisciplinary network capable of delivering the highest level of expertise.

Further research is warranted to elucidate the mechanistic underpinnings of LFS-associated orthopedic diseases and optimize screening strategies for prevention and early intervention.

FOOTNOTES

Author contributions: Pace V received the editorial invitation; Cenci G and Pace V designed the article, performed research and literature review, analyzed data, wrote and finalized the review.

Conflict-of-interest statement: The authors declare that they have no conflicts of interest.

Country of origin: Italy

ORCID number: Valerio Pace 0000-0002-4499-9157.

S-Editor: Luo ML
L-Editor: Filipodia
P-Editor: Zhao S

REFERENCES

1 **Rocca V**, Blandino G, D'Antona L, Iuliano R, Di Agostino S. Li-Fraumeni Syndrome: Mutation of TP53 Is a Biomarker of Hereditary Predisposition to Tumor: New Insights and Advances in the Treatment. *Cancers (Basel)* 2022; **14** [PMID: 35954327 DOI: 10.3390/cancers14153664]
2 **Kumamoto T**, Yamazaki F, Nakano Y, Tamura C, Tashiro S, Hattori H, Nakagawara A, Tsunematsu Y. Medical guidelines for Li-Fraumeni syndrome 2019, version 1.1. *Int J Clin Oncol* 2021; **26**: 2161-2178 [PMID: 34633580 DOI: 10.1007/s10147-021-02011-w]
3 **de Andrade KC**, Mirabello L, Stewart DR, Karlins E, Koster R, Wang M, Gapstur SM, Gaudet MM, Freedman ND, Landi MT, Lemonnier N, Hainaut P, Savage SA, Achatz MI. Higher-than-expected population prevalence of potentially pathogenic germline TP53 variants in individuals unselected for cancer history. *Hum Mutat* 2017; **38**: 1723-1730 [PMID: 28861920 DOI: 10.1002/humu.23320]
4 **Cecchinelli B**, Lavra L, Rinaldo C, Iacovelli S, Gurtner A, Gasbarri A, Ulivieri A, Del Prete F, Trovato M, Piaggio G, Bartolazzi A, Soddu S, Sciacchitano S. Repression of the antiapoptotic molecule galectin-3 by homeodomain-interacting protein kinase 2-activated p53 is required for p53-induced apoptosis. *Mol Cell Biol* 2006; **26**: 4746-4757 [PMID: 16738336 DOI: 10.1128/MCB.00959-05]
5 **Fuchs B**, Pritchard DJ. Etiology of osteosarcoma. *Clin Orthop Relat Res* 2002; 40-52 [PMID: 11953594 DOI: 10.1097/00003086-200204000-00007]
6 **Gargallo P**, Yáñez Y, Segura V, Juan A, Torres B, Balaguer J, Oltra S, Castel V, Cañete A. Li-Fraumeni syndrome heterogeneity. *Clin Transl Oncol* 2020; **22**: 978-988 [PMID: 31691207 DOI: 10.1007/s12094-019-02236-2]
7 **Wu CC**, Shete S, Amos CI, Strong LC. Joint effects of germ-line p53 mutation and sex on cancer risk in Li-Fraumeni syndrome. *Cancer Res* 2006; **66**: 8287-8292 [PMID: 16912210 DOI: 10.1158/0008-5472.CAN-05-4247]
8 **Wu CC**, Krahe R, Lozano G, Zhang B, Wilson CD, Jo EJ, Amos CI, Shete S, Strong LC. Joint effects of germ-line TP53 mutation, MDM2 SNP309, and gender on cancer risk in family studies of Li-Fraumeni syndrome. *Hum Genet* 2011; **129**: 663-673 [PMID: 21305319 DOI: 10.1007/s00439-011-0957-1]
9 **Aboulafia AJ**, Brooks F, Piratzky J, Weiss S. Osteosarcoma arising from heterotopic ossification after an electrical burn. A case report. *J Bone Joint Surg Am* 1999; **81**: 564-570 [PMID: 10225803 DOI: 10.2106/00004623-199904000-00015]
10 **Mirabello L**, Zhu B, Koster R, Karlins E, Dean M, Yeager M, Gianferante M, Spector LG, Morton LM, Karyadi D, Robison LL, Armstrong GT, Bhatia S, Song L, Pankratz N, Pinheiro M, Gastier-Foster JM, Gorlick R, de Toledo SRC, Petrilli AS, Patino-Garcia A, Lecanda F, Gutierrez-Jimeno M, Serra M, Hattinger C, Picci P, Scotlandi K, Flanagan AM, Tirabosco R, Amary MF, Kurucu N, Ilhan IE, Ballinger ML, Thomas DM, Barkauskas DA, Mejia-Baltodano G, Valverde P, Hicks BD, Zhu B, Wang M, Hutchinson AA, Tucker M, Sampson J, Landi MT, Freedman ND, Gapstur S, Carter B, Hoover RN, Chanock SJ, Savage SA. Frequency of Pathogenic Germline Variants in Cancer-Susceptibility Genes in Patients With Osteosarcoma. *JAMA Oncol* 2020; **6**: 724-734 [PMID: 32191290 DOI: 10.1001/jamaoncol.2020.0197]
11 **Consul N**, Amini B, Ibarra-Rovira JJ, Blair KJ, Moseley TW, Taher A, Shah KB, Elsayes KM. Li-Fraumeni Syndrome and Whole-Body MRI Screening: Screening Guidelines, Imaging Features, and Impact on Patient Management. *AJR Am J Roentgenol* 2021; **216**: 252-263 [PMID: 33151095 DOI: 10.2214/AJR.20.23008]
12 **Li FP**, Fraumeni JF Jr. Soft-tissue sarcomas, breast cancer, and other neoplasms. A familial syndrome? *Ann Intern Med* 1969; **71**: 747-752 [PMID: 5360287 DOI: 10.7326/0003-4819-71-4-747]
13 **Bougeard G**, Renaux-Petel M, Flaman JM, Charbonnier C, Fermey P, Belotti M, Gauthier-Villars M, Stoppa-Lyonnet D, Consolino E, Brugières L, Caron O, Benusiglio PR, Bressac-de Paillerets B, Bonadona V, Bonaïti-Pellié C, Tinat J, Baert-Desurmont S, Frebourg T. Revisiting Li-Fraumeni Syndrome From TP53 Mutation Carriers. *J Clin Oncol* 2015; **33**: 2345-2352 [PMID: 26014290 DOI: 10.1200/JCO.2014.59.5728]
14 **Magnusson S**, Gisselsson D, Wiebe T, Kristoffersson U, Borg Å, Olsson H. Prevalence of germline TP53 mutations and history of Li-Fraumeni syndrome in families with childhood adrenocortical tumors, choroid plexus tumors, and rhabdomyosarcoma: a population-based survey. *Pediatr Blood Cancer* 2012; **59**: 846-853 [PMID: 22653678 DOI: 10.1002/pbc.24223]
15 **Jaiswal S**, Vij M, Mehrotra A, Kumar B, Nair A, Jaiswal AK, Behari S, Jain VK. Choroid plexus tumors: A clinico-pathological and neuro-radiological study of 23 cases. *Asian J Neurosurg* 2013; **8**: 29-35 [PMID: 23741260 DOI: 10.4103/1793-5482.110277]
16 **Saboo SS**, Krajewski KM, O'Regan KN, Giardino A, Brown JR, Ramaiya N, Jagannathan JP. Spleen in haematological malignancies: spectrum of imaging findings. *Br J Radiol* 2012; **85**: 81-92 [PMID: 22096219 DOI: 10.1259/bjr/31542964]
17 **Zhu J**, Zhang J, Tang G, Hu S, Zhou G, Liu Y, Dai L, Wang Z. Computed tomography and magnetic resonance imaging observations of rhabdomyosarcoma in the head and neck. *Oncol Lett* 2014; **8**: 155-160 [PMID: 24959237 DOI: 10.3892/ol.2014.2094]
18 **Russo I**, Di Paolo V, Gurnari C, Mastronuzzi A, Del Bufalo F, Di Paolo PL, Di Giannatale A, Boldrini R, Milano GM. Congenital Rhabdomyosarcoma: a different clinical presentation in two cases. *BMC Pediatr* 2018; **18**: 166 [PMID: 29764408 DOI: 10.1186/s12887-018-1128-5]
19 **Keymling M**, Schlemmer HP, Kratz C, Pfeil A, Bickelhaupt S, Alsady TM, Renz DM. [Li-Fraumeni syndrome]. *Radiologie (Heidelb)* 2022; **62**: 1026-1032 [PMID: 36166074 DOI: 10.1007/s00117-022-01071-x]
20 **Tulcán EYB**, Pérez AV. Actualidad del melanoma dentro del espectro clínico del síndrome de Li FraumeniMelanoma within the clinical spectrum of Li Fraumeni syndrome: An update, Piel 2022, 37: 467-471 [DOI: 10.1016/j.piel.2021.11.012]
21 **Zhuang X**, Li Y, Cao H, Wang T, Chen J, Liu J, Lin L, Ye R, Li X, Liu S, Li W, Lv Y, Zhang J, He C, Xu X, Wang Z, Huang C, Liu X, Wang L. Case report of a Li-Fraumeni syndrome-like phenotype with a de novo mutation in CHEK2. *Medicine (Baltimore)* 2016; **95**: e4251 [PMID: 27442652 DOI: 10.1097/MD.0000000000004251]
22 **Alba-Pavón P**, Alaña L, Astigarraga I, Villate O. Splicing-Disrupting Mutations in Inherited Predisposition to Solid Pediatric Cancer. *Cancers (Basel)* 2022; **14** [PMID: 36497448 DOI: 10.3390/cancers14235967]

23 **Izawa N**, Matsumoto S, Manabe J, Tanizawa T, Hoshi M, Shigemitsu T, Machinami R, Kanda H, Takeuchi K, Miki Y, Arai M, Shirahama S, Kawaguchi N. A Japanese patient with Li-Fraumeni syndrome who had nine primary malignancies associated with a germline mutation of the p53 tumor-suppressor gene. *Int J Clin Oncol* 2008; **13**: 78-82 [PMID: 18307025 DOI: 10.1007/s10147-007-0692-8]

24 **Zhou J**, Li P, Feng J, Wu Q, You S. MiR-24-1-5p Hinders Malignant Phenotypes of Clear Cell Renal Cell Carcinoma by Targeting SHOX2. *Biochem Genet* 2023; **61**: 2004-2019 [PMID: 36917325 DOI: 10.1007/s10528-023-10353-5]

25 **Schiavi A**, Lavigne J, Turcotte R, Kasprzak L, Dumas N, Chong G, Freeman C, Alameldin M, Galiatsatos P, Palma L, Foulkes WD. Using a family history questionnaire to identify adult patients with increased genetic risk for sarcoma. *Curr Oncol* 2015; **22**: 317-325 [PMID: 26628864 DOI: 10.3747/co.22.2588]

26 **Huby M**, Brugières L, Mascard E, Gaspar N, Pannier S, Aurégan JC. Difficulties of Management of Multiple Synchronous Bone Tumors in Li-Fraumeni Syndrome. *Case Rep Orthop* 2019; **2019**: 8732089 [PMID: 31827960 DOI: 10.1155/2019/8732089]

27 **Shimatani A**, Aono M, Hoshi M, Oebisu N, Iwai T, Takada N, Hara J, Nitani C, Nakamura H. Secondary osteosarcoma in patients previously treated for childhood cancer: Three case reports. *Mol Clin Oncol* 2019; **10**: 153-158 [PMID: 30655991 DOI: 10.3892/mco.2018.1752]

28 **Pascoe EM**, Free M, Mackie PS, Donnan L, O'Sullivan M, Sullivan MJ, Heath JA. Osteosarcoma in a Child Below 2 Years of Age: Case Report and Review of the Literature. *J Pediatr Hematol Oncol* 2019; **41**: 410-412 [PMID: 30303869 DOI: 10.1097/MPH.0000000000001315]

29 **Yumrukçal F**, Dirik Y, Cinar A, Eralp L. Fourth primary malignant tumor in a patient with possible li-fraumeni syndrome: synchronous diagnosis of postirradiation sarcoma, cutaneous relapse of a previous soft tissue sarcoma, and lung adenocarcinoma. *Case Rep Orthop* 2014; **2014**: 597207 [PMID: 25506014 DOI: 10.1155/2014/597207]

30 **Blay JY**, Honoré C, Stoeckle E, Meeus P, Jafari M, Gouin F, Anract P, Ferron G, Rochwerger A, Ropars M, Carrere S, Marchal F, Sirveaux F, Di Marco A, Le Nail LR, Guiramand J, Vaz G, Machiavello JC, Marco O, Causeret S, Gimbergues P, Fiorenza F, Chaigneau L, Guillemin F, Guilloit JM, Dujardin F, Spano JP, Ruzic JC, Michot A, Soibinet P, Bompas E, Chevreau C, Duffaud F, Rios M, Perrin C, Firmin N, Bertucci F, Le Pechoux C, Le Loarer F, Collard O, Karanian-Philippe M, Brahmi M, Dufresne A, Dupré A, Ducimetière F, Giraud A, Pérol D, Toulmonde M, Ray-Coquard I, Italiano A, Le Cesne A, Penel N, Bonvalot S. Surgery in reference centers improves survival of sarcoma patients: a nationwide study. *Ann Oncol* 2019; **30**: 1407 [PMID: 31168580 DOI: 10.1093/annonc/mdz170]

World Journal of Clinical Cases

Submit a Manuscript: https://www.f6publishing.com

World J Clin Cases 2024 September 16; 12(26): 5845-5849

DOI: 10.12998/wjcc.v12.i26.5845

ISSN 2307-8960 (online)

EDITORIAL

Confocal laser endomicroscopy as a new diagnostic tool for poorly differentiated gastric adenocarcinoma

Giuseppe Evola, Marco Vacante, Francesco R Evola

Specialty type: Gastroenterology and hepatology

Provenance and peer review: Invited article; Externally peer reviewed.

Peer-review model: Single blind

Peer-review report's classification
Scientific Quality: Grade B
Novelty: Grade B
Creativity or Innovation: Grade B
Scientific Significance: Grade B

P-Reviewer: Liu TF, China

Received: March 20, 2024
Revised: May 7, 2024
Accepted: June 5, 2024
Published online: September 16, 2024
Processing time: 124 Days and 10.6 Hours

Giuseppe Evola, Department of Surgery, "Garibaldi" Hospital, Catania 95100, Italy

Marco Vacante, Department of General Surgery and Medical-Surgical Specialties, University of Catania, Catania 95123, Italy

Francesco R Evola, Department of Surgery, Division of Orthopedics and Trauma Surgery, "Cannizzaro" Hospital, Catania 95100, Italy

Corresponding author: Giuseppe Evola, MD, PhD, Former Contract Professor, Department of Surgery, "Garibaldi" Hospital, Piazza Santa Maria di Gesù n. 5 Catania 95100, Italy. giuseppe_evola@hotmail.it

Abstract

Gastric cancer (GC) is a multifactorial disease, where both environmental and genetic features can have an impact on its occurrence and development. GC represents one of the leading causes of cancer-related deaths worldwide. GC is most frequent in males and is believed to arise from a series of premalignant lesions. The detection of GC at an early stage is crucial because early GC, which is an invasive stomach cancer confined to the mucosal or submucosal lining, may be curable with a reported 5-year survival rate of more than 90%. Advanced GC usually has a poor prognosis despite current treatment standards. The diagnostic efficacy of conventional endoscopy (with light endoscopy) is currently limited. Confocal laser endomicroscopy is a novel imaging technique that allows real-time *in vivo* histological examination of mucosal surfaces during endoscopy. Confocal laser endomicroscopy may be of great importance in the surveillance of precancerous gastric lesions and in the diagnosis of GC. In this editorial we commented on the article about this topic published by Lou *et al* in the recent issue of the *World Journal of Clinical Cases*.

Key Words: Confocal laser endomicroscopy; *In vivo* microscopy; Optical histology; *Helicobacter pylori*; Intestinal metaplasia; Gastric atrophy; Gastric cancer; Early gastric cancer

Core Tip: Gastric cancer (GC) is one of the leading causes of death worldwide. Conventional white light endoscopy has a limited ability to detect GC and precancerous gastric lesions. Confocal laser endomicroscopy is an endoscopic modality developed to obtain very high magnification and resolution images of the mucosal layer of the gastrointestinal tract. Confocal laser endomicroscopy represents a substantial advancement in endoscopic imaging, as it may allow a direct histological observation of the *in vivo* tissue without the need for biopsy. Several studies have reported the value of this technique in the diagnosis of precancerous gastric lesions and early GC.

Citation: Evola G, Vacante M, Evola FR. Confocal laser endomicroscopy as a new diagnostic tool for poorly differentiated gastric adenocarcinoma. *World J Clin Cases* 2024; 12(26): 5845-5849
URL: https://www.wjgnet.com/2307-8960/full/v12/i26/5845.htm
DOI: https://dx.doi.org/10.12998/wjcc.v12.i26.5845

INTRODUCTION

Gastric cancer (GC) is the fifth most frequent tumor worldwide and represents the fourth-leading cause of death from cancer[1]. GC is a complex disease, where both genetic and environmental features can affect its incidence and progression. The vast majority of GC are adenocarcinomas and arise sporadically with no demonstrable inherited component. Hereditary cancer syndromes are linked to less than 3% of GC cases[2].

Traditionally, GC is divided into two main subtypes, intestinal and diffuse GC, on the basis of Lauren's classification [3]. These subtypes of GC have diverse molecular characteristics and show distinctive growth pathways. Intestinal-type GC commonly develops from a premalignant gastric alteration, such as chronic atrophic gastritis (CAG), intestinal metaplasia (GIM), and dysplasia, whereas diffuse GC does not seem to develop from this step-wise tumor progression but arises from normal gastric mucosa with no eventual premalignant stage.

The incidence of GC increases progressively with age; the median age of the patients with GC at diagnosis is 70 years (conventional GC), although around 10% of GCs are diagnosed at the age of 45 or younger (early-onset GC). Approximately 990000 people are diagnosed with GC in the world each year, of whom around 738000 eventually die[4]. GC is more frequent in males and is supposed to develop from a number of premalignant lesions through a series of stages from CAG, by way of GIM, through low-grade intraepithelial neoplasia and high-grade intraepithelial neoplasia (HGIN), to cancer[5].

The detection of GC at an early stage is crucial since early GC (EGC), which is an invasive stomach malignancy limited to the mucosal or submucosal regions, may be treatable, with a 5-year survival rate of more than 90%[6]. Advanced GC generally shows a poor prognosis, although current treatment standards (neoadjuvant/adjuvant chemotherapy, radical oncologic surgery with D2 lymph node dissection, targeted treatments) have led to significant improvements in survival [6]. Symptoms of GC tend to emerge late in the development of the disease, leading to a poor prognosis and a lack of curative therapeutic options; thus, prevention strategies are necessary to reduce the occurrence of GC and for its early detection.

The two main primary prevention strategies for GC at a population level include changes in dietary habits and a decreasing occurrence of *Helicobacter pylori* infection. The secondary prevention strategy is the early detection of GC using available resources, mainly esophagogastroduodenoscopy (EGD), which has been established as the gold standard for the diagnosis of GC. EGD with biopsies plays a crucial role in the diagnosis and follow-up of patients with precancerous lesions of the stomach, showing high sensitivity and specificity in the diagnosis of GC; furthermore, it is carried out for the minimally invasive treatment of early GC by endoscopic submucosal dissection and mucosal resection. However, despite increasing experience in the field of endoscopy, traditional white light endoscopy (WLE) showed a number of limitations in the observation of microscopic lesions and a remarkable rate of gastric tumors are actually undiagnosed.

A meta-analysis reported that 11.3% of upper gastrointestinal tract tumors were ignored at EGD up to 3 years before the diagnosis[7]. Immediate histological assessment of fresh tissue is fundamental for successful cancer diagnosis and therapy to allow the detection of tumor cells and to guarantee curative resection. Nonetheless, the conventional frozen section technique shows intrinsic limitations, such as suboptimal slide quality due to preparation artifacts, and a long processing time. So far, despite many attempts to overcome these limitations, alternative techniques have not been diffusely adopted in clinical practice. As the most valuable tools for GC screening, modern endoscopy techniques, such as confocal laser endomicroscopy (CLE), narrow-band imaging, and magnifying endoscopy, have been developed to improve the diagnostic process.

PRINCIPLES AND APPLICATIONS OF CLE

CLE shows benefits in identifying EGC and premalignant conditions, as it can offer a clear histological examination of the cells and subcellular areas *in vivo*[8-11] as well as reveal alterations in the mucosa that cannot be identified by WLE[12]. CLE can be used to study luminal structures, such as the esophagus, stomach, large bowel, and ductal structures, such as bile and the pancreatic ducts. CLE can magnify the structure of the mucosa by a factor of 1000, making it possible to view in real-time at the cellular or subcellular level[13]. CLE showed a sensitivity of 81.8%-92.6%, a specificity of 97.6%-100%,

and an accuracy of 94.2%-96.3% in differentiating gastric cancerous mucosa from normal mucosa as compared with histology findings[14,15]. CLE is generally not applied for the follow-up of large regions but is used for the characterization of lesions within a small field of view[16]. CLE utilizes a confocal laser microscope miniaturized to contain a flexible endoscope and can be used for the histological assessment of tissue during endoscopy, also known as virtual or optical biopsy[17].

The physical principle of CLE consists of light illumination of the gastric mucosal surface using a confocal laser and identifying the fluorescence returning back from the same area. The light source is focused at a definite depth, and the light from a single point on the focal plane can be selectively monitored and refocused through a pinhole confocal hole. Two types of CLE platforms are generally used: A scope-embedded type, which integrates a small confocal scanner into the tip of a flexible endoscope; and a miniature probe-type CLE, which can be passed through an accessory channel of a standard diagnostic scope[14,15]. CLE requires the use of a topical or intravenous fluorescent agent. Intravenous fluorescein sodium is most commonly used as it highlights cellular and subcellular details but does not stain the nuclei. The advantages of CLE are that it enhances the contrast and resolution of optical imaging and at the same time achieves the "*in vivo*" imaging of living tissues to avoid artifacts caused by tissue processing.

Zhang *et al*[18] examined the characteristics of gastric pits in various pathologies by means of eCLE and separated the gastric tips into different types: Normal gastric mucosa was classified as type A; CAG as type F; GIM as type E; signet-ring cell carcinoma and poorly differentiated tubular adenocarcinoma as type G1; and differentiated tubular adenocarcinoma as type G2. The type G pattern could predict GC with a high sensitivity (90.0%) and specificity (99.4%). The Miami classification system was suggested in order to standardize imaging acquisition and criteria for diagnosis of gastrointestinal mucosal alterations using CLE[19]. Four CLE diagnoses were obtained by evaluating the architecture of glands, cells, and microvessels (normal mucosa or benign inflammatory lesions, CAG and/or GIM, low-grade intraepithelial neoplasia and HGIN, cancer). In the Miami classification, EGC is described as a completely disorganized epithelium, fluorescein leakage, and dark irregular epithelium.

Li *et al*[20] suggested to add an index of blood vessel changes according to the Miami classification system for a more inclusive evaluation of gastric mucosa; this novel probe-type CLE classification includes three types of gastric pit patterns with seven subtypes and three types of vessel architecture. This classification also reports the blood vessel modifications in the pathological development of gastric mucosa and specifies the different pathological types, which may be more useful in clinical practice.

A number of studies have demonstrated the diagnostic importance of CLE for precancerous gastric alterations and GC [21-23]. In studies on GC, CLE has been found to reveal the final histopathology of the resection sample more accurately than traditional biopsies[16]. Furthermore, CLE permits the visualization of *Helicobacter pylori* in combination with acriflavine staining with 93% sensitivity and 86% specificity for the diagnosis of *Helicobacter pylori*-related gastritis[24,25].

ADVANTAGES AND LIMITATIONS OF CLE

As a novel imaging technique, CLE has different advantages: (1) It can minimize the amount of biopsies, allowing a high diagnostic sensitivity rate, decreasing the risk of mucosal injury, infection, loss of blood, and other complications due to multiple specimen collections; (2) It is more suitable for the long-term surveillance and follow-up of EGC; (3) It can assist doctors in making fast clinical assessments during endoscopy and decrease the waiting times for clinical decisions due to the time-consuming features of histology tests; (4) It shows advantages in the tumor margin evaluation of EGC, which will facilitate the effective endoscopic treatment of early tumors; and (5) It can evaluate the resection margins of gastrectomy, representing a noninvasive, real-time tool to help in the identification of tumor cells. In a large-scale prospective study with 1572 patients eCLE showed higher sensitivity (88.9%), specificity (99.3%), and accuracy (98.9%) than WLE in the diagnosis of superficial GC or HGIN[6].

Although these results highlighted the promising role of CLE, the technique has significant limitations that require improvement: (1) CLE cannot examine the whole gastric lumen because of the restricted field of vision and microscopic inspection within the stomach is unsteady and mobile due to respiratory excursions; (2) The use of a fluorescent dye is needed during CLE to visualize intestinal tissues (fluorescein cannot stain nuclei, so fluorescein-assisted CLE diagnoses is based exclusively on structural atypia); (3) Its low depth of tissue penetration limits the capability of CLE to visualize deeper tissues; and (4) The high cost of equipment and probes and the special training needed for image interpretation have delayed its extensive use. As a result of these disadvantages, it is impossible to use this method alone for early GC screening, so CLE will not be a viable alternative to forceps biopsy. However, despite these limitations, CLE is a promising imaging technique for the detection of upper digestive tract malignancies.

CONCLUSION

To date, CLE has not replaced histopathology; however, it may represent an advanced endoscopic imaging technology that permits the clear diagnosis of gastric lesions and achieves the early detection of malignancies in patients with a high risk of the development of cancer. The extensive use of CLE is limited by its high costs, low availability, and need for trained experts. Future technological advancements and joined applications with other new diagnostic techniques will help to overcome its intrinsic flaws and further support the accurate diagnosis of early gastrointestinal cancer.

ACKNOWLEDGEMENTS

We are grateful for the invitation to address this important issue in a reasoned editorial article.

FOOTNOTES

Author contributions: Evola G, Vacante M, and Evola FR contributed to this paper; Evola G and Vacante M designed the overall concept and outline of the manuscript; Evola FR contributed to the discussion and design of the manuscript; Evola G, Vacante M, and Evola FR contributed to the writing and editing of the manuscript and illustrations as well as a review of the literature.

Conflict-of-interest statement: Evola G, Vacante M and Evola FR have nothing to disclose.

Country of origin: Italy

ORCID number: Giuseppe Evola 0000-0002-3648-7063; Marco Vacante 0000-0002-6815-5012; Francesco Roberto Evola 0000-0002-0470-8343.

S-Editor: Bai Y
L-Editor: Filipodia
P-Editor: Zhao YQ

REFERENCES

1 **Sung H**, Ferlay J, Siegel RL, Laversanne M, Soerjomataram I, Jemal A, Bray F. Global Cancer Statistics 2020: GLOBOCAN Estimates of Incidence and Mortality Worldwide for 36 Cancers in 185 Countries. *CA Cancer J Clin* 2021; **71**: 209-249 [PMID: 33538338 DOI: 10.3322/caac.21660]
2 **Sereno M**, Aguayo C, Guillén Ponce C, Gómez-Raposo C, Zambrana F, Gómez-López M, Casado E. Gastric tumours in hereditary cancer syndromes: clinical features, molecular biology and strategies for prevention. *Clin Transl Oncol* 2011; **13**: 599-610 [PMID: 21865131 DOI: 10.1007/s12094-011-0705-y]
3 **Lauren P**. The two histological main types of gastric carcinoma: diffuse and so-called intestinal-type carcinoma. An attempt at a histo-clinical classification. *Acta Pathol Microbiol Scand* 1965; **64**: 31-49 [PMID: 14320675 DOI: 10.1111/apm.1965.64.1.31]
4 **Machlowska J**, Baj J, Sitarz M, Maciejewski R, Sitarz R. Gastric Cancer: Epidemiology, Risk Factors, Classification, Genomic Characteristics and Treatment Strategies. *Int J Mol Sci* 2020; **21** [PMID: 32512697 DOI: 10.3390/ijms21114012]
5 **Januszewicz W**, Turkot MH, Malfertheiner P, Regula J. A Global Perspective on Gastric Cancer Screening: Which Concepts Are Feasible, and When? *Cancers (Basel)* 2023; **15** [PMID: 36765621 DOI: 10.3390/cancers15030664]
6 **Li WB**, Zuo XL, Li CQ, Zuo F, Gu XM, Yu T, Chu CL, Zhang TG, Li YQ. Diagnostic value of confocal laser endomicroscopy for gastric superficial cancerous lesions. *Gut* 2011; **60**: 299-306 [PMID: 21193460 DOI: 10.1136/gut.2010.223586]
7 **Menon S**, Trudgill N. How commonly is upper gastrointestinal cancer missed at endoscopy? A meta-analysis. *Endosc Int Open* 2014; **2**: E46-E50 [PMID: 26135259 DOI: 10.1055/s-0034-1365524]
8 **Lou JX**, Wu Y, Huhe M, Zhang JJ, Jia DW, Jiang ZY. Diagnosis of poorly differentiated adenocarcinoma of the stomach by confocal laser endomicroscopy: A case report. *World J Clin Cases* 2024; **12**: 1481-1486 [PMID: 38576802 DOI: 10.12998/wjcc.v12.i8.1481]
9 **Han W**, Kong R, Wang N, Bao W, Mao X, Lu J. Confocal Laser Endomicroscopy for Detection of Early Upper Gastrointestinal Cancer. *Cancers (Basel)* 2023; **15** [PMID: 36765734 DOI: 10.3390/cancers15030776]
10 **Kollar M**, Krajciova J, Prefertusova L, Sticova E, Maluskova J, Vackova Z, Martinek J. Probe-based confocal laser endomicroscopy *vs* biopsies in the diagnostics of oesophageal and gastric lesions: A prospective, pathologist-blinded study. *United European Gastroenterol J* 2020; **8**: 436-443 [PMID: 32213027 DOI: 10.1177/2050640620904865]
11 **De Palma GD**. Confocal laser endomicroscopy in the "in vivo" histological diagnosis of the gastrointestinal tract. *World J Gastroenterol* 2009; **15**: 5770-5775 [PMID: 19998496 DOI: 10.3748/wjg.15.5770]
12 **Hoffman A**, Goetz M, Vieth M, Galle PR, Neurath MF, Kiesslich R. Confocal laser endomicroscopy: technical status and current indications. *Endoscopy* 2006; **38**: 1275-1283 [PMID: 17163333 DOI: 10.1055/s-2006-944813]
13 **ASGE Technology Committee**. Confocal laser endomicroscopy. *Gastrointest Endosc* 2014; **80**: 928-938 [PMID: 25442092 DOI: 10.1016/j.gie.2014.06.021]
14 **Kakeji Y**, Yamaguchi S, Yoshida D, Tanoue K, Ueda M, Masunari A, Utsunomiya T, Imamura M, Honda H, Maehara Y, Hashizume M. Development and assessment of morphologic criteria for diagnosing gastric cancer using confocal endomicroscopy: an *ex vivo* and *in vivo* study. *Endoscopy* 2006; **38**: 886-890 [PMID: 16981104 DOI: 10.1055/s-2006-944735]
15 **Kitabatake S**, Niwa Y, Miyahara R, Ohashi A, Matsuura T, Iguchi Y, Shimoyama Y, Nagasaka T, Maeda O, Ando T, Ohmiya N, Itoh A, Hirooka Y, Goto H. Confocal endomicroscopy for the diagnosis of gastric cancer in vivo. *Endoscopy* 2006; **38**: 1110-1114 [PMID: 17111332 DOI: 10.1055/s-2006-944855]
16 **Goetz M**. Characterization of lesions in the stomach: will confocal laser endomicroscopy replace the pathologist? *Best Pract Res Clin Gastroenterol* 2015; **29**: 589-599 [PMID: 26381304 DOI: 10.1016/j.bpg.2015.05.013]
17 **Fuks D**, Pierangelo A, Validire P, Lefevre M, Benali A, Trebuchet G, Criton A, Gayet B. Intraoperative confocal laser endomicroscopy for

real-time *in vivo* tissue characterization during surgical procedures. *Surg Endosc* 2019; **33**: 1544-1552 [PMID: 30232616 DOI: 10.1007/s00464-018-6442-3]

18 **Zhang JN**, Li YQ, Zhao YA, Yu T, Zhang JP, Guo YT, Liu H. Classification of gastric pit patterns by confocal endomicroscopy. *Gastrointest Endosc* 2008; **67**: 843-853 [PMID: 18440377 DOI: 10.1016/j.gie.2008.01.036]

19 **Wallace M**, Lauwers GY, Chen Y, Dekker E, Fockens P, Sharma P, Meining A. Miami classification for probe-based confocal laser endomicroscopy. Endoscopy 2011; 43: 882-891 [PMID: 21818734 DOI: 10.1055/s-0030-1256632]

20 **Li Z**, Zuo XL, Yu T, Gu XM, Zhou CJ, Li CQ, Ji R, Li YQ. Confocal laser endomicroscopy for *in vivo* detection of gastric intestinal metaplasia: a randomized controlled trial. *Endoscopy* 2014; **46**: 282-290 [PMID: 24473908 DOI: 10.1055/s-0033-1359215]

21 **Bae H**, Cho H, Jo Y, Heo SM, Chu J, Choi S, Hwang K, Kim K, Kim S. Real-time Histological Evaluation of Gastric Cancer Tissue by Using a Confocal Laser Endomicroscopic System. *In Vivo* 2024; **38**: 855-863 [PMID: 38418139 DOI: 10.21873/invivo.13511]

22 **Bai T**, Zhang L, Sharma S, Jiang YD, Xia J, Wang H, Qian W, Song J, Hou XH. Diagnostic performance of confocal laser endomicroscopy for atrophy and gastric intestinal metaplasia: A meta-analysis. *J Dig Dis* 2017; **18**: 273-282 [PMID: 28342261 DOI: 10.1111/1751-2980.12470]

23 **Zhang HP**, Yang S, Chen WH, Hu TT, Lin J. The diagnostic value of confocal laser endomicroscopy for gastric cancer and precancerous lesions among Asian population: a system review and meta-analysis. *Scand J Gastroenterol* 2017; **52**: 382-388 [PMID: 28078907 DOI: 10.1080/00365521.2016.1275770]

24 **Fugazza A**, Gaiani F, Carra MC, Brunetti F, Lévy M, Sobhani I, Azoulay D, Catena F, de'Angelis GL, de'Angelis N. Confocal Laser Endomicroscopy in Gastrointestinal and Pancreatobiliary Diseases: A Systematic Review and Meta-Analysis. *Biomed Res Int* 2016; **2016**: 4638683 [PMID: 26989684 DOI: 10.1155/2016/4638683]

25 **Kawai T**, Inoue H, Yao K, Kaise M, Kato M, Tanabe S, Sakata Y; Collaborators. Advanced diagnostic endoscopy in the upper gastrointestinal tract: Review of the Japan Gastroenterological Endoscopy Society core sessions. *Dig Endosc* 2023; **35**: 711-717 [PMID: 37183343 DOI: 10.1111/den.14594]

World Journal of Clinical Cases

Submit a Manuscript: https://www.f6publishing.com

World J Clin Cases 2024 September 16; 12(26): 5850-5853

DOI: 10.12998/wjcc.v12.i26.5850

ISSN 2307-8960 (online)

EDITORIAL

Proteomics for early prenatal screening of gestational diabetes mellitus

Liang Wu, Xiu-Ping Wang, Yun-Xia Zhu, Yan-Ping Tan, Chun-Ming Li

Specialty type: Endocrinology and metabolism

Provenance and peer review: Invited article; Externally peer reviewed.

Peer-review model: Single blind

Peer-review report's classification

Scientific Quality: Grade B

Novelty: Grade B

Creativity or Innovation: Grade B

Scientific Significance: Grade B

P-Reviewer: Gragnaniello V, Italy

Received: March 20, 2024

Revised: May 12, 2024

Accepted: June 4, 2024

Published online: September 16, 2024

Processing time: 124 Days and 12.7 Hours

Liang Wu, Xiu-Ping Wang, Yun-Xia Zhu, Chun-Ming Li, Department of Dermatology, The Second Affiliated Hospital, Jiangxi Medical College, Nanchang University, Nanchang 330006, Jiangxi Province, China

Yan-Ping Tan, Department of Dermatology, Jiangxi Provincial Maternal and Child Health Hospital, Nanchang 330000, Jiangxi Province, China

Co-corresponding authors: Yan-Ping Tan and Chun-Ming Li.

Corresponding author: Chun-Ming Li, PhD, Associate Chief Physician, Department of Dermatology, The Second Affiliated Hospital, Jiangxi Medical College, Nanchang University, No. 1 Minde Road, Nanchang 330006, Jiangxi Province, China. chunminglincu@163.com

Abstract

In this editorial, we comment on the article by Cao *et al*. Through applying isobaric tags for relative and absolute quantification technology coupled with liquid chromatography-tandem mass spectrometry, the researchers observed significant differential expression of 47 proteins when comparing serum samples from pregnant women with gestational diabetes mellitus (GDM) to the healthy ones. GDM symptoms may involve abnormalities in inflammatory response, complement system, coagulation cascade activation, and lipid metabolism. Retinol binding protein 4 and angiopoietin like 8 are potential early indicators of GDM. GDM stands out as one of the most prevalent metabolic complications during pregnancy and is linked to severe maternal and fetal outcomes like pre-eclampsia and stillbirth. Nevertheless, none of the biomarkers discovered so far have demonstrated effectiveness in predicting GDM. Our topic was designed to foster insights into advances in the application of proteomics for early prenatal screening of GDM.

Key Words: Gestational diabetes mellitus; Proteomics; Biomarker; Blood; Placenta

Core Tip: In this editorial, we comment on the article by Cao *et al*. Our topic was designed to foster insights into advances in the application of proteomics for early prenatal screening of gestational diabetes mellitus.

Citation: Wu L, Wang XP, Zhu YX, Tan YP, Li CM. Proteomics for early prenatal screening of gestational diabetes mellitus. *World J Clin Cases* 2024; 12(26): 5850-5853
URL: https://www.wjgnet.com/2307-8960/full/v12/i26/5850.htm
DOI: https://dx.doi.org/10.12998/wjcc.v12.i26.5850

INTRODUCTION

In this editorial, we comment on the article by Cao *et al*[1]. By applying isobaric tags for relative and absolute quantification (iTRAQ) technology coupled with liquid chromatography-tandem mass spectrometry, the researchers observed significant differential expression of 47 proteins when comparing serum samples from pregnant women with gestational diabetes mellitus (GDM) to the healthy ones. GDM symptoms may involve abnormalities in inflammatory response, complement system, coagulation cascade activation, and lipid metabolism. Retinol binding protein 4 and angiopoietin like 8 are potential early indicators of GDM.

GDM stands out as one of the most prevalent metabolic complications during pregnancy and is linked to severe maternal and fetal outcomes like pre-eclampsia and stillbirth. Furthermore, females diagnosed with GDM have an approximately ten-fold greater risk of developing diabetes later in life. Currently, the guidelines set by professional organizations suggest that all pregnant women should undergo universal screening for GDM using the 75 g oral glucose tolerance test between the 24th and 28th weeks of gestation. Selective screening for GDM during early pregnancy is suggested when certain maternal risk factors (higher maternal age, overweight/obesity, ethnicity, personal history of GDM, family history of diabetes, and previous macrosomia) are present. However, diagnosis of GDM is frequently delayed and confirmed after complications arise[2]. Hence, it is extremely crucial to explore potential biomarkers for GDM prediction during pregnancy to accurately identify pregnant women at high risk of GDM and to develop effective interventions. Nevertheless, none of the biomarkers discovered so far have demonstrated effectiveness in predicting GDM.

Mass spectrometry-based proteomic techniques are powerful tools for large-scale analysis of protein modifications and have been utilized in a wide range of biomedical research areas to uncover novel biomarkers. Our topic was designed to foster insights into advances in the application of proteomics for early prenatal screening of GDM. We ultimately ended up with nine research papers.

Blood proteomics for early prenatal screening of GDM

Zhao *et al*[3] obtained blood samples from pregnant females during the 12-16 wk of gestation. Thirty of these pregnant females were later diagnosed with GDM at 24 to 28 wk of gestation and chosen as the subjects for the study. Using iTRAQ analysis, 33 differentially expressed proteins (DEPs) were identified in the serum samples. This study highlights the roles of the complement system, blood coagulation, and the inflammatory and immune responses in the pathogenesis of GDM. Specifically, the authors noted that a panel of four candidate proteins (insulin-like growth factor-binding protein 5, fibrinogen alpha chain, coagulation factor IX, and apolipoprotein E) were able to distinguish women who later developed GDM from controls, demonstrating excellent sensitivity and specificity. Another nested case-control study was conducted by Ravnsborg *et al*[4], who applied a proteomics approach to first-trimester sera from 60 obese women. Serum proteomic profiling revealed 25 proteins whose levels significantly differed between the cases and controls. The more significant finding of this study was that three proteins, vitronectin, serum amyloid P-component, and afamin, were further confirmed as biomarkers of GDM. Shen *et al*[5] reported that 31 and 27 DEPs were identified in the serum samples collected from pregnant females later diagnosed with GDM during 12-16 wk of gestation and GDM patients at 24-28 wk. These proteins were linked to diabetes and maternal and perinatal complications. This study highlights the roles of the blood clotting cascade and the complement system in the development of GDM. DEPs could serve as potential biomarkers for prediction and diagnosis of GDM in the future. In the study of Mavreli *et al*[6], plasma samples collected from five women who developed GDM and five nondiabetic women in the first trimester were analysed using iTRAQ-based proteomics. Enzyme-linked immunosorbent assay was used in an independent cohort of 25 patients with GDM and 25 normal controls for verification. Notable differences in expression were observed between the two groups for thrombospondin-4, basement membrane-specific heparan sulfate proteoglycan core protein, extracellular matrix protein 1, beta-ala-his dipeptidase, and prenylcysteine oxidase 1. These DEPs are primarily linked to complement and coagulation cascades.

Placental proteomics for early prenatal screening of GDM

Using data-independent acquisition proteomics, Wei *et al*[7] conducted a study to compare the protein expression profiles of placental tissue between patients with GDM and healthy controls. They identified 37 proteins that were differently expressed between the two groups. This study provided preliminary evidence that CD248 and CD109 can serve as predictive markers for GDM during early pregnancy. Ge *et al*[8] used iTRAQ for proteomic screening of DEPs in the placenta from GDM patients and healthy women. A total of 68 DEPs in the placenta of GDM patients were identified, comprising 47 downregulated and 21 upregulated DEPs. Fourteen specific proteins (EXOSC7, PHGDH, SPTBN2L, ANK1, SPTB, RAB21, CIRBP, SLC4A1, RAB3B, EPPK1, HNRNPA3, HNRNP, HNRNPAB, and HNRNPA2B1) were found to be differentially expressed in the placenta. These proteins may play a crucial role in regulating the occurrence and development of GDM through multilink and multichannel regulation. Chen *et al*[9] investigated the protein expression profiles of placental samples from 89 women with GDM and 83 with normal glucose tolerance. The study identified 123

DEPs in the placenta involved in oxidative phosphorylation, inflammatory signaling, ribosomal function, and the pancreatic secretion pathway. In addition, the plasma total triglyceride and galectin 3 binding protein levels had good predictive and diagnostic value during early pregnancy.

Urine proteomics for early prenatal screening of GDM

Due to its accessibility in large quantities, noninvasive collection, and easy preparation, urine has become a good biological sample for biomarker identification. Ramachandrarao *et al*[10] analysed the exosome proteome content in 24-h urine samples obtained at 20 wk of pregnancy from pregnant women with GDM, pregnant women with pregestational type 2 diabetes (PGD), and controls (CTRLs). A total of 856, 734, and 646 proteins in exosomes were identified in the 24-h urine samples from patients in the PGD, GDM, and CTRL groups, respectively. The S100 calcium-binding protein A9 was found to be significantly increased in both PGD and GDM patients. Guo *et al*[11] collected urine samples from 889 healthy young pregnant women in the early second trimester, 69 of whom were subsequently diagnosed with GDM at 24 to 28 wk of gestation. Through iTRAQ-based quantitative proteomics, a total of 1901 proteins were identified in this study, including 119 significantly DEPs. This study suggested that CD59 and interleukin 1 receptor antagonist (IL1RA) in urine could be early, noninvasive diagnostic predictors of GDM in young pregnant women, and that IL1RA has greater diagnostic power than CD59.

CONCLUSION

Over the past few decades, there has been a growing focus on predicting GDM at an early stage. However, finding "ideal biomarkers" that offer exceptional sensitivity, specificity, and reproducibility to identify women at risk of GDM is still a challenge. Hence, further efforts are required to determine definitive GDM biomarkers.

FOOTNOTES

Author contributions: Wu L contributed to data collection and manuscript writing; Zhu YX and Wang XP contributed to data analysis; Tan YP contributed to conceptualization and supervision; Li CM contributed to manuscript polishing and editing; all authors have read and approved the final manuscript. Both Tan YP and Li CM have played important and indispensable roles in the writing and editing of the manuscript and review of the literature as the co-corresponding authors. Tan YP conceptualized and supervised the whole process of the project. She searched the literature, and revised and submitted the early version of the manuscript. Li CM was instrumental and responsible for polishing, editing, and submission of the current version of the manuscript.

Conflict-of-interest statement: All the authors declare that they have no conflict of interest to disclose.

Country of origin: China

ORCID number: Liang Wu 0009-0004-6926-3236; Xiu-Ping Wang 0009-0003-0348-8427; Yun-Xia Zhu 0000-0001-5102-3817; Yan-Ping Tan 0009-0002-1210-7086; Chun-Ming Li 0009-0000-1998-5311.

S-Editor: Liu JH
L-Editor: A
P-Editor: Cai YX

REFERENCES

1 **Cao WL**, Yu CP, Zhang LL. Serum proteins differentially expressed in gestational diabetes mellitus assessed using isobaric tag for relative and absolute quantitation proteomics. *World J Clin Cases* 2024; **12**: 1395-1405 [PMID: 38576811 DOI: 10.12998/wjcc.v12.i8.1395]

2 **Yanachkova V**, Staynova R, Stankova T, Kamenov Z. Placental Growth Factor and Pregnancy-Associated Plasma Protein-A as Potential Early Predictors of Gestational Diabetes Mellitus. *Medicina (Kaunas)* 2023; **59** [PMID: 36837599 DOI: 10.3390/medicina59020398]

3 **Zhao D**, Shen L, Wei Y, Xie J, Chen S, Liang Y, Chen Y, Wu H. Identification of candidate biomarkers for the prediction of gestational diabetes mellitus in the early stages of pregnancy using iTRAQ quantitative proteomics. *Proteomics Clin Appl* 2017; **11** [PMID: 28220636 DOI: 10.1002/prca.201600152]

4 **Ravnsborg T**, Svaneklink S, Andersen LLT, Larsen MR, Jensen DM, Overgaard M. First-trimester proteomic profiling identifies novel predictors of gestational diabetes mellitus. *PLoS One* 2019; **14**: e0214457 [PMID: 30917176 DOI: 10.1371/journal]

5 **Shen L**, Zhao D, Chen Y, Zhang K, Chen X, Lin J, Li C, Iqbal J, Zhao Y, Liang Y, Wei Y, Feng C. Comparative Proteomics Analysis of Serum Proteins in Gestational Diabetes during Early and Middle Stages of Pregnancy. *Proteomics Clin Appl* 2019; **13**: e1800060 [PMID: 31162828 DOI: 10.1002/prca.201800060]

6 **Mavreli D**, Evangelinakis N, Papantoniou N, Kolialexi A. Quantitative Comparative Proteomics Reveals Candidate Biomarkers for the Early Prediction of Gestational Diabetes Mellitus: A Preliminary Study. *In Vivo* 2020; **34**: 517-525 [PMID: 32111749 DOI: 10.21873/invivo.11803]

7 **Wei Y**, He A, Huang Z, Liu J, Li R. Placental and plasma early predictive biomarkers for gestational diabetes mellitus. *Proteomics Clin Appl* 2022; **16**: e2200001 [PMID: 35385222 DOI: 10.1002/prca.202200001]

8 **Ge L**, Huang P, Miao H, Yu H, Wu D, Chen F, Lin Y, Lin Y, Li W, Hua J. The new landscape of differentially expression proteins in placenta tissues of gestational diabetes based on iTRAQ proteomics. *Placenta* 2023; **131**: 36-48 [PMID: 36473392 DOI: 10.1016/j.placenta.2022.11.012]

9 **Chen F**, Li M, Fei X, Chen X, Zhang Z, Zhu W, Shen Y, Mao Y, Liu J, Xu J, Du J. Predictive plasma biomarker for gestational diabetes: A case-control study in China. *J Proteomics* 2023; **271**: 104769 [PMID: 36372392 DOI: 10.1016/j.jprot.2022.104769]

10 **Ramachandrarao SP**, Hamlin AA, Awdishu L, Overcash R, Zhou M, Proudfoot J, Ishaya M, Aghania E, Madrigal A, Kokoy-Mondragon C, Kao K, Khoshaba R, Bounkhoun A, Ghassemian M, Tarsa M, Naviaux RK. Proteomic analyses of Urine Exosomes reveal New Biomarkers of Diabetes in Pregnancy. *Madridge J Diabetes* 2016; **1**: 11-22 [PMID: 31448371 DOI: 10.18689/mjd-1000103]

11 **Guo Y**, Han Z, Guo L, Liu Y, Li G, Li H, Zhang J, Bai L, Wu H, Chen B. Identification of urinary biomarkers for the prediction of gestational diabetes mellitus in early second trimester of young gravidae based on iTRAQ quantitative proteomics. *Endocr J* 2018; **65**: 727-735 [PMID: 29760307 DOI: 10.1507/endocrj.EJ17-0471]

World Journal of Clinical Cases

Submit a Manuscript: https://www.f6publishing.com

World J Clin Cases 2024 September 16; 12(26): 5854-5858

DOI: 10.12998/wjcc.v12.i26.5854

ISSN 2307-8960 (online)

EDITORIAL

Paired box proteins as diagnostic biomarkers for endocervical adenocarcinoma

Jia-Hui Zhou, Xiang-Ning Zhang

Specialty type: Medicine, research and experimental

Provenance and peer review: Invited article; Externally peer reviewed.

Peer-review model: Single blind

Peer-review report's classification

Scientific Quality: Grade D

Novelty: Grade C

Creativity or Innovation: Grade C

Scientific Significance: Grade C

P-Reviewer: Ozaki T, Japan

Received: April 5, 2024

Revised: May 12, 2024

Accepted: May 23, 2024

Published online: September 16, 2024

Processing time: 108 Days and 22.4 Hours

Jia-Hui Zhou, Pathology Department, Lishui Central Hospital, Lishui 323000, Zhejiang Province, China

Xiang-Ning Zhang, Pathophysiology Department, Guangdong Medical University, Dongguan 523808, Guangdong Province, China

Corresponding author: Xiang-Ning Zhang, MD, PhD, Associate Professor, Pathophysiology Department, Guangdong Medical university, No. 1 Xincheng Avenue, Songshan Lake Scientific and Industrial Park, Dongguan 523808, Guangdong Province, China.
zhangxn_2006@126.com

Abstract

In this editorial, we commented on the article by Akers *et al* published in the recent issue of the *World Journal of Clinical Cases*. We focused specifically on the role of the transcription factor paired box protein 8 (PAX8) belonging to the family PAX in the carcinogenesis of a gynecologic tumor, endocervical adenocarcinoma, arising from the tissue of mesonephric origin, and the potential diagnostic value for the same type of neoplasms. The global vaccination program of human papillomavirus (HPV) has dramatically reduced the incidence of cervical cancer, including cases of adenocarcinoma. The type of adenoid epithelial origin has a lower frequency of HPV detection but tends to be more aggressive and fatal. Cases of endocervical adenocarcinoma occurring in females of menopause age have been described in the 2023 volume of the *World Journal of Clinical Cases* and in our study recently published in *Oncol Lett*. The histopathological findings and immunohistochemical assays showed that the lesions had glandular morphology, and the specimens in these two reports were immunohistochemically positive for the transcription factor PAX8, albeit that they had opposing expression profiles of tumor suppressor p16 and estrogen receptor and the presence of the HPV genome. The presence of a mucin protein, MUC 5AC, as revealed in both studies suggested target molecules for the diagnosis of mucinous adenoid type of uterine tumor and other histological origins. The clinical outcome was unfavorable due to metastasis and recurrence. This prompted the improvement of the antitumor modality, with the introduction of precise targeting therapy. Mucin has now been reported to be the therapeutic target for adenocarcinomas.

Key Words: Cervical adenocarcinoma; Diagnostic biomarker; Paired box protein 8; Embryogenesis; Transcription factor

Core Tip: Paired box proteins (PAXs) are a family of transcription factors that play an important role in the embryogenesis of different tissues through the regulation of gene expression. PAX 2, 5, and 8 are expressed in the sites of mesonephric tissues, and their deregulation contributes to the genesis of urogenital tumors such as cervical and ovarian cancers. Immunohistochemical staining and in situ hybridization tests revealed that the specimens of endocervical adenocarcinoma were positive for the transcription factor PAX8 and human papillomavirus. It is proposed that combined with mucin of glandular tumor, PAX8 can be used as a diagnostic marker for cervical adenocarcinoma.

Citation: Zhou JH, Zhang XN. Paired box proteins as diagnostic biomarkers for endocervical adenocarcinoma. *World J Clin Cases* 2024; 12(26): 5854-5858
URL: https://www.wjgnet.com/2307-8960/full/v12/i26/5854.htm
DOI: https://dx.doi.org/10.12998/wjcc.v12.i26.5854

INTRODUCTION

In 2023, a report by Akers *et al*[1] published in the *World Journal of Clinical Cases* described a case of distant metastasis of cervical adenocarcinoma with alterations in several biomarkers including tumor suppressor p16, estrogen receptor, and transcription factor paired box protein 8 (PAX8). The case was also positive for human papillomavirus (HPV)[1]. We recently reported 2 cases of gastric-type endocervical adenocarcinoma; one of the patients was immunohistochemically positive for PAX8[2]. Because PAX protein expression related to the tissue origin of lesions during embryogenesis and published data on the involvement of PAX proteins in the cancers of the ovary and uterine cervix, we aimed to dissect the possible significance of using PAX proteins, especially PAX8, as diagnostic and therapeutic targets of cervical adenocarcinoma.

Role of PAX proteins in mesonephric embryogenesis and carcinogenesis

Gynecologic tumors such as ovarian and cervical cancers arise from the tissues of mesonephric origin during embryogenesis. The transcription factors regulate embryonic development and play a role in organogenesis. The aberrant expression is responsible for the genesis of malignancies. Some members of the PAX family are implicated in these processes.

The PAX family comprises nine members, namely PAX1-9. They are divided into four groups based on their distinct molecular motif composition. The transcription factors are preferentially expressed in different anatomic sites during human embryogenesis to regulate gene expression; in relation to this, the PAX protein family molecules also contribute to carcinogenesis in specific parts of the body.

The members of the PAX family preferentially contribute to the regulation of gene expression of different organs; early expression of PAX2 is essential for the formation of the mesonephric duct[3]. It also compensates for the reduced expression of PAX8 throughout kidney development; the expression of PAX8 is activated in kidney and thyroid tissue during their organogenesis process[4]. In addition, PAX1 and PAX9 are implicated in the development of the skeleton. PAX2, 3, 5, 6, 7, and 8 are implicated in the development of the central nervous system[5], and aberrant expression of these PAX family members contributes to malignancies of the kidneys, thyroid gland, ovary, fallopian tube, and uterine cervix[6-8]. Table 1 summarizes the biological classification and activities of PAX family proteins including their role in tumorigenicity.

Role of PAX proteins in the genesis of cervical adenocarcinoma

Two major types of tumors, squamous carcinoma and adenocarcinoma[9,10], arise in the epithelial lining of the uterine cervix. Cervical cancer predominantly of squamous epithelial origin is associated with infection of high-risk HPV like types 16 and 18. The high incidence of HPV infection in cell cervical carcinoma offers an opportunity for global eradication through HPV vaccination[11]. Cervical adenocarcinomas, however, form a spectrum from well-differentiated adenoma malignum (a mucinous variant of minimal deviation adenocarcinoma) to poorly differentiated, invasive gastric-type adenocarcinoma[12,13]. Endocervical carcinoma, specifically gastric-type cervical adenocarcinoma, has a low incidence of HPV infection.

Generally, adenocarcinoma of the cervix has a poor prognosis. Regarding distant metastasis, cervical cancer typically metastasizes to local structures through direct invasion, hematogenous dissemination, or dissemination through the lymphatic system[14,15]. It was reported that breast metastases of cervical cancer occurred in the case of high-grade adenocarcinoma with mucinous features that we discussed in our case study[2].

Table 1 Classification, embryogenesis, and tumorigenicity of paired box protein family proteins

Group in PAX family	Member in PAX family	Expression site during embryogenesis	Involvement in tumorigenicity
I	PAX1	Skeleton, thymus, pharyngeal pouch	
	PAX9	Skeleton, teeth, thymus	
	PAX2	Kidney, CNS	Bladder and renal cancers
II	PAX5	B cells, CNS	Lymphomas
	PAX8	Kidneys, thyroid gland, CNS	Thyroid, ovarian, and cervical cancers
III	PAX3	Neural crest, CNS, muscle	Melanoma, rhabdomyosarcoma
	PAX7	Same as above	Rhabdomyosarcoma
IV	PAX4	Pancreas, gut	
	PAX5	Pancreas, gut, and eyes	Gastrointestinal cancers

CNS: Central nervous system; PAX: Paired box protein.

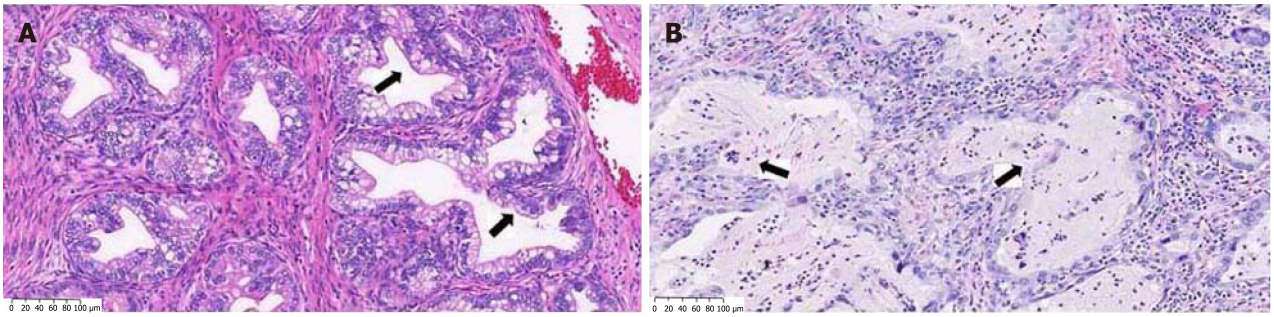

Figure 1 Histopathologic presentation of endocervical adenocarcinoma. Representative microscopic images of 2 cases of gastric-type endocervical adenocarcinoma. A: Case 1; B: Case 2. The scale bar is a length of 100 μm.

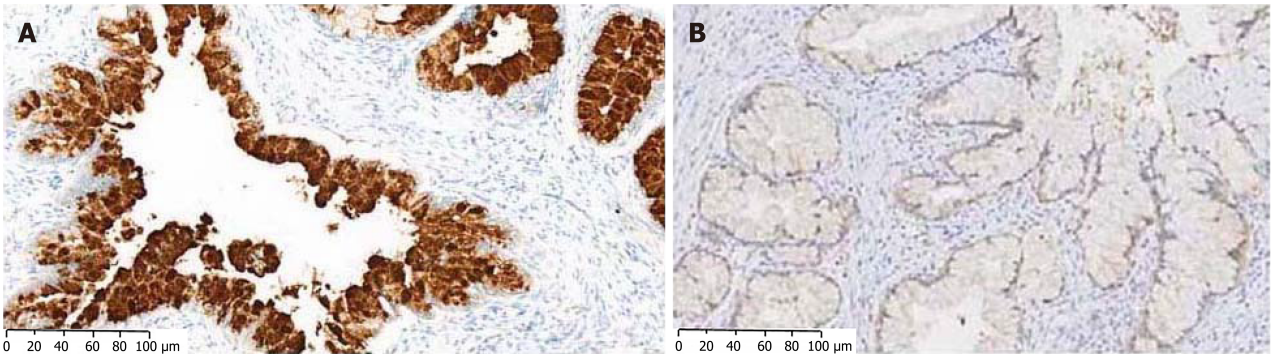

Figure 2 Immunohistochemical staining of gastric endocervical adenocarcinoma. A: Positive staining for a mucin protein, MUC 5AC, which is a biomarker of mucinous glandular tumor of the uterine cervix; B: Positive staining for the transcription factor paired box protein 8. The scale bar represents a length of 100 μm.

In situ hybridization test revealed that the case of cervical adenocarcinoma was positive for HPV and the transcription factor PAX8. Similarly, we reported 2 cases of gastric-type endocervical adenocarcinoma with one case being positive for PAX8[2]. Our cases presented as lesions of glandular appearance, and microscopically the tumor cells presented as cells of adenoid epithelium (Figure 1). In addition to PAX8 they were positive for a mucin protein, MUC 5AC (Figure 2), and negative for HPV. Furthermore, in contrast to the present report, our cases were negative for both estrogen receptor and the tumor suppressor p16.

Both PAX2 and PAX8 play an important role in the genesis of the anatomic structure of the ovary, uterus cervix, and uterus corpus during embryonic development. It has been shown that PAX8 is expressed in tumors of the thyroid gland, kidneys, and Müllerian tube, such as malignancies of ovary and endometrium, and its incidence of detection is high in ovarian cancer[16-20]. The possible involvement of PAX8 has been revealed in the genesis of cervical cancer[21,22].

PAX 8 has been recognized as a DNA binding transcription factor. A binding site for it has been identified in the promoter region in Wilms' tumor gene (*WT1*), coding for a product for the development of kidney and gonadal glands. The data suggested that part of its role in kidney development was as a modulator of WT1 expression in the kidney[23]. It remains to be tested whether tumors of the cervix and ovary have altered expression of WT1. While high PAX8 level is present in thyroid cancers, it has been reported that the coding region of *PAX8* is mutated in patients of thyroid dysgenesis, and it is responsible for elevated thyroid-stimulating hormone levels in congenital hypothyroidism[24]. Given this, the molecules of particular members of the PAX family are proposed to be indicators or biomarkers for the diagnosis of cervical adenocarcinoma or cancer of the cervix in general.

The expression of PAX8 has been noted in tumors of thyroid, renal, and Müllerian tube origins, like neoplasms originating from ovary and endometrium. Meanwhile, however, PAX8 was reported to be expressed in all 20 cases (100%) of benign endocervical epithelium specimens. Additionally, it was expressed in 97%-100% of adenocarcinoma in situ and in 0%-87% of endocervical adenocarcinoma specimens[25,26]. These findings suggest that the incidence of PAX proteins is low with the progression of the tumor and that the aberrant expression profile of tissue antigen due to the differentiation status in malignancy may account for negative PAX8 expression in 1 of our reported cases. The study of numerous clinical samples is needed to clarify this issue.

CONCLUSION

Multiple drivers of cancer involve the genesis of cervical cancer. We immunohistochemically detected the presence of mutant p53 in our reports. However, the oncogenicity-related changes could be highly heterogeneous; our study revealed the absence of mutant *k-ras* as assayed using a PCR-based amplification refractory mutant system[2]. Our early work showed that in HPV-positive cervical cancer cases, oncogene *c-myc* was overexpressed due to exon alteration[27] and the change in c-myc, which cooperates with mutant k-ras, results in malignancy, as reported in another study[28]. The gain-of-function mutations of oncogenes together with the mutation of tumor suppressor genes are common changes in malignancies but less specific to particular neoplasms of certain histologic origins. It is therefore proposed that molecules implicated in organogenesis related to tumors can be used as therapeutic targets for adenocarcinomas. The PAX family proteins may fulfill such demands[29,30].

FOOTNOTES

Author contributions: Zhou JH and Zhang XN conceived the idea and performed the study; Zhou JH prepared the primary draft, figures, and table; Zhang XN corrected the manuscript and revised the figures and table; Both authors read and approved the final version of the paper and agreed on its submission.

Conflict-of-interest statement: All the authors report having no relevant conflicts of interest for this article.

Country of origin: China

ORCID number: Jia-Hui Zhou 0000-0002-9735-685x; Xiang-Ning Zhang 0000-0002-7875-5548.

S-Editor: Liu H
L-Editor: Filipodia
P-Editor: Zhao S

REFERENCES

1 **Akers A**, Read S, Feldman J, Gooden C, English DP. Diagnostic challenges and individualized treatment of cervical adenocarcinoma metastases to the breast: A case report. *World J Clin Cases* 2024; **12**: 412-417 [PMID: 38313645 DOI: 10.12998/wjcc.v12.i2.412]
2 **Zhou J**, Zhang X, Mao W, Zhu Y, Yan L, Jiang J, Zhang M. Pathological features of gastric-type endocervical adenocarcinoma: A report of two cases. *Oncol Lett* 2024; **27**: 149 [PMID: 38406594 DOI: 10.3892/ol.2024.14282]
3 **Dressler GR**, Wilkinson JE, Rothenpieler UW, Patterson LT, Williams-Simons L, Westphal H. Deregulation of Pax-2 expression in transgenic mice generates severe kidney abnormalities. *Nature* 1993; **362**: 65-67 [PMID: 8383297 DOI: 10.1038/362065a0]
4 **Mansouri A**, Chowdhury K, Gruss P. Follicular cells of the thyroid gland require Pax8 gene function. *Nat Genet* 1998; **19**: 87-90 [PMID: 9590297 DOI: 10.1038/ng0598-87]
5 **Lang D**, Powell SK, Plummer RS, Young KP, Ruggeri BA. PAX genes: roles in development, pathophysiology, and cancer. *Biochem Pharmacol* 2007; **73**: 1-14 [PMID: 16904651 DOI: 10.1016/j.bcp.2006.06.024]
6 **Daniel L**, Lechevallier E, Giorgi R, Sichez H, Zattara-Cannoni H, Figarella-Branger D, Coulange C. Pax-2 expression in adult renal tumors.

Hum Pathol 2001; **32**: 282-287 [PMID: 11274636 DOI: 10.1053/hupa.2001.22753]
7 **Heidarpour M**, Tavanafar Z. Diagnostic utility of PAX8 in differentiation of mullerian from non-mullerian tumors. *Adv Biomed Res* 2014; **3**: 96 [PMID: 24800185 DOI: 10.4103/2277-9175.129366]
8 **Laury AR**, Hornick JL, Perets R, Krane JF, Corson J, Drapkin R, Hirsch MS. PAX8 reliably distinguishes ovarian serous tumors from malignant mesothelioma. *Am J Surg Pathol* 2010; **34**: 627-635 [PMID: 20414098 DOI: 10.1097/PAS.0b013e3181da7687]
9 **Adegoke O**, Kulasingam S, Virnig B. Cervical cancer trends in the United States: a 35-year population-based analysis. *J Womens Health (Larchmt)* 2012; **21**: 1031-1037 [PMID: 22816437 DOI: 10.1089/jwh.2011.3385]
10 **Guo F**, Cofie LE, Berenson AB. Cervical Cancer Incidence in Young U.S. Females After Human Papillomavirus Vaccine Introduction. *Am J Prev Med* 2018; **55**: 197-204 [PMID: 29859731 DOI: 10.1016/j.amepre.2018.03.013]
11 **Bewley S**. HPV vaccination and cervical cancer screening. *Lancet* 2022; **399**: 1939 [PMID: 35598621 DOI: 10.1016/S0140-6736(22)00110-6]
12 **Cree IA**, White VA, Indave BI, Lokuhetty D. Revising the WHO classification: female genital tract tumours. *Histopathology* 2020; **76**: 151-156 [PMID: 31846528 DOI: 10.1111/his.13977]
13 **Kojima A**, Mikami Y, Sudo T, Yamaguchi S, Kusanagi Y, Ito M, Nishimura R. Gastric morphology and immunophenotype predict poor outcome in mucinous adenocarcinoma of the uterine cervix. *Am J Surg Pathol* 2007; **31**: 664-672 [PMID: 17460448 DOI: 10.1097/01.pas.0000213434.91868.b0]
14 **Kumar L**, Pokharel YH, Dawar R, Thulkar S. Cervical cancer metastatic to the breast: a case report and review of the literature. *Clin Oncol (R Coll Radiol)* 1999; **11**: 414-416 [PMID: 10663334 DOI: 10.1053/clon.1999.9095]
15 **Cholmondeley K**, Callan L, Sangle N, D'Souza D. Metastatic cervical adenocarcinoma to the breast: A case report and literature review. *Gynecol Oncol Rep* 2019; **28**: 33-36 [PMID: 30815528 DOI: 10.1016/j.gore.2019.01.011]
16 **Maulbecker CC**, Gruss P. The oncogenic potential of Pax genes. *EMBO J* 1993; **12**: 2361-2367 [PMID: 8099544 DOI: 10.1002/j.1460-2075.1993.tb05890.x]
17 **Corona RI**, Seo JH, Lin X, Hazelett DJ, Reddy J, Fonseca MAS, Abassi F, Lin YG, Mhawech-Fauceglia PY, Shah SP, Huntsman DG, Gusev A, Karlan BY, Berman BP, Freedman ML, Gayther SA, Lawrenson K. Non-coding somatic mutations converge on the PAX8 pathway in ovarian cancer. *Nat Commun* 2020; **11**: 2020 [PMID: 32332753 DOI: 10.1038/s41467-020-15951-0]
18 **Fu DJ**, De Micheli AJ, Bidarimath M, Ellenson LH, Cosgrove BD, Flesken-Nikitin A, Nikitin AY. Cells expressing PAX8 are the main source of homeostatic regeneration of adult mouse endometrial epithelium and give rise to serous endometrial carcinoma. *Dis Model Mech* 2020; **13** [PMID: 32998907 DOI: 10.1242/dmm.047035]
19 **Di Palma T**, Lucci V, de Cristofaro T, Filippone MG, Zannini M. A role for PAX8 in the tumorigenic phenotype of ovarian cancer cells. *BMC Cancer* 2014; **14**: 292 [PMID: 24766781 DOI: 10.1186/1471-2407-14-292]
20 **Ramachandran D**, Wang Y, Schürmann P, Hülse F, Mao Q, Jentschke M, Böhmer G, Strauß HG, Hirchenhain C, Schmidmayr M, Müller F, Runnebaum I, Hein A, Koch M, Ruebner M, Beckmann MW, Fasching PA, Luyten A, Dürst M, Hillemanns P, Dörk T. Association of genomic variants at PAX8 and PBX2 with cervical cancer risk. *Int J Cancer* 2021 [PMID: 33905146 DOI: 10.1002/ijc.33614]
21 **Wu Y**, Li H, Wang H, Zhang F, Cao H, Xu S. MSK2 promotes proliferation and tumor formation in squamous cervical cancer *via* PAX8/RB-E2F1/cyclin A2 axis. *J Cell Biochem* 2019; **120**: 11432-11440 [PMID: 30756420 DOI: 10.1002/jcb.28421]
22 **Li CG**, Nyman JE, Braithwaite AW, Eccles MR. PAX8 promotes tumor cell growth by transcriptionally regulating E2F1 and stabilizing RB protein. *Oncogene* 2011; **30**: 4824-4834 [PMID: 21602887 DOI: 10.1038/onc.2011.190]
23 **Fraizer GC**, Shimamura R, Zhang X, Saunders GF. PAX 8 regulates human WT1 transcription through a novel DNA binding site. *J Biol Chem* 1997; **272**: 30678-30687 [PMID: 9388203 DOI: 10.1074/jbc.272.49.30678]
24 **Macchia PE**, Lapi P, Krude H, Pirro MT, Missero C, Chiovato L, Souabni A, Baserga M, Tassi V, Pinchera A, Fenzi G, Grüters A, Busslinger M, Di Lauro R. PAX8 mutations associated with congenital hypothyroidism caused by thyroid dysgenesis. *Nat Genet* 1998; **19**: 83-86 [PMID: 9590296 DOI: 10.1038/ng0598-83]
25 **Shukla A**, Thomas D, Roh MH. PAX8 and PAX2 expression in endocervical adenocarcinoma in situ and high-grade squamous dysplasia. *Int J Gynecol Pathol* 2013; **32**: 116-121 [PMID: 23202787 DOI: 10.1097/PGP.0b013e318257df46]
26 **Goyal A**, Yang B. Differential patterns of PAX8, p16, and ER immunostains in mesonephric lesions and adenocarcinomas of the cervix. *Int J Gynecol Pathol* 2014; **33**: 613-619 [PMID: 25272301 DOI: 10.1097/PGP.0000000000000102]
27 **Huang SL**, Liu ZQ, Zhang XN, Li MJ. Human papillomavirus, human cytomegalovirus and oncogene C-myc in cervical carcinoma and cervicitis. *Chin Med J (Engl)* 1993; **106**: 208-210 [PMID: 8391967]
28 **Stenzel A**, Semczuk A, Rózyńskal K, Jakowicki J, Wojcierowski J. "Low-risk" and "high-risk" HPV-infection and K-ras gene point mutations in human cervical cancer: a study of 31 cases. *Pathol Res Pract* 2001; **197**: 597-603 [PMID: 11569923]
29 **Yemelyanova A**, Gown AM, Wu LS, Holmes BJ, Ronnett BM, Vang R. PAX8 expression in uterine adenocarcinomas and mesonephric proliferations. *Int J Gynecol Pathol* 2014; **33**: 492-499 [PMID: 25083965 DOI: 10.1097/PGP.0b013e3182a54afa]
30 **Danialan R**, Assaad M, Burghardt J, Newcomb P, Cartun RW, Mandavilli S. The utility of PAX8 and IMP3 immunohistochemical stains in the differential diagnosis of benign, premalignant, and malignant endocervical glandular lesions. *Gynecol Oncol* 2013; **130**: 383-388 [PMID: 23618832 DOI: 10.1016/j.ygyno.2013.04.020]

World Journal of Clinical Cases

Submit a Manuscript: https://www.f6publishing.com

World J Clin Cases 2024 September 16; 12(26): 5859-5862

DOI: 10.12998/wjcc.v12.i26.5859

ISSN 2307-8960 (online)

EDITORIAL

Endoscopic ultrasound-guided biliary drainage using electrocautery-enhanced lumen-apposing metal stent for malignant biliary obstruction: A promising procedure

Si-Ze Wu

Specialty type: Gastroenterology and hepatology

Provenance and peer review: Invited article; Externally peer reviewed.

Peer-review model: Single blind

Peer-review report's classification

Scientific Quality: Grade C, Grade D

Novelty: Grade B, Grade C

Creativity or Innovation: Grade B, Grade C

Scientific Significance: Grade B, Grade C

P-Reviewer: Kitamura K, Japan

Received: April 20, 2024

Revised: May 19, 2024

Accepted: June 7, 2024

Published online: September 16, 2024

Processing time: 94 Days and 0.2 Hours

Si-Ze Wu, Department of Ultrasound, The First Affiliated Hospital of Hainan Medical University, Haikou 570102, Hainan Province, China

Corresponding author: Si-Ze Wu, MD, Chief Physician, Professor, Department of Ultrasound, The First Affiliated Hospital of Hainan Medical University, No. 31 Longhua Road, Haikou 570102, Hainan Province, China. wsz074@aliyun.com

Abstract

In this editorial, we comment on the article by Peng *et al*. Palliative drainage for biliary obstruction resulting from unresectable malignant lesions includes internal and external drainage. The procedures of biliary drainage are usually guided by fluoroscopy or transcutaneous ultrasound, endoscopic ultrasound (EUS), or both. Endoscopic retrograde cholangiopancreatography (ERCP) has been primarily recommended for the management of biliary obstruction, while EUS-guided biliary drainage and percutaneous transhepatic biliary drainage (PTBD) are alternative choices for cases where ERCP has failed or is impossible. PTBD is limited by shortcomings of a higher rate of adverse events, more reinterventions, and severe complications. EUS-guided biliary drainage has a lower rate of adverse events than PTBD. EUS-guided biliary drainage with electrocautery-enhanced lumen-apposing metal stent (ECE-LAMS) enables EUS-guided biliary-enteric anastomosis to be performed in a single step and does not require prior bile duct puncture or a guidewire. The present meta-analysis showed that ECE-LAMS has a high efficacy and safety in relieving biliary obstruction in general, although the results of LAMS depending on the site of biliary obstruction. This study has highlighted the latest advances with a larger sample-based comprehensive analysis.

Key Words: Malignant biliary obstruction; Biliary drainage; Percutaneous transhepatic biliary drainage; Electrocautery-enhanced lumen-apposing metal stents; Transcutaneous ultrasound; Endoscopic ultrasound; Endoscopic retrograde cholangiopancreatography

Core Tip: Some malignant distal biliary obstructions require drainage for palliative treatment, and endoscopic retrograde cholangiopancreatography (ERCP) with placement of a stent has been a first choice. However, ERCP can fail or may not be suitable for some challenging cases. Endoscopic ultrasound (EUS)-guided biliary drainage with electrocautery-enhanced lumen-apposing metal stent can be an alternative choice for ERCP, with the strength to perform biliary-enteric anastomosis under EUS guidance in a single step without the need for prior bile duct puncture or a guidewire. In this editorial, the efficacy and safety of it have been discussed, and the latest advances are highlighted.

Citation: Wu SZ. Endoscopic ultrasound-guided biliary drainage using electrocautery-enhanced lumen-apposing metal stent for malignant biliary obstruction: A promising procedure. *World J Clin Cases* 2024; 12(26): 5859-5862
URL: https://www.wjgnet.com/2307-8960/full/v12/i26/5859.htm
DOI: https://dx.doi.org/10.12998/wjcc.v12.i26.5859

INTRODUCTION

Jaundice caused by biliary obstruction is common in the adult population in clinical practice. The locations of biliary obstruction include intrahepatic biliary duct, perihilar duct, and distal biliary duct. The underlying diseases that can lead to this condition include stones in the bile ducts, bile duct carcinoma, chronic cholangitis, periampullary adenocarcinoma, pancreatic head carcinoma infiltration, tumoral compression, trauma, other conditions affecting the bile ducts, and iatrogenic diseases. The treatment of obstructive jaundice includes radical cure and palliative treatment. Currently, there are several procedures for the palliative treatment of obstructive jaundice through biliary drainage, including internal drainage and external drainage. Internal drainage mainly refers to endoscopic retrograde cholangiopancreatography (ERCP) with the placement of a stent, as well as endoscopic ultrasound (EUS)-guided biliary duct drainage. External drainage procedures include percutaneous transhepatic biliary drainage (PTBD), endoscopic nasobiliary drainage, and postoperative T-tube drainage.

The ERCP procedure can be used to investigate the structures and lesions of the extrahepatic bile duct, pancreatic ducts, and ampulla, and can also be used to perform some interventional treatments[1]. Despite having various complications such as post-procedure pancreatic inflammation, bleeding, infection, and perforation of the intestines, ERCP with placement of stent in the tumor remains the primary choice for bile drainage in the palliative treatment of patients with distal malignant obstructive jaundice[1,2]. However, the initial failure rate of ERCP is reported to be as high as 10% to 20%[1]. The main reasons for failures include inaccessibility of the papilla due to tumor infiltration of the duodenum or papilla, aberrant regional anatomy due to previous procedures of cephalic duodenopancreatectomy and gastrectomy, or other surgeries, prior intervention and stenting of the ampulla, and cannulation failure[1]. For cases where ERCP fails, alternative techniques such as PTBD and EUS-guided biliary drainage are considered[1-3]. In terms of technical and clinical success, the two procedures have shown comparable effectiveness[4]. However, EUS-guided biliary drainage performed in expert centers frequently shows substantially better clinical success, fewer adverse events, and fewer reinterventions[4]. Compared to patients undergoing EUS-guided biliary drainage, PTBD patients using different routes of drainage (trans-hepatic or extra-hepatic) undergo considerably additional reinterventions (4.9 *vs* 1.3), experience more pain (4.1 *vs* 1.9), and encounter more delayed adverse events (53.8% *vs* 6.6%)[5]. In another study, it was found that 205 of the 331 patients (61.9%) who underwent PTCD developed complications, including infections in 91 patients (40.6%) and non-infectious complications in 114 of the 331 patients (34.4%)[6]. Patients undergoing PTBD often have a poor quality of life, and the procedure is inconvenient for most patients due to the associated external ducts and bags. On the other hand, EUS-guided biliary drainage using conventional procedure and stents involves multiple steps, which can significantly increase the rate of adverse events[7].

EUS and ERCP can be combined for biliary drainage. A clinical trial showed that ERCP and EUS in combination exhibited significantly lower rates of recurrent biliary obstruction at 3 months and 6 months compared to bilateral PTBD, with similar rates of adverse events and no significant difference in mortality. The lower morbidity is associated with a significantly reduced risk of biliary reintervention[1,8].

PTBD and ERCP used to be fluoroscopy-guided procedures, and later both procedures were introduced with US-guided imaging or a combination of both. All imaging guidance techniques allow for visualization of the duct lumen, helping to avoid blind operations. Biliary puncture under US guidance has been shown to be safe and effective due to its low complication rate and high success rate[9]. Additionally, fluoroscopy-guided PTBD (F-PTBD) increases the exposure of patients and operators to radiation. A comparative study of 195 patients, including 207 F-PTBDs and 44 ultrasound-guided PTBDs (US-PTBDs), showed a higher success rate for F-PTBD from the biliary ducts in the right lobe of the liver compared to US-PTBD (91.9% *vs* 75%; $P = 0.033$), and a trend of a higher success rate for US-PTBD from the biliary ducts in the left lobe of the liver (82.9% *vs* 95.8%; $P = 0.223$). F-PTBD appears to be superior to US-PTBD for the drainage of biliary obstruction in the right liver lobe. However, major complications occur more frequently with F-PTBD. There was no significant difference between the two procedures in regard to overall procedure success (90% *vs* 86.4%), overall interventional complication rates (10.6% *vs* 9.1%), fluoroscopy times, intervention times, or sedative dosages[10].

Biliary duct puncture per se is not a difficult procedure but is associated with a potential risk of higher bleeding complications. Performing biliary duct drainage under imaging guidance or with the aid of an endoscope can enhance the clinical success rate, reduce adverse events, and save time. US-guidance includes transcutaneous US-guidance and EUS-

guidance. Apart from being free of ionization and radiation, both methods can display dilated bile ducts and associated lesions, visualize structures beyond the intestine and bile duct lumen, scan the region of interest from multiple dimensions, and allow for repeated scanning. These features are advantageous for performance and can increase the operator's confidence. The combined use of fluoroscopy and US-guided PTBD is safer and more effective for puncture and guidewire insertion in the PTBD procedure, significantly reducing fluoroscopy time and radiation doses. One of the shortcomings of US-guidance is its inability to display a wide field in a single scan and difficulty in showing small-sized bile ducts due to limited spatial resolution[9]. EUS allows clear visualization of previously inaccessible anatomical regions of the pancreatic and biliary ducts, as well as some structures adjacent to the gastrointestinal tract. With the aid of a biopsy device, it also enables the acquisition of tissue for histological diagnosis and access to regional fluid collections and other abnormalities[11]. The endoscope provides an advantage in obtaining an acute and detailed view of the region of interest and the capability to acquire target tissues for histological study. Radiocontrast agent-enhanced X-ray radiography can display a large field of the biliary tree, pancreatic ducts, and small-sized bile ducts. However, it cannot detect detailed structures outside the lumen of bile ducts, pancreatic ducts, and the gastrointestinal tract. On the other hand, it has side effects of ionization and radiation, and the use of iodine-based radiocontrast agents may not be suitable for patients who are allergic to iodine or have concomitant renal failure. Both PTBD and ERCP can be used for the drainage of distal bile duct obstruction, but ERCP is usually not used for hepatic perihilar biliary obstruction.

In 2013, a new technology of EUS-guided biliary drainage with placement of electrocautery-enhanced lumen-apposing metal stent (ECE-LAMS) was introduced. This technology allows for the performance of EUS-guided biliary-enteric anastomosis in a single step and is free from prior bile duct puncture or the use of a guidewire[12]. The ECE-LAMS significantly simplifies the procedure and is particularly suitable for frail patients or those with other conditions that make them intolerant to other procedures. A retrospective study demonstrated that both expert operators (4 out of 12) and non-expert operators (8 out of 12) achieved similar satisfactory success rates in performing ECE-LAMS[13]. Another retrospective multicenter study showed that ECE-LAMS has high technical and clinical success rates for various indications of interventional EUS. This suggests that it can be considered as an alternative treatment method for cases where ERCP has failed, as well as for other challenging cases. The procedure was found to be reproducible and generalizable[12]. However, it is important to note that these studies have a retrospective design with small sample sizes, which may limit the generalizability of the conclusions. Further investigation is necessary to validate these findings.

UPDATED EVALUATION OF EUS-GUIDED BILIARY DRAINAGE WITH ECE-LAMS

Peng *et al*[14], address the progress in recent years by conducting an updated meta-analysis to assess the efficacy and safety of EUS-guided biliary drainage with placement of ECE-LAMS for the palliation of distal biliary obstruction. In this meta-analysis, two prospective studies and 12 retrospective cohort studies were included after an extensive and intensive search of databases and data curation. This meta-analysis is an updated and comprehensive systematic review, as the quality of the included studies was independently evaluated, details of the procedures and methods in each study were thoroughly reviewed and curated, and adequate statistical analyses were performed. In this meta-analysis, a total of 620 participants from 14 eligible studies were included, which is more than twice the number of patients included in previous analyses. These findings highlight the efficacy, safety, adverse events, and other new discoveries[14]. The pooled rates of technical success, clinical success, adverse events, and overall reintervention were 96.7%, 91.0%, 17.5%, and 7.3%, respectively. The main limitation of the meta-analysis was that most of the enrolled studies were of retrospective design, which may have introduced selection bias. Moving forward, more randomized trials and well-designed prospective studies are needed to further investigate, confirm, and validate the previous findings.

CLINICAL IMPLICATIONS

The results of this study indicate that ECE-LAMS has a favorable success rate with acceptable adverse events in biliary drainage for malignant distal biliary obstruction, especially indicative for those who have failed using ERCP or not suitable to perform ERCP. ECE-LAMS cannot be used for the biliary drainage of intrahepatic or hepatic perhilar biliary obstruction. The consistent body of evidence across most subgroups suggests that ECE-LAMS is a reproducible and generalizable approach, giving the procedure great technical implementation and widespread application. Future studies are needed to improve the clinical success and safety rate of EUS-guided ECE-LAMS implantation and to expand its application to other indications.

CONCLUSION

Increased evidence supports that EUS-guided biliary drainage using ECE-LAMS for the palliative treatment of malignant distal biliary obstruction after ERCP failure or when ERCP is not feasible has shown high efficacy and safety. In the future, well-designed prospective studies with larger sample sizes are needed to further understand EUS-guided biliary drainage with ECE-LAMS.

FOOTNOTES

Author contributions: Wu SZ conceptualized and wrote the manuscript.

Conflict-of-interest statement: No benefits in any form have been received or will be received from a commercial party related directly or indirectly to the subject of this article.

Country of origin: China

ORCID number: Si-Ze Wu 0000-0002-1086-764X.

S-Editor: Liu JH
L-Editor: Filipodia
P-Editor: Zhao YQ

REFERENCES

1 **Dumonceau JM**, Tringali A, Papanikolaou IS, Blero D, Mangiavillano B, Schmidt A, Vanbiervliet G, Costamagna G, Devière J, García-Cano J, Gyökeres T, Hassan C, Prat F, Siersema PD, van Hooft JE. Endoscopic biliary stenting: indications, choice of stents, and results: European Society of Gastrointestinal Endoscopy (ESGE) Clinical Guideline - Updated October 2017. *Endoscopy* 2018; **50**: 910-930 [PMID: 30086596 DOI: 10.1055/a-0659-9864]

2 **Giovannini M**, Moutardier V, Pesenti C, Bories E, Lelong B, Delpero JR. Endoscopic ultrasound-guided bilioduodenal anastomosis: a new technique for biliary drainage. *Endoscopy* 2001; **33**: 898-900 [PMID: 11571690 DOI: 10.1055/s-2001-17324]

3 **Dietrich CF**, Braden B, Burmeister S, Aabakken L, Arciadacono PG, Bhutani MS, Götzberger M, Healey AJ, Hocke M, Hollerbach S, Ignee A, Jenssen C, Jürgensen C, Larghi A, Moeller K, Napoléon B, Rimbas M, Săftoiu A, Sun S, Bun Teoh AY, Vanella G, Fusaroli P, Carrara S, Will U, Dong Y, Burmester E. How to perform EUS-guided biliary drainage. *Endosc Ultrasound* 2022; **11**: 342-354 [PMID: 36255022 DOI: 10.4103/EUS-D-21-00188]

4 **Sharaiha RZ**, Khan MA, Kamal F, Tyberg A, Tombazzi CR, Ali B, Tombazzi C, Kahaleh M. Efficacy and safety of EUS-guided biliary drainage in comparison with percutaneous biliary drainage when ERCP fails: a systematic review and meta-analysis. *Gastrointest Endosc* 2017; **85**: 904-914 [PMID: 28063840 DOI: 10.1016/j.gie.2016.12.023]

5 **Hassan Z**, Gadour E. Percutaneous transhepatic cholangiography *vs* endoscopic ultrasound-guided biliary drainage: A systematic review. *World J Gastroenterol* 2022; **28**: 3514-3523 [PMID: 36158274 DOI: 10.3748/wjg.v28.i27.3514]

6 **Turan AS**, Jenniskens S, Martens JM, Rutten MJCM, Yo LSF, van Strijen MJL, Drenth JPH, Siersema PD, van Geenen EJM. Complications of percutaneous transhepatic cholangiography and biliary drainage, a multicenter observational study. *Abdom Radiol (NY)* 2022; **47**: 3338-3344 [PMID: 34357434 DOI: 10.1007/s00261-021-03207-4]

7 **Anderloni A**, Troncone E, Fugazza A, Cappello A, Del Vecchio Blanco G, Monteleone G, Repici A. Lumen-apposing metal stents for malignant biliary obstruction: Is this the ultimate horizon of our experience? *World J Gastroenterol* 2019; **25**: 3857-3869 [PMID: 31413524 DOI: 10.3748/wjg.v25.i29.3857]

8 **Kongkam P**, Orprayoon T, Boonmee C, Sodarat P, Seabmuangsai O, Wachiramatharuch C, Auan-Klin Y, Pham KC, Tasneem AA, Kerr SJ, Romano R, Jangsirikul S, Ridtitid W, Angsuwatcharakon P, Ratanachu-Ek T, Rerknimitr R. ERCP plus endoscopic ultrasound-guided biliary drainage *vs* percutaneous transhepatic biliary drainage for malignant hilar biliary obstruction: a multicenter observational open-label study. *Endoscopy* 2021; **53**: 55-62 [PMID: 32515005 DOI: 10.1055/a-1195-8197]

9 **Park SE**, Nam IC, Baek HJ, Ryu KH, Lim SG, Won JH, Kim DR. Effectiveness of ultrasound-guided percutaneous transhepatic biliary drainage to reduce radiation exposure: A single-center experience. *PLoS One* 2022; **17**: e0277272 [PMID: 36331963 DOI: 10.1371/journal.pone.0277272]

10 **Nennstiel S**, Treiber M, Faber A, Haller B, von Delius S, Schmid RM, Neu B. Comparison of Ultrasound and Fluoroscopically Guided Percutaneous Transhepatic Biliary Drainage. *Dig Dis* 2019; **37**: 77-86 [PMID: 30253406 DOI: 10.1159/000493120]

11 **van der Merwe SW**, van Wanrooij RLJ, Bronswijk M, Everett S, Lakhtakia S, Rimbas M, Hucl T, Kunda R, Badaoui A, Law R, Arcidiacono PG, Larghi A, Giovannini M, Khashab MA, Binmoeller KF, Barthet M, Perez-Miranda M, van Hooft JE. Therapeutic endoscopic ultrasound: European Society of Gastrointestinal Endoscopy (ESGE) Guideline. *Endoscopy* 2022; **54**: 185-205 [PMID: 34937098 DOI: 10.1055/a-1717-1391]

12 **Mangiavillano B**, Moon JH, Crinò SF, Larghi A, Pham KD, Teoh AYB, Paduano D, Lee YN, Yoo HW, Shin IS, Rizzatti G, Robles-Medranda C, Oleas R, Conti Bellocchi MC, Auriemma F, Lamonaca L, Spatola F, Conigliaro R, Facciorusso A, Gabbrielli A, Repici A. Safety and efficacy of a novel electrocautery-enhanced lumen-apposing metal stent in interventional EUS procedures (with video). *Gastrointest Endosc* 2022; **95**: 115-122 [PMID: 34339667 DOI: 10.1016/j.gie.2021.07.021]

13 **Jacques J**, Privat J, Pinard F, Fumex F, Valats JC, Chaoui A, Cholet F, Godard B, Grandval P, Legros R, Kerever S, Napoleon B. Endoscopic ultrasound-guided choledochoduodenostomy with electrocautery-enhanced lumen-apposing stents: a retrospective analysis. *Endoscopy* 2019; **51**: 540-547 [PMID: 30347424 DOI: 10.1055/a-0735-9137]

14 **Peng ZX**, Chen FF, Tang W, Zeng X, Du HJ, Pi RX, Liu HM, Lu XX. Endoscopic-ultrasound-guided biliary drainage with placement of electrocautery-enhanced lumen-apposing metal stent for palliation of malignant biliary obstruction: Updated meta-analysis. *World J Gastrointest Surg* 2024; **16**: 907-920 [PMID: 38577086 DOI: 10.4240/wjgs.v16.i3.907]

World Journal of Clinical Cases

Submit a Manuscript: https://www.f6publishing.com

World J Clin Cases 2024 September 16; 12(26): 5863-5867

DOI: 10.12998/wjcc.v12.i26.5863

ISSN 2307-8960 (online)

EDITORIAL

Cardiac implications in myasthenia gravis

Praveen Reddy Elmati, Gowthami Sai Kogilathota Jagirdhar, Salim Surani

Specialty type: Medicine, research and experimental

Provenance and peer review: Invited article; Externally peer reviewed.

Peer-review model: Single blind

Peer-review report's classification

Scientific Quality: Grade B
Novelty: Grade B
Creativity or Innovation: Grade B
Scientific Significance: Grade B

P-Reviewer: Kumawat VS, India

Received: May 5, 2024
Revised: June 3, 2024
Accepted: June 14, 2024
Published online: September 16, 2024
Processing time: 78 Days and 9.3 Hours

Praveen Reddy Elmati, Department of Anesthesiology, Saint Clair Hospital, Dover, NJ 07801, United States

Gowthami Sai Kogilathota Jagirdhar, Department of Medicine, Saint Michaels Medical Center, Newark, NJ 07107, United States

Salim Surani, Department of Medicine and Pharmacology, Texas A&M University, College Station, TX 77843, United States

Corresponding author: Salim Surani, FACP, FCCP, MD, MHSc, Adjunct Professor, Department of Medicine and Pharmacology, Texas A&M University, 40 Bizzell Street, College Station, TX 77843, United States. srsurani@hotmail.com

Abstract

This editorial aimed to consolidate the current evidence in literature on the association between myasthenia gravis (MG) and cardiac involvement, focusing on the impact of thymoma, antistriational antibodies, and late-onset MG. Additionally, the study aimed to explore the influence of genetic differences among populations on the association with cardiac disease. We conducted a review of existing literature in PubMed and Google Scholar to find relevant studies on cardiac involvement in MG. We created search criteria using a combination of free text words, including MG, antistriational antibodies, thymectomy, cardiomyopathy, myocarditis, arrhythmias, autonomic dysfunction. Relevant articles published in English language were analyzed and incorporated. The findings indicate a strong association between thymoma, myasthenic crisis, antistriational antibodies, and late-onset MG with cardiac involvement. The study also revealed that genetic differences among populations influence the risk of cardiac disease and electrocardiography (ECG) abnormalities in MG patients. Autonomic dysfunctions altered cardiac autonomic response and increased susceptibility to arrhythmias and sudden cardiac death in MG patients. The study supports the significance of thymoma, antistriational antibodies, and late-onset MG as key factors associated with cardiac involvement in MG patients. It emphasizes the importance of ECG as the initial test in managing MG patients, particularly in the perioperative period, to identify and genetic testing if needed to address their cardiac risk effectively.

Key Words: Myasthenia gravis; Antistriational antibodies; Thymectomy; Cardiomyopathy; Myocarditis; Arrhythmias; Autonomic dysfunction

Core Tip: Preoperative cardiac screening is crucial for patients with myasthenia gravis (MG), especially those with thymoma, late-onset MG, or antistriational antibodies. Understanding the link between MG and cardiac conditions such as cardiomyopathy, myocarditis, takotsubo cardiomyopathy, autonomic dysfunction, and arrhythmias is essential for perioperative surgical management. Electrocardiography and Troponin T can be important initial screening tests in patients with high risk suspicion. Comprehensive screening protocols are necessary to mitigate cardiac risks and optimize outcomes in MG patients undergoing surgery.

Citation: Elmati PR, Jagirdhar GSK, Surani S. Cardiac implications in myasthenia gravis. *World J Clin Cases* 2024; 12(26): 5863-5867
URL: https://www.wjgnet.com/2307-8960/full/v12/i26/5863.htm
DOI: https://dx.doi.org/10.12998/wjcc.v12.i26.5863

INTRODUCTION

Myasthenia gravis (MG) is a disorder that affects the skeletal and cardiac muscles. Patients have autoantibodies against the Acetylcholine receptor, muscle-specific tyrosine kinase, and low-density lipoprotein receptor-related protein four. Based on the literature, the incidence of MG is 4.1 to 30 per 100000, and prevalence is 150-to 200 per 100000[1]. The exact cardiac prevalence of MG is unknown in current literature. In the presence of thymoma the prevalence can range from 10%-15%[2]. Patients post thymectomy had decreased cardiac involvement[3]. Perioperative considerations in MG patients are related to cardiorespiratory manifestations and myasthenic crisis. MG patients can also have antistriational autoantibodies, including anti-titin, ryanodine receptor, anti-muscular voltage-gated potassium channel (Kv1.4), and myositis-specific antibodies. Antistriational exists because of their binding in a cross-striation pattern to skeletal and heart muscle tissue sections.

Romi *et al*[4] in their study of Caucasian patients with MG, found that patients with anti Kv1.4 antibodies had late onset and mild MG, which is in contrast to Japanese patients with similar antibodies who had severe MG symptoms, including thymoma, myasthenic crisis, myocarditis, and QT prolongation[4-6]. This could be due to other contributing factors, including genetic differences in this population, and thus, disease severity may not be related to anti-Kv1.4 antibodies alone. Perioperative cardiac testing in MG patients ensures the identification of cardiac issues that can be effectively managed in the operative period. In this editorial, we discuss Nag *et al*[7] manuscript on perioperative cardiac risks in MG patients.

INCREASED CARDIAC RISK IN MG PATIENTS

Heart and skeletal muscle are proposed autoimmune targets for MG patients. Evidence in the literature reports the association of antistriational autoantibodies with cardiac manifestations. Anti-titin antibodies have also been reported to be associated with thymoma-associated MG[8,9]. The clarity regarding the frequency and intensity of the association remains uncertain. Nag *et al*[7] do not provide information on cardiac screening tests in MG patients and algorithms for screening considerations. Patients with myasthenic crisis and underlying cardiac disease, including hypertensive cardiomyopathy, atrial fibrillation, and ischemic heart disease, had an increased risk of non-invasive ventilation failure on attempting weaning from mechanical ventilation[10]. In a study by Kato *et al*[11] on MG patients, the authors found electrocardiography (ECG) as the best initial step for screening MG to assess patients for cardiac risk. Common ECG abnormalities observed were persistent atrial fibrillation, atrioventricular block, ST segment depression and negative T waves, early repolarization, left ventricular hypertrophy, and prolonged QTc interval[11,12]. Echocardiography should be considered as the next step if abnormalities are noted in ECG or in patients presenting with heart failure, arrhythmias, or signs of myocarditis[11]. Kato *et al*[11] and Tsugawa *et al*[12] described that around 56%-62% have ECG abnormalities in MG patients, particularly those not on immunosuppressant therapy. In a study by Furlund Owe *et al*[13] on MG patients compared to healthy controls on echocardiography, left ventricular systolic and diastolic function did not differ between the groups. This further strengthens the recommendation to consider ECG as the screening step to identify cardiac involvement in MG patients. For symptomatic patients with dyspnea, chest pain, and ECG changes or ECHO abnormalities, troponin levels can also be considered. Elevated cardiac troponins also mean that the patients' MG is not well controlled, and treatment with immunosuppressive therapy is required[14]. The cardiopulmonary function can be tested using the 6-minute walk distance in MG patients with poor functional status since low walk distance was associated with longer hospital stays after thymectomy[15,16].

CARDIOMYOPATHY, MYOCARDITIS IN MG

MG has been associated with dilated cardiomyopathy (DCM) based on prior studies by Zhou *et al*[17] on genetic analysis. The authors state midline 1 interacting protein 1 and PI3K-interacting protein 1 in MG-associated DCM[17]. Myocarditis,

thymoma, and late-onset MG were associated with antistriational antibodies on a flow cytometry analysis of patient samples over 13 years in a study by Kufukihara *et al*[18]. All myocarditis patients had at least one of these autoantibodies, and 70% had thymoma. Suzuki *et al*[6] report that out of 924 patients with MG, three patients developed myocarditis and seven patients had at least one Antistriational antibody positive, and four had thymoma. Nag *et al*[7] state also state that the presence of thymoma increases the risk of cardiac complications in MG patients to 10%-15% based on current literature. In a study of 247 patients with MG, the presence of anti-titin antibodies was associated with myocarditis in 17 of 25 patients. The authors also reported that anti-titin antibodies and Myasthenic crisis were associated with myocarditis, but no association was found with thymoma[19]. Thus, there is strong literature on the association of antistriational antibodies in association with myocarditis. However, the association of thymoma with myocarditis is still conflicted. Cheng *et al*[20] in their systematic review on myocarditis in MG patients state dyspnea as the commonest presentation and reports a 50% hospital mortality rate in these patients.

Chen *et al*[21] on their retrospective study of hospitalized patients with MG found increasing age, presence of infection, immune checkpoint inhibitors therapy and ongoing myasthenic crisis, and thymoma were associated with elevated troponin T levels (> 14 ng/L). High troponins, female sex, thymoma and infection were a predictor of death in hospitalization. This measuring biomarkers in hospitalized patients with MG may be beneficial. Patients with autoimmune disease, particularly MG, are at increased risk for Takutsubo cardiomyopathy (TCM) based on multiple pieces of evidence in the literature and are often mistaken for acute coronary syndrome. Farjoud Kouhanjani *et al*[22] describe 18.8% of patients with autoimmune disease had TCM. The EKG findings in TCM commonly include normal EKG, T wave inversions, ST segment elevations, prolongation of the QT interval, and transient q waves. Nag *et al*[7] describe TCM in MG, particularly those with myasthenic crisis. Rathish and Karalliyadda[23] performed a systematic review of TCM in MG patients and found that all patients were in myasthenic crisis at presentation. They also document that half the patients had no prior diagnosis of MG prior to presentation.

CARDIAC ARRHYTHMIAS IN MG

Nag *et al*[7] describe arrhythmia, sick sinus syndrome, and heart block in MG patients. Gandhi *et al*[3] in their retrospective study on MG for 10 years found the prevalence of cardiac arrhythmias to be around 17%. The authors also state patients with thymectomy had less cardiac involvement suggesting that thymoma was associated with higher cardiac risk [3]. Evidence in the literature also reports MG patients with severe bradycardia with positive anti-striation antibodies, anti-muscular voltage-gated potassium channel-complex (Kv1.4) antibodies, and anti-titin antibodies[24].

Multiple pieces of evidence in the literature report atrial fibrillation in myasthenic crisis patients. These patients often had acetylcholinesterase receptor antibody positive[25].

The authors fail to mention in detail the autonomic functions that are altered in MG patients, including cardiac autonomic response, sympathetic and parasympathetic dysfunction, particularly during periods of hemodynamic instability, lower sensitivity of baroreflexes, and higher sympathetic and vagal balance at rest, and orthostatic alterations[26-28]. These authors found abnormalities in cardiovascular reflux testing; heart rate variability was assessed using a 20-minute ECG recording, 24-hour ECG monitoring, Valsalva maneuver, and orthostasis. These autonomic dysfunctions can predispose patients with MG to develop arrhythmias and sudden cardiac death[28,29]. Arrhythmic episodes are often noted during periods of stress and surgery, including thymectomy[30].

FUTURE RECOMMENDATIONS

Future studies should focus on antibody and genetic testing in MG patients to apply precision medicine in managing patients in the perioperative period and in assessing their cumulative cardiac risk. The is an increased need for more pathological testing to confirm the cardiac risks associated with MG. This will provide a clear direction for future research and aid in early diagnosis of cardiac involvement.

CONCLUSION

We agree with the authors Nag *et al*[7] that thymoma, antistriational antibodies, and late onset MG are associated with cardiac involvement. Genetic differences and thymoma among populations also tend to influence the association with cardiac disease, ECG abnormalities and troponin T levels. The presence of thymoma, myasthenic crisis, and antistriational antibodies appears to have a stronger risk for cardiac involvement. ECG serves as the best initial step to screen MG patients in the perioperative period. Including Troponin T for hospitalized patients undergoing surgery may be beneficial to detect cardiac injury.

FOOTNOTES

Author contributions: Elmati PR designed the overall concept and outline of the manuscript; Elmati PR and Kogilathota Jagirdhar GS performed the research and literature review; Elmati PR, Kogilathota Jagirdhar GS, and Surani S analyzed the studies and wrote the

manuscript; All authors have read and approved the final manuscript.

Conflict-of-interest statement: None of the authors have any conflict of interest to disclose.

Country of origin: United States

ORCID number: Praveen Reddy Elmati 0000-0003-1283-2368; Gowthami Sai Kogilathota Jagirdhar 0000-0003-1855-0863; Salim Surani 0000-0001-7105-4266.

Corresponding Author's Membership in Professional Societies: American College of Chest Physician.

S-Editor: Gao CC
L-Editor: A
P-Editor: Zhao YQ

REFERENCES

1 **Dresser L**, Wlodarski R, Rezania K, Soliven B. Myasthenia Gravis: Epidemiology, Pathophysiology and Clinical Manifestations. *J Clin Med* 2021; **10** [PMID: 34064035 DOI: 10.3390/jcm10112235]
2 **Shivamurthy P**, Parker MW. Cardiac manifestations of myasthenia gravis: A systematic review. *IJC Metabolic & Endocrine* 2014; **5**: 3-6 [DOI: 10.1016/j.ijcme.2014.08.003]
3 **Gandhi R**, Boddepalli R, Govindarajan R, Salgado E. Prevalence of Cardiac Arrhythmia in Myasthenia Gravis (P7.057). *Neurology* 2015; **84** [DOI: 10.1212/wnl.84.14_supplement.p7.057]
4 **Romi F**, Suzuki S, Suzuki N, Petzold A, Plant GT, Gilhus NE. Anti-voltage-gated potassium channel Kv1.4 antibodies in myasthenia gravis. *J Neurol* 2012; **259**: 1312-1316 [PMID: 22167224 DOI: 10.1007/s00415-011-6344-y]
5 **Suzuki S**, Satoh T, Yasuoka H, Hamaguchi Y, Tanaka K, Kawakami Y, Suzuki N, Kuwana M. Novel autoantibodies to a voltage-gated potassium channel Kv1.4 in a severe form of myasthenia gravis. *J Neuroimmunol* 2005; **170**: 141-149 [PMID: 16182377 DOI: 10.1016/j.jneuroim.2005.08.017]
6 **Suzuki S**, Utsugisawa K, Nagane Y, Satoh T, Terayama Y, Suzuki N, Kuwana M. Classification of myasthenia gravis based on autoantibody status. *Arch Neurol* 2007; **64**: 1121-1124 [PMID: 17698702 DOI: 10.1001/archneur.64.8.1121]
7 **Nag DS**, Chatterjee A, Mahanty PR, Sam M, Bharadwaj MK. Perioperative cardiac risks in myasthenia gravis. *World J Clin Cases* 2024; **12**: 2147-2150 [PMID: 38808348 DOI: 10.12998/wjcc.v12.i13.2147]
8 **Moura J**, Sousa AP, Samões R, Carneiro P, Neves E, Silva AM, Santos E. Anti-titin antibodies in a cohort of myasthenia gravis patients. *J Thorac Dis* 2024; **16**: 973-978 [PMID: 38505076 DOI: 10.21037/jtd-23-94]
9 **Suzuki S**, Utsugisawa K, Nagane Y, Suzuki N. Three types of striational antibodies in myasthenia gravis. *Autoimmune Dis* 2011; **2011**: 740583 [PMID: 21785709 DOI: 10.4061/2011/740583]
10 **Iori E**, Ariatti A, Mazzoli M, Bastia E, Gozzi M, Agnoletto V, Marchioni A, Galassi G. Cardiac disorders worsen the final outcome in myasthenic crisis undergoing non-invasive mechanical ventilation: a retrospective 20-year study from a single center. *Acta Myol* 2022; **41**: 15-23 [PMID: 35465341 DOI: 10.36185/2532-1900-064]
11 **Kato T**, Hirose S, Kumagai S, Ozaki A, Matsumoto S, Inoko M. Electrocardiography as the First Step for the Further Examination of Cardiac Involvement in Myasthenia Gravis. *Biomed Res Int* 2016; **2016**: 8058946 [PMID: 26885517 DOI: 10.1155/2016/8058946]
12 **Tsugawa J**, Ogura H, Mera H, Fukae J, Tsuboi Y. Analyzing clinical characteristics of patients with myasthenia gravis through repetitive nerve stimulation testing. *Neurology & Clinical Neurosc* 2019; **7**: 71-74 [DOI: 10.1111/ncn3.12270]
13 **Furlund Owe J**, Skulstad Davidsen E, Eide GE, Gerdts E, Gilhus NE. Left ventricular long-axis function in myasthenia gravis. *J Neurol* 2008; **255**: 1777-1784 [PMID: 19156489 DOI: 10.1007/s00415-008-0049-x]
14 **Kumagai S**, Kato T, Ozaki A, Hirose S, Minamino E, Kimura Y, Nakane E, Miyamoto S, Izumi T, Haruna T, Nohara R, Inoko M. Serial measurements of cardiac troponin I in patients with myasthenia gravis-related cardiomyopathy. *Int J Cardiol* 2013; **168**: e79-e80 [PMID: 23886525 DOI: 10.1016/j.ijcard.2013.07.046]
15 **Hayashi K**, Fukumoto K, Yokoi K, Nagaya M, Inoue T, Ito S, Nakajima H, Hattori K, Kadono I, Nishida Y. Post-operative delayed ambulation after thymectomy is associated withpre-operative six-minute walk distance. *Disabil Rehabil* 2018; **40**: 1900-1905 [PMID: 28415886 DOI: 10.1080/09638288.2017.1315182]
16 **Cata JP**, Lasala JD, Williams W, Mena GE. Myasthenia Gravis and Thymoma Surgery: A Clinical Update for the Cardiothoracic Anesthesiologist. *J Cardiothorac Vasc Anesth* 2019; **33**: 2537-2545 [PMID: 30219643 DOI: 10.1053/j.jvca.2018.07.036]
17 **Zhou G**, Wang S, Lin L, Lu K, Lin Z, Zhang Z, Zhang Y, Cheng D, Szeto K, Peng R, Luo C. Screening for immune-related biomarkers associated with myasthenia gravis and dilated cardiomyopathy based on bioinformatics analysis and machine learning. *Heliyon* 2024; **10**: e28446 [PMID: 38571624 DOI: 10.1016/j.heliyon.2024.e28446]
18 **Kufukihara K**, Watanabe Y, Inagaki T, Takamatsu K, Nakane S, Nakahara J, Ando Y, Suzuki S. Cytometric cell-based assays for anti-striational antibodies in myasthenia gravis with myositis and/or myocarditis. *Sci Rep* 2019; **9**: 5284 [PMID: 30918333 DOI: 10.1038/s41598-019-41730-z]
19 **Kim KH**, Kim SW, Cho J, Chung HY, Shin HY. Anti-titin antibody is associated with more frequent hospitalization to manage thymoma-associated myasthenia gravis. *Front Neurol* 2022; **13**: 978997 [PMID: 36277908 DOI: 10.3389/fneur.2022.978997]

20 **Cheng W**, Sun T, Liu C, Zhou Z, Duan J, Zhao Y, Yang M, Chen P. A systematic review of myasthenia gravis complicated with myocarditis. *Brain Behav* 2021; **11**: e2242 [PMID: 34105901 DOI: 10.1002/brb3.2242]

21 **Chen H**, Kong L, Zhang Y, Lin X, Shi Z, Du Q, Wang X, Lang Y, Cai L, Mou Z, Luo W, Li S, Zhou H. Myocardial Injury in Hospitalized Patients with Myasthenia Gravis. *J Clin Med* 2022; **11** [PMID: 36498680 DOI: 10.3390/jcm11237106]

22 **Farjoud Kouhanjani M**, Hosseini SA, Mousavi SM, Noroozi Z, Sadeghi P, Jokar-Derisi A, Jamshidi Mouselou MS, Ahmadi M, Attar A. Takotsubo Cardiomyopathy and Autoimmune Disorders: A Systematic Scoping Review of Published Cases. *Int J Clin Pract* 2024; **2024**: 7259200 [PMID: 38414580 DOI: 10.1155/2024/7259200]

23 **Rathish D**, Karalliyadda M. Takotsubo syndrome in patients with myasthenia gravis: a systematic review of previously reported cases. *BMC Neurol* 2019; **19**: 281 [PMID: 31718587 DOI: 10.1186/s12883-019-1523-z]

24 **Fujita R**, Matoba S, Morihata H, Inoue M. [Anti-striational antibodies detected in a patient with late-onset myasthenia gravis suffering from severe bradycardia: a case report]. *Rinsho Shinkeigaku* 2021; **61**: 543-546 [PMID: 34275952 DOI: 10.5692/clinicalneurol.cn-001592]

25 **Jacobs DH**. Myasthenia Gravis Crisis and Atrial Fibrillation. *Neurologist* 2020; **25**: 1-3 [PMID: 31876650 DOI: 10.1097/NRL.0000000000000246]

26 **Zawadka-Kunikowska M**, Rzepiński Ł, Tafil-Klawe M, Veronese N, Barbagallo M, Habek M, Gilhus NE. Altered Cardiac Autonomic Regulation in Individuals with Myasthenia Gravis-A Systematic Review and Meta-Analysis. *Neurol Int* 2023; **15**: 1140-1154 [PMID: 37755362 DOI: 10.3390/neurolint15030071]

27 **Elsais A**, Kerty E, Russell K, Toska K. Does cardiovascular autonomic dysfunction contribute to fatigue in myasthenia gravis? *Physiol Res* 2022; **71**: 79-91 [PMID: 35043646 DOI: 10.33549/physiolres.934660]

28 **Nikolić A**, Perić S, Nišić T, Popović S, Ilić M, Stojanović VR, Lavrnić D. The presence of dysautonomia in different subgroups of myasthenia gravis patients. *J Neurol* 2014; **261**: 2119-2127 [PMID: 25119843 DOI: 10.1007/s00415-014-7465-x]

29 **Peric S**, Rakocevic-Stojanovic V, Nisic T, Pavlovic S, Basta I, Popovic S, Damjanovic S, Lavrnic D. Cardiac autonomic control in patients with myasthenia gravis and thymoma. *J Neurol Sci* 2011; **307**: 30-33 [PMID: 21658726 DOI: 10.1016/j.jns.2011.05.028]

30 **Pandey R**, Garg R, Chandralekha, Darlong V, Punj J, Sinha R, Jyoti B, Mukundan C, Elakkumanan LB. Robot-assisted thoracoscopic thymectomy: perianaesthetic concerns. *Eur J Anaesthesiol* 2010; **27**: 473-477 [PMID: 20216070 DOI: 10.1097/EJA.0b013e3283309cea]

World Journal of Clinical Cases

Submit a Manuscript: https://www.f6publishing.com

World J Clin Cases 2024 September 16; 12(26): 5868-5876

DOI: 10.12998/wjcc.v12.i26.5868

ISSN 2307-8960 (online)

ORIGINAL ARTICLE

Case Control Study

Multivariate analysis of oral mucosal ulcers during orthodontic treatment

Jing Chang, Xue Li

Specialty type: Dentistry, oral surgery and medicine

Provenance and peer review: Unsolicited article; Externally peer reviewed.

Peer-review model: Single blind

Peer-review report's classification

Scientific Quality: Grade D

Novelty: Grade C

Creativity or Innovation: Grade C

Scientific Significance: Grade B

P-Reviewer: Camacho AID, Mexico

Received: March 11, 2024

Revised: May 6, 2024

Accepted: May 24, 2024

Published online: September 16, 2024

Processing time: 133 Days and 23 Hours

Jing Chang, Xue Li, The Fifth Clinic, Peking University School and Hospital of Stomatology, National Center for Stomatology, National Clinical Research Center for Oral Diseases, National Engineering Research Center of Oral Biomaterials and Digital Medical Devices Beijing 100081, China

Corresponding author: Xue Li, PhD, Doctor, The Fifth Clinic, Peking University School and Hospital of Stomatology, National Center for Stomatology, National Clinical Research Center for Oral Diseases, National Engineering Research Center of Oral Biomaterials and Digital Medical Devices, No. 22 Zhongguancun South Street, Beijing 100081, China.
lixue4337@126.com

Abstract

BACKGROUND

Orthodontic treatment can easily cause local soft tissue reactions in the oral cavity of patients under mechanical stress, leading to oral mucosal ulcers and affecting their quality of life. At present, only limited literature has explored the factors leading to oral ulcers in orthodontic treatment, and these research results are still controversial.

AIM

To investigate the current status and related factors of oral mucosal ulcers during orthodontic treatment, aiming to provide a valuable reference for preventing this disease in clinical practice.

METHODS

A total of 587 patients who underwent orthodontic treatment at the Peking University School of Stomatology and Hospital of Stomatology between 2020 and 2022 were selected and allocated to an observation or control group according to the incidence of oral mucosal ulcers during orthodontic therapy. A questionnaire survey was constructed to collect patient data, including basic information, lifestyle and eating habits, treatment details, mental factors, and trace element levels, and a comparative analysis of this data was performed between the two groups.

RESULTS

A logistic regression model with oral ulcers as the dependent variable was established. The regression results showed that age (≥ 60 years: odds ratio [OR]: 6.820; 95% confidence interval [CI]: 2.226–20.893), smoking history (smoking: OR: 4.434;

95%CI: 2.527–7.782), toothbrush hardness (hard: OR: 2.804; 95%CI: 1.746–4.505), dietary temperature (hot diet: OR: 1.399; 95%CI: 1.220–1.722), treatment course (> 1 year: OR: 3.830; 95%CI: 2.203–6.659), and tooth brushing frequency (> 1 time per day: OR: 0.228; 95%CI: 0.138–0.377) were independent factors for oral mucosal ulcers (P < 0.05). Furthermore, Zn level (OR: 0.945; 95%CI: 0.927–0.964) was a protective factor against oral ulcers, while the SAS (OR: 1.284; 95%CI: 1.197–1.378) and SDS (OR: 1.322; 95%CI: 1.231–1.419) scores were risk factors.

CONCLUSION

Age ≥ 60 years, smoking history, hard toothbrush, hot diet, treatment course for > 1 year, tooth brushing frequency of ≤ 1 time per day, and mental anxiety are independent risk factors for oral mucosal ulcers. Therefore, these factors should receive clinical attention and be incorporated into the development and optimization of preventive strategies for reducing oral ulcer incidence.

Key Words: Orthodontic treatment; Oral ulcers; Multivariate; Logistic regression; Prevent disease

Core Tip: Currently, there is limited literature exploring the factors leading to oral ulcers during orthodontic treatment, with considerable controversy. Therefore, this study uses retrospective data to explore and analyze the current situation and related factors of oral mucosal ulcers during orthodontic treatment in our hospital, providing a reference for the clinical prevention of this disease.

Citation: Chang J, Li X. Multivariate analysis of oral mucosal ulcers during orthodontic treatment. *World J Clin Cases* 2024; 12(26): 5868-5876
URL: https://www.wjgnet.com/2307-8960/full/v12/i26/5868.htm
DOI: https://dx.doi.org/10.12998/wjcc.v12.i26.5868

INTRODUCTION

Orthodontic treatment traditionally refers to the correction of teeth and the removal of malocclusion and deformed teeth, with the diagnosis and treatment procedures primarily involving determining the etiology and mechanism of the malocclusion to achieve an aesthetic modification of the affected teeth. Although this treatment can effectively ameliorate dental and skeletal problems, utilizing orthodontic appliances to adjust the coordination between facial bones, teeth, nerves, and muscles in the maxillofacial region can easily cause the reaction of the local soft tissues in the patient's oral cavity following mechanical stress and ultimately result in the accumulation of oral bacteria[1]. In the initial treatment stage, oral mucosal ulcers can sometimes occur due to the contact of the mucosa with orthodontic brackets[2-4]. Oral mucosal ulcers are a prevalent adverse reaction in patients undergoing orthodontic treatment, often presenting on the surface of the mouth and tongue margin and triggering a burning sensation and pain (Figure 1). Thus, the speech and diet of the patients are affected to a certain degree by these ulcers, which generally heal spontaneously within 1–2 week. However, oral mucosal ulcers tend to occur as repeated attacks, with some patients experiencing multiple infections over a short period that affect their quality of life. Currently, only limited literature has explored the factors leading to oral ulcers during orthodontic treatment, and those study results remain debated. Therefore, this study utilized retrospective data to investigate the current status and factors linked to oral mucosal ulcers during orthodontic treatment in our hospital, aiming to provide a reliable reference for improving the clinical prevention of this disease.

MATERIALS AND METHODS

A total of 587 patients who underwent orthodontic treatment at the Peking University School and Hospital of Stomatology between January 2020 and January 2022 were enrolled and assigned to an observation or control group according to the incidence of oral mucosal ulcers during orthodontic treatment. The relevant data of the patients in the two groups were obtained using a pre-designed questionnaire survey.

Inclusion criteria

The patients were included if they met the following criteria: (1) Underwent orthodontics in our hospital; (2) Age of ≥ 18 years; and (3) No history of other dental diseases or abnormal dental morphology.

Exclusion criteria

The patients were excluded if they met any of the following criteria: (1) Severe systemic diseases (hypertension, diabetes, or cardiovascular diseases); (2) Communication difficulties that hindered the ability to independently complete the

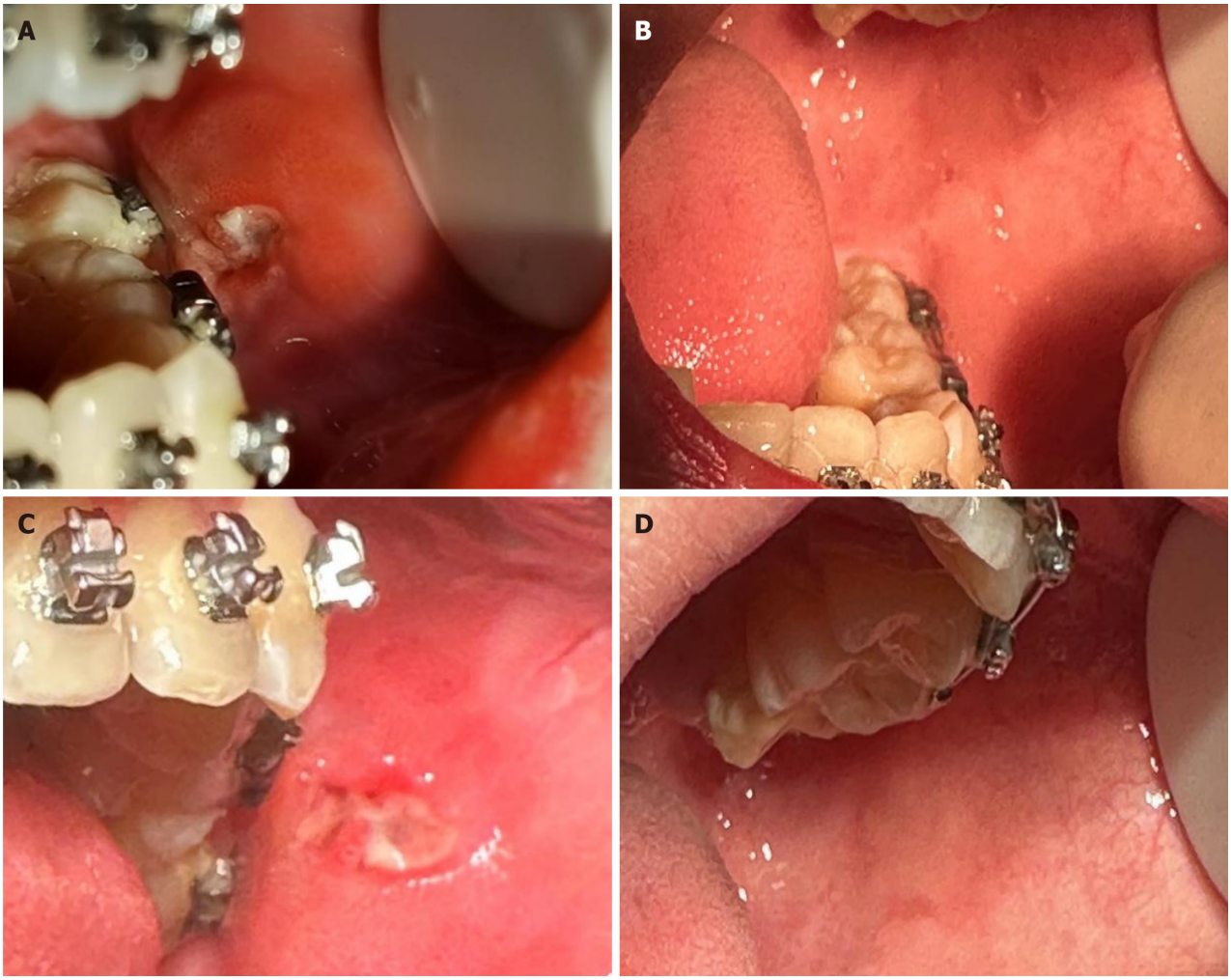

Figure 1 Schematic diagram of oral ulcers. A: Tongue mucosa; B and C: Oral-retropharyngeal approach; D: Gingiva.

questionnaire; (3) Mental health disorders; or (4) Pregnant or breast-feeding women or other patients deemed not suitable to participate in this research.

All enrolled patients were informed of the research purpose, and signed informed consent was obtained from each patient.

Data collection

A unified questionnaire was administered to the included patients *via* telephone interviews to collect the following information: basic information (age, sex, and smoking and drinking history), lifestyle and eating habits (tooth brushing frequency, toothbrush hardness, dietary preference for meat, and dietary temperature), treatment details (treatment course, tooth position, disease type, and orthodontic appliance type), mental factors (anxiety and depression), and trace element levels (zinc, copper, and iron concentrations). Oral mucosal ulcers refer to persistent defects or destruction of the oral epithelium integrity, accompanied by surface necrosis and detachment that result in the formation of a depression. These ulcers can be classified as primary (recurrent aphthous ulcers) and secondary ulcers. The diagnostic criteria for oral mucosal ulcers were according to the criteria specified in the *Diseases of Oral Mucosa*, 4th edition, People's Medical Publishing House[5]. Additionally, the recurrence of the symptoms in the patients with oral ulcers was recorded. Recurrence was defined as an increase in the area and number of ulcers (*i.e.* > 1 attack per month) that recurred 3 months following successful treatment.

The study data were entered by trained professionals using EpiData3.1 software *via* double entry of the collected data and verification of consistency. Finally, the data were logically reviewed and quality-controlled to ensure authenticity, accuracy, and reliability.

Research methods

Detection of trace elements: After obtaining consent from the patients, 20 μL of peripheral blood was collected from each patient by the senior chief doctor of our hospital. Subsequently, the quantitative measurement of the trace elements, such as zinc, copper, and iron, in the blood samples was conducted utilizing an atomic absorption spectrometer. Quantitative analysis of the trace elements by an atomic absorption spectrometer is based on the principle of light radiation absorption by gaseous atoms, with the wavelength of absorbed light corresponding to the specific emission spectrum of the stimu-

lated atom. Based on this concept, the concentration of trace elements in patient serum was quantitatively determined according to the intensity of the absorbed radiation.

Anxiety and depression scores: The Self-Rating Anxiety Scale (SAS) and Self-Rating Depression Scale (SDS) were used to assess the anxiety and depression levels of the patients. The two scales comprise 20 items each, and both scales have a 1–4 scoring system for rating the respondents' feelings during the most recent week. The cumulative scores of each item are weighted to obtain the total SAS or SDS scores, with higher total scores suggesting greater levels of anxiety or depression, respectively. The current cut-off value for the standard deviation is 50 points, with scores of 50–59, 60–69, and > 69 indicating mild, moderate, and severe anxiety/depression, respectively.

Statistical analyses

All data were analyzed using SPSS 22.0 statistical software. Measurement data were expressed as mean ± standard deviation or median (interquartile range), while count data were presented as numbers (percentage). Furthermore, the measurement data were tested for normality. Normally distributed data were compared between groups *via* *t*-test, whereas the Wilcoxon rank sum test was employed for non-normally distributed data. Intergroup comparisons of count data were performed utilizing the χ^2 test. After conducting a univariate analysis with oral ulcer occurrence (with/without) as the dependent variable, variables with $P < 0.1$ were selected for subsequent modeling. A binary logistic regression model was then used to identify the independent risk factors for oral ulcers. Similarly, a binary logistic regression model with recurrence as a dependent variable was applied to detect the independent risk factors for oral ulcer recurrence.

The test level was set at $\alpha = 0.05$ (two-tailed test), and $P < 0.05$ was considered statistically significant.

RESULTS

General patient information

As demonstrated in Table 1, the basic data of all 587 patients were analyzed after grouping them based on the incidence and recurrence of oral ulcers. Patients with oral ulcers had a mean age of 52.53 ± 11.10 years, and those without oral ulcers exhibited a mean age of 52.98 ± 11.94 years, with no significant difference in age between these two groups ($P > 0.05$). Among the patients who developed oral ulcers, 153 (26.06%) presented with recurrent symptoms. Except for drinking history, disease type, tooth position, and orthodontic appliance type, all other factors were significantly different between the two groups. Therefore, these factors were included in the models constructed for further comparison analyses.

Multivariate analysis of factors associated with oral ulcers

Variables were assigned values as outlined in Table 2, and the independent variables with significant differences ($P < 0.1$) were included in the univariate analysis to establish the model with oral ulcers as the dependent variable. Age (60 years: odds ratio [OR]: 6.820; 95% confidence interval [CI]: 2.226–20.893), smoking history (smoking: OR: 4.434; 95%CI: 2.527–7.782), toothbrush hardness (hard: OR: 2.804; 95%CI: 1.746–4.505), dietary temperature (hot diet: OR: 1.399; 95%CI: 1.220–1.722), treatment course (> 1 year, OR: 3.830; 95%CI: 2.203–6.659), and tooth brushing frequency (> 1 time per day: OR: 0.228; 95%CI: 0.138–0.377) were found to be independent factors for oral mucosal ulcers ($P < 0.05$). Furthermore, the level of the trace element Zn (OR: 0.945; 95%CI: 0.927–0.964) was a protective factor against oral ulcers, while the SAS (OR: 1.284; 95%CI: 1.197–1.378) and SDS (OR: 1.322; 95%CI: 1.231–1.419) scores were demonstrated to be risk factors. Table 3 provides the complete details of the analysis.

Multivariate analysis of factors associated with recurrent oral ulcers

We further analyzed the recurrence of oral ulcers by modeling, with disease recurrence as the dependent variable and independent variables such as smoking history and tooth brushing frequency. The results showed that smoking history (smoking: OR: 3.588; 95%CI: 1.829–7.040), disease type (dentofacial deformity: OR: 0.396; 95%CI: 0.199–0.786), toothbrush hardness (hard: OR: 7.905; 95%CI: 4.044–15.451), dietary habits (non-dietary preference for meat: OR: 0.517; 95%CI: 0.263–0.984), disease location (anterior tooth region: OR: 2.319; 95%CI: 1.206–4.462), and tooth brushing frequency (≤ 1 time per day, OR: 2.894; 95%CI: 1.452–5.770) were independent factors for oral ulcer recurrence ($P < 0.05$). See Table 4 for further details.

DISCUSSION

Current status of oral ulcers during orthodontic treatment

In recent years, the proportion of people paying attention to the beauty and alignment of their teeth has been increasing due to the expanding and evolving social relationships and aesthetic needs[6]. Related research has shown that the number of individuals receiving orthodontic treatment in China has been growing at present, with an emerging trend in the younger population[7,8]. Although orthodontic treatment provides a good diagnostic effect and can improve facial beauty, it can also lead to numerous complications, such as enamel demineralization and oral mucosal ulcers, owing to the use of external appliances. Oral ulcers usually present within 2 week after commencing orthodontic treatment. At the

Table 1 Comparison of the general data of the patients grouped according to the presence and recurrence of oral ulcers

Categories	Indicators	Oral ulcer group, *n* = 297	Non-oral ulcer group, *n* = 290	*P* value	Recurrence group, *n* = 144	Non-recurrence group, *n* = 153	*P* value
Sex	Male	113 (38.05)	236 (81.38)	< 0.001	51 (35.42)	62 (40.52)	0.365
	Female	184 (61.95)	54 (18.62)		93 (64.58)	91 (59.48)	
Smoking	No	178 (59.93)	258 (88.9)	< 0.001	93 (64.58)	85 (55.56)	0.113
	Yes	119 (40.07)	32 (11.03)		51 (35.42)	68 (44.44)	
Drinking history	No	97 (32.66)	109 (37.59)	0.211	44 (30.56)	53 (34.64)	0.453
	Yes	200 (67.34)	181 (62.41)		100 (69.44)	100 (65.36)	
Disease type	Dental caries	152 (51.18)	149 (51.38)	0.484	69 (47.92)	83 (54.25)	0.253
	Dentofacial deformity	72 (24.24)	60 (20.69)		41 (28.47)	31 (20.26)	
	Periodontal disease	73 (24.58)	81 (27.93)		34 (23.61)	39 (25.49)	
Toothbrush hardness	Soft	151 (50.84)	199 (68.62)	< 0.001	95 (65.97)	56 (36.60)	< 0.001
	Hard	146 (49.16)	91 (31.38)		49 (34.03)	97 (63.40)	
Dietary preference for meat	No	218 (73.40)	243 (83.79)	0.002	108 (75.00)	110 (71.90)	0.545
	Yes	79 (26.60)	47 (16.21)		36 (25.00)	43 (28.10)	
Dietary temperature	Warm	76 (25.59)	105 (36.21)	0.005	39 (27.08)	37 (24.18)	0.567
	Hot	221 (74.41)	185 (63.79)		105 (72.92)	116 (75.82)	
Treatment course	≤ 1 year	84 (28.28)	157 (54.14)	< 0.001	47 (32.64)	37 (24.18)	0.106
	> 1 year	213 (71.72)	133 (45.86)		97 (67.36)	116 (75.82)	
Tooth position	Non-anterior tooth region	158 (53.20)	136 (46.90)	0.127	89 (61.81)	69 (45.10)	0.004
	Anterior tooth region	139 (46.80)	154 (53.10)		55 (38.19)	84 (54.90)	
Orthodontic appliance type	Straight-wire bracket	138 (46.46)	120 (41.38)	0.215	67 (46.53)	71 (46.41)	0.983
	Conventional straight wire	159 (53.54)	170 (58.62)		77 (53.47)	82 (53.59)	
Age	< 60 years	179 (60.27%)	226 (77.93%)	< 0.001	95 (65.97)	84 (54.90)	0.051
	≥ 60 years	118 (39.73%)	64 (22.07%)		49 (34.03)	69 (45.10)	
SAS score		44.66 (5.58)	37.31 (5.54)	< 0.001	44.69 (5.67)	44.64 (5.51)	0.940
SDS score		47.04 (7.51)	37.16 (5.15)	< 0.001	47.13 (7.12)	46.96 (7.88)	0.849
Zn		97.95 (20.53)	127.88 (26.83)	< 0.001	98.91 (21.36)	97.05 (19.74)	0.434
Cu		17.04 (6.40)	17.70 (6.03)	0.201	17.15 (6.48)	16.93 (6.35)	0.773
Fe		9.14 (1.50)	9.31 (1.52)	0.158	9.16 (1.49)	9.12 (1.51)	0.830

SAS: Self-Rating Anxiety Scale; SDS: Self-Rating Depression Scale. SAS and SDS scores and the trace element levels are presented as mean (standard deviation), whereas the remaining categories are expressed as the number of patients (percentage).

initial treatment stage, the mucosa can become ulcerated following contact with orthodontic brackets. Ulcers may also appear during treatment because of the irritation at the end of the ligature or archwire. In this study, 153 patients (26.06%) experienced the symptoms of recurrent oral ulcers, similar to the recurrence rate of 22.24% (117 of 526 patients) in an investigation by Liu *et al*[9]. Oral ulcers are a multifactorial disease, with the risk factors varying across studies. Moreover, the research findings may exhibit deviations in populations from different regions and ethnicities. Therefore, this study explored the current status of oral ulcers during orthodontic treatment and the related factors in 587 patients, providing useful reference and evidence for the clinical prevention of this disease.

Table 2 Assignment of values to the variables

Variable	Assigned values
Sex	Male = 1; female = 2
Smoking history	No = 0; yes = 1
Drinking history	No = 0; yes = 1
Tooth brushing frequency	≤ 1 time per day = 0; > 1 time per day = 1
Toothbrush hardness	Soft = 0; hard = 1
Dietary preference for meat	No = 0; yes =1
Dietary temperature	Warm = 0; hot =1
Treatment course	≤ 1 year = 0; > 1 year = 1
Tooth position	Non-anterior tooth region = 0; anterior tooth region = 1
Disease type	Dental caries = 1; dentofacial deformity = 2; periodontal disease =3
Orthodontic appliance type	Straight-wire bracket = 1; conventional straight-wire = 2
Recurrence	Without = 0; with = 1

Multifactor analysis of factors associated with oral ulcers

According to this study results, age < 60 years, smoking history, hard toothbrush, hot diet, treatment course for > 1 year, and tooth brushing frequency of > 1 time per day were associated with oral ulcer occurrence. Additionally, Zn level (OR: 0.945; 95%CI: 0.927–0.964) served as a protective factor for oral ulcers, while the SAS (OR: 1.284; 95%CI: 1.197–1.378) and SDS (OR: 1.322; 95%CI: 1.231–1.419) scores were risk factors. Age ≥60 years was identified as an independent risk factor for oral ulcer development, potentially because older patients were more likely to develop oral mucosal ulcers and experience more severe symptoms than those who were younger due to the aging-related effects of decreased metabolism, poor oral mucosal adaptability, and reduced oral mucosal elasticity. Furthermore, most older people have systemic diseases, which in turn increase the possibility of oral ulcers to some extent. Furthermore, smoking habit has been shown to be a risk factor for intractable oral ulcers[10]. Toxic substances, including nicotine in cigarettes, can damage the oral mucosa, thereby diminishing the protective function of the mucosa and exacerbating the susceptibility of the oral cavity to bacterial or viral invasions and infections. The habit of smoking can also cause recurrent and intractable oral mucosal ulcers, consistent with our finding of smoking history as a risk factor for oral ulcer recurrence (OR: 3.588; 95%CI: 1.829–7.040). Moreover, the close relation between a hard toothbrush and oral ulcers may be attributed to the oral mucosal damage that can be easily caused by a hard toothbrush, ultimately leading to the occurrence and recurrence of oral ulcers[11].

Previous studies have also suggested that high dietary temperature is an independent risk factor for oral ulcers[12]. The consumption of food that is excessively hot or at a high temperature can lead to the destruction of oral mucosal cells. Such extremely hot dietary temperatures can result in the scalding of the oral mucosa and traumatic ulcer development, even in the absence of orthodontic treatment. A longer treatment course (*i.e.* > 1 year) and tooth brushing frequency of ≤ 1 time per day were also found to be risk factors for oral mucosal ulcers in this study. Good brushing habits are known to have a positive impact on oral cleanliness and bacterial elimination in the oral cavity. Conversely, an inadequate frequency of tooth brushing can lead to an unclean internal environment in the oral cavity that facilitates the proliferation of oral bacteria, thus escalating the likelihood of oral ulcers. Further, a dietary preference for meat can induce oral mucosal ulcers. In contrast, prior studies have suggested that vitamin B and trace elements in vegetables and fruits have therapeutic effects on oral ulcers[13]. The current study revealed that the trace element Zn had a protective role against oral mucosal ulcers, demonstrating a long-term healing effect on ulcers and inflammation. However, the relation between a dietary preference for meat and oral ulcers was significant only in the univariate analysis but not in the multivariate analysis, possibly due to the linear relationship with other variables, including trace elements. Therefore, future studies should control for other variables and employ larger sample sizes to comprehensively investigate the relationship between dietary preference for meat and oral ulcers.

Finally, the influence of mental factors on oral ulcers during orthodontic treatment was examined. Our results found that the SAS (OR: 1.284; 95%CI: 1.197–1.378) and SDS (OR: 1.322; 95%CI: 1.231–1.419) scores were risk factors for oral ulcers. Correspondingly, long-term anxiety and depression have been suggested to cause neurological dysfunction in patients[14,15]. A possible explanation for these observations may be that the increased nervousness during orthodontic treatment may activate sympathetic adrenal hormones and induce emotional tension, ultimately reducing patient immunity and causing oral ulcer disease.

Multivariate analysis of factors associated with oral ulcer recurrence

In addition to identifying the risk factors for oral ulcers, we further determined the factors linked to oral ulcer recurrence. Our analysis demonstrated that disease type (dentofacial deformity: OR: 0.396; 95%CI: 0.199–0.786) and disease location (anterior tooth region: OR: 2.319; 95%CI: 1.206–4.462) were associated with recurrent oral ulcers. Compared to the other

Table 3 Logistic regression analysis of factors associated with oral ulcers

Parameters	Univariate model			Multivariate model		
	OR	95%CI	*P* value	OR	95%CI	*P* value
Age						
< 60 years	1.000			1.000		
≥ 60 years	7.116	4.880–10.377	< 0.001	6.820	2.226–20.893	< 0.001
Smoking history						
No	1.000			1.000		
Yes	5.390	3.491–8.323	< 0.001	4.434	2.527–7.782	< 0.001
Toothbrush hardness						
Soft	1.000			1.000		
Hard	2.114	1.510–2.960	< 0.001	2.804	1.746–4.505	< 0.001
Dietary preference for meat						
No	1.000			1.000		
Yes	1.874	1.250–2.808	0.002	1.719	0.994–2.973	0.053
Dietary temperature						
Warm	1.000			1.000		
Hot	1.650	1.158–2.351	0.006	1.399	1.220–1.722	0.002
Treatment course						
≤ 1 year	1.000			1.000		
> 1 year	2.993	2.126–4.215	< 0.001	3.830	2.203–6.659	< 0.001
Sex						
Male	1.000			1.000		
Female	2.328	1.621–3.343	< 0.001	1.610	0.933–2.780	0.087
Tooth brushing frequency						
≤ 1 time per day	1.000			1.000		
> 1 time per day	0.309	0.218–0.437	< 0.001	0.228	0.138–0.377	< 0.001
Zn level	0.947	0.938–0.957	< 0.001	0.945	0.927–0.964	< 0.001
SAS score	1.262	1.213–1.314	< 0.001	1.284	1.197–1.378	< 0.001
SDS score	1.278	1.228–1.331	< 0.001	1.322	1.231–1.419	< 0.001

CI: Confidence interval; OR: Odds ratio; SAS: Self-Rating Anxiety Scale; SDS: Self-Rating Depression Scale.

Table 4 Logistic regression analysis of factors associated with oral ulcer recurrence

Indicators	B	SE	Wald	*P* value	OR	95%CI
Smoking history	1.278	0.344	13.806	< 0.001	3.588	1.829–7.040
Tooth brushing frequency ≤ 1 time per day	1.063	0.352	9.111	0.003	2.894	1.452–5.770
Dentofacial deformity	−0.927	0.350	7.008	0.008	0.396	0.199–0.786
Hard toothbrush	2.067	0.342	36.555	< 0.001	7.905	4.044–15.451
Non-dietary preference for meat	−0.659	0.345	3.639	0.046	0.517	0.263–0.984
Disease in anterior tooth region	0.841	0.334	6.354	0.012	2.319	1.206–4.462

CI: Confidence interval; OR: Odds ratio.

disease types (*i.e.* dental caries and periodontal disease), dentofacial deformities were not prone to oral ulcer recurrence after orthodontic treatment. This result implied that dentofacial deformities have a specific protective effect against recurrent mouth ulcers. Considering that the anterior tooth region is an area of oral exposure and a frequently used area of the oral cavity, this region may be more prone to recurrent oral mucosal ulcers[16].

CONCLUSION

In summary, age ≥ 60 years, smoking history, hard toothbrush, hot diet, treatment course for > 1 year, tooth brushing frequency of ≤ 1 time per day, and mental anxiety are independent risk factors for oral mucosal ulcers during orthodontic treatment. Therefore, the incidence of oral ulcers during orthodontic treatment can be reduced by enhancing the protective measures for older patients. Moreover, efforts should be made to promote oral health-related knowledge and encourage patients to maintain good lifestyle habits after orthodontic treatment, including adopting a healthy diet with more vegetables and fruits, supplementing with trace elements and vitamins, employing correct tooth brushing methods, adjusting mentality, and alleviating anxiety and depression. All these strategies will contribute to improving immunity and preventing oral mucosal ulcers in patients during orthodontic treatment.

FOOTNOTES

Author contributions: Chang J and Li X wrote, revised, and reviewed the final manuscript.

Institutional review board statement: This study was approved by the Ethics Committee of the School and Hospital of Stomatology of Peking University on January 2, 2020.

Informed consent statement: All enrolled patients were informed of the research purpose, and signed informed consent was obtained from each patient.

Conflict-of-interest statement: All the authors declare that they have no conflict of interest.

Data sharing statement: All data and materials are available from the corresponding author upon reasonable request.

STROBE statement: The authors have read the STROBE Statement—checklist of items, and the manuscript was prepared and revised according to the STROBE Statement—checklist of items.

Country of origin: China

ORCID number: Xue Li 0009-0006-3286-1640.

S-Editor: Liu JH
L-Editor: Filipodia
P-Editor: Zhao YQ

REFERENCES

1 **Jiang WX**, Xia CL, Ding X, Liu MX, Liu GR. Effects of Periodontal-Orthodontic Combined Treatment on Periodontal Function, Gingival Crevicular Fluid TSLP and IL-33 and its Influence Factors Study of Prognosis in Patients with Invasive Periodontitis. *Xiandai Shengwu Yixue Jinzhan* 2022; **22**: 3972-3976+3981 [DOI: 10.13241/j.cnki.pmb.2022.20.034]

2 **Brancher JA**, Spada PP, Meger MN, Fatturri AL, Dalledone M, de Paiva Bertoli FM, Deeley K, Scariot R, Vieira AR, Küchler EC, de Souza JF. The association of genetic polymorphisms in serotonin transporter and catechol-O-methyltransferase on temporomandibular disorders and anxiety in adolescents. *J Oral Rehabil* 2019; **46**: 597-604 [PMID: 30811655 DOI: 10.1111/joor.12783]

3 **Kretschmer WB**, Baciuţ G, Baciuţ M, Sader R. Effect of bimaxillary orthognathic surgery on dysfunction of the temporomandibular joint: a retrospective study of 500 consecutive cases. *Br J Oral Maxillofac Surg* 2019; **57**: 734-739 [PMID: 31255372 DOI: 10.1016/j.bjoms.2019.06.010]

4 **Lin L**, Duan N, Wang X, Song YF, Wang WM. Study on the correlation between common diseases of oral mucosa and psychological factors. *Kouqiang Jibing Fangzhi* 2019; **27**: 236-240 [DOI: 10.12016/j.issn.2096-1456.2019.04.006]

5 **Chen QM**. Oral Mucosal Diseases. 4th Edition. People's Health Publishing House, 2012

6 **Richter GM**, Kruppa J, Munz M, Wiehe R, Häsler R, Franke A, Martins O, Jockel-Schneider Y, Bruckmann C, Dommisch H, Schaefer AS. A combined epigenome- and transcriptome-wide association study of the oral masticatory mucosa assigns CYP1B1 a central role for epithelial

health in smokers. *Clin Epigenetics* 2019; **11**: 105 [PMID: 31331382 DOI: 10.1186/s13148-019-0697-y]

7 **Gong F**, Wang QQ, Ma L. The effect of fluoxetine in adjuvant treatment of erosive ulcer oral mucosal disease and its influence on patients' anxiety,depression and quality of life. *Guoji Jingshenbingxue Zazhi* 2021; **48**: 703-706 [DOI: 10.13479/j.cnki.jip.2021.04.036]

8 **Lv L**. Effect of systematic nursing intervention on the occurrence and quality of life of oral mucosal ulcers in patients with nasopharyngeal carcinoma undergoing intensity-modulated radiotherapy. *Xiandai Zhenduan Yu Zhiliao* 2018; **29**: 3009-3010 [DOI: 10.3969/j.issn.1001-8174.2018.18.079]

9 **Liu J**, Xu H, Tang G, Liu H, Sun Z, Zhou G, Cheng B, Wang W, He H, Guo B, Meng W, Liu Q, Wang J, Luo X, Zhou Y, Jiang L, Zeng X, Dan H, Chen Q. A multi-center cross-sectional study of 1495 Chinese oral lichen planus patients. *Oral Dis* 2023 [PMID: 37994276 DOI: 10.1111/odi.14798]

10 **Lv XD**, Wu MM, Zhang LR, Shi YH. Er: Clinical observation of YAG Laser-assisted Ultrasound Therapy in the Treatment of Severe Periodontitis. *Linchuang Kouqiang Yixue Zazhi* 202; **38**: 356-359 [DOI: 10.3969/j.issn.1003-1634.2022.06.011]

11 **Zhao Y**, Yin Y, Tao L, Nie P, Tang Y, Zhu M. Er:YAG laser *vs* scaling and root planing as alternative or adjuvant for chronic periodontitis treatment: a systematic review. *J Clin Periodontol* 2014; **41**: 1069-1079 [PMID: 25164559 DOI: 10.1111/jcpe.12304]

12 **Fitzpatrick SG**, Cohen DM, Clark AN. Ulcerated Lesions of the Oral Mucosa: Clinical and Histologic Review. *Head Neck Pathol* 2019; **13**: 91-102 [PMID: 30701449 DOI: 10.1007/s12105-018-0981-8]

13 **Hu SL**, Qin F, Zheng JH. Dai M. A study on the correlation between polymorphisms of IL-4, IL-6, and IL-13 genes and chronic periodontitis. *Hainan Yixue* 2016; **27**: 3455-3457 [DOI: 10.3969/j.issn.1003-6350.2016.21.005]

14 **Tang Y**, Liu YP, Li YC. Analysis of the relationship between anxiety-depression and TCM syndrome types in patients with oral lichen planus. *Zhongguo Yiyao Kexue* 2020; **10**: 6-9+22 [DOI: 10.3969/j.issn.2095-0616.2020.07.002]

15 **Mainville GN**, Marsh WL, Allen CM. Oral ulceration associated with concurrent herpes simplex virus, cytomegalovirus, and Epstein-Barr virus infection in an immunocompromised patient. *Oral Surg Oral Med Oral Pathol Oral Radiol* 2015; **119**: e306-e314 [PMID: 25544404 DOI: 10.1016/j.oooo.2014.10.019]

16 **Diwan B**, Shirbhate U, Bajaj P, Reche A, Pahade A. Conventional Scalpel and Diode Laser Approach for the Management of Traumatic Fibroma. *Cureus* 2023; **15**: e47810 [PMID: 38021932 DOI: 10.7759/cureus.47810]

World Journal of Clinical Cases

Submit a Manuscript: https://www.f6publishing.com

World J Clin Cases 2024 September 16; 12(26): 5877-5884

DOI: 10.12998/wjcc.v12.i26.5877

ISSN 2307-8960 (online)

ORIGINAL ARTICLE

Case Control Study

Impact of web-based positive psychological intervention on emotions, psychological capital, and quality of life in gastric cancer patients on chemotherapy

Yu-Yu Xin, Dan Zhao

Specialty type: Medicine, research and experimental

Provenance and peer review: Unsolicited article; Externally peer reviewed.

Peer-review model: Single blind

Peer-review report's classification

Scientific Quality: Grade C

Novelty: Grade B

Creativity or Innovation: Grade B

Scientific Significance: Grade C

P-Reviewer: Tavares Lacerda AL

Received: May 10, 2024

Revised: June 13, 2024

Accepted: July 1, 2024

Published online: September 16, 2024

Processing time: 73 Days and 14.2 Hours

Yu-Yu Xin, Department of General Medicine, The Fourth Affiliated Hospital of Soochow University (Suzhou Dushu Lake Hospital), Suzhou 215000, Jiangsu Province, China

Dan Zhao, Department of Nursing, The Fourth Affiliated Hospital of Soochow University (Suzhou Dushu Lake Hospital), Suzhou 215000, Jiangsu Province, China

Corresponding author: Dan Zhao, MNurs, Associate Chief Nurse, Nursing Department, The Fourth Affiliated Hospital of Soochow University (Suzhou Dushu Lake Hospital), No. 9 Chongwen Road, Suzhou Industrial Park, Suzhou 215000, Jiangsu Province, China. zhaod0102@163.com

Abstract

BACKGROUND

Gastric cancer is a malignant digestive tract tumor that originates from the epithelium of the gastric mucosa and occurs in the gastric antrum, particularly in the lower curvature of the stomach.

AIM

To evaluate the impact of a positive web-based psychological intervention on emotions, psychological capital, and quality of survival in gastric cancer patients on chemotherapy.

METHODS

From January 2020 to October 2023, 121 cases of gastric cancer patients on chemotherapy admitted to our hospital were collected and divided into a control group (n = 60) and an observation group (n = 61) according to the admission order. They were given either conventional nursing care alone and conventional nursing care combined with web-based positive psychological interventions, respectively. The two groups were compared in terms of negative emotions, psychological capital, degree of cancer-caused fatigue, and quality of survival.

RESULTS

After intervention, the number of patients in the observation group who had negative feelings toward chemotherapy treatment was significantly lower than that of the control group ($P < 0.05$); the Positive Psychological Capital Questionnaire score was considerably higher than that of the control group ($P < 0.05$);

the degree of cancer-caused fatigue was significantly lower than that of the control group ($P < 0.05$); and the Quality of Life Scale for Cancer Patients (QLQ-30) score was significantly higher than that of the control group ($P < 0.05$).

CONCLUSION

Implementing a web-based positive psychological intervention for gastric cancer chemotherapy patients can effectively improve negative emotions, enhance psychological capital, and improve the quality of survival.

Key Words: Internet; Positive psychology; Gastric cancer chemotherapy; Negative emotions; Psychological capital; Quality of survival

Core Tip: Scientific and well-designed nursing interventions hold significant potential in mitigating negative emotions, enhancing psychological capital, and improving the overall quality of life for patients undergoing cancer chemotherapy. These interventions are crucial in supporting patients' mental and physical well-being.

Citation: Xin YY, Zhao D. Impact of web-based positive psychological intervention on emotions, psychological capital, and quality of life in gastric cancer patients on chemotherapy. *World J Clin Cases* 2024; 12(26): 5877-5884
URL: https://www.wjgnet.com/2307-8960/full/v12/i26/5877.htm
DOI: https://dx.doi.org/10.12998/wjcc.v12.i26.5877

INTRODUCTION

According to the latest cancer data in China[1], there are 397000 new cases of gastric cancer each year, with the morbidity and mortality both ranking 3rd among various malignant tumors, and the new cases account for 44% of the global cases. Therefore, it is also known as "Chinese-style cancer". Considering the small number of cancer cells that may remain after laparoscopic radical gastric cancer surgery, most patients, except for a few, need postoperative chemotherapy to kill tumor cells further and prolong the survival period[2]. However, chemotherapy has high side effects, easily increases somatic discomfort, affects patients' confidence in treatment, and reduces the quality of survival[3]. Therefore, strengthening nursing measures is crucial in relieving psychological pressure, promoting the smooth progress of chemotherapy, and improving treatment success rates. Thus, this study proposed the application of web-based positive psychological interventions in such patients to provide a sufficient theoretical basis for clinically relevant nursing work.

Gastric cancer is a malignant digestive tract tumor that originates from the epithelium of the gastric mucosa and occurs in the gastric antrum, particularly in the lower curvature of the stomach[4,5]. Laparoscopic radical gastrectomy for gastric cancer, as the main treatment modality for this disease, can effectively resect local lesions and clear lymph nodes[6]. Postoperative supplementation with chemotherapy can further prevent the recurrence and metastasis of cancer cells and improve the prognosis of surgery[7]. However, in practice[8], most patients are affected by disease, surgery, drugs, and other factors and often suffer from malnutrition among others. In addition, chemotherapy inevitably damages normal tissue cells while acting on cancer cells, triggering related toxicity and side effects, impacting patients' physical and mental health, and subsequently affecting chemotherapy compliance and cancer-related fatigue (CRF), which is not conducive to the establishment of confidence in treatment. Therefore, the implementation of scientific and efficient nursing interventions plays a crucial role in reducing the negative emotions of patients receiving gastric cancer chemotherapy, constructing psychological capital, and improving their quality of survival. In recent years, the advantages of "Internet + " have gradually come to the fore, and the use of artificial intelligence technology to build a network platform has also become a new trend in medical and healthcare management. mHealth refers to providing medical services and information through mobile communication technology, specifically in the mobile Internet field, and is based on medical and healthcare applications for mobile terminal systems, such as Android and IOS[9,10]. Web-based positive psychological intervention is an Internet information-based care model that overcomes conventional disease care's time and spatial limitations and aims to provide patients with online and offline integrated mental health care services through Internet channels.

MATERIALS AND METHODS

General information

From January 2020 to October 2023, 121 gastric cancer patients on chemotherapy admitted to our hospital were enrolled and divided into a control group ($n = 60$) and an observation group ($n = 61$), according to the admission order. The baseline data of the two groups were well-balanced and comparable ($P > 0.05$; Table 1).

Table 1 Comparison of baseline information between the two groups

Group	Baseline information									
	Gender (M:F), *n* (%)	Age (year)	Lesion site				Tumor stage			
			Corpus	Fundus	Antrum	Multisite	Ia	Ib	II	III
Observation (n = 61)	31 (50.82):30 (49.18)	54.69 ± 5.14	16 (26.23)	15 (24.59)	28 (45.90)	2 (3.28)	12 (31.25)	18 (52.08)	26 (16.67)	5 (16.67)
Control (n = 60)	30 (50.00):30 (50.00)	54.33 ± 5.29	14 (23.33)	15 (25.00)	29 (48.33)	2 (3.33)	10 (16.67)	19 (31.67)	25 (41.67)	6 (10.00)
t/χ^2	0.008	0.380	0.136	0.003	0.072	0.242	0.184	0.066	0.011	0.119
P value	0.928	0.705	0.712	0.958	0.789	0.623	0.668	0.797	0.915	0.730

The inclusion criteria were as follows: (1) Patients who were diagnosed with gastric cancer; (2) Patients who had a certain cultural level, were conscious, and could think independently; (3) Patients who had complete medical records; (4) Patients who had no contraindications to chemotherapy and were treated with chemotherapy; and (6) Patients who were aware of the purpose of this study and provided informed consent.

The exclusion criteria were as follows: (1) Patients who had other malignant tumors; (2) Those with mental diseases, such as long-term consciousness disorder and mental abnormality; (3) Those who died in the middle of the course or gave up the treatment; (4) Those with cancer cell infiltration and metastasis; and (5) Those with coagulation dysfunction.

Methods of care

Control group: The control group underwent routine nursing. We systematically assessed the patients' condition, provided them with a good ward environment, understood their basic situation, provided one-on-one verbal health education, fully informed them of the precautions during chemotherapy treatment. We strengthened the monitoring of vital signs and care of complications, advised patients to comply with the doctor's advice on regular use of medication, and provide nursing services in terms of safety, life, diet, and other aspects. We increased the number of ward rounds, strictly performed the daily nursing handover, and fully implemented the nursing work. We asked the patients about their psychological status and specific conditions during the morning check-up every day and promptly carried out symptomatic interventions in the event of any abnormalities.

Observation group: The observation group underwent routine care combined with a positive web-based psychological intervention. The former is the same as described above. The web-based positive psychological intervention consisted of the following stages: (1) Pre-preparation: A team was established, which involved selecting experienced and thoughtful medical staff, comprising one N3-level nurse in charge, two attending physicians, one N2-level nurse in charge, five nurses in charge, and two network publicity officers, all supervised and guided by the N3-level nurse in charge. A clear division of responsibilities was assigned, with the N3-level nurse responsible for ensuring progress in nursing care; attending physicians and nurses in charge responsible for implementing nursing content; and network publicity officers responsible for maintaining network security. In the month before the implementation of the intervention, on a weekly basis, the department director and the head nurse led the team in ensuring that the attending physicians and nurses in charge were able to implement nursing content and the network publicity officers could maintain network security. Likewise, in the month before the implementation of the intervention, the head of the department and the head nurse, led the team in holding a bi-weekly (every Monday and Friday) "network-based positive psychological intervention" training meeting. Each week, 1-2 members of the team were designated as responsible for the collection of defective cases from the department. They had to prepare an individualized analysis of each case and explain the case to the remaining members of the team during their shift the next morning or during the second meeting of the week. This was meant to comprehensively improve the quality of the nursing staff, enrich their cognitive skills, and cultivate in them the spirit of "prudence and solitude." Regular outings were also organized for them to deepen the connotations of nursing care and network technology in their work; (2) Designing the mobile technology based intervention: We requested the network information department of the hospital for developing a mobile technology based treatment application (app) for patients undergoing gastric cancer chemotherapy. The app was developed with the approval of the management of the hospital. The group members who developed the app browsed through authoritative literature and typical cases treated at the hospital in the past years. They searched the databases of Wanfang, Zhi.com, PubMed, the full-text database of China's journals, and Cochrane, among others, using keywords such as "network," "positive psychological intervention," "gastric cancer chemotherapy," "negative emotions," "psychological intervention" and "psychological capital," and "quality of life" in the literature search. Considering the actual situation of the department, they prioritized the needs of patients, collated and summarized the useful information, and began brainstorming to develop the app containing the following five modules: "Health education and popular science," "Breathing, meditation, and relaxation," "Communication and exchange of information," "About us," and "Notes." The unified implementation plan was constantly adjusted during the implementation period; (3) Modules 1 to 3: The first module, "Health education and popular science," included information on the pathogenesis of gastric cancer, causes, epidemiology, clinical manifestations, principles of chemotherapy, adverse reactions, and the latest research results at home and abroad, among others. Patients were instructed to browse and watch this in their spare time and focus on learning the relevant contents, such as "principles of chemotherapy" and "adverse reactions," to enhance their understanding of the process of chemotherapy. The second module, "Breathing, meditation, and relaxation," was a tutorial with video playback. Specifically, patients were guided

through sessions of deep breathing techniques and total relaxation, followed by meditation in a secluded environment with no external stimulation. They were asked to sit quietly and relax, without any turmoil in their minds, play their personal favorite soothing music to create a suitable atmosphere, breathe deeply and slowly *as per* the instructions softly spoken, gently close their eyes, feel the airflow and rhythm of every breath, and synchronize their body rhythm with their breath. They were asked to imagine their body swaying in unison with their breath and accept any thoughts that come into their mind. This session was conducted 3 times/d, 8–10 min each time. In the "Communication and exchange of information" module, a WeChat group of "gastric cancer chemotherapy patients" was formed inviting patients to join a group chat. Their personal name cards were changed to reflect their real names so that the medical staff could identify them. The necessary applications of the WeChat group chat were conveyed to ensure that patients possess the basic skills of sending and receiving text, making voice calls, sending pictures, and video chatting. The attending physician answered questions online every Friday from 9 to 10 a.m. The rest of the time, the nursing staff posted small videos and health quizzes, mostly relating to knowledge about chemotherapy for gastric cancer. These were accompanied by voice instructions and explanations asking patients to pay close attention to changes in their own emotions, understand their psychological state, learn to control their emotions, and contact the medical staff in time for psychological counseling if or when they were overwhelmed by their own negative emotions. In terms of medication, they were strictly prohibited from adjusting their dosage of medication without authorization or from stopping medication on their own. They were also counseled on their diet and advised to refrain from eating greasy and spicy food; (4) Module 4: The "About us" section contains a brief introduction of the medical team, departmental contact channels, and patient feedback services among others; and (5) Module 5: The "Notes" section contained instructions on how to set a specific period to operate reminders. It also contained automatic generation of nursing shift content for facilitating nursing staff to standardize the content of the shift handover.

The intervention was conducted for 12 consecutive weeks during which observations from both groups were noted.

Observation indicators

Negative emotions: The observation indicators included: (1) Forced psychology: Resistance to chemotherapy treatment and having to make themselves obey against their own will; (2) Nervousness: Excessive worry about the effect of chemotherapy, being in a spirit state of high readiness, and being unable to cooperate with the nursing staff; and (3) Fear of psychology: In the face of chemotherapy, because of the fear of the pain accompanied by attempts to get rid of the pain but cannot do anything about it, resulting in fear of strong repression of the emotional experience.

Psychological capital: The Positive Psychological Capital Questionnaire (PPQ)[7] was used, including four dimensions of optimism (42 points), hope (42 points), self-efficacy (49 points), and psychological resilience (49 points), with 28 entries and a total score of 182 points. The score is positively related to psychological capital.

Degree of cancer-caused fatigue: The Revised Piper Fatigue Scale (RPFS)[8] was used, which consists of four dimensions of physical symptoms, cognitive level, affective symptoms, and behavioral changes, with 22 items, all of which are assigned a score of 0–10. The scores are positively related to the degree of fatigue.

Self-perceived burden: The Self-Perceived Burden Scale[9] was used, and the content included physical burden (10 points), emotional burden (30 points), and economic burden (10 points), with a total of 10 entries scored on a Likert scale of 5, with a total score of 50 points. The higher the score, the heavier the self-perceived burden.

Survival quality: The Quality of Life Scale for Cancer Patients (QLQ-30)[10] was used, four functional dimensions of which were selected, namely, general condition (100 points), psychology (100 points), physiology (100 points), and social adaptation (100 points). The higher the score, the better the quality of life.

Statistical analysis

Data were statistically analyzed using SPSS Windows software version 26.0. Measurement data meeting a normal distribution, presented as the mean ± SD, were compared by independent or paired-samples *t* tests. Measurement data not meeting a normal distribution, expressed as median with interquartile range, were compared by the Wilcoxon signed-rank test. Counting data, expressed as percentages (%), were compared by the χ^2 test. $P < 0.05$ was considered statistically significant.

RESULTS

Comparison of negative emotions

After intervention, the number of patients in the observation group who had negative emotions about chemotherapy treatment was significantly lower than that of the control group ($P < 0.05$). Further details are presented in Table 2.

Comparison of psychological capital

The psychological capital of the two groups was comparable before care ($P > 0.05$). After intervention, the PPQ score of the observation group was significantly higher than that of the control group ($P < 0.05$). Further details are presented in Table 3.

Table 2 Comparison of negative emotions, *n* (%)

Group	Cases	Obsessive-compulsive disorder	Nervousness	Fearfulness
Observation	61	4 (6.56)	3 (4.92)	2 (3.28)
Control	60	12 (60.00)	11 (18.33)	9 (15.00)
χ^2		4.763	5.321	5.028
P value		0.029	0.021	0.025

Table 3 Comparison of psychological capital (mean ± SD, points)

Group	Cases	Pessimism		Wish		Self-efficacy		Mental toughness	
		Before care	After care	Before care	After care	Before care	After care	Before care	After care
Observation	61	25.28 ± 3.72	35.30 ± 2.64[a]	25.21 ± 3.75	36.28 ± 2.69[a]	33.33 ± 2.91	40.22 ± 3.58[a]	32.35 ± 3.61	40.30 ± 2.66[a]
Control	60	25.25 ± 3.74	31.89 ± 2.50[a]	25.28 ± 3.72	32.88 ± 2.65[a]	33.36 ± 2.87	37.85 ± 3.57[a]	32.31 ± 3.59	35.90 ± 2.61[a]
t value		0.044	3.016	0.141	4.610	0.185	4.784	0.061	2.922
P value		0.965	0.003	0.888	< 0.001	0.853	< 0.001	0.951	0.004

[a]*P* < 0.05 compared to pre-care.

Comparison of degree of cancer-caused fatigue

The degree of CRF in the two groups was comparable before care ($P > 0.05$). After intervention, the degree of cancer-induced fatigue in the observation group was significantly lower than that of the control group ($P < 0.05$). Further details are presented in Table 4.

Comparison of self-perceived burden

The self-perceived burdens of the two groups before care were comparable ($P > 0.05$). After intervention, the self-perceived burden of the observation group was significantly lower than that of the control group ($P < 0.05$). Further details are presented in Table 5.

Comparison of quality of survival

Before care, there was no significant difference in the quality of survival scores between the two groups ($P > 0.05$). After intervention, the QLQ-30 scores of the observation group were significantly higher than those of the control group ($P < 0.05$). Further details are presented in Table 6.

DISCUSSION

This study showed that after the joint use of a web-based positive psychological intervention, the number of patients in the observation group who had negative emotions about chemotherapy treatment was significantly lower than that of the control group, and the PPQ score was significantly higher than that of the control group ($P < 0.05$). These results suggest that web-based positive psychological interventions can alleviate adverse emotions in patients undergoing gastric cancer chemotherapy. Conventional care often ignores individualized differences among patients and therefore has a poor effect. However, in modern society, along with the innovative transformation of the medical model, the bio-psycho-social integrated model has emerged, which explicitly proposes that a variety of integrated factors mostly cause modern diseases. Therefore, it is necessary to consider the role of four major factors, emotion, personality, maladaptive behaviors, and psychological stress, while carrying out all-around diagnostic treatment[11]. A large number of studies have fully confirmed[12] that psychological factors occupy an important position in the process of disease occurrence, development, and regression. Therefore, clinical care workers should try to meet the psychological needs of patients, help them regulate their social roles, stabilize mood fluctuations, alleviate psychological pressure and stress, enhance their ability to adapt to the disease, and build confidence in their treatment. Positive psychological intervention, as a kind of consciousness nursing, is based on the theory of positive psychology, with the characteristics of being "comprehensive," "hierarchical," and "systemic," aiming to fully incorporate love, empathy, and psychological stress into the whole nursing process to reduce patients' mental stress and alleviate their negative emotions[13]. Simultaneously, the implementation of positive psychological interventions based on the Internet can meet the physical, mental, and spiritual needs of patients, aiming to implement the whole process of assisted care through information technology; information release is convenient, and resource sharing is strong, which can effectively compensate for the limitations of conventional care[14].

Table 4 Comparison of degree of cancer-caused fatigue (mean ± SD, points)

Group	Cases	Somatic symptoms		Cognitive level		Emotional symptoms		Behavioral changes	
		Before care	After care	Before care	After care	Before care	After care	Before care	After care
Observation	61	5.28 ± 0.70	4.33 ± 0.84[a]	5.23 ± 0.75	4.26 ± 0.69[a]	5.31 ± 0.91	4.24 ± 0.58[a]	5.34 ± 0.61	4.31 ± 0.66[a]
Control	60	5.26 ± 0.74	4.84 ± 0.70[a]	5.25 ± 0.72	4.89 ± 0.65[a]	5.36 ± 0.85	4.83 ± 0.57[a]	5.37 ± 0.59	4.95 ± 0.61[a]
t value		0.123	2.913	0.120	4.150	0.251	4.531	0.221	4.447
P value		0.903	0.005	0.905	< 0.001	0.803	< 0.001	0.826	< 0.001

[a]*P* < 0.05 compared to pre-care.

Table 5 Comparison of self-perceived burdens (mean ± SD, points)

Group	Cases	Physical burden		Emotional burden		Economic burden		Physical burden	
		Before care	After care	Before care	After care	Before care	After care	Before care	After care
Observation	61	8.39 ± 0.33	2.54 ± 0.30[a]	26.10 ± 1.02	11.81 ± 1.11[a]	8.16 ± 0.19	2.42 ± 0.16[a]	8.39 ± 0.33	2.54 ± 0.30[a]
Control	60	8.42 ± 0.36	5.42 ± 0.34[a]	26.31 ± 1.07	15.05 ± 1.17[a]	8.13 ± 0.13	5.05 ± 0.17[a]	8.42 ± 0.36	5.42 ± 0.34[a]
t value		0.478	49.428	1.105	15.629	1.012	87.646	0.478	49.428
P value		0.634	< 0.001	0.271	< 0.001	0.314	< 0.001	0.634	< 0.001

[a]*P* < 0.05 compared to pre-care.

Table 6 Comparison of quality of survival (mean ± SD, points)

Group	Cases	Overall situation		Psychology		Physiology		Social adaptation	
		Before care	After care	Before care	After care	Before care	After care	Before care	After care
Observation	61	59.31 ± 5.84	88.85 ± 4.78[a]	60.24 ± 5.23	90.60 ± 4.39[a]	60.28 ± 4.22	90.22 ± 4.98[a]	62.31 ± 5.84	91.85 ± 5.74[a]
Control	60	59.26 ± 5.62	80.55 ± 3.97[a]	60.35 ± 5.12	86.28 ± 4.65[a]	60.36 ± 4.27	85.55 ± 3.07[a]	62.26 ± 5.62	86.55 ± 4.93[a]
t value		0.048	10.382	0.117	5.256	0.104	6.197	0.048	5.445
P value		0.962	< 0.001	0.907	< 0.001	0.918	< 0.001	0.962	< 0.001

[a]*P* < 0.05 compared to pre-care.

CRF is a feeling of fatigue or exhaustion related to cancer or cancer treatment. It is a painful, persistent, subjective feeling of fatigue or exhaustion with somatic, emotional, or cognitive aspects[15]. Fox *et al*[16] noted that CRF is prevalent in patients receiving chemotherapy; more than 75% of metastatic tumor patients experience cancer-caused fatigue, and the quality of their survival is severely affected, which is an essential factor hindering the daily life of cancer patients. In this study, we found that the degree of CRF in the observation group was significantly lower than that of the control group, and the burden of self-perception was reduced after the web-based positive psychological intervention ($P < 0.05$). These results suggest that web-based positive psychology programs can improve CRF in patients with gastric cancer. After the patients were admitted to the hospital, the nursing staff explained in detail the basic knowledge about chemotherapy for gastric cancer and helped them quickly identify their conditions. Further, the nursing staff highlighted the risk factors and adverse reactions accompanying chemotherapy to make the patients fully aware that this is a normal phenomenon without excessive panic. Moreover, the patients only needed to actively cooperate with the treatment, and they were guided to form a correct cognition, further relieve their psychological burden, improve their health literacy, and enhance their confidence in chemotherapy through subconsciousness, notably confidence, in chemotherapy to improve the quality of life[17-19].

While the current study provides valuable insights into the impact of web-based positive psychological interventions on gastric cancer chemotherapy patients, there are some limitations that need to be acknowledged. First, the sample size of 121 patients, although sufficient for initial findings, may not fully represent the broader population of gastric cancer patients on chemotherapy. Second, the study was conducted in a single hospital, limiting the generalization of the results to other healthcare settings. Additionally, the duration of the intervention and follow-up period were relatively short, limiting the ability to assess the long-term effects of the web-based positive psychological interventions. Furthermore, the

study relied primarily on self-reported measures, which may be subject to recall bias or participant subjectivity. Finally, other factors that could potentially influence the outcomes, such as social support and comorbidities, were not fully considered in the analysis.

CONCLUSION

Web-based positive psychological intervention for gastric cancer patients can significantly reduce negative emotions such as compulsion, fear, and nervousness, improve their psychological capital, and enhance the quality of their survival. This can be used as an ideal care method for postoperative gastric cancer patients undergoing chemotherapy.

FOOTNOTES

Author contributions: Xin YY designed the research study; Xin YY and Zhao D performed the primary literature review and data extraction; Xin YY and Zhao D analyzed the data and wrote the manuscript; Xin YY was responsible for revising the manuscript for important intellectual content; all authors read and approved the final version.

Institutional review board statement: This study was reviewed and approved by The Fourth Affiliated Hospital of Soochow University (Suzhou Dushu Lake Hospital) (2024 Lunyan Approval No. 241013).

Informed consent statement: All study participants or their legal guardian provided informed written consent about personal and medical data collection prior to study enrolment.

Conflict-of-interest statement: The authors have no financial relationships to disclose.

Data sharing statement: No additional data are available.

STROBE statement: The authors have read the STROBE statement-checklist of items, and the manuscript was prepared and revised according to the STROBE statement-checklist of items.

Country of origin: China

ORCID number: Yu-Yu Xin 0009-0005-6469-7593; Dan Zhao 0009-0000-6650-316X.

S-Editor: Lin C
L-Editor: Wang TQ
P-Editor: Zhao S

REFERENCES

1 **Wei XN**, Cai WY, Wu KL, Zeng FG. Application effect of gastrointestinal bundle nursing on the protection of gastrointestinal function in patients with gastric cancer. *Medicine (Baltimore)* 2023; **102**: e34308 [PMID: 37478274 DOI: 10.1097/MD.0000000000034308]
2 **Zamani M**, Alizadeh-Tabari S. Anxiety and depression prevalence in digestive cancers: a systematic review and meta-analysis. *BMJ Support Palliat Care* 2023; **13**: e235-e243 [PMID: 34417285 DOI: 10.1136/bmjspcare-2021-003275]
3 **Zou G**, Li Y, Xu R, Li P. Resilience and positive affect contribute to lower cancer-related fatigue among Chinese patients with gastric cancer. *J Clin Nurs* 2018; **27**: e1412-e1418 [PMID: 29266530 DOI: 10.1111/jocn.14245]
4 **Fu L**, Feng X, Jin Y, Lu Z, Li R, Xu W, Chang VT, Hu Y, Ye X. Symptom Clusters and Quality of Life in Gastric Cancer Patients Receiving Chemotherapy. *J Pain Symptom Manage* 2022; **63**: 230-243 [PMID: 34537311 DOI: 10.1016/j.jpainsymman.2021.09.003]
5 **Methods In Medicine CAM**. Retracted: Outcome of Nursing Based on Health Belief United with Knowledge, Belief, and Practice Mode on Gastroscopy of Patients with Gastric Cancer. *Comput Math Methods Med* 2023; **2023**: 9783730 [PMID: 38124968 DOI: 10.1155/2023/9783730]
6 **He F**, He RX. Systematic nursing interventions in gastric cancer: A randomized controlled study. *World J Clin Cases* 2022; **10**: 1843-1851 [PMID: 35317163 DOI: 10.12998/wjcc.v10.i6.1843]
7 **Sexton RE**, Al Hallak MN, Diab M, Azmi AS. Gastric cancer: a comprehensive review of current and future treatment strategies. *Cancer Metastasis Rev* 2020; **39**: 1179-1203 [PMID: 32894370 DOI: 10.1007/s10555-020-09925-3]
8 **Wang M**, Wang S, Su Q, Ma T. Effect of Combining Early Chemotherapy with Zhipu Liujunzi Decoction under the Concept of Strengthening and Consolidating Body Resistance for Gastric Cancer Patients and Nursing Strategy. *Contrast Media Mol Imaging* 2021; **2021**: 2135924 [PMID: 34934408 DOI: 10.1155/2021/2135924]
9 **Sousa P**, Duarte E, Ferreira R, Esperança A, Frontini R, Santos-Rocha R, Luís L, Dias SS, Marques N. An mHealth intervention programme to

promote healthy behaviours and prevent adolescent obesity (TeenPower): A study protocol. *J Adv Nurs* 2019; **75**: 683-691 [PMID: 30397934 DOI: 10.1111/jan.13905]

10 **Kaya G**, Eskin Bacaksiz F. The relationships between nurses' positive psychological capital, and their employee voice and organizational silence behaviors. *Perspect Psychiatr Care* 2022; **58**: 1793-1800 [PMID: 34888883 DOI: 10.1111/ppc.12990]

11 **Montagut-Martínez P**, Pérez-Cruzado D, Gutiérrez-Sánchez D. Cancer-related fatigue measures in palliative care: A psychometric systematic review. *Eur J Cancer Care (Engl)* 2022; **31**: e13642 [PMID: 35822246 DOI: 10.1111/ecc.13642]

12 **Meyer G**, Merkle R, Schinkel S, Spelsberg F, Weidenhagen R, Schildberg FW. [Postoperative endoscopy for the diagnosis and therapy of complications]. *Chirurg* 2002; **73**: 9-21 [PMID: 11974469 DOI: 10.1007/s104-002-8023-z]

13 **Dempster M**, Howell D, McCorry NK. Illness perceptions and coping in physical health conditions: A meta-analysis. *J Psychosom Res* 2015; **79**: 506-513 [PMID: 26541550 DOI: 10.1016/j.jpsychores.2015.10.006]

14 **Lee JY**, Jang Y, Hyung W. Mediating Effect of Illness Perception on Psychological Distress in Patients With Newly Diagnosed Gastric Cancer: Based on the Common-Sense Model of Self-regulation. *Cancer Nurs* 2023; **46**: E138-E145 [PMID: 35324505 DOI: 10.1097/NCC.0000000000001103]

15 **Tauber NM**, O'Toole MS, Dinkel A, Galica J, Humphris G, Lebel S, Maheu C, Ozakinci G, Prins J, Sharpe L, Smith AB, Thewes B, Simard S, Zachariae R. Effect of Psychological Intervention on Fear of Cancer Recurrence: A Systematic Review and Meta-Analysis. *J Clin Oncol* 2019; **37**: 2899-2915 [PMID: 31532725 DOI: 10.1200/JCO.19.00572]

16 **Peixoto TADSM**, Peixoto NMDSM, Pinto CAS, Santos CSVB. Nursing strategies to support psychological adaptation in adult cancer patients: a scoping review. *Rev Esc Enferm USP* 2021; **55**: e03690 [PMID: 33886916 DOI: 10.1590/S1980-220X2019039203690]

17 **Cao XL**, Wang X, Li P, Ju W. Psychological effects of advanced care on patients received endoscopic gastric cancer resection. *Medicine (Baltimore)* 2019; **98**: e17497 [PMID: 31593116 DOI: 10.1097/MD.0000000000017497]

18 **Wu X**, Zhang W. Reminiscence therapy-based care program alleviates anxiety and depression, as well as improves the quality of life in recurrent gastric cancer patients. *Front Psychol* 2023; **14**: 1133470 [PMID: 37351436 DOI: 10.3389/fpsyg.2023.1133470]

19 **Fox RS**, Ancoli-Israel S, Roesch SC, Merz EL, Mills SD, Wells KJ, Sadler GR, Malcarne VL. Sleep disturbance and cancer-related fatigue symptom cluster in breast cancer patients undergoing chemotherapy. *Support Care Cancer* 2020; **28**: 845-855 [PMID: 31161437 DOI: 10.1007/s00520-019-04834-w]

World Journal of Clinical Cases

Submit a Manuscript: https://www.f6publishing.com

World J Clin Cases 2024 September 16; 12(26): 5885-5892

DOI: 10.12998/wjcc.v12.i26.5885

ISSN 2307-8960 (online)

ORIGINAL ARTICLE

Retrospective Cohort Study

Risk factors and clinical significance of posterior slip of the proximal vertebral body after lower lumbar fusion

Jia-Jun Zhu, Yi Wang, Jun Zheng, Sheng-Yang Du, Lei Cao, Yu-Ming Yang, Qing-Xi Zhang, Ding-Ding Xie

Specialty type: Medicine, research and experimental

Provenance and peer review: Unsolicited article; Externally peer reviewed.

Peer-review model: Single blind

Peer-review report's classification

Scientific Quality: Grade C

Novelty: Grade B

Creativity or Innovation: Grade B

Scientific Significance: Grade B

P-Reviewer: Foroozanfar S

Received: March 18, 2024

Revised: June 7, 2024

Accepted: June 25, 2024

Published online: September 16, 2024

Processing time: 126 Days and 13.4 Hours

Jia-Jun Zhu, Yi Wang, Jun Zheng, Sheng-Yang Du, Lei Cao, Yu-Ming Yang, Qing-Xi Zhang, Ding-Ding Xie, Department of Spinal Surgery, Xuzhou First People's Hospital, Xuzhou 221112, Jiangsu Province, China

Jia-Jun Zhu, Yi Wang, Jun Zheng, Sheng-Yang Du, Lei Cao, Yu-Ming Yang, Qing-Xi Zhang, Ding-Ding Xie, Department of Spinal Surgery, The Affiliated Xuzhou Municipal Hospital of Xuzhou Medical University, Xuzhou 221112, Jiangsu Province, China

Jia-Jun Zhu, Yi Wang, Jun Zheng, Sheng-Yang Du, Lei Cao, Yu-Ming Yang, Qing-Xi Zhang, Ding-Ding Xie, Department of Spinal Surgery, The Affiliated Hospital of China University of Mining and Technology, Xuzhou 221112, Jiangsu Province, China

Co-first authors: Jia-Jun Zhu and Yi Wang.

Corresponding author: Ding-Ding Xie, MM, Attending Doctor, Department of Spinal Surgery, Xuzhou First People's Hospital, No. 269 Daxue Road, Xuzhou 221112, Jiangsu Province, China. dd2225@126.com

Abstract

BACKGROUND

Adjacent segment disease (ASD) after fusion surgery is frequently manifests as a cranial segment instability, disc herniation, spinal canal stenosis, spondylolisthesis or retrolisthesis. The risk factors and mechanisms of ASD have been widely discussed but never clearly defined.

AIM

To investigate the risk factors and clinical significance of retrograde movement of the proximal vertebral body after lower lumbar fusion.

METHODS

This was a retrospective analysis of the clinical data of patients who underwent transforaminal lumbar interbody fusion surgery between September 2015 and July 2021 and who were followed up for more than 2 years. Ninety-one patients with degenerative lumbar diseases were included (22 males and 69 females), with an average age of 52.3 years (40-73 years). According to whether there was retrograde movement of the adjacent vertebral body on postoperative X-rays, the patients were divided into retrograde and nonretrograde groups. The sagittal parameters of the spine and pelvis were evaluated before surgery, after surgery,

and at the final follow-up. At the same time, the Oswestry Disability Index (ODI) and Visual Analogue Scale (VAS) were used to evaluate the patients' quality of life.

RESULTS

Nineteen patients (20.9%) who experienced retrograde movement of proximal adjacent segments were included in this study. The pelvic incidence (PI) of the patients in the retrograde group were significantly higher than those of the patients in the nonretrograde group before surgery, after surgery and at the final follow-up ($P < 0.05$). There was no significant difference in lumbar lordosis (LL) between the two groups before the operation, but LL in the retrograde group was significantly greater than that in the nonretrograde group postoperatively and at the final follow-up. No significant differences were detected in terms of the |PI–LL|, and there was no significant difference in the preoperative lordosis distribution index (LDI) between the two groups. The LDIs of the retrograde group were 68.1% ± 11.5% and 67.2% ± 11.9%, respectively, which were significantly lower than those of the nonretrograde group (75.7% ± 10.4% and 74.3% ± 9.4%, respectively) ($P < 0.05$). Moreover, the patients in the retrograde group had a greater incidence of a LDI < 50% than those in the nonretrograde group ($P < 0.05$). There were no significant differences in the ODI or VAS scores between the two groups before the operation, but the ODI and VAS scores in the retrograde group were significantly worse than those in the nonretrograde group after the operation and at the last follow-up, ($P < 0.05$).

CONCLUSION

The incidence of posterior slippage after lower lumbar fusion was approximately 20.9%. The risk factors are related to a higher PI and distribution of lumbar lordosis. When a patient has a high PI and insufficient reconstruction of the lower lumbar spine, adjacent segment compensation *via* posterior vertebral body slippage is one of the factors that significantly affects surgical outcomes.

Key Words: Adjacent segment disease; Posterior vertebral slip; Sagittal alignment of spine-pelvis; Lower lumbar fusion; Quality of life

Core Tip: Sagittal alignment of the spine and pelvis was assessed for patients with or without retrograde of the adjacent vertebra body on postoperative X-rays. We concluded that the risk factors of the posterior slip of the proximal vertebra body after lower lumbar fusion are related to a higher pelvic incidence (PI) and distribution of lumbar lordosis. When a patient has a high PI and insufficient reconstruction of the lower lumbar spine, adjacent segment compensation *via* posterior vertebra body slippage is one of the factors that significantly affects surgical outcomes.

Citation: Zhu JJ, Wang Y, Zheng J, Du SY, Cao L, Yang YM, Zhang QX, Xie DD. Risk factors and clinical significance of posterior slip of the proximal vertebral body after lower lumbar fusion. *World J Clin Cases* 2024; 12(26): 5885-5892
URL: https://www.wjgnet.com/2307-8960/full/v12/i26/5885.htm
DOI: https://dx.doi.org/10.12998/wjcc.v12.i26.5885

INTRODUCTION

Adjacent segment disease (ASD) has become a highly concerning complication following low lumbar fusion surgery. Okuda *et al*[1] reported that incidence of radiologically ASD after posterior lumbar interbody fusion with pedicle screw fixation reached 19%, 49%, and 75% at 2, 5 and 10 years, respectively. In addition, ASD is an important factor affecting clinical outcomes[1]. Owing to the different definitions of ASD, its radiographic features differ presenting as adjacent segment instability, disc herniation, spinal canal stenosis, spondylolisthesis or retrolisthesis of the adjacent vertebra[2,3]. The clinical characteristics of ASD differ on different imaging modalities appearing as adjacent segment instability, spondylolisthesis or retrolisthesis appear at the short-term follow-up, or disc herniation and spinal canal stenosis of the adjacent segment at the long-term follow-up. Different pathogeneses can thus result in different imaging results[1,2]. Retrograde movement of cranial adjacent segments is common after transforaminal lumbar interbody fusion (TLIF). Although the risk factors for ASD have been previously investigated, no study has focus on the retrograde movement of cranial adjacent segments. However, to the best of our knowledge, there has been no study of the risk factors or clinical value of retrolisthesis of cranial adjacent segments. The present study was designed to quantitatively evaluate the radiographic and clinical data of patients who underwent TLIF, to identify the incidence, risk factors and clinical value of retrolisthesis of cranial adjacent segments.

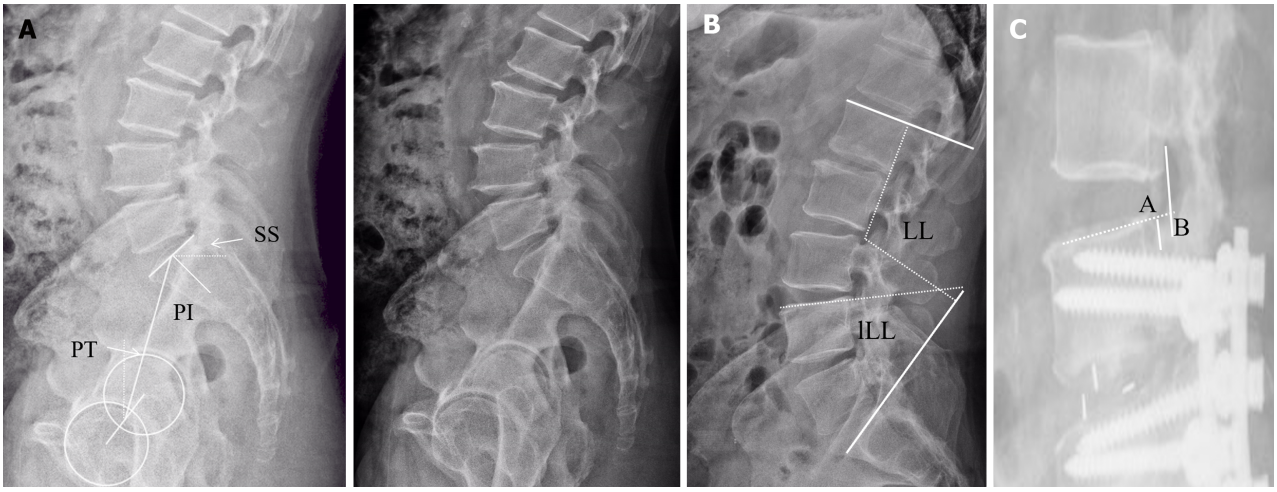

Figure 1 Pelvic and spinal parameters and retrograde distance of cranial adjacent segments. A: Pelvic incidence: The angle between the line perpendicular to the sacral plate at its midpoint and the line connecting this point to the axis of the femoral heads; Pelvic tilt: The angle between the line connecting the midpoint of the sacral plate to the femoral head axis and the vertical axis; Sacral slope: The angle between the superior plate of S1 and a horizontal line; B: Lumbar lordosis (LL): The angle between the superior endplate of the L1 vertebra and the superior endplate of the S1; Lower LL: The angle between the superior endplate of the L4 vertebra and the superior endplate of the S1; C: Retrograde distance of cranial adjacent segments: The distance between point A and point B; point A: The dorsal edges of the cranial endplate of the inferior vertebral, point B: The intersection point between the line crossing the dorsal edges of the caudal endplate of the superior vertebral and perpendicular to the cranial endplate of the inferior vertebral. PI: Pelvic incidence; PT: Pelvic tilt; LL: Lumbar lordosis; lLL: Lower LL; SS: Sacral slope.

MATERIALS AND METHODS

Subjects

The study was approved by the Institutional Review Board, and the clinical data of all patients who were diagnosed with degenerative lumbar disease and who underwent TLIF at our department between September 2015 and July 2021 were retrospectively reviewed. Inclusion criteria: (1) A diagnosis of degenerative lumbar disease, including lumbar disc herniation, lumbar spinal stenosis, lumbar spondylolisthesis; (2) Followed up for more than 2 years; and (3) Complete preoperative, postoperative and follow-up X-rays. Patients who previously underwent lumbar surgery or had a congenital spine deformity were excluded. In total, 91 patients, including 22 males and 69 females with an average age of 52.3 years (40-73 years), were ultimately enrolled. The mean duration of follow-up were 27.3 months (range 24-51 months). According to whether there was retrograde movement of the adjacent vertebral body on postoperative X-rays, the patients were divided into retrograde and nonretrograde groups.

Radiological assessment

Sagittal alignment of the spine and pelvis was assessed with Surgimap Spine software (Nemaris, Inc., New York, NY, United States). In line with previously described methods[4-7], three pelvic and three spinal parameters were measured on upright standing lateral radiographs of the lumbar spine: (1) Pelvic incidence (PI): The angle between the line perpendicular to the sacral plate at its midpoint and the line connecting this point to the axis of the femoral heads; (2) Pelvic tilt (PT): The angle between the line connecting the midpoint of the sacral plate to the femoral head axis and the vertical axis; (3) Sacral slope (SS): The angle between the superior plate of S1 and a horizontal line[8-11]; (4) Lumbar lordosis (LL): The angle between the superior endplate of the L1 vertebra and the superior endplate of the S1 vertebra; (5) Lower LL (lLL): The angle between the superior endplate of the L4 vertebra and the superior endplate of the S1 vertebra; and (6) Upper LL (uLL): The angle of LL minus lLL (Figure 1A and B). A positive angle was defined as lordosis and a negative angle was defined as kyphosis.

Retrograde distance of cranial adjacent segments: Distance between point A and point B (Figure 1C); point A: The dorsal edges of the cranial endplate of the inferior vertebra, point B: The intersection point between the line crossing the dorsal edges of the caudal endplate of the superior vertebra and the line perpendicular to the cranial endplate of the inferior vertebra. A distance > 3 mm was defined as unstable vertebral body slip.

|PI-LL| > 10° was defined as PT and LL mismatch. The lordosis distribution index (LDI) was defined as lLL/LL × 100%. A normal LDI was defined as 50%-80%. A LDI < 50% indicates insufficient lLL, and a LDI > 80% indicates excessive lLL[3,8,9].

Quality of life assessment

The Oswestry Disability Index (ODI) and Visual Analogue Scale (VAS) were used for preoperative, postoperative and final follow-up evaluations. The questionnaire results were recorded and statistically analyzed by two independent orthopedic surgeons, and inconclusive results were statistically analyzed again.

Statistical analysis

Data analysis was performed with SPSS 17.0 software (SPSS, Chicago, IL, United States). Continuous data are described as the mean ± SD (range). Paired *t* test was used to compare continuous variables between the two groups. Comparisons of categorical variables were analyzed with the χ^2 test. A *P*-value < 0.05 indicated statistical significance.

RESULTS

Ninety-one patients with degenerative lumbar diseases were included (22 males and 69 females), with an average age of 52.3 years (40-73 years). Retrograde movement of cranial adjacent segments was observed in 19 (20.9%) patients at the last follow-up (Figure 2). Table 1 summarizes the demographic data of the patients in the two groups. Age and the sex ratio were similar between the two groups. No significant differences were noted between the two groups in terms of the operation time, blood loss volume, follow-up time, fixed segment, fusion segment, or fixation of S1.

The surgery was successful in all patients. In the nonretrograde group, two patients experienced fat liquefaction, which healed after debridement. One patient experienced cerebrospinal fluid leakage but showed good recovery 9 days after endorhachis repair. In the retrograde group, one patient developed an infection and was cured after anti-inflammatory therapy. One patient presented with nerve root irritation, which disappeared on the seventh day after treatment with methylprednisolone and mecobalamin. There was no cage shifting, screw fracture or internal fixation loosening during the follow-up period in the nonretrograde group. One patient underwent revision surgery due to internal fixation failure. At the final follow-up, 4 patients in the nonretrograde group and 7 patients in the retrograde group were diagnosed with ASD.

Comparisons of the pelvic parameters and sagittal lumbar parameters between the two groups are presented in Table 2. The PI, SS and uLL were significantly greater in the retrograde group preoperatively, postoperatively and at the final follow-up ($P < 0.05$). Compared with those in the nonretrograde group, LL was significantly greater postoperatively and at the final follow-up ($P < 0.05$), but did not significantly differ before the operation ($P > 0.05$). In addition, the PT and lLL did not significantly differ between the two groups preoperatively, postoperatively or at the final follow-up ($P > 0.05$).

The sagittal morphology of the lumbar spine was also compared between the two groups (Table 3). No significant differences were detected in terms of |PI-LL| preoperatively, postoperatively or at the final follow-up ($P > 0.05$). There was no significant difference in the preoperative LDI between the two groups. The LDIs of the retrograde group were 68.1% ± 11.5% and 67.2% ± 11.9%, respectively, which were significantly lower than those of the nonretrograde group (75.7% ± 10.4% and 74.3% ± 9.4%, respectively) ($P < 0.05$). Moreover, patients in the retrograde group were noted had a higher incidence of insufficient lLL than those in the nonretrograde group ($P < 0.05$).

The ODI and VAS scores were significantly better in nonretrograde group postoperatively and at the final follow-up ($P < 0.05$), but did not significantly differ before the operation between the two groups ($P > 0.05$) (Table 4).

DISCUSSION

Lumbar retrolisthesis is a common occurrence, and its incidence and mechanism have been described in several studies. However, all of the studies concentrated on patients who did not undergo surgery. In a retrospective study by Zhu *et al* [5], the sagittal spinopelvic parameters of 105 patients (60 patients with retrolisthesis and 45 patients with anterolisthesis) and 40 healthy age-matched adults were measured and analyzed. They reported that the sagittal vertical axis, PI, SS, and LL in the retrolisthesis group were significantly lower than those in the anterolisthesis group and in the control group, whereas the thoracolumbar kyphosis (TLK) in the retrolisthesis group was significantly greater than that in the other 2 groups. They concluded that a low PI may contribute to the occurrence and progression of retrolisthesis. In contrast, another similar study reported that lumbar retrolisthesis could also occur under in patients with a high PI[10]. They concluded that lumbar retrolisthesis in patients with a high PI might be primarily associated with increased backward sliding forces at the hyper tilted vertebra in the large TLK segment and lumbar instability caused by disc degeneration and facet arthritis[10]. Currently, the mechanism underlying the backward displacement of the vertebra is unclear, and cannot provided a reliable theoretical reference for lumbar retrolisthesis following TLIF.

In our study, the patients in the retrograde group had a high PI preoperatively, postoperatively and at the final follow-up. The LL and uLL were significantly greater in the retrograde group postoperatively and at the final follow-up; however, the LL preoperatively and the lLL preoperatively, postoperatively and at the final follow-up did not significantly differ between the two groups. In the healthy adult population, the loss of lLL is the most important factor. Reconstruction of the lLL is the key point for ideal sagittal spine resconstruction[6]. For patients who underwent lLL short-segment spina fusion surgery, insufficient reestablishment of the lLL was compensated for hyperextension of the unfused uLL, which resulted in excessive cranial adjacent intervertebral space expansion to compensate for insufficient LL. According to a finite element analysis of biomechanics, Senteler *et al*[7] concluded that insufficient reestablishment of the lLL results in increased segmental joint loads in the unfused and fused lumbar spine, and predisposes patients to ASD after lumbar spinal fusion[7]. Our study also revealed that backward displacement of the cranial adjacent vertebra following low spinal fusion was correlated with insufficient reestablishment of the lLL for patients with a high PI. Patients with a high PI and who experience lLL reconstruction deficiency can cause forward progression the trunk. The uLL increases to maintain gravity balance, which results in an increase in adjacent segment backward shear force, and

Table 1 Patient demographic data, mean ± SD

	Nonretrograde group	Retrograde group	*t* value	*P* value
Age (year)	51.7 ± 10.6	52.4 ± 11.3	0.258	0.797
Sex (male/female)	18/54	4/15	0.128	0.721
Operation time (minute)	257.3 ± 46.9	264.7 ± 43.8	0.619	0.540
Blood loss (mL)	219.6 ± 49.3	207.7± 56.5	0.907	0.367
Follow-up time (month)	27.4 ± 6.3	26.9 ± 7.0		
Fixed segment	2.4 ±0.69	2.5 ± 0.74	0.554	0.581
Fusion segment				
1	59	14	0.646	0.421
2	13	5		
Fixation of S1				
Yes	12	5	0.921	0.337
No	60	14		

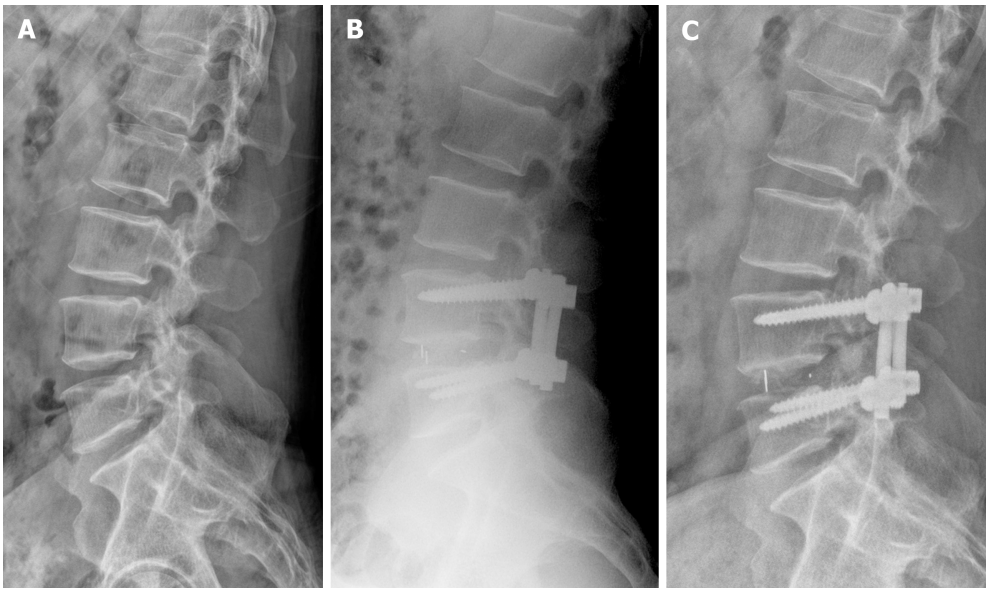

Figure 2 X-rays of a patient who underwent transforaminal lumbar interbody fusion surgery. A: Male, 51 years, lumbar disc herniation; B: postoperative X-ray: Pelvic incidence (PI) 57°, lumbar lordosis (LL) 59°, Lower lumbar lordosis 32°, |PI-LL| 2°, lordosis distribution index 54.2%; C: 27 months after the operation: Retrograde distance of cranial adjacent segments 4mm.

thus leads to backward sliding of the adjacent segment of the vertebra.

To determine the mechanical of properties cranial adjacent vertebra retrolisthesis following lumbar fusion surgery, PI-LL matching and sagittal lumbar morphology data were collected. There was no significant difference between the two groups with respect to PI-LL matching. However, in term of the distribution of LL, the LDI of the retrograde group was significantly lower postoperatively and at the final follow-up. Moreover, the proportion of patients with a LDI < 50% was significantly greater in the retrograde group than in the nonretrograde group. The results support the theoretical foundation of the mechanism of retrolisthesis in patients with a high PI. Based on these results, we believe that the distribution of LL should be considered as important as PI-LL matching in patients who undergo lumbar fusion surgery. Yilgor *et al*[11] evaluated the sagittal spinal parameters of patients following long-segment spine fusion surgery and reported that the PI-LL may be insufficient for predicting the proximal junction mechanics and internal fixation complications postoperatively. A low LDI should be considered; moreover, a lower LDI indicates significantly higher risks of mechanical and internal fixation complications. This study revealed that all of the following factors should be considered prior to reconstruction of LL through lumbar spinal surgery: The segments responsible for preoperative lordosis loss, the PI, and the distribution of LL. A full intervertebral bone graft and larger cage were selected and placed as front as possible in the intervertebral space to obtain satisfactory intervertebral lordosis and LL.

Table 2 Radiography parameters of the two groups, mean ± SD

	Nonretrograde group	Retrograde group	*t* value	*P* value
PI (°)				
Preoperative	47.9 ± 9.2	57.8 ± 10.6	4.041	< 0.001
Postoperative	49.2 ± 9.6	58.1 ± 11.4	3.454	0.008
Final follow-up	49.6 ± 10.3	57.2 ± 11.9	2.768	< 0.001
PT (°)				
Preoperative	20.5 ± 6.2	21.5 ± 6.4	0.621	0.536
Postoperative	15.6 ± 4.4	14.8 ± 5.6	0.665	0.508
Final follow-up	14.9 ± 3.9	15.3 ± 5.0	0.374	0.709
SS (°)				
Preoperative	27.9 ± 8.3	35.1 ± 8.2	3.371	< 0.001
Postoperative	35.8 ± 7.9	42.7 ± 10.8	3.123	0.002
Final follow-up	37.1 ± 9.4	41.9 ± 7.7	2.049	0.043
LL (°)				
Preoperative	34.1 ± 10.2	38.9 ± 14.8	1.649	0.103
Postoperative	48.7 ± 12.6	57.1 ± 10.6	2.664	0.009
Final follow-up	48.9 ± 9.7	56.3 ± 9.2	2.988	0.003
lLL (°)				
Preoperative	24.9 ± 4.8	27.0 ± 6.8	1.546	0.126
Postoperative	38.1 ± 8.9	38.7 ± 9.9	0.255	0.799
Final follow-up	37.4 ± 9.6	38.9 ± 8.5	0.619	0.537
uLL (°)				
Preoperative	8.1 ± 3.4	10.9 ± 4.7	2.934	0.004
Postoperative	12.5 ± 4.3	18.2 ± 6.4	4.605	< 0.001
Final follow-up	12.7 ± 5.6	17.6 ± 5.4	3.417	< 0.001

PI: Pelvic incidence; PT: Pelvic tilt; SS: Sacral slope; LL: Lumbar lordosis; lLL: Lower LL; uLL: Upper LL.

The ODI and VAS scores were significantly lower in the retrograde group postoperatively and at the final follow-up, which might be related to the local stress concentration and the nonideal distribution of LL. Adjacent segment shear forces and the burden on the functional units of the spine increase because the proximal adjacent intervertebral space expands and cranial adjacent vertebra retrolisthesis occurs, which leads to back pain[7]. At the same time, the long-term inability of the spine to perform compensatory function decreases the effect of surgery and lead to a lower quality of life [8]. Yilgor *et al*[11] confirmed that the distribution of LL is closely associated with long-term surgical effects and that the ideal distribution of LL could maintain long-term satisfactory quality of life.

Limitations of our study include its retrospective design, short follow-up duration and lack of systematic evaluation of the relationship between vertebral retrolisthesis and ASD. Vertebra retrolisthesis is a time-dependent complication, and a longer follow-up duration is needed to observe its incidence and clinical outcome. Theoretically, vertebral retrolisthesis is a form of ASD. Seven patients in the retrograde group and 4 patients in the nonretrograde group were diagnosed with ASD. Whether intraoperative facet joint damage could affect the posterior displacement of the vertebra was not mentioned in this study.

CONCLUSION

The incidence of proximal adjacent vertebra retrolisthesis after lower lumbar fusion is 20.9%, and a high PI and inappropriate LDI are risk factors. Backward sliding of the cranial adjacent vertebra to compensate for insufficient restoration of LL in patients with a high PI significantly affects surgical outcomes.

Table 3 Lumbar sagittal images of the patients in the two groups, mean ± SD

	Nonretrograde group	Retrograde group	*t* value	*P* value
|PI-LL| (°)				
Preoperative	13.9 ± 5.2	15.3 ± 5.8	1.019	0.311
Postoperative	1.9 ± 4.3	1.4 ± 3.6	0.465	0.643
Final follow-up	0.9 ± 2.1	1.2 ± 3.0	0.671	0.504
PI-LL matching				
Yes	63	16	0.142	0.706
No	9	3		
LDI (%)				
Preoperative	75.9 ± 14.9	71.1 ± 16.7	1.217	0.226
Postoperative	75.7 ± 10.4	68.1 ± 11.5	2.772	0.006
Final follow-up	74.3 ± 9.4	67.2 ± 11.9	2.764	0.006
Distribution of LL				
LDI < 50%	6	7	49.937	< 0.001
50% ≤ LDI < 80%	64	12		
80 ≤ LDI	2	0		

PI: Pelvic incidence; LL: Lumbar lordosis; ILL: Lower LL; LDI: Lordosis distribution index.

Table 4 Quality of life of the patients in the two groups, mean ± SD

	Nonretrograde group	Retrograde group	*t* value	*P* value
ODI score				
Preoperative	41.4 ± 11.9	40.8 ± 10.3	0.201	0.841
Postoperative	21.1 ± 7.2	26.1 ± 7.4	2.677	< 0.001
Final follow-up	18.0 ± 6.3	24.2 ± 4.6	4.009	< 0.001
VAS score				
Preoperative	7.0 ± 2.2	7.4 ± 2.5	0.685	0.495
Postoperative	2.2 ± 1.2	3.1 ± 1.6	2.703	0.008
Final follow-up	1.8 ± 1.1	2.9 ± 1.4	3.654	< 0.001

ODI: Oswestry Disability Index; VAS: Visual Analogue Scale.

ACKNOWLEDGEMENTS

I would like to express my gratitude to all those who helped me during the writing of this paper. My deepest gratitude goes first and foremost to my team members for their contribution to this paper, including research designed and performed, data collected and analyzed, manuscript wrote. Secondly, I would like to express my heartfelt gratitude to Professor Pei-An Lou, who helped me a lot about data analyzed. Finally, I am indebted to the editor and the reviewers for the time and effort on our paper.

FOOTNOTES

Author contributions: Xie DD, Zhu JJ, Zheng J, Cao L and Du SY designed the research study; Xie DD, Zhu JJ, Wang Y, Yang YM and Zhang QX performed the research; Zhu JJ and Wang Y contributed analytic tools; Xie DD, Zhu JJ and Wang Y analyzed the data and wrote the manuscript. All authors have read and approve the final manuscript.

Supported by The Youth Medicine Technology Innovation Project of Xuzhou Health Commission, No. XWKYHT20200026.

Institutional review board statement: The study was reviewed and approved by the Xuzhou First people's Hospital Institutional Review Board.

Informed consent statement: All study participants, or their legal guardian, provided informed written consent prior to study enrollment.

Conflict-of-interest statement: All the authors declare no conflicts of interest.

Data sharing statement: Technical appendix, statistical code, and dataset available from the corresponding author at dd2225@126.com.

STROBE statement: The authors have read the STROBE Statement-checklist of items, and the manuscript was prepared and revised according to the STROBE Statement-checklist of items.

Country of origin: China

ORCID number: Ding-Ding Xie 0009-0009-2100-8451.

S-Editor: Liu H
L-Editor: A
P-Editor: Cai YX

REFERENCES

1 **Okuda S**, Nagamoto Y, Matsumoto T, Sugiura T, Takahashi Y, Iwasaki M. Adjacent Segment Disease After Single Segment Posterior Lumbar Interbody Fusion for Degenerative Spondylolisthesis: Minimum 10 Years Follow-up. *Spine (Phila Pa 1976)* 2018; **43**: E1384-E1388 [PMID: 29794583 DOI: 10.1097/BRS.0000000000002710]

2 **Jeong TS**, Son S, Lee SG, Ahn Y, Jung JM, Yoo BR. Comparison of adjacent segment disease after minimally invasive versus open lumbar fusion: a minimum 10-year follow-up. *J Neurosurg Spine* 2022; **36**: 525-533 [PMID: 34740178 DOI: 10.3171/2021.7.SPINE21408]

3 **Bae JS**, Lee SH, Kim JS, Jung B, Choi G. Adjacent segment degeneration after lumbar interbody fusion with percutaneous pedicle screw fixation for adult low-grade isthmic spondylolisthesis: minimum 3 years of follow-up. *Neurosurgery* 2010; **67**: 1600-7; discussion 1607 [PMID: 21107190 DOI: 10.1227/NEU.0b013e3181f91697]

4 **Scemama C**, Magrino B, Gillet P, Guigui P. Risk of adjacent-segment disease requiring surgery after short lumbar fusion: results of the French Spine Surgery Society Series. *J Neurosurg Spine* 2016; **25**: 46-51 [PMID: 26967992 DOI: 10.3171/2015.11.SPINE15700]

5 **Zhu F**, Bao H, Liu Z, Zhu Z, He S, Qiu Y. Lumbar Retrolisthesis in Aging Spine: What are the Associated Factors? *Clin Spine Surg* 2017; **30**: E677-E682 [PMID: 28632553 DOI: 10.1097/BSD.0000000000000198]

6 **Kim SI**, Min HK, Ha KY, Park HY, Cho CH, Cho RK, Kim YH. Effects of Restoration of Sagittal Alignment on Adjacent Segment Degeneration in Instrumented Lumbar Fusions. *Spine (Phila Pa 1976)* 2020; **45**: E1588-E1595 [PMID: 32956253 DOI: 10.1097/BRS.0000000000003682]

7 **Senteler M**, Weisse B, Snedeker JG, Rothenfluh DA. Pelvic incidence-lumbar lordosis mismatch results in increased segmental joint loads in the unfused and fused lumbar spine. *Eur Spine J* 2014; **23**: 1384-1393 [PMID: 24647596 DOI: 10.1007/s00586-013-3132-7]

8 **Yilgor C**, Sogunmez N, Boissiere L, Yavuz Y, Obeid I, Kleinstück F, Pérez-Grueso FJS, Acaroglu E, Haddad S, Mannion AF, Pellise F, Alanay A; European Spine Study Group (ESSG). Global Alignment and Proportion (GAP) Score: Development and Validation of a New Method of Analyzing Spinopelvic Alignment to Predict Mechanical Complications After Adult Spinal Deformity Surgery. *J Bone Joint Surg Am* 2017; **99**: 1661-1672 [PMID: 28976431 DOI: 10.2106/JBJS.16.01594]

9 **Rothenfluh DA**, Mueller DA, Rothenfluh E, Min K. Pelvic incidence-lumbar lordosis mismatch predisposes to adjacent segment disease after lumbar spinal fusion. *Eur Spine J* 2015; **24**: 1251-1258 [PMID: 25018033 DOI: 10.1007/s00586-014-3454-0]

10 **Zhu W**, Kong C, Zhang S, Wang P, Sun X, Lu S. The radiographic characteristics and developmental mechanism of the lumbar degenerative retrolisthesis under a high-grade PI. *J Orthop Sci* 2021; **26**: 103-109 [PMID: 32205019 DOI: 10.1016/j.jos.2020.02.012]

11 **Yilgor C**, Sogunmez N, Yavuz Y, Abul K, Boissiére L, Haddad S, Obeid I, Kleinstück F, Sánchez Pérez-Grueso FJ, Acaroğlu E, Mannion AF, Pellise F, Alanay A; European Spine Study Group. Relative lumbar lordosis and lordosis distribution index: individualized pelvic incidence-based proportional parameters that quantify lumbar lordosis more precisely than the concept of pelvic incidence minus lumbar lordosis. *Neurosurg Focus* 2017; **43**: E5 [PMID: 29191103 DOI: 10.3171/2017.8.FOCUS17498]

World Journal of Clinical Cases

Submit a Manuscript: https://www.f6publishing.com

World J Clin Cases 2024 September 16; 12(26): 5893-5900

DOI: 10.12998/wjcc.v12.i26.5893

ISSN 2307-8960 (online)

ORIGINAL ARTICLE

Retrospective Study

Predictive value of diaphragm ultrasound for mechanical ventilation outcome in patients with acute exacerbation of chronic obstructive pulmonary disease

Lei-Lei Qu, Wen-Ping Zhao, Ji-Ping Li, Wei Zhang

Specialty type: Medicine, research and experimental

Provenance and peer review: Unsolicited article; Externally peer reviewed.

Peer-review model: Single blind

Peer-review report's classification

Scientific Quality: Grade C

Novelty: Grade B

Creativity or Innovation: Grade B

Scientific Significance: Grade B

P-Reviewer: Segal-Abramovich T

Received: May 7, 2024

Revised: June 7, 2024

Accepted: July 1, 2024

Published online: September 16, 2024

Processing time: 76 Days and 14.9 Hours

Lei-Lei Qu, Ji-Ping Li, Wei Zhang, The First Department of Respiratory and Critical Care Medical Center, The First People's Hospital of Baiyin City, Baiyin 730900, Gansu Province, China

Wen-Ping Zhao, Department of Nursing, The First People's Hospital of Baiyin City, Baiyin 730900, Gansu Province, China

Co-first authors: Lei-Lei Qu and Wen-Ping Zhao.

Co-corresponding authors: Ji-Ping Li and Wei Zhang.

Corresponding author: Ji-Ping Li, MBBS, Doctor, The First Department of Respiratory and Critical Care Medical Center, The First People's Hospital of Baiyin City, No. 222 Silong Road, Baiyin District, Baiyin 730900, Gansu Province, China. f18706985775@163.com

Abstract

BACKGROUND

Acute exacerbation of chronic obstructive pulmonary disease (AECOPD) is often combined with respiratory failure, which increases the patient's morbidity and mortality. Diaphragm ultrasound (DUS) has developed rapidly in the field of critical care in recent years. Studies with DUS monitoring diaphragm-related rapid shallow breathing index have demonstrated important results in guiding intensive care unit patients out of the ventilator. Early prediction of the indications for withdrawal of non-invasive ventilator and early evaluation of patients to avoid or reduce disease progression are very important.

AIM

To explore the predictive value of DUS indexes for non-invasive ventilation outcome in patients with AECOPD.

METHODS

Ninety-four patients with AECOPD who received mechanical ventilation in our hospital from January 2022 to December 2023 were retrospectively analyzed, and they were divided into a successful ventilation group (68 cases) and a failed ventilation group (26 cases) according to the outcome of ventilation. The clinical data of patients with successful and failed noninvasive ventilation were compared, and the independent predictors of noninvasive ventilation outcomes in

AECOPD patients were identified by multivariate logistic regression analysis.

RESULTS

There were no significant differences in gender, age, body mass index, complications, systolic pressure, heart rate, mean arterial pressure, respiratory rate, oxygen saturation, partial pressure of oxygen, oxygenation index, or time of inspiration between patients with successful and failed mechanical ventilation ($P > 0.05$). The patients with successful noninvasive ventilation had shorter hospital stays and lower partial pressure of carbon dioxide ($PaCO_2$) than those with failed treatment, while potential of hydrogen (pH), diaphragm thickening fraction (DTF), diaphragm activity, and diaphragm movement time were significantly higher than those with failed treatment ($P < 0.05$). pH [odds ratio (OR) = 0.005, $P < 0.05$], $PaCO_2$ (OR = 0.430, $P < 0.05$), and DTF (OR = 0.570, $P < 0.05$) were identified to be independent factors influencing the outcome of mechanical ventilation in AECOPD patients.

CONCLUSION

The DUS index DTF can better predict the outcome of non-invasive ventilation in AECOPD patients.

Key Words: Diaphragm ultrasound; Mechanical ventilation; Acute exacerbation of chronic obstructive pulmonary disease; Predictive value; Diaphragm thickening fraction; Diaphragm activity

Core Tip: There are few relevant literature reports on the predictive value of diaphragm ultrasound (DUS) indexes for mechanical ventilation therapy, so we conducted a study in which the clinical data of patients with successful and failed noninvasive ventilation were compared, and the independent predictors of noninvasive ventilation outcomes in acute exacerbation of chronic obstructive pulmonary disease (AECOPD) patients were identified by multivariate logistic regression analysis. It was found that the DUS index DTF can better predict the outcome of non-invasive ventilation therapy in AECOPD patients.

Citation: Qu LL, Zhao WP, Li JP, Zhang W. Predictive value of diaphragm ultrasound for mechanical ventilation outcome in patients with acute exacerbation of chronic obstructive pulmonary disease. *World J Clin Cases* 2024; 12(26): 5893-5900
URL: https://www.wjgnet.com/2307-8960/full/v12/i26/5893.htm
DOI: https://dx.doi.org/10.12998/wjcc.v12.i26.5893

INTRODUCTION

Chronic obstructive pulmonary disease (COPD), a common chronic respiratory disease, has become the third leading cause of death and is one of the most serious public health problems worldwide[1,2]. The definition of COPD is constantly being updated, and according to the 2021 Global Initiative for Chronic Obstructive Lung Disease, COPD was defined as a common, preventable, and treatable disease characterized by breathing difficulties and restricted airflow due to abnormalities in the airways and alveoli, which is often associated with high exposure to toxic particulates and gases [3]. COPD patients often suffer from acute exacerbation under infection, stress, and other factors. When acute exacerbation of COPD (AECOPD) occurs, it is often combined with respiratory failure, which increases the patient's morbidity and mortality[4]. Current studies have shown that dynamic pulmonary hyperinflation and intrinsic positive end expiratory pressure are the most important respiratory mechanical changes in COPD patients with respiratory failure[5, 6]. In patients with AECOPD, the above two respiratory mechanical functional abnormalities are further worsened, resulting in a significant increase in oxygen consumption and respiratory load of patients, exceeding the effective compensatory capacity of respiratory muscles such as the diaphragm, resulting in different degrees of hypoxemia and hypercapnia, and ultimately leading to type II respiratory failure[7,8]. If not rescued in time, respiratory failure can seriously endanger the patient's life. Currently, in addition to routine anti-infection, antispasmodic, reducing cough relieving, and removing phlegm, proper respiratory support is an important part of treatments for AECOPD[9,10].

Mechanical ventilation establishes a pressure difference between the airway opening and the alveoli to keep the airway open, thereby improving oxygenation and reversing hypoxia and carbon dioxide retention in the body[11]. Mechanical ventilation is clinically divided into two categories: Invasive ventilation and noninvasive ventilation[12]. Invasive ventilation involves the connection to the ventilator by invasive means such as tracheal intubation or tracheotomy, which is mostly used for critically ill patients. It can rapidly correct hypoxemia and hypercapnia, but it may also have unavoidable complications, such as ventilator-associated pneumonia and pneumatic injuries, and will bring a huge economic burden to the patient[13]. Noninvasive ventilation is a non-invasive way to connect a ventilator through a nasal mask or mask. It can provide patients with double-level pressure support and retain the natural defense function of the respiratory tract. Meanwhile, it can avoid lung injury and infection caused by invasive ventilation to the greatest extent. The value of noninvasive ventilation in the treatment of respiratory failure caused by AECOPD has been recognized, and the effective rate is more than 80% in patients with different degrees of carbon dioxide retention[14]. However, in clinical

application, due to the occurrence of adverse reactions such as man-machine incoordination, poor sputum drainage, suppressed fear, flatulence, and facial pressure sores, about 20% of patients cannot tolerate the treatment[15].

The diaphragm is one of the main respiratory muscles in the human body, and it is responsible for nearly 60% to 80% of respiratory activities. Function decline or even dysfunction of the diaphragm is one of the important factors leading to dyspnea and even respiratory failure in patients with AECOPD[16]. Therefore, the assessment of diaphragm function status becomes very important in the diagnosis and treatment of AECOPD[17]. Recently, the development of ultrasound medicine has led to a wide range of clinical studies using ultrasound to evaluate the structure and function of the diaphragm. Ultrasonography can more directly observe the changes in the diaphragm and has the advantages of being safe, non-invasive, economical, portable, accurate, and reproducible. Therefore, it is increasingly widely used in clinical assessment of diaphragm structure and function[18]. Diaphragm ultrasound (DUS) is rapidly developing in the field of critical care. Relevant studies have shown that the use of DUS to monitor the diaphragm-related rapid shallow breathing index to guide the weaning of ICU patients from the ventilator has achieved important research results. It can be used to early predict the indications for the withdrawal of non-invasive ventilators in AECOPD, and to assess the prognosis of patients in order to avoid or reduce the progression of the disease[19]. However, there are few relevant literature reports on the predictive value of DUS indicators for mechanical ventilation therapy, so we conducted such a study and now reports the results as follows.

MATERIALS AND METHODS

Patients

Ninety-four patients with AECOPD who received mechanical ventilation in our hospital from January 2022 to December 2023 were retrospectively analyzed, and they were divided into either a successful ventilation group (successful withdrawal, 68 cases) or a failed ventilation group (unsuccessful withdrawal, 26 cases) according to the outcome of ventilation. All enrolled patients provided written informed consent.

Inclusion and exclusion criteria

The inclusion criteria were: (1) Patients with a definite diagnosis of AECOPD; (2) Patients meeting the indications for noninvasive ventilation, such as those with respiratory acidosis or severe dyspnea but without contraindications to mechanical ventilation; and (3) Patients with complete clinical follow-up data.

The exclusion criteria were: (1) Patients with other serious life-threatening diseases, such as cerebrovascular diseases, lung malignancies, and airway obstruction; (2) Patients with severe pneumothorax, atelectasis, pneumonia, or interstitial lung disease, or those who planned to undergo surgery recently; (3) Patients with altered mental state, being prone to aspiration and unable to cooperate with the treatment; (4) Patients who had received systemic treatment for COPD before admission; and (5) Patients who were intolerant to respiratory muscle masks or needed emergency tracheal intubation.

Methods

The clinical data such as gender, age, body mass index (BMI), comorbidities, length of stay, systolic blood pressure, blood oxygen saturation, mean arterial pressure, respiratory rate, heart rate, blood gas analysis results, and DUS indexes were collected.

All patients were given basic treatment, including intravenous infusion of methylprednisolone. During hospitalization, the use and dosage of antibiotics were adjusted according to clinical symptoms and signs, sputum culture test, and the results of inflammatory marker detection. Meanwhile, treatments such as reducing phlegm and relieving asthma and maintaining internal environment were given. Noninvasive ventilator was used to give non-invasive ventilation treatment (oral and nasal mask ventilation). The ventilation mode was self-dominant touch/time-switching mode. The oxygen concentration fraction (FiO_2) in inhaled air was 30% to 60%, the inspiratory pressure was 8 to 14 cmH_2O, the expiratory pressure was 4 to 8 cmH_2O, the ratio of inhalation to exhalation was (1.5 to 2.0):1, and the respiratory rate was 10-14 times /min. When the pressure rose, the parameters would be adjusted at any time to make the blood oxygen saturation > 90%. Real-time attention was paid to the sputum excretion capacity of patients, and sputum drainage was performed regularly.

Evaluation of diaphragm ultrasound indicators

A doctor skilled in ultrasound operation performed ultrasound examination under the guidance of a superior doctor to evaluate diaphragm activity (DE), diaphragm movement time (E-T) index, and diaphragm thickening fraction (DTF). The patient was placed in the supine region with the head of the bed elevated by 20° to 40°, and the wide-frequency line array probe was placed at the junction of the anterior axillary line and the lower edge of the costal arch. The liver or spleen was used as the diaphragm transducer window. The DE was measured by M-mode ultrasound, and the average value was obtained by repeating the measurement three times. DE was calculated as the distance of the diaphragm from baseline at the end of inhalation - distance of the diaphragm from baseline at the end of expiration. E-T index was calculated as DE × time of inspiration (TI). For the measurement and evaluation of DTF, the ultrasound probe was placed at the 8th to 10th intercostal spaces in the right axillary midline for continuous observation, the patient was instructed to take 10-15 deep breaths, the changes in the thickness of the right diaphragm were captured during the respiration process, and the thicknesses of the diaphragm at the end of inhalation and expiration were measured on the images. After measuring five respiratory cycles, the average DTF was calculated. DTF was calculated as (end-inspiratory diaphragm thickness - end-

expiratory diaphragm thickness)/end-expiratory diaphragm thickness × 100%.

Statistical analysis

SPSS 27.0 software was applied for statistical analyses. Measurement data, expressed as the mean ± SD, were compared by the *t*-test. Count data, described as percentages, were compared between groups using the χ^2 test. Parameters with statistically significant differences in univariate analysis were included in the multivariate logistic regression model for analysis. The receiver operating characteristic (ROC) curve was drawn to analyze the predictive efficacy of each index for the treatment effect of non-invasive ventilation in AECOPD patients. The area under the ROC curve (AUC) was calculated. $P < 0.05$ was considered statistically significant.

RESULTS

General clinical information

Table 1 shows that there were no significant differences in gender, BMI, age, complications, systolic pressure, heart rate, mean arterial pressure, respiratory rate, oxygen saturation, partial pressure of oxygen, oxygenation index (PaO_2/FiO_2), or TI between patients with successful and failed mechanical ventilation ($P > 0.05$). Patients with successful noninvasive ventilation had lower hospital stays and partial pressure of carbon dioxide ($PaCO_2$) than those with failed treatment, while potential of hydrogen (pH), DTF, DE, and E-T index were significantly higher in patients with successful noninvasive ventilation than in those with failed treatment ($P < 0.05$).

Multivariate logistic regression analysis

Using the ventilation outcome as the dependent variable, and hospital stays, pH, $PaCO_2$, DTF, DE, and E-T index as independent variables, the multivariate logistic regression analysis indicated that pH [odds ratio (OR) = 0.005, $P < 0.05$], $PaCO_2$ (OR = 0.430, $P < 0.05$), and DTF (OR = 0.570, $P < 0.05$) were independent factors influencing the outcome of mechanical ventilation in AECOPD patients (Table 2).

Predictive efficacy for noninvasive ventilation

As shown in Table 3 and Figure 1, the AUC values of pH, $PaCO_2$, and DTF in predicting the outcome of non-invasive ventilation in AECOPD patients were 0.690, 0.833, and 0.876, respectively, suggesting good predictive efficacy ($P < 0.05$). The optimal cut-off values of pH, $PaCO_2$ and DTF were 7.33, 63.50 mmHg, and 21.35%, respectively.

DISCUSSION

AECOPD occurs often due to pneumothorax and pulmonary embolism caused by upper respiratory tract infection. Moreover, AECOPD can further aggravate the lung function damage and greatly increase the morbidity and mortality, seriously threatening the physical and mental health and life of the patients[20]. Non-invasive ventilation increases the minute ventilation of the lungs by giving constant volume or pressure, thus preventing alveolar collapse, reducing intrapulmonary shunts, improving the ventilation and blood flow ratio, promoting gas exchange, preserving spontaneous respiration in patients with AECOPD, and effectively decreasing the rate of endotracheal intubation[21]. The diaphragm is the most important respiratory muscle that performs 70% of the respiratory muscle functions, belongs to the muscle-fiber structure, and is located between the thoracic cavity and the abdominal cavity. In mechanical ventilation, ventilation failure is frequently seen, which is mainly due to diaphragm dysfunction[22]. Therefore, clinicians must objectively assess the function of the patient's diaphragm, so as to provide a reference basis for the successful withdrawal of the machine. In clinical practice, DUS is widely used for the assessment of diaphragm function due to its advantages of safety, feasibility, and reproducibility[23,24]. Our study results indicated that the $PaCO_2$ of patients with successful noninvasive ventilation was lower than that of patients with treatment failure, and the pH, DTF, DE, and E-T index were markedly higher than those of patients with treatment failure.

In patients with AECOPD, the decrease in expiratory time and restriction of expiratory flow along with the increase in respiratory rate lead to lung hyperinflation and expiratory restriction. If the mechanical load on the diaphragm is resistive, DE and TI will increase accordingly, resulting in an increase in the E-T index[25]. When the mechanical load is elastic, the diaphragm can counteract the pressure, and although TI decreases, DE may increase, resulting in a constant E-T index. However, if the diaphragm's contractile force decreases and is insufficient to overcome the excessive increase in mechanical load, mechanical injury will eventually occur as the diaphragm quickly depletes its functional reserve, resulting in a decrease in the E-T index[26]. Previous studies have demonstrated that DE and DTF are significantly reduced in patients with AECOPD, and diaphragmatic activity in COPD is closely related to airway obstruction, lung hyperinflation, ventilatory capacity, and dyspnea[27,28]. In a study of 30 mechanically ventilated COPD patients, Saeed *et al*[29] found that a DE of 11 mm had a sensitivity of 0.864, specificity of 0.875, and accuracy of 0.895 for predicting off-exit outcomes during a spontaneous respiration test. Since DE is related to inspiratory volume and creates pressure by increasing the patient's respiration, DE indicators are clinically significant only in the absence of ventilation support. In addition, since diaphragm movement is not only the result of diaphragm contraction and relaxation, DE may be affected by the position, which is more obvious when the patient is supine or sitting. And when the abdominal or chest pressure changes (ascites and atelectasis), the patient's diaphragm movement is significantly reduced, but it has nothing to do with

Table 1 Comparison of clinical data between two groups

Variable	Successful ventilation group (*n* = 68)	Failed ventilation group (*n* = 26)	t/χ^2	*P* value
Male [*n* (%)]	35 (51.47)	16 (61.54)	0.768	0.381
Age (years)	64.74 ± 4.25	65.77 ± 4.48	1.040	0.301
BMI (kg/m^2)	23.41 ± 2.12	23.62 ± 2.15	0.428	0.669
Complications [*n* (%)]				
Hypertension	39 (57.35)	16 (61.54)	0.136	0.713
Asthma	26 (38.24)	12 (46.15)	0.490	0.484
Diabetes	22 (32.35)	11 (42.31)	0.818	0.366
Systolic pressure (mmHg)	109.85 ± 21.09	107.77 ± 13.19	0.469	0.640
Mean arterial pressure (mmHg)	91.98 ± 9.79	90.85 ± 10.43	0.496	0.621
Heart rate (times/min)	83.79 ± 12.37	88.92 ± 12.56	1.790	0.077
Oxygen saturation (%)	87.93 ± 4.01	88.73 ± 5.39	0.788	0.433
Respiratory rate (times/min)	21.85 ± 3.24	23.04 ± 3.36	1.569	0.120
Hospital stays (d)	8.89 ± 3.14	11.46 ± 4.34	3.172	0.002
Blood gas analysis results				
pH	7.32 ± 0.16	7.21 ± 0.15	2.936	0.004
PaO_2 (mmHg)	47.69 ± 5.41	46.69 ± 5.66	0.790	0.432
$PaCO_2$ (mmHg)	62.21 ± 3.69	66.54 ± 3.02	5.334	< 0.001
PaO_2/FiO_2	98.35 ± 5.24	96.32 ± 5.16	1.687	0.095
Diaphragm ultrasound				
DTF (%)	24.18 ± 3.02	19.12 ± 3.18	7.172	< 0.001
DE (mm)	21.02 ± 2.26	17.42 ± 2.14	7.010	< 0.001
TI (s)	1.14 ± 0.19	1.06 ± 0.14	1.920	0.058
E-T index	2.39 ± 0.47	1.84 ± 0.33	5.411	< 0.001

pH: Potential of hydrogen; PaO2: Partial pressure of oxygen; PaCO2: Partial pressure of carbon dioxide; PaO2/FiO2: Oxygenation index; DTF: Diaphragm thickening fraction; DE: Diaphragm activity; E-T: Diaphragm movement time; TI: Time of inspiration.

Table 2 Multivariate logistic regression analysis of predictive indicators for non-invasive ventilation outcome in acute exacerbation of chronic obstructive pulmonary disease patients

Index	β	SE	Wald	*P* value	OR	95%CI
Hospital stays	0.221	0.156	1.999	0.157	1.247	0.918-1.694
pH	5.367	2.731	3.861	0.049	0.005	0.000-0.986
$PaCO_2$	0.845	0.350	5.841	0.016	0.430	0.216-0.852
DTF	0.562	0.219	6.613	0.010	0.570	0.371-0.875
DE	0.190	0.219	0.758	0.384	1.210	0.788-1.857
E-T index	2.401	2.020	1.413	0.234	0.091	0.002-4.747

OR: Odds ratio; CI: Confidence interval; pH: Potential of hydrogen; PaCO2: Partial pressure of carbon dioxide; DTF: Diaphragm thickening fraction; DE: Diaphragm activity; E-T: Diaphragm movement time.

Table 3 Predictive efficacy of potential of hydrogen, partial pressure of carbon dioxide, and diaphragm thickening fraction for non-invasive ventilation outcomes in patients with acute exacerbation of chronic obstructive pulmonary disease

Index	AUC	95%CI	*P* value	Sensitivity	Specificity
pH	0.690	0.576-0.804	0.005	0.885	0.500
$PaCO_2$	0.833	0.745-0.920	< 0.001	0.923	0.691
DTF	0.873	0.793-0.953	< 0.001	0.808	0.809

pH: Potential of hydrogen; PaCO2: Partial pressure of carbon dioxide; DTF: Diaphragm thickening fraction; AUC: Area under curve; CI: Confidence interval.

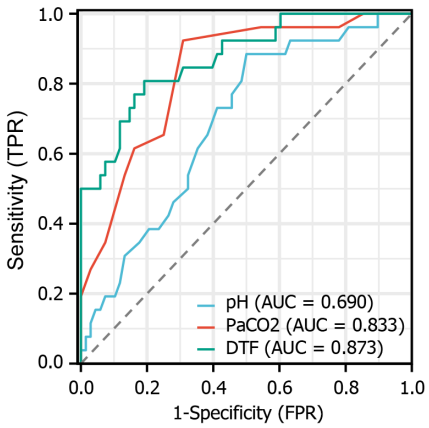

Figure 1 Receiver operating characteristic curves of potential of hydrogen, partial pressure of carbon dioxide, and diaphragm thickening fraction to predict outcome of non-invasive ventilation in acute exacerbation of chronic obstructive pulmonary disease patients. TPR: True positive rate; FPR: False positive rate; AUC: Area under curve; pH: Potential of hydrogen; PaCO2: Partial pressure of carbon dioxide; DTF: Diaphragm thickening fraction.

the diaphragm contractile function itself, so the accuracy is low.

The results of multivariate analysis in our study showed that pH, $PaCO_2$, and DTF were independent predictors of the therapeutic effect of noninvasive ventilation. Previous studies have consistently shown that the severity of hypercapnia and acidosis is related to the therapeutic effect of early non-invasive ventilation in AECOPD patients[30]. ROC curve analysis in our study displayed that the AUC of pH in predicting the therapeutic effect of noninvasive ventilation was 0.690, and when the optimal cut-off value was 7.33, the sensitivity and specificity were 0.885 and 0.500, respectively. $PaCO_2$ had an AUC of 0.833, with a sensitivity of 0.923 and specificity of 0.691 at the optimal cut-off value of 63.50 mmHg. In most patients with AECOPD, non-invasive ventilation should be given early when pH < 7.35 and $PaCO_2$ > 48.75 mmHg (6.5 kPa)[31]. Marchioni *et al*[32] showed that diaphragmatic dysfunction (DTF < 20%) on admission to the hospital in patients with AECOPD was an early predictor of failure of noninvasive ventilation, and was more accurate than baseline pH and $PaCO_2$. DTF is a good indicator of active diaphragm contraction compared with DE. In our study, the DTF of the failed group was significantly lower than that of the successful group, which was related to the decrease of diaphragm contraction function in the failed group. The optimal cut-off value of DTF was determined to be 21.35%, which is similar to the results of Antenora *et al*[33] (DTF < 20% is closely associated with failure of noninvasive ventilation in AECOPD patients). The study by Dres and Demoule[34] has shown that DTF is the gold standard for assessing diaphragm dysfunction. However, this study also had some limitations, such as single-center study, small sample size, no lung volume assessment, and no dynamic assessment of diaphragm function.

CONCLUSION

The DUS index DTF can better predict the outcome of non-invasive ventilation in AECOPD patients.

ACKNOWLEDGEMENTS

We thank the members of the First People's Hospital of Baiyin City for helpful discussions. We apologize to the scientists whose work could not be cited due to space limitations.

FOOTNOTES

Author contributions: Qu LL and Zhao WP performed the research; Li JP and Zhang W contributed new reagents and analytic tools; Qu LL, Zhao WP, Li JP, and Zhang W designed the research study, analyzed the data, and wrote the manuscript; all authors have read and approved the final manuscript.

Institutional review board statement: The study was reviewed and approved by the First People's Hospital of Baiyin City Institutional Review Board.

Informed consent statement: All study participants, or their legal guardians, provided informed written consent prior to study enrollment.

Conflict-of-interest statement: The authors declare that they have no conflict of interest to disclose.

Data sharing statement: No other data is available.

Country of origin: China

ORCID number: Ji-Ping Li 0009-0009-6585-5628; Wei Zhang 0009-0008-8674-6132.

S-Editor: Fan M
L-Editor: Wang TQ
P-Editor: Zhao S

REFERENCES

1 **Ferrera MC**, Labaki WW, Han MK. Advances in Chronic Obstructive Pulmonary Disease. *Annu Rev Med* 2021; **72**: 119-134 [PMID: 33502902 DOI: 10.1146/annurev-med-080919-112707]
2 **Eaton Turner E**, Jenks M. Cost-effectiveness analysis of the use of high-flow oxygen through nasal cannula in intensive care units in NHS England. *Expert Rev Pharmacoecon Outcomes Res* 2018; **18**: 331-337 [PMID: 29187008 DOI: 10.1080/14737167.2018.1411804]
3 **Huang X**, Mu X, Deng L, Fu A, Pu E, Tang T, Kong X. The etiologic origins for chronic obstructive pulmonary disease. *Int J Chron Obstruct Pulmon Dis* 2019; **14**: 1139-1158 [PMID: 31213794 DOI: 10.2147/COPD.S203215]
4 **MacLeod M**, Papi A, Contoli M, Beghé B, Celli BR, Wedzicha JA, Fabbri LM. Chronic obstructive pulmonary disease exacerbation fundamentals: Diagnosis, treatment, prevention and disease impact. *Respirology* 2021; **26**: 532-551 [PMID: 33893708 DOI: 10.1111/resp.14041]
5 **Roesthuis LH**, van der Hoeven JG, Guérin C, Doorduin J, Heunks LMA. Three bedside techniques to quantify dynamic pulmonary hyperinflation in mechanically ventilated patients with chronic obstructive pulmonary disease. *Ann Intensive Care* 2021; **11**: 167 [PMID: 34862945 DOI: 10.1186/s13613-021-00948-9]
6 **Xu XT**, Sun Q, Xie JF, Pan C, Yang Y, Qiu HB, Liu L. [Effect of neurally adjusted ventilatory assist on trigger of mechanical ventilation in acute exacerbation of chronic obstructive pulmonary disease patients with intrinsic positive end-expiratory pressure]. *Zhonghua Nei Ke Za Zhi* 2019; **58**: 43-48 [PMID: 30605950 DOI: 10.3760/cma.j.issn.0578-1426.2019.01.008]
7 **Neder JA**, Rocha A, Berton DC, O'Donnell DE. Clinical and Physiologic Implications of Negative Cardiopulmonary Interactions in Coexisting Chronic Obstructive Pulmonary Disease-Heart Failure. *Clin Chest Med* 2019; **40**: 421-438 [PMID: 31078219 DOI: 10.1016/j.ccm.2019.02.006]
8 **Dennis CJ**, Menadue C, Schneeberger T, Leitl D, Schoenheit-Kenn U, Hoyos CM, Harmer AR, Barnes DJ, Koczulla AR, Kenn K, Alison JA. Bilevel Noninvasive Ventilation During Exercise Reduces Dynamic Hyperinflation and Improves Cycle Endurance Time in Severe to Very Severe COPD. *Chest* 2021; **160**: 2066-2079 [PMID: 34224690 DOI: 10.1016/j.chest.2021.06.050]
9 **Chuang ML**. Tidal volume expandability affected by flow, dynamic hyperinflation, and quasi-fixed inspiratory time in patients with COPD and healthy individuals. *Chron Respir Dis* 2022; **19**: 14799731221133390 [PMID: 36210794 DOI: 10.1177/14799731221133390]
10 **de Souza GHM**, Ferraresi C, Moreno MA, Pessoa BV, Damiani APM, Filho VG, Dos Santos GV, Zamunér AR. Acute effects of photobiomodulation therapy applied to respiratory muscles of chronic obstructive pulmonary disease patients: a double-blind, randomized, placebo-controlled crossover trial. *Lasers Med Sci* 2020; **35**: 1055-1063 [PMID: 31654154 DOI: 10.1007/s10103-019-02885-3]
11 **Koltsida G**, Konstantinopoulou S. Long term outcomes in chronic lung disease requiring tracheostomy and chronic mechanical ventilation. *Semin Fetal Neonatal Med* 2019; **24**: 101044 [PMID: 31706921 DOI: 10.1016/j.siny.2019.101044]
12 **Bhatt SP**, Patel SB, Anderson EM, Baugh D, Givens T, Schumann C, Sanders JG, Windham ST, Cutter GR, Dransfield MT. Video Telehealth Pulmonary Rehabilitation Intervention in Chronic Obstructive Pulmonary Disease Reduces 30-Day Readmissions. *Am J Respir Crit Care Med* 2019; **200**: 511-513 [PMID: 30978302 DOI: 10.1164/rccm.201902-0314LE]
13 **Sun J**, Li Y, Ling B, Zhu Q, Hu Y, Tan D, Geng P, Xu J. High flow nasal cannula oxygen therapy versus non-invasive ventilation for chronic obstructive pulmonary disease with acute-moderate hypercapnic respiratory failure: an observational cohort study. *Int J Chron Obstruct Pulmon Dis* 2019; **14**: 1229-1237 [PMID: 31239658 DOI: 10.2147/COPD.S206567]
14 **Macrea M**, Oczkowski S, Rochwerg B, Branson RD, Celli B, Coleman JM 3rd, Hess DR, Knight SL, Ohar JA, Orr JE, Piper AJ, Punjabi NM,

Rahangdale S, Wijkstra PJ, Yim-Yeh S, Drummond MB, Owens RL. Long-Term Noninvasive Ventilation in Chronic Stable Hypercapnic Chronic Obstructive Pulmonary Disease. An Official American Thoracic Society Clinical Practice Guideline. *Am J Respir Crit Care Med* 2020; **202**: e74-e87 [PMID: 32795139 DOI: 10.1164/rccm.202006-2382ST]

15 **Duan J**, Wang S, Liu P, Han X, Tian Y, Gao F, Zhou J, Mou J, Qin Q, Yu J, Bai L, Zhou L, Zhang R. Early prediction of noninvasive ventilation failure in COPD patients: derivation, internal validation, and external validation of a simple risk score. *Ann Intensive Care* 2019; **9**: 108 [PMID: 31565779 DOI: 10.1186/s13613-019-0585-9]

16 **do Nascimento IB**, Fleig R. Mobility impact and methods of diaphragm monitoring in patients with chronic obstructive pulmonary disease: a systematic review. *Clinics (Sao Paulo)* 2020; **75**: e1428 [PMID: 31939562 DOI: 10.6061/clinics/2020/e1428]

17 **Liu Q**, Duan H, Lian A, Zhuang M, Zhao X, Liu X. Rehabilitation Effects of Acupuncture on the Diaphragm Dysfunction in Chronic Obstructive Pulmonary Disease: A Systematic Review. *Int J Chron Obstruct Pulmon Dis* 2021; **16**: 2023-2037 [PMID: 34262271 DOI: 10.2147/COPD.S313439]

18 **Jain S**, Nair G, Nuchin A, Uppe A. Study of the diaphragm in chronic obstructive pulmonary disease using ultrasonography. *Lung India* 2019; **36**: 299-303 [PMID: 31290414 DOI: 10.4103/lungindia.lungindia_466_18]

19 **An TJ**, Yoo YJ, Lim JU, Seo W, Park CK, Rhee CK, Yoon HK. Diaphragm Ultrasound is an Imaging Biomarker that Distinguishes Exacerbation Status from Stable Chronic Obstructive Pulmonary Disease. *Int J Chron Obstruct Pulmon Dis* 2022; **17**: 3-12 [PMID: 35018095 DOI: 10.2147/COPD.S341484]

20 **Xiang G**, Wu Q, Wu X, Hao S, Xie L, Li S. Non-invasive ventilation intervention during exercise training in individuals with chronic obstructive pulmonary disease: A systematic review and meta-analysis. *Ann Phys Rehabil Med* 2021; **64**: 101460 [PMID: 33271344 DOI: 10.1016/j.rehab.2020.101460]

21 **Sehgal IS**, Kalpakam H, Dhooria S, Aggarwal AN, Prasad KT, Agarwal R. A Randomized Controlled Trial of Noninvasive Ventilation with Pressure Support Ventilation and Adaptive Support Ventilation in Acute Exacerbation of COPD: A Feasibility Study. *COPD* 2019; **16**: 168-173 [PMID: 31161812 DOI: 10.1080/15412555.2019.1620716]

22 **Schulz A**, Erbuth A, Boyko M, Vonderbank S, Gürleyen H, Gibis N, Bastian A. Comparison of Ultrasound Measurements for Diaphragmatic Mobility, Diaphragmatic Thickness, and Diaphragm Thickening Fraction with Each Other and with Lung Function in Patients with Chronic Obstructive Pulmonary Disease. *Int J Chron Obstruct Pulmon Dis* 2022; **17**: 2217-2227 [PMID: 36118281 DOI: 10.2147/COPD.S375956]

23 **Santana PV**, Cardenas LZ, de Albuquerque ALP, de Carvalho CRR, Caruso P. Diaphragmatic ultrasound findings correlate with dyspnea, exercise tolerance, health-related quality of life and lung function in patients with fibrotic interstitial lung disease. *BMC Pulm Med* 2019; **19**: 183 [PMID: 31638951 DOI: 10.1186/s12890-019-0936-1]

24 **Ogan N**, Aydemir Y, EVrin T, Ataç GK, Baha A, Katipoğlu B, Süzen B, Akpınar EE. Diaphragmatic thickness in chronic obstructive lung disease and relationship with clinical severity parameters. *Turk J Med Sci* 2019; **49**: 1073-1078 [PMID: 31293145 DOI: 10.3906/sag-1901-164]

25 **Sharma M**, Chandrik Babu S. Assessment of excursion and thickness of diaphragm by ultrasound during acute exacerbation of chronic obstructive pulmonary disease and correlation with severity of airway obstruction. *J Assoc Pulmonologist Tamilnadu* 2023; **6**: 2-6 [DOI: 10.4103/japt.japt_38_22]

26 **Palkar A**, Narasimhan M, Greenberg H, Singh K, Koenig S, Mayo P, Gottesman E. Diaphragm Excursion-Time Index: A New Parameter Using Ultrasonography to Predict Extubation Outcome. *Chest* 2018; **153**: 1213-1220 [PMID: 29353023 DOI: 10.1016/j.chest.2018.01.007]

27 **Zhang J**, Zhang C, Yan L, Zhang L, Wan Y, Wang Q, Wang P, Xu J. Shear wave elastography of the diaphragm in acute exacerbation of chronic obstructive pulmonary disease: A prospective observational study. *Medicine (Baltimore)* 2023; **102**: e33329 [PMID: 36930088 DOI: 10.1097/MD.0000000000033329]

28 **Erfan A**, Khalil M, Elmaraghy A, Abd Elkader M. Ultrasonographic assessment of diaphragmatic performance in two chronic obstructive pulmonary disease phenotypes admitted with acute exacerbation and its relation to outcome. *Egypt J Chest Dis Tuberc* 2023; **72**: 139-146 [DOI: 10.4103/ecdt.ecdt_57_22]

29 **Saeed AM**, El Assal GI, Ali TM, Hendawy MM. Role of ultrasound in assessment of diaphragmatic function in chronic obstructive pulmonary disease patients during weaning from mechanical ventilation. *Egypt J Bronchol* 2016; **10**: 167-172 [DOI: 10.4103/1687-8426.184363]

30 **Steriade AT**, Johari S, Sargarovschi N, Necula D, Tudose CE, Ionita D, Bogdan MA, Bumbacea D. Predictors of outcome of noninvasive ventilation in severe COPD exacerbation. *BMC Pulm Med* 2019; **19**: 131 [PMID: 31319839 DOI: 10.1186/s12890-019-0892-9]

31 **Haji K**, Royse A, Green C, Botha J, Canty D, Royse C. Interpreting diaphragmatic movement with bedside imaging, review article. *J Crit Care* 2016; **34**: 56-65 [PMID: 27288611 DOI: 10.1016/j.jcrc.2016.03.006]

32 **Marchioni A**, Castaniere I, Tonelli R, Fantini R, Fontana M, Tabbì L, Viani A, Giaroni F, Ruggieri V, Cerri S, Clini E. Ultrasound-assessed diaphragmatic impairment is a predictor of outcomes in patients with acute exacerbation of chronic obstructive pulmonary disease undergoing noninvasive ventilation. *Crit Care* 2018; **22**: 109 [PMID: 29703214 DOI: 10.1186/s13054-018-2033-x]

33 **Antenora F**, Fantini R, Iattoni A, Castaniere I, Sdanganelli A, Livrieri F, Tonelli R, Zona S, Monelli M, Clini EM, Marchioni A. Prevalence and outcomes of diaphragmatic dysfunction assessed by ultrasound technology during acute exacerbation of COPD: A pilot study. *Respirology* 2017; **22**: 338-344 [PMID: 27743430 DOI: 10.1111/resp.12916]

34 **Dres M**, Demoule A. Diaphragm dysfunction during weaning from mechanical ventilation: an underestimated phenomenon with clinical implications. *Crit Care* 2018; **22**: 73 [PMID: 29558983 DOI: 10.1186/s13054-018-1992-2]

World Journal of Clinical Cases

Submit a Manuscript: https://www.f6publishing.com

World J Clin Cases 2024 September 16; 12(26): 5901-5907

DOI: 10.12998/wjcc.v12.i26.5901

ISSN 2307-8960 (online)

ORIGINAL ARTICLE

Retrospective Study

Influence of perinatal factors on full-term low-birth-weight infants and construction of a predictive model

Liang Xu, Xue-Juan Sheng, Lian-Ping Gu, Zu-Ming Yang, Zong-Tai Feng, Dan-Feng Gu, Li Gao

Specialty type: Medicine, research and experimental

Provenance and peer review: Unsolicited article; Externally peer reviewed.

Peer-review model: Single blind

Peer-review report's classification

Scientific Quality: Grade C

Novelty: Grade B

Creativity or Innovation: Grade C

Scientific Significance: Grade C

P-Reviewer: Okui T

Received: May 16, 2024

Revised: July 9, 2024

Accepted: July 12, 2024

Published online: September 16, 2024

Processing time: 67 Days and 13.7 Hours

Liang Xu, Li Gao, Department of Neonatology, Suzhou Ninth People's Hospital, Suzhou 215200, Jiangsu Province, China

Xue-Juan Sheng, Lian-Ping Gu, Department of Obstetrics, Suzhou Ninth People's Hospital, Suzhou 215200, Jiangsu Province, China

Zu-Ming Yang, Zong-Tai Feng, Dan-Feng Gu, Department of Neonatology, Suzhou Municipal Hospital, Suzhou 215008, Jiangsu Province, China

Corresponding author: Xue-Juan Sheng, BMed, Attending Doctor, Department of Obstetrics, Suzhou Ninth People's Hospital, No. 2666 Ludang Road, Suzhou 215200, Jiangsu Province, China. 13776158198@163.com

Abstract

BACKGROUND

Being too light at birth can increase the risk of various diseases during infancy.

AIM

To explore the effect of perinatal factors on term low-birth-weight (LBW) infants and build a predictive model. This model aims to guide the clinical management of pregnant women's healthcare during pregnancy and support the healthy growth of newborns.

METHODS

A retrospective analysis was conducted on data from 1794 single full-term pregnant women who gave birth. Newborns were grouped based on birth weight: Those with birth weight < 2.5 kg were classified as the low-weight group, and those with birth weight between 2.5 kg and 4 kg were included in the normal group. Multiple logistic regression analysis was used to identify the factors influencing the occurrence of full-term LBW. A risk prediction model was established based on the analysis results. The effectiveness of the model was analyzed using the Hosmer–Leme show test and receiver operating characteristic (ROC) curve to verify the accuracy of the predictions.

RESULTS

Among the 1794 pregnant women, there were 62 cases of neonatal weight < 2.5 kg, resulting in an LBW incidence rate of 3.46%. The factors influencing full-term LBW included low maternal education level [odds ratio (OR) = 1.416], fewer

prenatal examinations (OR = 2.907), insufficient weight gain during pregnancy (OR = 3.695), irregular calcium supplementation during pregnancy (OR = 1.756), and pregnancy hypertension syndrome (OR = 2.192). The prediction model equation was obtained as follows: Logit (*P*) = 0.348 × maternal education level + 1.067 × number of prenatal examinations + 1.307 × insufficient weight gain during pregnancy + 0.563 × irregular calcium supplementation during pregnancy + 0.785 × pregnancy hypertension syndrome − 29.164. The area under the ROC curve for this model was 0.853, with a sensitivity of 0.852 and a specificity of 0.821. The Hosmer–Leme show test yielded χ^2 = 2.185, *P* = 0.449, indicating a good fit. The overall accuracy of the clinical validation model was 81.67%.

CONCLUSION

The occurrence of full-term LBW is related to maternal education, the number of prenatal examinations, weight gain during pregnancy, calcium supplementation during pregnancy, and pregnancy-induced hypertension. The constructed predictive model can effectively predict the risk of full-term LBW.

Key Words: Pregnant women; Perinatal care; Low-birth-weight infants; Influencing factors; Prediction model

Core Tip: Being too light at birth can increase the risk of various diseases during infancy. While premature birth is a significant factor causing low-birth-weight (LBW) infants, it involves many uncontrollable factors. Our research innovation lies in excluding premature infants and analyzing only the factors influencing LBW in full-term infants, thereby revealing the impact of other characteristics on LBW. We discovered that full-term LBW is related to maternal education level, frequency of prenatal examinations, weight gain during pregnancy, calcium supplementation during pregnancy, and factors associated with preeclampsia. Based on these findings, we constructed a risk prediction model that can effectively predict the risk of full-term LBW.

Citation: Xu L, Sheng XJ, Gu LP, Yang ZM, Feng ZT, Gu DF, Gao L. Influence of perinatal factors on full-term low-birth-weight infants and construction of a predictive model. *World J Clin Cases* 2024; 12(26): 5901-5907
URL: https://www.wjgnet.com/2307-8960/full/v12/i26/5901.htm
DOI: https://dx.doi.org/10.12998/wjcc.v12.i26.5901

INTRODUCTION

The birth weight of a newborn reflects fetal growth and development in utero and is an important indicator of maternal and child health in a community. Low-birth-weight (LBW) refers to a birth weight of less than 2.5 kg[1,2]. Babies who are underweight at birth are at an increased risk of various diseases and even death during infancy[3]. LBW is also closely related to physical and mental development during adolescence and chronic conditions such as cardiovascular disease and diabetes in adulthood[4-6]. Thus, newborn birth weight is crucial for their future health. The causes of LBW are complex, as any factor affecting the rate of fetal growth and development in the uterus can lead to being underweight at birth[7]. Premature birth has been recognized as a significant cause of LBW, but it involves many uncontrollable factors, such as multiple births and low placental position. This study excludes premature infants, focusing only on the influencing factors of LBW in full-term infants. By doing so, we aim to reveal the impact of other characteristics on LBW and develop a corresponding risk prediction model. This model will provide valuable insights for the clinical management of pregnant women's healthcare during pregnancy and promote the healthy growth of newborns.

MATERIALS AND METHODS

Research object

This study retrospectively analyzed data from 1794 women with singleton full-term pregnancies who delivered at Suzhou Ninth People's Hospital from January 2019 to December 2021. The newborns were grouped based on birth weight: Those weighing less than 2.5 kg were classified as the low-weight group, and those weighing between 2.5 kg and 4 kg were classified as the normal group. The perinatal data from both groups were analyzed to identify the factors influencing full-term LBW and to construct a prediction model. Additionally, maternal data from 300 women with singleton full-term pregnancies who delivered at Suzhou Ninth People's Hospital from January 2022 to December 2023 were used for model validation. The maternal data from both periods met the following conditions: (1) Pregnant women aged 18 years or older; (2) Gestational age at delivery between 37 and 42 weeks, and (3) No history of anemia or smoking. Exclusion criteria included the following: (1) The presence of a malignant tumor; (2) Pregnancy through assisted reproductive technology; (3) Multiple pregnancies; and (4) Macrosomia (newborn weight greater than 4 kg).

Research methods

Data were collected from the hospital information system on maternal age, education level, number of prenatal examinations, weight gain during pregnancy, calcium supplementation during pregnancy, pregnancy complications (*e.g.*, pregnancy hypertension syndrome, gestational diabetes mellitus, and pregnancy-associated thyroid disease), fetal distress, premature rupture of membranes, amniotic fluid volume, gestational age at delivery, and the newborn's weight and sex within 1 hour of birth.

Pregnancy weight gain (gestational weight gain) was calculated as weight at delivery (kg) minus the weight before pregnancy (kg). According to the guidelines for maternal weight gain during pregnancy, weight gain ranges are classified as follows[8]: 12.5–18.0 kg for underweight before pregnancy, 11.5–16.0 kg for normal weight before pregnancy, and 7.0–11.5 kg for overweight before pregnancy. Weight gain within these ranges is considered appropriate, below the lower limit is classified as insufficient, and above the upper limit is considered excessive.

Calcium supplementation during pregnancy was defined according to the "Dietary Guidelines for Pregnant Women" [9]. Regular calcium supplementation is considered an intake of ≥ 1000 mg/day from early pregnancy.

Less amniotic fluid was determined using B-ultrasound, with a maximum vertical depth of the amniotic fluid dark area ≤ 2 cm or an amniotic fluid index ≤ 5 cm[10].

Statistical analysis

The Statistical Package for the Social Sciences 19.0 software was used for data analysis. Measurement data are expressed as mean ± SD and were compared between the two groups using the *t*-test. Categorical variables are expressed as frequencies and were compared using the χ^2 test. Multivariate logistic regression was employed to analyze the factors influencing LBW in full-term infants, and a prediction model formula was constructed based on these factors. The Hosmer–Leme show test and receiver operating characteristic (ROC) curve analysis were used to evaluate the performance of the model. Maternal data from different time points were included to test the accuracy of the model's predictions. Statistical significance was set at $P < 0.05$.

RESULTS

Single-factor analysis of full-term LBW occurrence

Among 1794 neonates born to singleton full-term pregnant women, 62 cases had a birth weight of less than 2.5 kg (low-weight group), resulting in an incidence rate of 3.46%. The remaining 1732 neonates had a birth weight between 2.5 kg and 4.0 kg (normal group). Statistically significant differences ($P < 0.05$) were found between the low-weight and normal groups regarding maternal education level, number of prenatal examinations, weight gain during pregnancy, regular calcium supplementation during pregnancy, and pregnancy hypertension syndrome (Table 1).

Multivariate logistic regression analysis of full-term LBW occurrence

The dependent variable was whether full-term newborns were LBW (0 = no, 1 = yes). Independent variables included the statistically significant indicators from the single-factor analysis (Table 1). Multivariate logistic regression analysis showed that low maternal education level, fewer prenatal examinations, insufficient weight gain during pregnancy, irregular calcium supplementation during pregnancy, and pregnancy hypertension syndrome were all significant influencing factors of full-term LBW ($P < 0.05$) (Table 2).

Construction of a predictive model for the risk of full-term LBW

The predictive model was constructed based on the regression coefficients and constant terms of the influencing factors identified through multivariate logistic regression analysis (Table 2). The risk prediction model equation is as follows: Logit (P) = 0.348 × maternal education level (0 = high school and above; 1 = junior high school and below) + 1.067 × number of prenatal examinations (actual value) + 1.307 × insufficient weight gain during pregnancy (0 = no; 1 = yes) + 0.563 × calcium supplementation during pregnancy (0 = regular; 1 = irregular) + 0.785 × pregnancy hypertension syndrome (0 = no; 1 = yes) − 29.164. The area under the ROC curve of the risk prediction model was 0.853 (95%CI: 0.802–0.914), with a sensitivity of 0.852 and a specificity of 0.821 (Figure 1). The Hosmer–Leme show goodness-of-fit test showed that the predicted value of the model and the actual value were $\chi^2 = 2.185$, $P = 0.449$, demonstrating a good fit.

Validation effect of risk prediction model for full-term LBW

The model was validated using data from 300 full-term deliveries at Suzhou Ninth People's Hospital from January 2022 to December 2023. The sensitivity of the model in predicting the risk of full-term LBW was 83.33% (10/12), the specificity was 81.59% (235/288), and the accuracy rate was 81.67% (245/300) (Table 3).

DISCUSSION

The occurrence of full-term LBW is complex and likely results from the interaction of multiple factors. Previous research by Chinese scholars, who surveyed 103678 newborns in 39 hospitals across 14 provinces, found an LBW incidence of 7.21%[11]. In contrast, our study found the incidence of full-term LBW to be 3.46% (62/1794), which is significantly lower.

Table 1 Single-factor analysis of full-term low-birth-weight, *n* (%)

Factor	Low-weight group	Normal group	t/χ^2 value	*P* value
Maternal age (years) (mean ± SD)	28.24 ± 4.09	28.14 ± 4.39	0.685	0.495
Maternal education level			14.628	< 0.001
Junior high school and below	27 (43.55)	392 (22.63)		
High school and above	35 (56.45)	1340 (77.37)		
Frequency of prenatal examination (times) (mean ± SD)	10.01 ± 0.35	10.57 ± 0.39	8.278	< 0.001
Weight gain during pregnancy				
Insufficient	37 (59.68)	119 (6.87)	210.361	< 0.001
Suitable	21 (33.87)	1412 (81.52)		
Overweight	4 (6.45)	201 (11.61)		
Calcium supplementation during pregnancy			15.232	< 0.001
Rule	13 (20.97)	798 (46.07)		
Irregularity	49 (79.03)	934 (53.93)		
Pregnancy hypertension syndrome			12.162	< 0.001
Yes	9 (14.52)	81 (4.68)		
No	53 (85.48)	1651 (95.32)		
Gestational diabetes			0.548	0.459
Yes	7 (11.29)	254 (14.67)		
No	55 (88.71)	1478 (85.33)		
Pregnancy complicated with thyroid disease			0.254	0.614
Yes	4 (6.45)	87 (5.02)		
No	58 (93.55)	1645 (94.98)		
Fetal distress			1.386	0.239
Yes	8 (12.90)	149 (8.60)		
No	54 (87.10)	1583 (91.40)		
Premature rupture of membranes			2.547	0.110
Yes	6 (9.68)	88 (5.08)		
No	56 (90.32)	1644 (94.92)		
Oligohydramnios			2.968	0.085
Yes	5 (8.06)	65 (3.75)		
No	57 (91.94)	1667 (96.25)		
Gestational weeks at delivery (weeks) (mean ± SD)	38.43 ± 0.96	38.72 ± 1.13	1.515	0.132
Neonatal sex			2.882	0.090
Male	22 (35.48)	804 (46.42)		
Female	40 (64.52)	928 (53.58)		

This discrepancy may be due to the exclusion of premature births and multiple pregnancies in this study, as well as regional economic differences that impact LBW rates.

There is a correlation between an individual's educational level and their professional environment and living standards. Kundu *et al*[12] reported that low education levels in pregnant women, combined with a low family wealth index, have a cumulative effect on LBW, which is consistent with our findings. Pregnant women with higher education levels are more likely to have better knowledge of pregnancy care and maternal and child health, which promotes fetal development and growth. Conversely, those with lower education levels often have poorer economic conditions[13,14], leading to limited access to nutrition and healthcare[15]. This can result in neglect of nutrition and healthcare during pregnancy, adversely affecting fetal development and increasing the risk of LBW.

Table 2 Results of multivariate logistic regression analysis

Variable	β	SE	χ^2	*P* value	OR (95%CI)
Low level of maternal education	0.348	0.134	6.744	0.012	1.416 (1.058–2.975)
Low number of prenatal examinations	1.067	0.282	14.316	< 0.001	2.907 (1.893–6.278)
Insufficient weight gain during pregnancy	1.307	0.329	15.782	< 0.001	3.695 (2.092–7.455)
Irregular calcium supplementation during pregnancy	0.563	0.204	7.617	0.009	1.756 (1.146–3.984)
Pregnancy hypertension syndrome	0.785	0.226	12.065	< 0.001	2.192 (1.423–5.159)
Constant	−29.164	6.574	19.680	< 0.001	-

Table 3 Predicted and actual values of the model

Model prediction results	Actual results		Total	Sensitivity	Specificity	Accuracy
	LBW infants	Normal-birth-weight infants				
LBW infants	10	53	63			
Normal-birth-weight infants	2	235	237			
Total	12	288	300	83.33	81.59	81.67

LBW: Low-birth-weight.

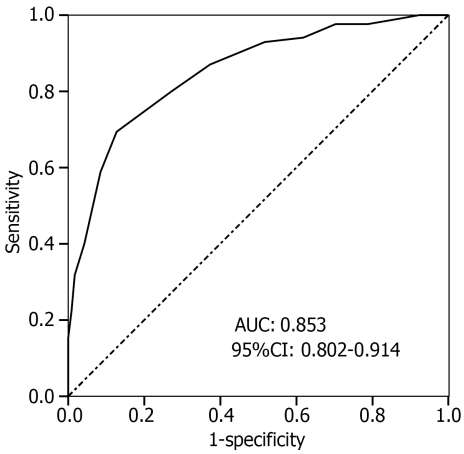

Figure 1 Evaluation of the receiver operating characteristic curve for the full-term low-birth-weight risk prediction model. AUC: Area under the receiver operating characteristic curve.

Prenatal examination is crucial for the timely detection of abnormal characteristics in pregnant women, such as gestational hypertension, umbilical cord abnormalities, and placental abnormalities. Bellizzi *et al*[16] demonstrated that inadequate prenatal care consultations are associated with LBW. Nagamine *et al*[17] similarly found that fewer prenatal examinations during pregnancy increased the risk of fetal LBW, aligning with the findings of this study. Some pregnant women may not undergo frequent prenatal examinations, which hinders doctors from timely monitoring the health status of both the pregnant woman and fetal development. This situation is particularly critical for pregnant women with abnormal conditions, potentially leading to missed treatment opportunities that are essential for normal fetal development and could have irreversible consequences. Weight gain during pregnancy significantly impacts maternal and infant outcomes[18]. Sun *et al*[19] showed that insufficient weight gain during pregnancy significantly affects newborn birth weight, consistent with the findings of this study. Insufficient weight gain is primarily linked to inadequate nutritional intake during pregnancy. Insufficient nutrition causes low energy substrate levels (such as lipids and amino acids) in the mother, which fails to provide adequate nutritional energy for the fetus, thereby affecting normal fetal development and increasing the risk of LBW. Moreover, poor maternal nutrition adversely affects the intrauterine environment, further compromising fetal development and increasing the risk of LBW.

Calcium is essential for the body and crucial for the health of pregnant women and normal fetal development[20,21]. China's dietary guidelines recommend a daily calcium supplement of 1000–1200 mg from early pregnancy[9]. Cormick *et al*[22] found that over 50% of pregnant women in China have insufficient calcium intake during pregnancy. This study

identified irregular calcium supplementation during pregnancy as a contributing factor to full-term LBW. Insufficient calcium supplementation may result from increased maternal blood volume during fetal growth, leading to decreased maternal blood calcium levels. Relying solely on daily meals may not meet the calcium needs of both the mother and fetus, potentially impairing fetal development and increasing LBW risk.

Pregnancy-induced hypertension is characterized by elevated blood pressure[23]. Getaneh *et al*[24] demonstrated that gestational hypertension significantly impacts newborn birth weight, consistent with our findings. The increase in blood pressure can induce continuous fluctuations and shear forces that damage vascular walls, leading to vascular endothelial injury and spasmodic contractions in uterine placental arteries[25,26]. This process results in placental and uterine ischemia and hypoxia, which in turn disrupts normal fetal development and increases the risk of LBW.

The occurrence of full-term LBW is primarily due to the lack of risk assessment for pregnant women during pregnancy, leading to insufficient early prevention. The logistic regression model, a generalized linear regression analysis model, is often used in clinical practice for disease diagnosis or to explore the influencing factors of diseases. This method can effectively demonstrate the relationship between independent variables and dependent variables. In this study, a predictive model was constructed based on the factors influencing the occurrence of full-term LBW. After validation, the model's overall accuracy was 81.67%, indicating that it is highly effective in predicting the risk of full-term LBW. This model can help identify high-risk populations in clinical practice. By incorporating factors such as the education level of pregnant women, frequency of prenatal examinations, weight gain during pregnancy, regular calcium supplementation during pregnancy, and the presence of preeclampsia, the model can calculate the potential risk of LBW for full-term fetuses. This enables the development of personalized management measures based on the probability of risk. For high-risk pregnant women, it is essential to strengthen pregnancy health education, guide them to adhere to standardized prenatal examinations, maintain a reasonable diet and nutrition, actively prevent pregnancy complications, and ultimately reduce the incidence of LBW.

This study is limited by its single-center retrospective design. Therefore, the clinical practicality and generalizability of the predictive model need to be further validated and optimized through prospective studies with larger sample sizes to improve the predictive performance of the model.

CONCLUSION

In summary, the occurrence of full-term LBW is related to low educational levels in pregnant women, fewer prenatal examinations, insufficient weight gain during pregnancy, irregular calcium supplementation during pregnancy, and pregnancy-induced hypertension. Based on these factors, the predictive model for full-term LBW risk demonstrates good discrimination.

FOOTNOTES

Author contributions: Xu L and Sheng XJ designed the study and wrote the manuscript; Xu L designed the study and provided clinical data; Xu L, Sheng XJ, Gu LP, Yang ZM, Feng ZT, Gu DF, and Gao L contributed to the data analysis; Xu L and Sheng XJ reviewed the research; all authors approved this research.

Institutional review board statement: The study was reviewed and approved by the Ethics Committee of Suzhou Ninth People's Hospital.

Informed consent statement: The study was reviewed and approved by the Ethics Committee of Suzhou Ninth People's Hospital approved the exemption for informed consent.

Conflict-of-interest statement: The authors declare no conflicts of interest.

Data sharing statement: The data used in this study can be obtained from the corresponding author upon request.

Country of origin: China

ORCID number: Xue-Juan Sheng 0009-0004-8260-0241.

S-Editor: Luo ML
L-Editor: A
P-Editor: Cai YX

REFERENCES

1 **Tchamo ME**, Prista A, Leandro CG. Low birth weight, very low birth weight and extremely low birth weight in African children aged between 0 and 5 years old: a systematic review. *J Dev Orig Health Dis* 2016; **7**: 408-415 [PMID: 27072315 DOI: 10.1017/S2040174416000131]

2 **Chung YH**, Hwang IS, Jung G, Ko HS. Advanced parental age is an independent risk factor for term low birth weight and macrosomia. *Medicine (Baltimore)* 2022; **101**: e29846 [PMID: 35777059 DOI: 10.1097/MD.0000000000029846]

3 **Gupta S**, Adhisivam B, Bhat BV, Plakkal N, Amala R. Short Term Outcome and Predictors of Mortality Among Very Low Birth Weight Infants - A Descriptive Study. *Indian J Pediatr* 2021; **88**: 351-357 [PMID: 32813195 DOI: 10.1007/s12098-020-03456-z]

4 **Durá-Travé T**, San Martín-García I, Gallinas-Victoriano F, Chueca Guindulain MJ, Berrade-Zubiri S. [Catch-up growth and associated factors in very low birth weight infants]. *An Pediatr (Engl Ed)* 2020; **93**: 282-288 [PMID: 31983650 DOI: 10.1016/j.anpedi.2019.06.017]

5 **Yadav DK**, Shukla GS, Gupta N, Shrestha N, Singh A, Kaphle HP. Maternal and Obstetric Factors Associated with Low Birth Weight. *J Nepal Health Res Counc* 2020; **17**: 443-450 [PMID: 32001846 DOI: 10.33314/jnhrc.v17i4.2263]

6 **Nakano Y**. Adult-Onset Diseases in Low Birth Weight Infants: Association with Adipose Tissue Maldevelopment. *J Atheroscler Thromb* 2020; **27**: 397-405 [PMID: 31866623 DOI: 10.5551/jat.RV17039]

7 **Bonnar K**, Fraser D. Extrauterine Growth Restriction in Low Birth Weight Infants. *Neonatal Netw* 2019; **38**: 27-33 [PMID: 30679253 DOI: 10.1891/0730-0832.38.1.27]

8 **Institute of Medicine (US) and National Research Council (US) Committee to Reexamine IOM Pregnancy Weight Guidelines**. Weight Gain During Pregnancy: Reexamining the Guidelines. Rasmussen KM, Yaktine AL, editors. Washington (DC): National Academies Press (US); 2009 [PMID: 20669500]

9 **Hovdenak N**, Haram K. Influence of mineral and vitamin supplements on pregnancy outcome. *Eur J Obstet Gynecol Reprod Biol* 2012; **164**: 127-132 [PMID: 22771225 DOI: 10.1016/j.ejogrb.2012.06.020]

10 **Zilberman Sharon N**, Pekar-Zlotin M, Kugler N, Accart Z, Nimrodi M, Melcer Y, Cuckle H, Maymon R. Oligohydramnios: how severe is severe? *J Matern Fetal Neonatal Med* 2022; **35**: 5754-5760 [PMID: 33645394 DOI: 10.1080/14767058.2021.1892068]

11 **Dong BQ**, You JP, Liang QY, Lyu W, Ma JF, Wei HW, Li H. [Study on the distribution and related factors of birth weight of live births in Guangxi Zhuang Autonomous Region of China from 2016 to 2018]. *Zhong hua Yu Fang Yi Xue Za Zhi* 2019; **53**: 1259-1264 [PMID: 31795583 DOI: 10.3760/cma.j.issn.0253-9624.2019.12.011]

12 **Kundu RN**, Ghosh A, Chhetri B, Saha I, Hossain MG, Bharati P. Regional with urban-rural variation in low birth weight and its determinants of Indian children: findings from National Family Health Survey 5 data. *BMC Pregnancy Childbirth* 2023; **23**: 616 [PMID: 37641012 DOI: 10.1186/s12884-023-05934-6]

13 **Altenhöner T**, Köhler M, Philippi M. The Relevance of Maternal Socioeconomic Characteristics for Low Birth Weight - a Case-Control Study. *Geburtshilfe Frauenheilkd* 2016; **76**: 248-254 [PMID: 27065486 DOI: 10.1055/s-0042-100204]

14 **Khatun S**, Rahman M. Quality of antenatal care and its dose-response relationship with birth weight in a maternal and child health training institute in Bangladesh. *J Biosoc Sci* 2008; **40**: 321-337 [PMID: 18005477 DOI: 10.1017/S0021932007002532]

15 **Sebayang SK**, Dibley MJ, Kelly PJ, Shankar AV, Shankar AH; SUMMIT Study Group. Determinants of low birthweight, small-for-gestational-age and preterm birth in Lombok, Indonesia: analyses of the birthweight cohort of the SUMMIT trial. *Trop Med Int Health* 2012; **17**: 938-950 [PMID: 22943372 DOI: 10.1111/j.1365-3156.2012.03039.x]

16 **Bellizzi S**, Padrini S. Quality utilization of antenatal care and low birth weight: evidence from 18 demographic health surveys. *East Mediterr Health J* 2020; **26**: 1381-1387 [PMID: 33226106 DOI: 10.26719/emhj.20.055]

17 **Nagamine M**, Matsumura K, Tsuchida A, Inadera H; Japan Environment and Children's Study (JECS) Group. Relationship between prenatal checkup status and low birth weight: a nationwide birth cohort-the Japan Environment and Children's Study. *Ann Epidemiol* 2023; **83**: 8-14 [PMID: 37094623 DOI: 10.1016/j.annepidem.2023.04.008]

18 **Dalfra' MG**, Burlina S, Lapolla A. Weight gain during pregnancy: A narrative review on the recent evidences. *Diabetes Res Clin Pract* 2022; **188**: 109913 [PMID: 35568262 DOI: 10.1016/j.diabres.2022.109913]

19 **Sun Y**, Shen Z, Zhan Y, Wang Y, Ma S, Zhang S, Liu J, Wu S, Feng Y, Chen Y, Cai S, Shi Y, Ma L, Jiang Y. Effects of pre-pregnancy body mass index and gestational weight gain on maternal and infant complications. *BMC Pregnancy Childbirth* 2020; **20**: 390 [PMID: 32631269 DOI: 10.1186/s12884-020-03071-y]

20 **Oh C**, Keats EC, Bhutta ZA. Vitamin and Mineral Supplementation During Pregnancy on Maternal, Birth, Child Health and Development Outcomes in Low- and Middle-Income Countries: A Systematic Review and Meta-Analysis. *Nutrients* 2020; **12**: 491 [PMID: 32075071 DOI: 10.3390/nu12020491]

21 **Farias PM**, Marcelino G, Santana LF, de Almeida EB, Guimarães RCA, Pott A, Hiane PA, Freitas KC. Minerals in Pregnancy and Their Impact on Child Growth and Development. *Molecules* 2020; **25**: 5630 [PMID: 33265961 DOI: 10.3390/molecules25235630]

22 **Cormick G**, Betrán AP, Romero IB, Lombardo CF, Gülmezoglu AM, Ciapponi A, Belizán JM. Global inequities in dietary calcium intake during pregnancy: a systematic review and meta-analysis. *BJOG* 2019; **126**: 444-456 [PMID: 30347499 DOI: 10.1111/1471-0528.15512]

23 **Reddy S**, Jim B. Hypertension and Pregnancy: Management and Future Risks. *Adv Chronic Kidney Dis* 2019; **26**: 137-145 [PMID: 31023448 DOI: 10.1053/j.ackd.2019.03.017]

24 **Getaneh T**, Negesse A, Dessie G, Desta M. The impact of pregnancy induced hypertension on low birth weight in Ethiopia: systematic review and meta-analysis. *Ital J Pediatr* 2020; **46**: 174 [PMID: 33243285 DOI: 10.1186/s13052-020-00926-0]

25 **Wang L**, Cheng L, Zhang S, Su M, Jin Y, Luo D. Mediation effect of pregnancy-induced hypertension on the association between assisted reproductive technology and adverse neonatal outcomes: a population-based study. *BMC Pregnancy Childbirth* 2023; **23**: 385 [PMID: 37231502 DOI: 10.1186/s12884-023-05694-3]

26 **Liu Y**, Li N, An H, Li Z, Zhang L, Li H, Zhang Y, Ye R. Impact of gestational hypertension and preeclampsia on low birthweight and small-for-gestational-age infants in China: A large prospective cohort study. *J Clin Hypertens (Greenwich)* 2021; **23**: 835-842 [PMID: 33507600 DOI: 10.1111/jch.14176]

World Journal of Clinical Cases

Submit a Manuscript: https://www.f6publishing.com

World J Clin Cases 2024 September 16; 12(26): 5908-5921

DOI: 10.12998/wjcc.v12.i26.5908

ISSN 2307-8960 (online)

ORIGINAL ARTICLE

Retrospective Study

Magnetic resonance imaging-based radiomics model for preoperative assessment of risk stratification in endometrial cancer

Zhi-Yao Wei, Zhe Zhang, Dong-Li Zhao, Wen-Ming Zhao, Yuan-Guang Meng

Specialty type: Medicine, research and experimental

Provenance and peer review: Unsolicited article; Externally peer reviewed.

Peer-review model: Single blind

Peer-review report's classification

Scientific Quality: Grade B

Novelty: Grade B

Creativity or Innovation: Grade B

Scientific Significance: Grade B

P-Reviewer: Kotelevets SM

Received: May 26, 2024

Revised: June 19, 2024

Accepted: July 3, 2024

Published online: September 16, 2024

Processing time: 57 Days and 11.2 Hours

Zhi-Yao Wei, Zhe Zhang, Dong-Li Zhao, Yuan-Guang Meng, Department of Obstetrics and Gynecology, Seventh Medical Center of Chinese People's Liberation Army General Hospital, Beijing 100700, China

Wen-Ming Zhao, National Genomics Data Center and Chinese Academy of Sciences Key Laboratory of Genome Sciences and Information, Beijing Institute of Genomics, Chinese Academy of Sciences and China National Center for Bioinformation, Beijing 100700, China

Corresponding author: Yuan-Guang Meng, PhD, Chief Doctor, Surgeon, Department of Obstetrics and Gynecology, Seventh Medical Center of Chinese People's Liberation Army General Hospital, No. 5 Nanmencang, Dongsishitiao, Dongcheng District, Beijing 100700, China. meng6512@vip.sina.com

Abstract

BACKGROUND

Preoperative risk stratification is significant for the management of endometrial cancer (EC) patients. Radiomics based on magnetic resonance imaging (MRI) in combination with clinical features may be useful to predict the risk grade of EC.

AIM

To construct machine learning models to predict preoperative risk stratification of patients with EC based on radiomics features extracted from MRI.

METHODS

The study comprised 112 EC patients. The participants were randomly separated into training and validation groups with a 7:3 ratio. Logistic regression analysis was applied to uncover independent clinical predictors. These predictors were then used to create a clinical nomogram. Extracted radiomics features from the T2-weighted imaging and diffusion weighted imaging sequences of MRI images, the Mann-Whitney *U* test, Pearson test, and least absolute shrinkage and selection operator analysis were employed to evaluate the relevant radiomic features, which were subsequently utilized to generate a radiomic signature. Seven machine learning strategies were used to construct radiomic models that relied on the screening features. The logistic regression method was used to construct a composite nomogram that incorporated both the radiomic signature and clinical independent risk indicators.

RESULTS
Having an accuracy of 0.82 along with an area under the curve (AUC) of 0.915 [95% confidence interval (CI): 0.806-0.986], the random forest method trained on radiomics characteristics performed better than expected. The predictive accuracy of radiomics prediction models surpassed that of both the clinical nomogram (AUC: 0.75, 95%CI: 0.611-0.899) and the combined nomogram (AUC: 0.869, 95%CI: 0.702-0.986) that integrated clinical parameters and radiomic signature.

CONCLUSION
The MRI-based radiomics model may be an effective tool for preoperative risk grade prediction in EC patients.

Key Words: Endometrial cancer; Risk stratification; Radiomics; Machine learning; Nomogram

Core Tip: Our research focused on the utilization of clinical features and radiomics derived from magnetic resonance imaging (MRI) in order to predict the risk grade of endometrial cancer (EC). In our studies, we constructed a predictive model capable of predicting preoperative EC risk. The MRI-based radiomics model put forth in this research showed strong predictive ability and great potential value for assessing the level of EC risk. The integration of predictive models into clinical practice would greatly enhance the preoperative selection of customized therapy.

Citation: Wei ZY, Zhang Z, Zhao DL, Zhao WM, Meng YG. Magnetic resonance imaging-based radiomics model for preoperative assessment of risk stratification in endometrial cancer. *World J Clin Cases* 2024; 12(26): 5908-5921
URL: https://www.wjgnet.com/2307-8960/full/v12/i26/5908.htm
DOI: https://dx.doi.org/10.12998/wjcc.v12.i26.5908

INTRODUCTION

Endometrial cancer (EC), characterized by the abnormal growth of cells in the lining of the uterus, is a prevalent gynecologic malignancy with a significant global health impact for females[1]. The early detection rate of EC is normally high, with approximately 80% of cases being diagnosed in stage I, with almost 95% 5-year survival rates[2]. However, if a disease has spread regionally or far away, the 5-year survival rate is substantially lower (68% and 17%, respectively)[3].

According to the European Society for Medical Oncology, the European Society for Radiotherapy and Oncology, and the European Society of Gynaecological Oncology Consensus Conference non-molecular risk classification of EC from 2020[4], patients who are at a heightened risk demonstrate the presence of at least one of the subsequent histologic characteristics: Deep infiltration into the myometrium (DMI); a tumor of high grade; a histological subtype that is non-endometrioid; lymph-vascular spaces invasion (LVSI); spread beyond the uterus; or involvement of lymph nodes.

Bilateral salpingo-oophorectomy and total abdominal hysterectomy are the standard treatments for low-risk EC. Although numerous clinical trials have sought to demonstrate the benefits of adjuvant therapy and lymphadenectomy (LA) for EC in its early stages, whether it truly meets the needs of patients remains controversial[5]. Approximately 7%-10% of patients undergoing lymph node dissection have postoperative lymphatic fistula, and roughly 23% of people are said to have lower extremity lymphedema on average[6]. According to the guidelines, individuals diagnosed with low-risk endometrioid carcinoma exhibit a diminished likelihood of lymph node involvement, hence LA is not advised for these patients. However, high-risk patients who had previously had partial surgery who needed LA to complete staging may be a good candidate for this procedure. For patients with intermediate-risk and high-risk endometrial carcinoma, surgical tumor debulking including enlarged lymph nodes and adjuvant treatment is recommended.

Therefore, we merged intermediate and high-risk groups as the high-risk group. Hence, identifying an effective approach for accurately evaluating risk stratification in EC cancer before treatment is crucial to ensure precise decision-making. Precise evaluation of the primary tumor, lymph nodes, and distant metastases is crucial for predicting the risk stratification of EC, particularly in the context of DMI.

Transvaginal ultrasonography is inferior to magnetic resonance imaging (MRI), which provides higher diagnostic performance[7,8]. Preoperative evaluation of EC staging using combined MRI T2-weighted imaging (T2WI) sequences is considered the best way for accurate assessment of DMI, particularly in cases where there is disappearance of the junctional zone (commonly seen in postmenopausal patients) and poor tumor-myometrial contrast[9]. Nevertheless, there is often an overestimation of the stage in instances where the tumor affects the uterine horns, when the tumor extends extensively into the uterine wall causing thinning of the myometrium, or in the event it occurs in a leiomyomatous uterus marked due to the varied signal strength observed in the myometrium[10,11].

The utilization of radiomics within clinical decision systems has witnessed a notable surge in recent years, leading to enhanced precision in the realms of diagnosis, prognosis, and prediction[12,13]. The primary objective of radiomics is transforming medical pictures into digital information that encompasses physiological and fundamental descriptive variables, such as contrast enhancement, diffusion properties, and tracer pickup. Additionally, it encompasses funda-

mental describing metrics, among which are dimension, form, intensity, and texture[14]. The application of radiomics is frequently observed in the field of oncology. According to reports, medical imaging characteristics were useful in differentiating across EC risk groups[15,16].

In the assessment of the predictive capacity of three risk stratification models for lymph node transfer in endometrioid EC, Korkmaz *et al*[17] found that the model that exhibited the highest performance attained an area under the curve (AUC) value of 0.780. Liu *et al*[18] concluded that the utilization of texture analysis exhibited promising prospects in its capacity to function as imaging indicators for evaluating preoperative risk. However, additional study is required to examine the evaluation of MRI-based radiomic analysis in conjunction with clinical factors for the purpose of preoperative risk stratification in patients with EC.

The objective of the present research was to inquire into the utilization of clinical features and radiomics derived from MRI in order to predict the risk grade of EC.

MATERIALS AND METHODS

Patients

The retrospective inquiry in question was exempt from the requirement of informed consent as it had obtained approval from the institutional review board. We reviewed 315 patients with EC that had postoperative pathological results between January 2018 and January 2020 in our hospital. Based on the following criteria, 112 cases were included in the study. Patients were first stratified according to the European Society of Gynaecological Oncology, the European Society for Medical Oncology, and the European Society of Pathology 2020 guidelines and then divided into two groups: Low-risk (including patients belonging to the low-risk class according to the 2020 guidelines classification); and high-risk (including intermediate, intermediate-high, and high-risk classes).

The inclusion criteria were: (1) Patients with pathologically confirmed EC who received an MRI exam 2 wk before surgery; and (2) Individuals who had not received any therapeutic interventions, including surgical procedures, biopsies, radiation therapy, chemotherapy, or hormone therapy, prior to their MRI. The exclusion criteria were: (1) Patients with missing clinical data; (2) Poor MRI image quality or significant artifacts that did not match the requirement of analysis; and (3) Lesions with a diameter of less than 5 mm. A random assignment method was used to allocate patients in a 7:3 ratio between the training group (n = 78) and the validation cohort (n = 34). The research flowchart is portrayed in Figure 1.

Data and images collection

Clinical and histopathological traits of all selected patients, such as age, histological grade and subtype, International Federation of Gynaecology and Obstetrics staging, body mass index, hypertension, hyperlipidemia, diabetes mellitus, menstruation, menopause status, fertility history, serum cancer antigen (CA) 125 level, serum CA19-9 level, and drinking and smoking history, were collected. These data were obtained through consultation of the medical record system. MRI pictures of all patients in digital imaging and communications in the medicine type were exported.

All MRI examinations were performed using 3.0 T system MRI scanners (Magnetom Aera; Siemens Healthcare, Germany). The standard scanning protocol comprised axial fast spin-echo (FSE) T1-weighted images, axial FSE T2WI, axial fat suppression FSE T2WI, and sagittal FSE T2WI. The b values utilized in diffusion weighted imaging (DWI) encompassed the values of 0 and 1000 s/mm^2. In the study, uterus-sagittal position T2WI were acquired for lesion segmentation. Other imaging was used as a reference for lesion segmentation. Then, the radiomics features were extracted based on T2WI and DWI sequences. Table 1 displays the MRI parameters in detail.

Image segmentation and radiomic features extraction

The open-source software three-dimensional (3D) slicer (version 5.2.1), which may be accessed at https://www.slicer.org, was employed for the purpose of image segmentation. Segmentation was performed independently and manually by two experienced doctors who were unaware of the pathological result of the patient. The entire tumor was included in the 3D volume of interest (VOI), which the medical professionals defined, divided, and fused for a layer after layer screen. In the event of a disagreement, the two doctors talked it out until an agreement was reached.

The VOIs underwent resampling to a voxel size of 3 mm × 3 mm × 3 mm before extracting features to produce isotropic voxels; to ensure that the gray-level values of all photos were dispersed over the same range, image normalization was carried out. The VOI of each patient was utilized to extract radiomics features using the free and publicly accessible python program pyradiomics (https://pypi.org/project/pyradiomics/). The following categories were created from the extracted features: First-order features; two-dimensional features; gray-level cooccurrence matrix (GLCM); gray-level dependence matrix; gray-level size-zone matrix; gray-level run-length matrix; and neighboring gray tone difference matrix[19]. In total, 1037 radiomics characteristics were retrieved.

Radiomic feature picking and signature building

To mitigate interference across the feature dimensions, the features underwent standardization making use of the Z-score method, which involves deducting the average value and dividing by the standard deviation. Initially, to assess what features could individually separate the low-risk group from the high-risk group, we conducted the Mann-Whitney U test. Only features exhibiting a P value of 0.05 were retained. Subsequently, to eliminate highly correlated features, we removed the features with $P > 0.9$. The utilization of the least absolute shrinkage and selection operator (Lasso) in data analysis allows for the reduction of coefficients associated with variables that are not relevant to survival to zero while

Table 1 Magnetic resonance imaging scanning parameters

Sequence	TR/TE in ms	FOV in mm × mm	Matrix	Slice gap in mm	Slice thickness in mm
Axial T1WI	500/8.6	310 × 310	224 × 320	1	6
Axial T2WI	6200/95	310 × 310	307 × 384	1	6
Axial (FS)-T2WI	4000/93	310 × 310	256 × 320	1	5
Sagittal (FS)-T2WI	6000/86	240 × 240	205 × 256	1	6
Axial DWI	5000/69	327 × 245	115 × 192	1	4

DWI: Diffusion weighted imaging; FOV: Field of view; FS: Fat suppression; T1WI: T1-weighted images; T2WI: T2-weighted imaging; TE: Echo Time; TR: Repetition time.

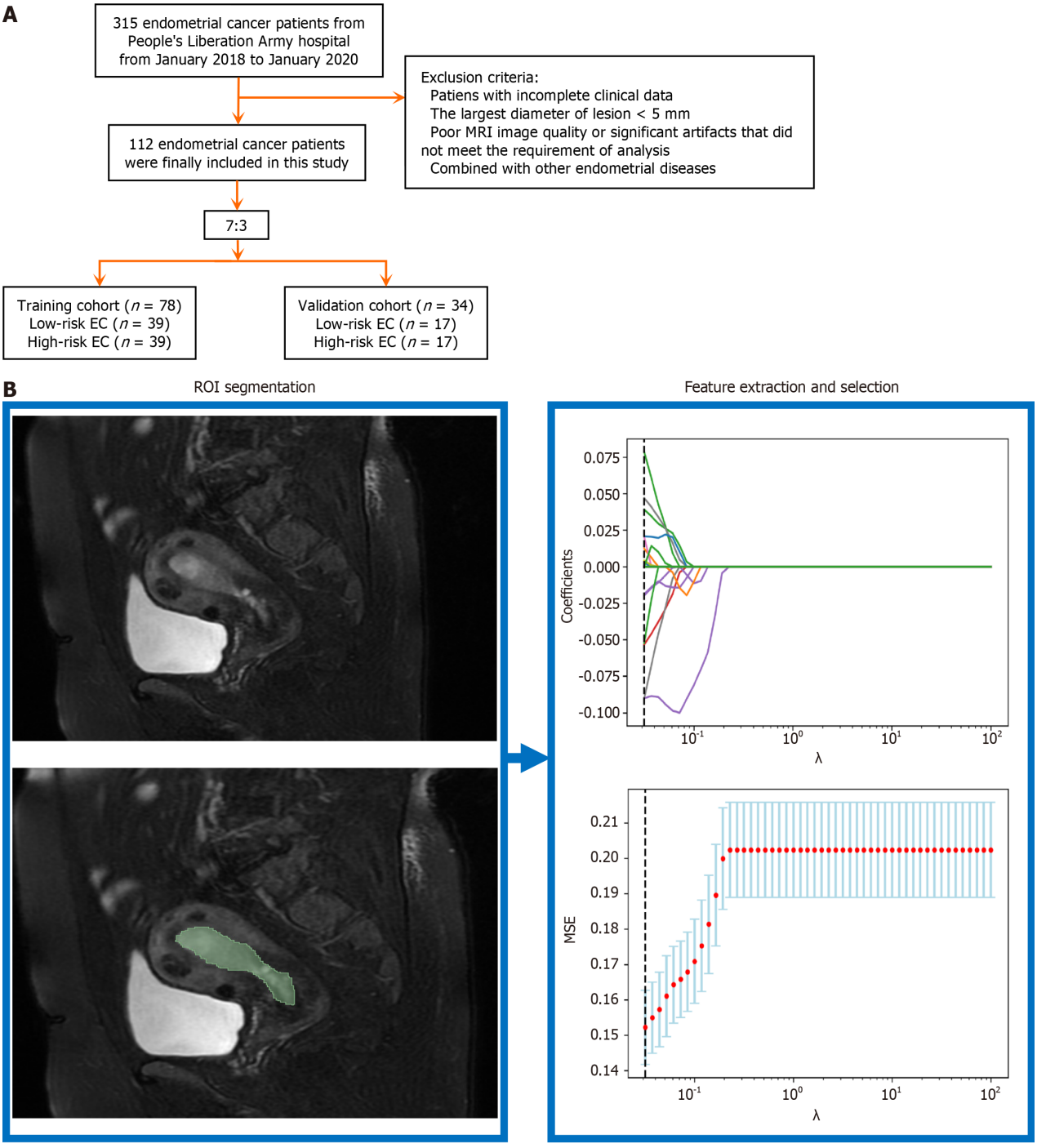

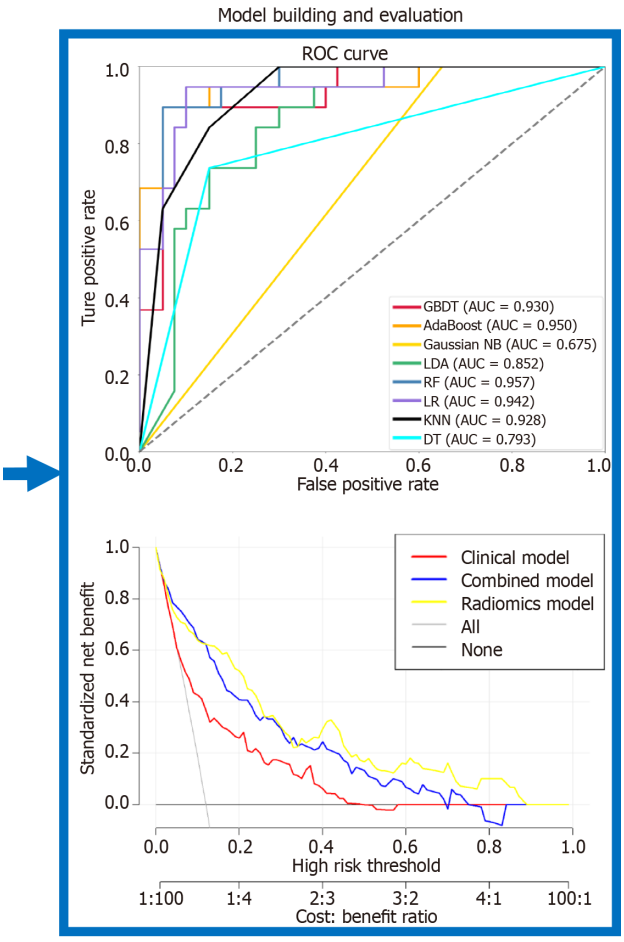

Figure 1 Technology roadmap for this research. A: Flow chart of patient enrollment; B: Workflow of radiomics analysis process. AUC: Area under the curve; DT: Decision tree; EC: Endometrial cancer; KNN: K-nearest neighbor; LDA: Linear discriminant analysis; LR: Logistic regression; MRI: Magnetic resonance imaging; MSE: Mean-square error; RF: Random forest; ROC: Receiver operating characteristic; ROI: Region of interest.

retaining features that have coefficients that are not equal to zero[20,21]. In this study, the Lasso method was employed to identify radiomics properties with the highest impact, and a 10-fold cross-validation approach was implemented within the training cohort. The minimum criteria (minimum lambda) were used to identify the ideal tuning parameter.

The radiomic signature (radscore) was calculated by adding up all of the filtered eigen values and multiplying the total by the appropriate coefficients. Radscore = $\beta 1X1 + \beta 2X2 + \ldots \beta nXn$, with the radiomic signature denoted as radscore, βn was the coefficient, and Xn was the eigenvalue[22]. The assessment of the consistency between radscore in the training and testing sets was conducted by employing the Wilcoxon rank sum Mann-Whitney *U* test.

Model construction

By applying univariate and multivariate regression analysis, the clinical independent predictors were discovered. Applying the independent predictors, a clinical nomogram was then produced. To categorize the EC based on their radiomics features because we needed a model to solve a binary classification problem and we did not have a very large sample size, seven popular binary machine learning algorithms [logistic regression (LR), K-nearest neighbor (KNN), decision tree (DT), random forest (RF), gradient boosting (GB), eXtreme GB (XGBoost), and GBDT] with good explanations were used. A combined prediction multivariate logistic regression model was developed by including the radiomic signature (radscore) and clinically significant predictors that demonstrated statistical significance in a multivariate regression analysis.

Model performance and comparison and statistical analysis

The building of the ideal radiomics model was accomplished by employing a machine learning technique that demonstrated the maximum AUC value in the validation cohort[23]. AUCs of the models were compared *via* the Delong test [24]. The calibration was verified using calibration curves. The method of decision curve analysis was employed in order to assess and quantify the clinical value associated with each model[25].

Statistical tests suitable for the data type were employed to compare the baseline data between the training and validation cohorts. Specifically, the χ^2 test or the Fisher exact test were used for categorical variables, while the continuous variables were assessed using either the two-sample *t*-test or the Mann-Whitney *U* test. Statistical significance was attributed to data sets with *P* values lower than 0.05. Statistical analyses were performed utilizing the statistical product

and service solutions (version 26.0, international business machines corporation, https://www.ibm.com/spss), R software (version 3.5.1, https://www.r-project.org/), and Python (version 3.5.6, https://www.python.org/).

RESULTS

Demographic characteristics

A sample size of 112 individuals, aged between 31 years and 84 years (average age of 58.35 ± 11.75 years), was partitioned into two separate sections: Low-risk (n = 56) and high-risk (n = 56; including 42 intermediate risk cases and 14 high-risk cases). The participants were randomized to the training and validation subgroups in a random manner, following a 7:3 ratio. In the training subgroup, there were 39 patients classified as low-risk and an equal number of 39 patients classified as high-risk. Similarly, in the validation cohort, there were 17 patients classified as low-risk and an equal number of 17 patients classified as high-risk. The training and validation cohorts did not significantly differ in either clinical or histological characteristics. Table 2 displays the fundamental characteristics of the individuals.

Radiomic feature selection and radiomic signature construction

The 3D Slicer software was utilized to extract a total of 1037 quantitative imaging feature parameters for each patient. Following deredundancy processing, 788 features were kept, and 15 feature parameters were chosen using the Lasso dimensionality reduction approach (Figure 2). The radiomics score for each patient was computed *via* a linear equation using the following formula:

Radscore = (0.085 × original_firstorder_Minimum) + (0.046 × original_glcm_ldmn) + [(-0.039) × log-sigma-4-4-mm-3D_firstorder_Energy] + [(-0.075) × log-sigma-4-4-mm-3D_firstorder_Maximum] + [(-0.133) × wavelet-LLH_firstorder_Median] + (0.072 × wavelet-LLH_firstorder_Skewness) + [(-0.057) × wavelet-LLH_glszm_LowGrayLevelZoneEmphasis] + [(-0.077) × wavelet-LHL_firstorder_Median] + (0.048 × wavelet-LHL_glcm_ClusterProminence) + (0.145 × wavelet-LHH_glcm_ClusterProminence) + (0.046 × wavelet-HHL_glcm_JointEnergy) + [(-0.088) × wavelet-HHH_glcm_MCC] + [(-0.075) × wavelet-LHH_gldm_LargeDependenceLowGrayLevelEmphasis] + [(-0.038) × wavelet-LLL_glrlm_LongRunHighGrayLevelEmphasis] + (0.046 × wavelet-LLL_glszm_LargeAreaLowGrayLevelEmphasis).

The study observed that the radscore exhibited greater values in the high-risk subgroup in comparison to the low-risk subgroup. Additionally, statistical analysis demonstrated that the radscore had a strong capability to differentiate between EC patients with low risk and those with high risk, as observed in both the training and validation cohorts. Low-risk EC patients had a radscore of 0.25 ± 0.20 in the training cohort compared to high-risk patient radscores of 0.75 ± 0.15 (P = 0.000); in the validation cohort, low-risk EC patients had a radscore of 0.24 ± 0.39 compared to high-risk patient radscores of 0.67 ± 0.21 (P = 0.000) (Figure 3).

Development and validation of the clinical model

Logistic regression analysis, both univariate and multivariate, was used to filter out all of the clinically suspicious risk factors (Table 3). The findings revealed that age, CA125, and CA19-9 were clinical independent predictors. A clinical model was constructed with the predictors. The AUC was 0.751 [95% confidence interval (CI): 0.611-0.899] in validation set, and accuracy was 0.706. Figure 4A depicts the clinical prediction model nomogram.

Development and validation of the radiomics models

Radiomics models were created using LR, KNN, DT, RF, GB, XGBoost, and GBDT. The model performance information is displayed in Table 4. The discrimination of the RF algorithm model outperformed the others.

Development and validation of the combined model

The LR technique was employed to generate a nomogram that integrated the variables of age, CA125, CA19-9, and radscore into a combined model. The AUC in the test collection demonstrated outstanding discrimination, with a value of 0.869 (95%CI: 0.702-0.986). Figure 4B displays the nomogram representing the combined prediction models.

Comparison of models

Figure 5 including the receiver operating characteristic curves, calibration curves, and decision curve analysis, presents a comparative analysis of the performance between a clinical model, the best radiomics model, and the combined model. According to the Delong test (P < 0.05), the radiomics model exhibited superior discriminatory performance compared to both the clinical and combined models.

DISCUSSION

This study involved the development of three models that were based on clinical independent risk factors, radiomics features, and the combination of clinical risk factors with radscore. The objective was to predict risk stratification for EC. This study demonstrated that the MRI-based radiomics models and the clinical models have good efficacy when assessing the risk grade of EC. The diagnostic efficacy of the combined model (AUC: 0.869, 95%CI: 0.702-0.986) was higher than the clinical model (AUC: 0.75, 95%CI: 0.611-0.899), and the radiomics model (AUC: 0.915, 95%CI: 0.806-0.986)

Table 2 Characteristics of endometrial cancer patients in the training and validation cohorts

Characteristics	Training cohort	Validation cohort	*P* value
Number	78	34	
Age in yr	58.04 ± 11.54	59.06 ± 12.04	0.367
Histological grade[1]			0.465
G1/G2	58	23	
G3	20	11	
Risk classes			1.000
Low-risk	39	17	
High-risk	39	17	
Histological subtype[1]			0.018
Endometrioid	66	22	
Serous	6	5	
Clear cell	4	4	
Carcinosarcoma	2	3	
FIGO staging			0.765
I	50	21	
II	11	7	
III	9	4	
IV	8	2	
BMI			
> 24	44	19	0.959
≤ 24	34	15	
Hypertension			0.812
Positive	20	8	
Negative	58	26	
DM			0.605
Positive	15	8	
Negative	63	26	
Hyperlipidemia			0.338
Positive	5	4	
Negative	73	30	
Menstruation			0.395
Regular	48	18	
Irregular	30	16	
Menopausal status			
Premenopausal	57	27	0.477
Postmenopausal	21	7	
Fertility			0.669
Fertility	69	31	
Nonfertility	9	3	
CA125			0.617
< 35 U/mL	61	28	

≥ 35 U/mL	17	6	
CA19-9			0.631
< 27 U/mL	67	28	
≥ 27 U/mL	11	6	
Family history of cancer			0.292
Positive	10	7	
Negative	68	27	
Drinking history			0.915
Positive	5	2	
Negative	73	32	
Smoking history			0.606
Positive	4	1	
Negative	74	33	

[1]Histological grade and subtype of endometrioid adenocarcinoma from surgical specimen.
Data are *n* or mean ± standard deviation. FIGO: The International Federation of Gynaecology and Obstetrics; BMI: Body mass index; CA125: Cancer antigen 125; CA19-9: Cancer antigen 19-9; DM: Diabetes mellitus.

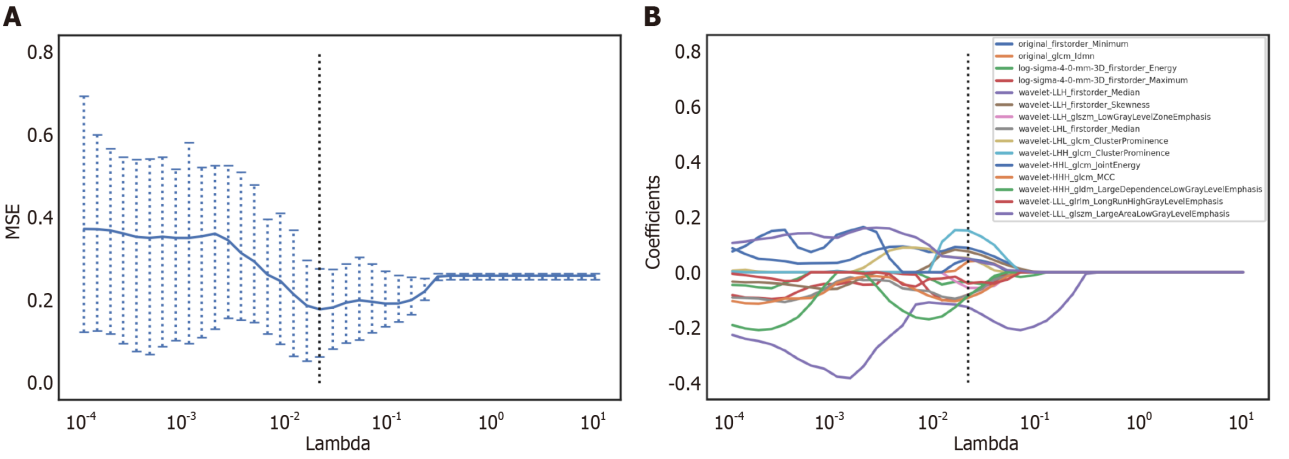

Figure 2 Least absolute shrinkage and selection operator regression model for screening the radiomics characteristics of the training group. A: Screening of the radiomics features was performed through least absolute shrinkage and selection operator (Lasso) regression. The cross validation for Lasso regression, where the parameter λ was adjusted to find the best function set, is shown. The vertical dotted line on the left panel represents the log(λ) corresponding to the optimal λ; B: Screening of the radiomics features was performed through Lasso regression. The coefficients of texture parameters changed with λ. The vertical line corresponds to the 10 features selected with non-zero Lasso cross-validation coefficients. MSE: Mean-square error.

developed based on the imaging features extracted from the T2WI and DWI sequence had the highest efficacy. The RF model performed best in this investigation out of various classifiers utilized to build the radiomics predictive model. This study showcased the efficacy of utilizing a comprehensive tumor radiomics-based analysis to evaluate the risk classification of EC before surgical intervention. The radiomics model may be clinically effective in the individualized surgical care of EC patients since radiomics may extract relevant data about high-risk indicators prior to surgery.

Some studies have explored preoperative prediction of EC risk stratification. Yan *et al*[26] found that variables for high-risk EC included metabolic syndrome, CA125, age, and tumor grade after curettage. Saarelainen *et al*[27] also concluded that CA125 paired with other serum indicators was superior to CA125 alone in predicting the recurrence of disease in EC patients. CA125 is a factor that relates to high-risk EC. In line with this, age, CA125, and CA19-9 were independent risk factors associated with EC risk stratification in this study.

Previous studies have noted that patients with EC, particularly those exhibiting unfavorable prognostic factors such as tumor recurrences, grade 3 tumors, DMI, lymph node metastasis, and extrauterine disease, utilize CA125 as a biomarker for tumor detection[28]. CA125 has been integrated into many pre-surgery prediction models, with varying levels of effectiveness. In clinical settings, the utilization of a threshold value of 35 U/mL for CA125 can prove to be a valuable diagnostic tool due to its high sensitivity. This is evidenced by the fact that a mere 1% of females who are in good health exhibit CA125 levels surpassing this cutoff point[29]. Therefore, this widely used cutoff was also used in this study.

Table 3 Univariate regression analysis and multivariate regression analysis

Characteristics	Univariate regression OR (95%CI)	*P* value	Multivariate regression OR (95%CI)	*P* value
Age	Reference 1.091 (1.038-1.147)	0.000	Reference 1.10 (1.000-1.019)	0.048
BMI				
> 24	Reference			
≤ 24	2.333 (0.933-5.833)	0.070		
Hypertension				
Positive	Reference			
Negative	0.438 (0.152-1.256)	0.124		
Diabetes mellitus				
Positive	Reference			
Negative	0.848 (0.274-2.619)	0.774		
Hyperlipidemia				
Positive	Reference			
Negative	0.649 (0.102-4.113)	0.646		
Menstruation				
Regular	Reference			
Irregular	1.591 (0.615-4.114)	0.338		
Menopausal status				
Premenopausal	Reference			
Postmenopausal	2.560 (0.898-7.296)	0.079		
Reproductive history				
Positive	Reference			
Negative	0.777 (0.192-3.142)	0.724		
CA125				
< 35 U/mL	Reference		Reference	
≥ 35 U/mL	26.435 (3.284-29.776)	0.002	1.515 (1.163-1.973)	0.003
CA19-9			Reference	
< 27 U/mL	Reference		1.355 (1.030-1.783)	0.033
≥ 27 U/mL	5.550 (1.114-27.648)	0.036		
Family history of cancer				
Negative	Reference			
Positive	1.000 (0.265-3.772)	1.000		
Drinking history				
Negative	Reference			
Positive	4.343 (0.463-40.749)	0.199		
Smoke history				
Negative	Reference			
Positive	0.316 (0.031-3.177)	0.328		
Radscore	1.027 (1.002-1.054)	0.038	1.025 (0.990-1.060)	0.016

BMI: Body mass index; CA125: Cancer antigen 125; CA19-9: Cancer antigen 19-9; CI: Confidence interval; OR: Odds ratio.

Table 4 Outcomes of radiomics models in validation set

Algorithms	AUC (95%CI)	Accuracy	Sensitivity	Specificity
LR	0.794 (0.706-0.976)	0.794	0.765	0.824
KNN	0.893 (0.766-0.971)	0.765	0.823	0.705
DT	0.676 (0.529-0.824)	0.676	0.529	0.824
RF	0.915 (0.806-0.986)	0.824	0.824	0.824
GB	0.907 (0.792-0.979)	0.794	0.706	0.882
XGBoost	0.869 (0.739-0.965)	0.765	0.706	0.824
GBDT	0.872 (0.742-0.958)	0.765	0.647	0.882

AUC: Area under the curve; CI: Confidence interval; DT: Decision tree; GB: Gradient boosting; GBDT: Gradient boosting decision tree; KNN: K-nearest neighbor; LR: Logistic regression; RF: Random forest; XGBoost: eXtreme gradient boosting.

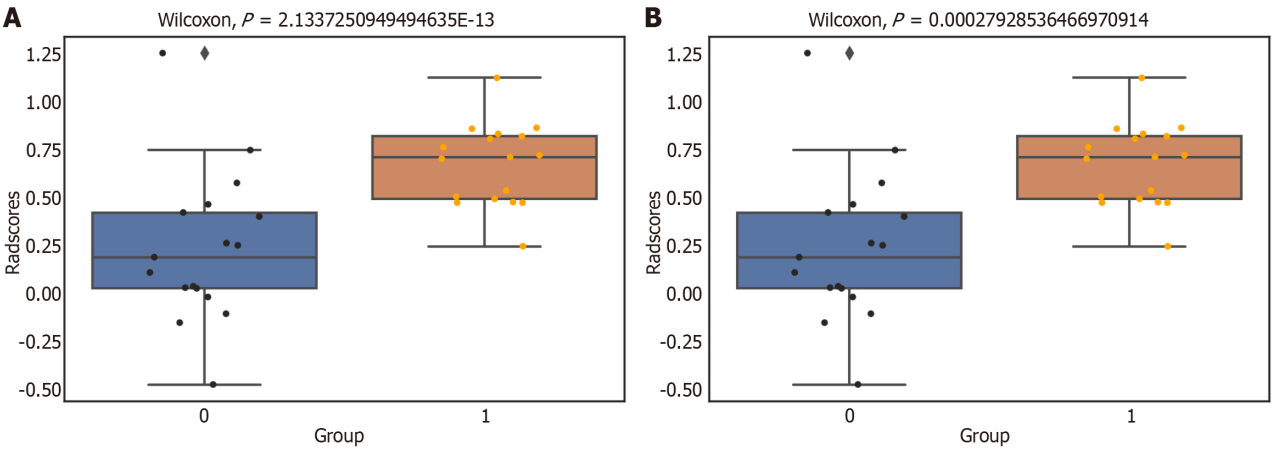

Figure 3 Comparison of low-risk and high-risk endometrial cancer radscores. A: Training groups; B: Testing groups. 1: Low-risk endometrial cancer; 0: High-risk endometrial cancer.

Furthermore, there is research that has demonstrated notable correlations between International Federation of Gynaecology and Obstetrics staging and several other characteristics. These factors encompass inadequate histological classification, progressed clinical stage, existence of metastatic lymph nodes, and heightened blood CA19-9 levels[30]. Elderly females are more likely to have metabolic syndrome, have worse basic health status, and are more likely to develop high-risk EC. A study showed that reproductive history was a high-risk indicator for the emergence of EC[31]. In the current study, however, this conclusion was not found, suggesting that reproductive history may be more related to the incidence of EC instead of risk grade.

Previous studies have found a connection between the characteristics of tumor texture and diagnosis and grading[32,33]. Celli *et al*[34] found that the differentiation of low-risk EC from other risk categories, as well as the identification of the existence of LVSI, can be achieved with moderate to high accuracy by the utilization of MRI-based whole-tumor radiomics and radio-genomic investigations. Using MRI texture features, Ueno *et al*[35] established preliminary mathematical modelling that showed a correlation with DMI, LVSI, and high tumor grade. The AUC of the model in predicting high-risk EC was 0.83, but they did not perform the volumetric analysis. High-throughput parameters were extracted for the current investigation, and 15 statistically significant features were then found to create a radiomics model. The model performed well in identifying low-risk and high-risk EC; the sensitivity and specificity of the validation cohort were 82.4% and 82.4%, and the AUC was 0.915.

The GLCM feature characterizes the spatial arrangement of grey intensity in a two-dimensional manner by quantifying the probability of observing specific pixel pairs with particular grey values[36,37]. The chosen feature in this study comprised six GLCM features, indicating a close association between the distribution of texture and spatial heterogeneity within tumors and tumor differentiation. Moreover, alterations in the internal texture of tumors play a crucial role in determining tumor risk grading.

Among the seven machine learning algorithms we used to develop a radiomics model, the RF model performed best. It is based on DT analysis; the algorithm builds DTs by employing a random selection process to determine a subset of the samples and a subset of the features to be used for the split at each node. This greatly reduces the variance term in the diagnostic error. This is an advantage over bagging of the DTs[38]. In the area of biomedical research, the characteristics of RF make it the perfect material for creating diagnostic models.

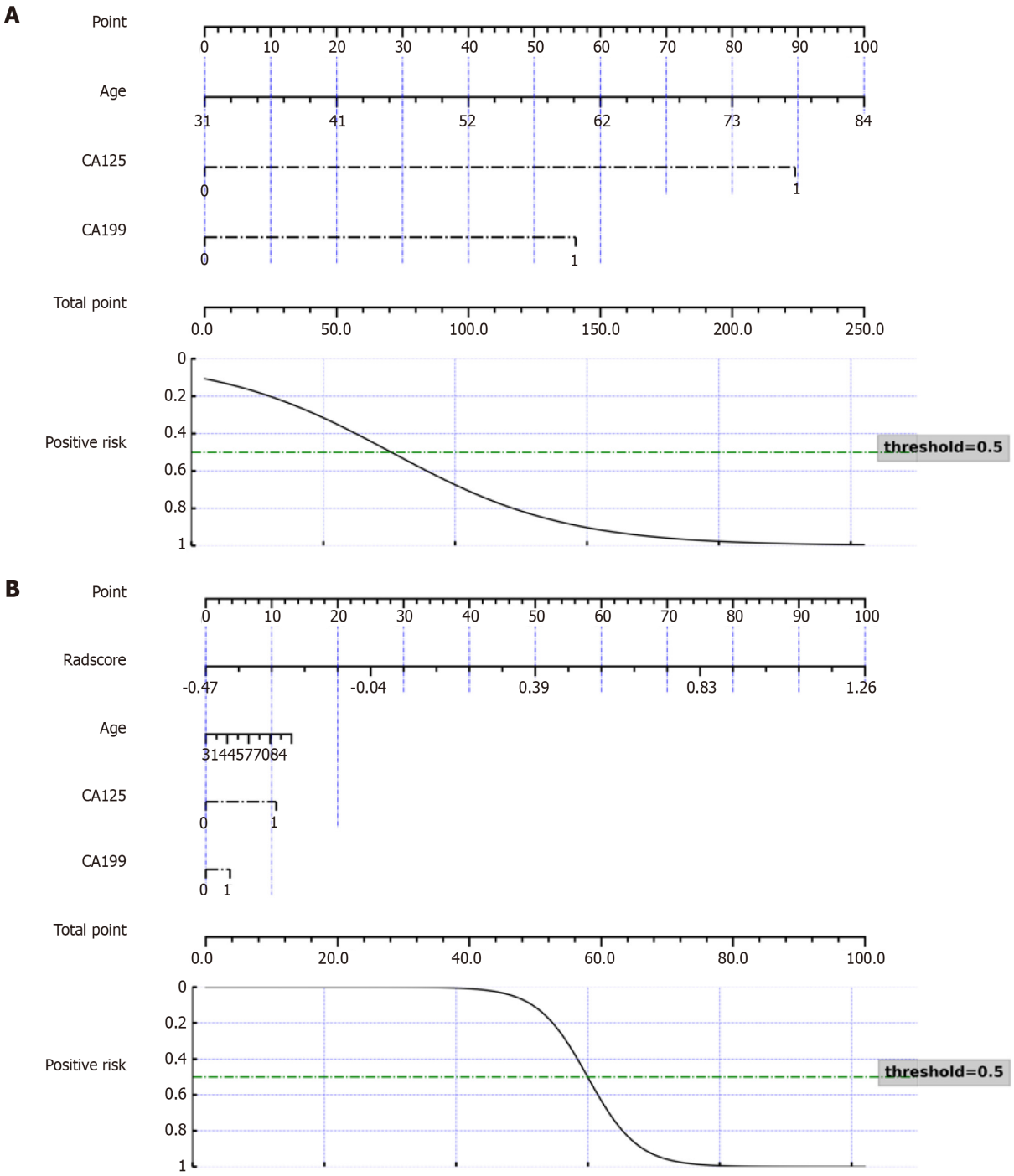

Figure 4 Nomogram to predict endometrial cancer risk. Cancer antigen (CA) 125 label 1 corresponds to serum levels below 35 U/mL, and label 0 corresponds to serum levels higher than 35 U/mL. CA19-9 label 1 corresponds to serum levels below 27 U/mL, and label 0 corresponds to serum levels higher than 27 U/mL. A: Nomogram developed by clinical predictors; B: Radiomics-clinical combined nomogram.

Our study had some limitations. First, our model might have been overfitted because we only included 112 patients in this early investigation. Second, even though the MRI was performed according to a set protocol, the retrospective nature of the study could result in inhomogeneity un the imaging data. Although normalization was used in the picture analysis, image standardization and normalization techniques still require research. Third, we included only T2WI map images in our model, which may potentially enable missing significant data. To limit the potential of biases from only one sequence, future studies should use multiparametric techniques.

CONCLUSION

The MRI-based radiomics model put forth in this research showed strong predictive ability and great potential value for assessing the level of EC risk. The integration of predictive models into clinical practice would greatly enhance the

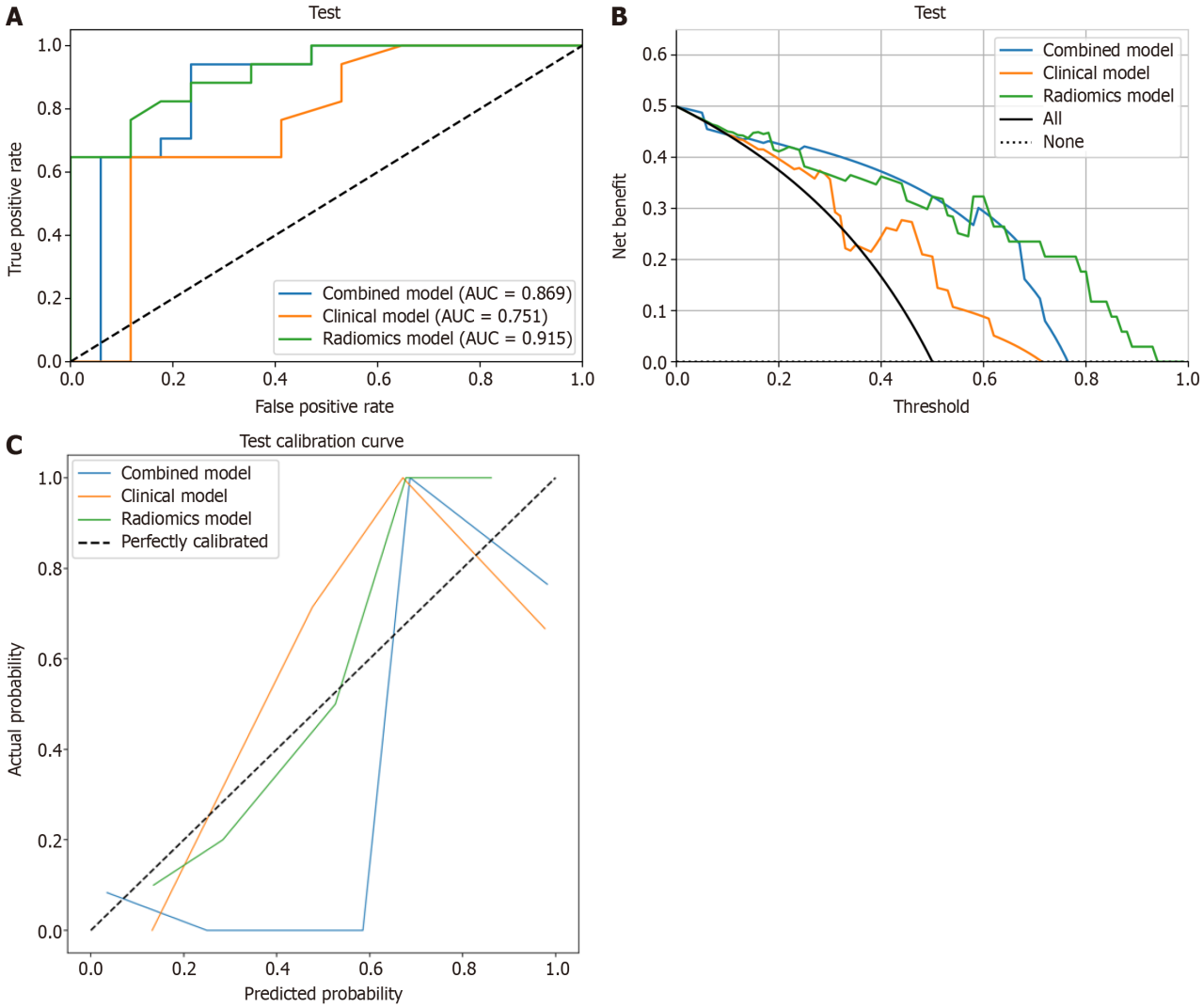

Figure 5 Evaluation of the radiomics model, clinical model, and combined model for predicating endometrial cancer risk grading. A: Receiver operating characteristic curve; B: Calibration curve; C: Decision curve analysis. AUC: Area under the curve.

preoperative selection of customized therapy.

ACKNOWLEDGEMENTS

The authors express their heartfelt thanks to the staff of the Department of Obstetrics and Gynecology of our hospital.

FOOTNOTES

Author contributions: Wei ZY, Zhang Z, and Zhao DL contributed to methodology; Wei ZY contributed to writing the original draft and formal analysis; Meng YG contributed to writing, reviewing, and editing; Wei ZY and Zhao DL contributed to supervision; All authors contributed to data curation and conceptualization and read and approved the final manuscript.

Institutional review board statement: This study was performed in line with the principles of the Declaration of Helsinki. The Institutional Ethics Review Board approved this retrospective study and waived the requirement for written informed consent (No: 2022-403).

Informed consent statement: The retrospective inquiry in question was exempt from the requirement of informed consent as it had obtained approval from the institutional review board.

Conflict-of-interest statement: The authors declare that they have no competing interests.

Data sharing statement: The datasets generated and analyzed during the current study are not publicly available but are available from

the corresponding author on reasonable request.

Country of origin: China

ORCID number: Yuan-Guang Meng 0000-0002-4957-3999.

S-Editor: Fan M
L-Editor: Filipodia
P-Editor: Wang WB

REFERENCES

1 **Sung H**, Ferlay J, Siegel RL, Laversanne M, Soerjomataram I, Jemal A, Bray F. Global Cancer Statistics 2020: GLOBOCAN Estimates of Incidence and Mortality Worldwide for 36 Cancers in 185 Countries. *CA Cancer J Clin* 2021; **71**: 209-249 [PMID: 33538338 DOI: 10.3322/caac.21660]
2 **Pintican R**, Bura V, Zerunian M, Smith J, Addley H, Freeman S, Caruso D, Laghi A, Sala E, Jimenez-Linan M. MRI of the endometrium - from normal appearances to rare pathology. *Br J Radiol* 2021; **94**: 20201347 [PMID: 34233457 DOI: 10.1259/bjr.20201347]
3 **PDQ Adult Treatment Editorial Board**. Endometrial Cancer Treatment (PDQ®): Health Professional Version. 2024 Feb 8. In: PDQ Cancer Information Summaries [Internet]. Bethesda (MD): National Cancer Institute (US); 2002- [PMID: 26389270]
4 **Gultekin M**, Guler OC, Yuce Sari S, Akkus Yildirim B, Onal C, Celik H, Yuce K, Ayhan A, Arik Z, Kose F, Altundag O, Zoto Mustafayev T, Atalar B, Bolukbasi Y, Yildiz F. Multi-institutional validation of the ESMO-ESGO-ESTRO consensus conference risk grouping in Turkish endometrial cancer patients treated with comprehensive surgical staging. *J Obstet Gynaecol* 2021; **41**: 414-420 [PMID: 32347768 DOI: 10.1080/01443615.2020.1737661]
5 **Jang JW**, Lee LJ. External Beam, Brachytherapy, or Chemotherapy? Defining Adjuvant Therapy for Early-Stage and High- and High-Intermediate-Risk Endometrial Cancer. *J Clin Oncol* 2019; **37**: 1778-1784 [PMID: 31163010 DOI: 10.1200/JCO.19.00362]
6 **Yost KJ**, Cheville AL, Al-Hilli MM, Mariani A, Barrette BA, McGree ME, Weaver AL, Dowdy SC. Lymphedema after surgery for endometrial cancer: prevalence, risk factors, and quality of life. *Obstet Gynecol* 2014; **124**: 307-315 [PMID: 25004343 DOI: 10.1097/AOG.0000000000000372]
7 **Kinkel K**, Forstner R, Danza FM, Oleaga L, Cunha TM, Bergman A, Barentsz JO, Balleyguier C, Brkljacic B, Spencer JA; European Society of Urogenital Imaging. Staging of endometrial cancer with MRI: guidelines of the European Society of Urogenital Imaging. *Eur Radiol* 2009; **19**: 1565-1574 [PMID: 19194709 DOI: 10.1007/s00330-009-1309-6]
8 **Sala E**, Crawford R, Senior E, Shaw A, Simcock B, Vrotsou K, Palmer C, Rajan P, Joubert I, Lomas D. Added value of dynamic contrast-enhanced magnetic resonance imaging in predicting advanced stage disease in patients with endometrial carcinoma. *Int J Gynecol Cancer* 2009; **19**: 141-146 [PMID: 19258956 DOI: 10.1111/IGC.0b013e3181995fd9]
9 **Wu LM**, Xu JR, Gu HY, Hua J, Haacke EM, Hu J. Predictive value of T2-weighted imaging and contrast-enhanced MR imaging in assessing myometrial invasion in endometrial cancer: a pooled analysis of prospective studies. *Eur Radiol* 2013; **23**: 435-449 [PMID: 22865275 DOI: 10.1007/s00330-012-2609-9]
10 **Haldorsen IS**, Husby JA, Werner HM, Magnussen IJ, Rørvik J, Helland H, Trovik J, Salvesen ØO, Espeland A, Salvesen HB. Standard 1.5-T MRI of endometrial carcinomas: modest agreement between radiologists. *Eur Radiol* 2012; **22**: 1601-1611 [PMID: 22453859 DOI: 10.1007/s00330-012-2400-y]
11 **Bi Q**, Chen Y, Wu K, Wang J, Zhao Y, Wang B, Du J. The Diagnostic Value of MRI for Preoperative Staging in Patients with Endometrial Cancer: A Meta-Analysis. *Acad Radiol* 2020; **27**: 960-968 [PMID: 31636004 DOI: 10.1016/j.acra.2019.09.018]
12 **Wang Q**, Li Q, Mi R, Ye H, Zhang H, Chen B, Li Y, Huang G, Xia J. Radiomics Nomogram Building From Multiparametric MRI to Predict Grade in Patients With Glioma: A Cohort Study. *J Magn Reson Imaging* 2019; **49**: 825-833 [PMID: 30260592 DOI: 10.1002/jmri.26265]
13 **Manganaro L**, Nicolino GM, Dolciami M, Martorana F, Stathis A, Colombo I, Rizzo S. Radiomics in cervical and endometrial cancer. *Br J Radiol* 2021; **94**: 20201314 [PMID: 34233456 DOI: 10.1259/bjr.20201314]
14 **Lambin P**, Leijenaar RTH, Deist TM, Peerlings J, de Jong EEC, van Timmeren J, Sanduleanu S, Larue RTHM, Even AJG, Jochems A, van Wijk Y, Woodruff H, van Soest J, Lustberg T, Roelofs E, van Elmpt W, Dekker A, Mottaghy FM, Wildberger JE, Walsh S. Radiomics: the bridge between medical imaging and personalized medicine. *Nat Rev Clin Oncol* 2017; **14**: 749-762 [PMID: 28975929 DOI: 10.1038/nrclinonc.2017.141]
15 **Bi WL**, Hosny A, Schabath MB, Giger ML, Birkbak NJ, Mehrtash A, Allison T, Arnaout O, Abbosh C, Dunn IF, Mak RH, Tamimi RM, Tempany CM, Swanton C, Hoffmann U, Schwartz LH, Gillies RJ, Huang RY, Aerts HJWL. Artificial intelligence in cancer imaging: Clinical challenges and applications. *CA Cancer J Clin* 2019; **69**: 127-157 [PMID: 30720861 DOI: 10.3322/caac.21552]
16 **Moro F**, Albanese M, Boldrini L, Chiappa V, Lenkowicz J, Bertolina F, Mascilini F, Moroni R, Gambacorta MA, Raspagliesi F, Scambia G, Testa AC, Fanfani F. Developing and validating ultrasound-based radiomics models for predicting high-risk endometrial cancer. *Ultrasound Obstet Gynecol* 2022; **60**: 256-268 [PMID: 34714568 DOI: 10.1002/uog.24805]
17 **Korkmaz V**, Meydanli MM, Yalçın I, Sarı ME, Sahin H, Kocaman E, Haberal A, Dursun P, Güngör T, Ayhan A. Comparison of three different risk-stratification models for predicting lymph node involvement in endometrioid endometrial cancer clinically confined to the uterus. *J Gynecol Oncol* 2017; **28**: e78 [PMID: 29027396 DOI: 10.3802/jgo.2017.28.e78]
18 **Liu Z**, Wang S, Dong D, Wei J, Fang C, Zhou X, Sun K, Li L, Li B, Wang M, Tian J. The Applications of Radiomics in Precision Diagnosis and Treatment of Oncology: Opportunities and Challenges. *Theranostics* 2019; **9**: 1303-1322 [PMID: 30867832 DOI: 10.7150/thno.30309]

19 **van Griethuysen JJM**, Fedorov A, Parmar C, Hosny A, Aucoin N, Narayan V, Beets-Tan RGH, Fillion-Robin JC, Pieper S, Aerts HJWL. Computational Radiomics System to Decode the Radiographic Phenotype. *Cancer Res* 2017; **77**: e104-e107 [PMID: 29092951 DOI: 10.1158/0008-5472.CAN-17-0339]

20 **Sauerbrei W**, Royston P, Binder H. Selection of important variables and determination of functional form for continuous predictors in multivariable model building. *Stat Med* 2007; **26**: 5512-5528 [PMID: 18058845 DOI: 10.1002/sim.3148]

21 **Vasquez MM**, Hu C, Roe DJ, Chen Z, Halonen M, Guerra S. Least absolute shrinkage and selection operator type methods for the identification of serum biomarkers of overweight and obesity: simulation and application. *BMC Med Res Methodol* 2016; **16**: 154 [PMID: 27842498 DOI: 10.1186/s12874-016-0254-8]

22 **Huang Y**, Liu Z, He L, Chen X, Pan D, Ma Z, Liang C, Tian J, Liang C. Radiomics Signature: A Potential Biomarker for the Prediction of Disease-Free Survival in Early-Stage (I or II) Non-Small Cell Lung Cancer. *Radiology* 2016; **281**: 947-957 [PMID: 27347764 DOI: 10.1148/radiol.2016152234]

23 **Rui W**, Qiao N, Wu Y, Zhang Y, Aili A, Zhang Z, Ye H, Wang Y, Zhao Y, Yao Z. Radiomics analysis allows for precise prediction of silent corticotroph adenoma among non-functioning pituitary adenomas. *Eur Radiol* 2022; **32**: 1570-1578 [PMID: 34837512 DOI: 10.1007/s00330-021-08361-3]

24 **DeLong ER**, DeLong DM, Clarke-Pearson DL. Comparing the areas under two or more correlated receiver operating characteristic curves: a nonparametric approach. *Biometrics* 1988; **44**: 837-845 [PMID: 3203132 DOI: 10.2307/2531595]

25 **Steyerberg EW**, Vickers AJ, Cook NR, Gerds T, Gonen M, Obuchowski N, Pencina MJ, Kattan MW. Assessing the performance of prediction models: a framework for traditional and novel measures. *Epidemiology* 2010; **21**: 128-138 [PMID: 20010215 DOI: 10.1097/EDE.0b013e3181c30fb2]

26 **Yan BC**, Li Y, Ma FH, Feng F, Sun MH, Lin GW, Zhang GF, Qiang JW. Preoperative Assessment for High-Risk Endometrial Cancer by Developing an MRI- and Clinical-Based Radiomics Nomogram: A Multicenter Study. *J Magn Reson Imaging* 2020; **52**: 1872-1882 [PMID: 32681608 DOI: 10.1002/jmri.27289]

27 **Saarelainen SK**, Peltonen N, Lehtimäki T, Perheentupa A, Vuento MH, Mäenpää JU. Predictive value of serum human epididymis protein 4 and cancer antigen 125 concentrations in endometrial carcinoma. *Am J Obstet Gynecol* 2013; **209**: 142.e1-142.e6 [PMID: 23583212 DOI: 10.1016/j.ajog.2013.04.014]

28 **Shawn LyBarger K**, Miller HA, Frieboes HB. CA125 as a predictor of endometrial cancer lymphovascular space invasion and lymph node metastasis for risk stratification in the preoperative setting. *Sci Rep* 2022; **12**: 19783 [PMID: 36396713 DOI: 10.1038/s41598-022-22026-1]

29 **Bast RC Jr**, Klug TL, St John E, Jenison E, Niloff JM, Lazarus H, Berkowitz RS, Leavitt T, Griffiths CT, Parker L, Zurawski VR Jr, Knapp RC. A radioimmunoassay using a monoclonal antibody to monitor the course of epithelial ovarian cancer. *N Engl J Med* 1983; **309**: 883-887 [PMID: 6310399 DOI: 10.1056/NEJM198310133091503]

30 **Bian J**, Sun X, Li B, Ming L. Clinical Significance of Serum HE4, CA125, CA724, and CA19-9 in Patients With Endometrial Cancer. *Technol Cancer Res Treat* 2017; **16**: 435-439 [PMID: 27562869 DOI: 10.1177/1533034616666644]

31 **Sponholtz TR**, Palmer JR, Rosenberg L, Hatch EE, Adams-Campbell LL, Wise LA. Reproductive factors and incidence of endometrial cancer in U.S. black women. *Cancer Causes Control* 2017; **28**: 579-588 [PMID: 28361447 DOI: 10.1007/s10552-017-0880-4]

32 **Xu X**, Li H, Wang S, Fang M, Zhong L, Fan W, Dong D, Tian J, Zhao X. Multiplanar MRI-Based Predictive Model for Preoperative Assessment of Lymph Node Metastasis in Endometrial Cancer. *Front Oncol* 2019; **9**: 1007 [PMID: 31649877 DOI: 10.3389/fonc.2019.01007]

33 **Chu H**, Pang P, He J, Zhang D, Zhang M, Qiu Y, Li X, Lei P, Fan B, Xu R. Value of radiomics model based on enhanced computed tomography in risk grade prediction of gastrointestinal stromal tumors. *Sci Rep* 2021; **11**: 12009 [PMID: 34103619 DOI: 10.1038/s41598-021-91508-5]

34 **Celli V**, Guerreri M, Pernazza A, Cuccu I, Palaia I, Tomao F, Di Donato V, Pricolo P, Ercolani G, Ciulla S, Colombo N, Leopizzi M, Di Maio V, Faiella E, Santucci D, Soda P, Cordelli E, Perniola G, Gui B, Rizzo S, Della Rocca C, Petralia G, Catalano C, Manganaro L. MRI- and Histologic-Molecular-Based Radio-Genomics Nomogram for Preoperative Assessment of Risk Classes in Endometrial Cancer. *Cancers (Basel)* 2022; **14** [PMID: 36497362 DOI: 10.3390/cancers14235881]

35 **Ueno Y**, Forghani B, Forghani R, Dohan A, Zeng XZ, Chamming's F, Arseneau J, Fu L, Gilbert L, Gallix B, Reinhold C. Endometrial Carcinoma: MR Imaging-based Texture Model for Preoperative Risk Stratification-A Preliminary Analysis. *Radiology* 2017; **284**: 748-757 [PMID: 28493790 DOI: 10.1148/radiol.2017161950]

36 **Park HJ**, Park B, Lee SS. Radiomics and Deep Learning: Hepatic Applications. *Korean J Radiol* 2020; **21**: 387-401 [PMID: 32193887 DOI: 10.3348/kjr.2019.0752]

37 **Chu H**, Lin X, He J, Pang P, Fan B, Lei P, Guo D, Ye C. Value of MRI Radiomics Based on Enhanced T1WI Images in Prediction of Meningiomas Grade. *Acad Radiol* 2021; **28**: 687-693 [PMID: 32418785 DOI: 10.1016/j.acra.2020.03.034]

38 **Breiman L**. Bagging predictors. *Mach Learn* 1996; **24**: 123-140 [DOI: 10.1007/bf00058655]

World Journal of Clinical Cases

Submit a Manuscript: https://www.f6publishing.com

World J Clin Cases 2024 September 16; 12(26): 5922-5929

DOI: 10.12998/wjcc.v12.i26.5922

ISSN 2307-8960 (online)

ORIGINAL ARTICLE

Observational Study

Application of real-time shear wave elastography to Achilles tendon hardness evaluation in older adults

Xuan He, Xin Wei, Jia Hou, Wei Tan, Ping Luo

Specialty type: Medicine, research and experimental

Provenance and peer review: Unsolicited article; Externally peer reviewed.

Peer-review model: Single blind

Peer-review report's classification

Scientific Quality: Grade B

Novelty: Grade C

Creativity or Innovation: Grade C

Scientific Significance: Grade B

P-Reviewer: Leotoing L

Received: May 7, 2024

Revised: June 17, 2024

Accepted: June 27, 2024

Published online: September 16, 2024

Processing time: 76 Days and 14.3 Hours

Xuan He, Xin Wei, Jia Hou, Wei Tan, Ping Luo, Department of Functional Examination, Sichuan Province Orthopedic Hospital, Chengdu 610041, Sichuan Province, China

Corresponding author: Jia Hou, BM BCh, Department of Functional Examination, Sichuan Province Orthopedic Hospital, No. 132 Section 1 West of 1st Ring Road, Wuhou District, Chengdu 610041, Sichuan Province, China. 19908051666@163.com

Abstract

BACKGROUND

Real-time shear wave elastography (SWE) is a non-invasive imaging technique used to measure tissue stiffness by generating and tracking shear waves in real time. This advanced ultrasound-based method provides quantitative information regarding tissue elasticity, offering valuable insights into the mechanical properties of biological tissues. However, the application of real-time SWE in the musculoskeletal system and sports medicine has not been extensively studied.

AIM

To explore the practical value of real-time SWE for assessing Achilles tendon hardness in older adults.

METHODS

A total of 60 participants were enrolled in the present study, and differences in the elastic moduli of the bilateral Achilles tendons were compared among the following categories: (1) Age: 55-60, 60-65, and 65-70-years-old; (2) Sex: Male and female; (3) Laterality: Left and right sides; (4) Tendon state: Relaxed and tense state; and (5) Tendon segment: Proximal, middle, and distal.

RESULTS

There were no significant differences in the elastic moduli of the bilateral Achilles tendons when comparing by age or sex ($P > 0.05$). There were, however, significant differences when comparing by tendon side, state, or segment ($P < 0.05$).

CONCLUSION

Real-time SWE plays a significant role compared to other examination methods in the evaluation of Achilles tendon hardness in older adults.

Key Words: Aged Achilles tendon; Real-time; Shear wave elastography; Young's modulus; Muscle stiffness

Core Tip: We aimed to quantify Achilles tendon stiffness in older adults using real-time shear wave elastography (SWE) technology, and to analyze the overall change in Achilles tendon elasticity at different ages. Sixty participants were enrolled in the present study, and the differences in the elastic moduli of the bilateral Achilles tendons were compared among participants of different ages and sexes, as well as those with different tendon sides, states, and segments. After the research, we concluded that real-time SWE plays a significant role compared to other examination methods in the evaluation of Achilles tendon hardness in older adults.

Citation: He X, Wei X, Hou J, Tan W, Luo P. Application of real-time shear wave elastography to Achilles tendon hardness evaluation in older adults. *World J Clin Cases* 2024; 12(26): 5922-5929
URL: https://www.wjgnet.com/2307-8960/full/v12/i26/5922.htm
DOI: https://dx.doi.org/10.12998/wjcc.v12.i26.5922

INTRODUCTION

The Achilles tendon is the largest tendon in the human body and is comprised of three component parts: the tendon-muscle junction, tendon, and tendon-heel bone junction. It plays very important roles in human locomotion, including walking, running, jumping, and even climbing stairs, and is also the tendon most prone to rupture during exercise[1]. The unique biomechanical properties of the Achilles tendon mean that it is strong enough to withstand the high tensile stresses of muscle contraction, as well as the compressive and shear forces which occur during angulation[2]. When the Achilles tendon undergoes chronic degeneration, which occurs due to a variety of factors, such as decreased blood supply, aging, repeated trauma, and drug-related effects, the internal collagen fiber structure and arrangement, nuclear morphology, and morphological diversity changes. In turn, the normal function and biomechanical properties of the tendon are affected, making it easy for the tendon to rupture under the action of an external force[3,4]. With the ongoing improvement to people's living standards, increased emphasis regarding health awareness and delayed retirement ages, the proportion of older adults aged 55-70 years who continue to contribute to their jobs and engage in physical exercise has increased significantly. Owing to the degeneration of body functions in older adults, even minor activities may cause soft tissue damage, and the pain may not be obvious, or may be difficult to detect. Due to such delayed detection, therefore, it is likely that the optimal treatment window will be missed[5].

Various tissues in the body have different elastic coefficients, and strains (primarily morphological changes) to these tissues change after the application of external forces or alternating vibrations. Ultrasound elastography collects the signals of each segment of a designated area during a certain period of time, which are then comprehensively analyzed using a combined autocorrelation method. The subsequent results produce gray-scale or color-coded image[6]. Real-time shear wave elastography (SWE) is a new real-time two-dimensional (2D) elastography method for estimating stiffness quantitatively in kilopascals (kPa). Real-time SWE uses focused ultrasonic beams to induce a radiation force in tissues, as well as ultrasonic imaging sequences capable of observing movement in real-time[7]. In real-time SWE, a transducer emits ultrasound waves that induce shear waves within the tissue of interest. These shear waves propagate through the tissue and their velocity is directly related to the tissue's stiffness. By analyzing the propagation speed of these shear waves, the technique can calculate the elastic modulus of the tissue, which reflects its stiffness or hardness[8]. Real-time SWE can provide information surrounding tissue texture, elastic hardness, elastic value, shape and area ratios, and establish another independent dimension regarding tissue information, which has broad prospects for clinical applications involving almost all organs of the human body[9]. Real-time SWE has been widely used to evaluate the liver, gallbladder, spleen, pancreas, kidney, thyroid, breast, cardiovascular, nerve, prostate, uterine tissues, and various lesions in tissues, as well as in radiofrequency ablation and anti-angiogenesis tumor therapies[10].

Real-time SWE is a popular research topic in the field of ultrasound imaging[11]; Using SWE, Caroline Ewertsen and colleagues examined the biceps brachii, gastrocnemius, and quadriceps muscles of healthy volunteers[12]. Wang *et al*[13] used SWE to measure shear wave velocity of supraspinatus tendons and muscles to help predict residual tendon mass and found that this is one of the key factors in successful rotator cuff repair. A recent study using the SWE technique found that ankle joint position and probe frequency are factors that affect the elastic value of the Achilles tendon[14]. Another study evaluated the association of renal elasticity with renal fibrosis in patients with chronic kidney disease using real-time SWE[15]. However, the application of real-time SWE in the musculoskeletal system and sports medicine in older adults of different ages has not been extensively studied.

With the increased clinical promotion and application of real-time SWE, it is also being increasingly applied to study the skeletal muscle system. The purpose of the present study, therefore, was to collect data concerning Achilles tendon stiffness in older adults, aged 55-70 years old, to quantify Achilles tendon stiffness in these older adults using real-time SWE technology, and to analyze the overall change in Achilles tendon elasticity at different ages, and promote further research regarding the use of real-time SWE to evaluate the health status of tendons in different populations and provide information for clinical decision-making.

MATERIALS AND METHODS

General information

A total of 60 subjects without any obvious limitations in terms of ankle motion were randomly selected from inpatients in our hospital and were enrolled in the present study. The subjects were between 55 and 70 (average 62.15 ± 1.25) years old. Of the 60 subjects, 45 were women and 15 were men. The participants were divided into three groups: 55-60 years old (n = 35), 61-65 years old (n = 14), and 66-70 years old (n = 11).

Inclusion criteria: (1) Age between 55 and 70 years; and (2) No activity.

Exclusion criteria: (1) Patients with a history of neuromuscular diseases or musculoskeletal injuries involving the lower extremities; (2) Patients who had recently (within 1 month) taken drugs that affect muscle function; (3) Patients with an obvious unilateral dominant foot (the maximum circumference difference between the calf and thigh on both sides should be < 10%); (4) Heart disease or severe asthma; (5) Abnormal gait (caused by central nervous system or peripheral nerve injury, bone and joint disease, lesions, or vascular skin disease); and (6) Systemic diseases such as fibromyalgia, degenerative joint disease, calcific Achilles tendinitis, chronic Achilles tendon pain, rheumatoid arthritis, and neuropathy.

Instruments and methods

Real-time SWE procedure: The present study utilized a Supersonic Aixplorer (France Acoustics) ultrasound instrument and a linear array probe to perform SWE examinations, with the probe frequency set at 4-15 MHz and probe model L11-3U. Patients were instructed to lay in the prone position with their legs stretched and relaxed, feet hanging off the edge of the examination table, toes pointed down and perpendicular to the horizontal plane, and Achilles tendon fully exposed. SWE examination was performed at least 10 minutes after the tendon is completely relaxed, using the L18-5 linear probe and then using the L20-6 hockey stick probe, which was selected by default musculoskeletal parameters. The Q-box depth was set to 1 cm. After a uniform color diagram was obtained, it was measured three times and the average values were taken for further analysis. Between each collection, the probe was removed from the patient's skin.

First, with the Achilles tendon in a relaxed state, the parameter mode was adjusted so that the Achilles tendon and its surrounding tissues were clearly displayed in 2D ultrasound mode. The Achilles tendon was divided into proximal (muscle-tendon junction), middle (2-6 cm above the attached end of Achilles tendon), and distal segments (attached end of Achilles tendon), and each segment was scanned vertically and continuously along the maximum long-axis section. After obtaining a stable image, SWE was performed using a 1.0 cm × 1.0 cm sampling frame. Once the elasticity map was complete, stable, and without defects, 3 mm regions of interest were used to measure and record the elastic modulus (kPa). Three measurements were obtained from each section of the Achilles tendon, at different locations on the elasticity map, from which average values were obtained. The average elastic modulus of the Achilles tendon on each side was calculated from the mean values of the three sections. The patient was then asked to stretch the dorsum of the foot by 15°, stretching the Achilles tendon to its greatest extent, such that the tendon was in a tense state. The elastic modulus of the three segments of the Achilles tendon was measured again. The average value for each segment and that for each unilateral Achilles tendon were calculated separately. All measurements were obtained by the same sonographer.

Statistical analysis

SPSS v.26.0 software was used for data processing, and measurement data are described by mean ± SD. Analysis of variance was used to compare multiple groups of measured data, and the least significant difference method was used to compare groups. Statistical significance was set as $P < 0.05$.

RESULTS

Comparison of elastic moduli in different age groups, relaxed state

Elastic moduli of the bilateral Achilles tendons in the relaxed state did not significantly differ among the groups categorized by age ($P > 0.05$). Further details are presented in Table 1.

Comparison of elastic moduli between sexes, relaxed state

Elastic moduli of the bilateral Achilles tendons in the relaxed state did not significantly differ between the groups categorized by sex ($P > 0.05$). Further details are presented in Table 2.

Comparison of elastic moduli between left and right sides, relaxed state

Elastic moduli of the Achilles tendon in the relaxed state differed significantly between the left and right sides ($P < 0.05$). Further details are presented in Table 3.

Comparison of elastic moduli of the bilateral Achilles tendon, various states

Elastic moduli of the Achilles tendon differed significantly based on the state of relaxation and tension ($P < 0.05$). Further details are presented in Table 4.

Comparison of elastic moduli among the three segments, relaxed state

Elastic moduli of the Achilles tendon in the relaxed state differed significantly based on the segment involved ($P < 0.05$). Further details are presented in Table 5.

Table 1 Elastic modulus of bilateral Achilles tendon in relaxed state among multiple groups of measurement data, mean ± SD

Variable		55-60 (*n* = 35)	61-65 (*n* = 14)	66-70 (*n* = 11)	*F* value	*P* value
Relaxed modulus of elasticity	Left average	326.39 ± 81.44	315.09 ± 57.09	365.51 ± 63.38	1.609	0.209
	Right average	354.63 ± 90.1	321.42 ± 59.88	406.98 ± 127.42	2.666	0.078

Table 2 Elastic modulus of bilateral Achilles tendon in relaxed state, mean ± SD

variable		Male (*n* = 15)	Female (*n* = 45)	*t* value	*P* value
Relaxed modulus of elasticity	Left average	323.69 ± 61.47	333.33 ± 78.55	-0.433	0.667
	Right average	352.33 ± 78.6	357.86 ± 100.4	-0.194	0.847

Table 3 Elastic modulus of Achilles tendon in relaxed state, mean ± SD

Variable	Left average	Right average	*t* value	*P* value
Relaxed modulus of elasticity	330.92 ± 74.27	356.48 ± 94.81	-2.849	0.006

Table 4 Elastic modulus of bilateral Achilles tendon, mean ± SD

Variable	Relaxed modulus of elasticity	Elastic modulus under tension	*t* value	*P* value
Left average	330.92 ± 74.27	762.92 ± 26.02	-44.262	< 0.001
Right average	356.48 ± 94.81	768.74 ± 24.05	-34.413	< 0.001

Table 5 Elastic modulus of two groups of three segments of bilateral Achilles tendon in relaxed state, mean ± SD

Variable	Relaxed modulus of elasticity	*t* value	*P* value
Far left	288.19 ± 83.67	-4.288	<0.001
Middle left	328.11 ± 81.92		
Far left	288.19 ± 83.67	-6.206	<0.001
Near left	376.46 ± 105.42		
Middle left	328.11 ± 81.92	-4.326	<0.001
Near left	376.46 ± 105.42		
Far right	329.61 ± 118.97	-2.309	0.024
Middle right	353.75 ± 98.01		
Far right	329.61 ± 118.97	-4.424	<0.001
Near right	386.08 ± 103.78		
Middle right	353.75 ± 98.01	-3.144	0.003
Near right	386.08 ± 103.78		

DISCUSSION

The power behind the activity of the lower limb muscle group primarily originates from the muscle action of the lower limbs and trunk. Muscle activity helps to maintain balance, absorb shock, accelerate and decelerate motion, and promote limb movements[16]. The quadriceps are integral in hip flexion and knee extension, and act as a knee extensor in the first 20% of the jogging cycle. After the heel departs the ground, the quadriceps also play a role in hip flexion and knee extension. When the anterior thigh muscles, such as the quadriceps, relax, the posterior thigh muscles, such as the biceps femoris, contract to flex the calf. When quadriceps and other anterior thigh muscles contract, the biceps femoris and other posterior thigh muscles relax, working in tandem to flex and extend the calf. When the gastrocnemius lifts the heel off the ground, its concentric forceful contraction reaches a peak, producing a powerful kicking action that forces the body's

center of gravity forward. The tibialis anterior is the dorsiflexor of the ankle, contracting when the heel strikes and the toes leave the ground during jogging to control the plantar flexion of the ankle joint[17]. The Achilles tendon is the largest tendon in the human body, formed by fusion of the calf triceps muscles (soleus, gastrocnemius inner, and outer heads) approximately 15 cm above the heel. It is primarily composed of dense connective tissue with a scarce blood supply and connects the muscle groups at the back of the calf to the calcaneus. The primary function of the Achilles tendon is to flex the calf and plantarflex the foot. Together with the calf muscles, it plays an important role in numerous movements, such as standing upright, jumping, and running. During physiological exercise, the physical characteristics of the muscles change dynamically to adapt to the needs of various physiological and motor functions. Quantification of muscle physical properties helps in understanding their physiological function, of which muscle stiffness is an important parameter[18]. Muscle stiffness can change under a variety of conditions, such as active contraction and passive stretching, and is important for muscles to function efficiently[19]. Moreover, a strong linear relationship exists among muscle stiffness, strength, and tension[20].

The Achilles tendon, as a viscoelastic tendon structure that maintains the stability of ankle joint activities, has unique biomechanical properties, and its elasticity and hardness are a manifestation of these biomechanical properties. Achilles tendon injuries are the most common types of tendon injuries, and their incidence has increased in recent years. Because the Achilles tendon is a poorly vascularized tissue, it is prone to numerous post-injury complications, and is difficult to repair and heal. Stress and injury to the Achilles tendon affect its mechanical properties[21]; therefore, quantification of muscle stiffness aids in understanding the physiological functions of skeletal muscles. Understanding changes in muscle stiffness in older adults who have suffered an Achilles tendon injury is necessary to guide the management of clinical treatment and rehabilitation training. In sports medicine, quantifying the elastic characteristics of skeletal muscle is helpful for understanding the impact of changes in muscle stiffness on pain or injury in older adults with Achilles tendon injury, along with its underlying mechanisms. Numerous methods, such as soft tissue ultrasound palpation and magnetic resonance elastography, are available for measuring muscle stiffness[22,23]. In the diagnosis of Achilles tendon injury, traditional ultrasound technology is inexpensive, noninvasive, reproducible, and can detect morphological changes in muscles; however, biomechanical evaluations and quantitative analyses cannot be performed.

In most skeletal muscle examinations performed using ultrasound, an operator applies manual pressure to the patient's body using an ultrasound probe, causing the tissue to deform, with softer tissues deforming more and experiencing stress. In contrast to harder tissues, the corresponding strain rate can be obtained by comparing the strain rate in the static state. A major problem with semiquantitative analysis is that the operator may find it challenging to maintain a constant pressure each time a force is applied. SWE is a new generation of elasticity imaging technology that obtains information concerning hardness of the examined tissues based on the elastic modulus calculated during an elasticity test performed without compressing the tissue[24]. SWE is used to quantify tissue stiffness using the shear wave method, and those data are used to analyze the results. In the SWE method, $3\rho C2$ (E = Young's modulus, ρ is tissue density, C is shear wave velocity, and the resulting Young's modulus (in Pascal) can directly characterize mechanical properties of the tissue. SWE allows for the real-time quantitative analysis of the elastic properties of tissues, and the resulting color-coded map can distinguish between various tissues based on their degree of elasticity. The color range reflects the stiffness of the tissue; that is, Young's modulus. When the Young's modulus was elevated, the SWV was higher, indicating greater tissue stiffness[25]. Researchers first used ultrasound elastography to study the musculoskeletal structure of healthy adults, and found that musculoskeletal tissue has a relatively high hardness[26]. Additionally, the experimental results of other studies have shown a good linear relationship between the Young's modulus obtained by SWE and muscle activity reflected by electroencephalogram results. Because muscle mechanical properties are nonlinear, Young's modulus should exhibit a certain relationship with muscle tension; therefore, SWE can accurately reflect and evaluate muscle tension[27]. As SWE is a real-time, full-amplitude, and fully quantitative imaging system for human tissue stiffness evaluation, this technology was used in a previous multicenter study to evaluate the Achilles tendon in normal people. The results showed that there were significant differences in elasticity of the Achilles tendon in different postures, although the parallelism between the probe and Achilles tendon affected the test results. Therefore, when testing elasticity of the Achilles tendon, the foot on the side being tested should be allowed to hang naturally, and the probe should be placed parallel to the tendon. Simultaneously, the examiner should move calmly, gently lower the probe, and obtain the most stable Young's modulus values when the long axis of the Achilles tendon is clearly visible.

The results of the present study showed that among the 60 older adult participants, there was no statistically significant difference in the elastic moduli of the Achilles tendon in a relaxed state based on age or sex (see Tables 1 and 2, respectively, for details). Achilles tendon stiffness does not increase or decrease regularly with age, and the changes between sexes have no definitive significance. Although the change in Achilles tendon stiffness in this age group is not specific, and the correlation with different sexes was not close enough, we obtained a corresponding reference range for estimating the normal Achilles tendon elastic modulus value in older adults. When the Achilles tendon was in the relaxed state, the elastic moduli of the two sides were different (see Table 3 for details), with that of the right side higher than that of the left. This result is most likely related to the fact that the right lower limb plays a key role in controlling various bodily activities. With the Achilles tendon in relaxed and tense states, there was a significant difference in its elastic modulus, as the hardness in the tense state was significantly higher than that in the relaxed state (Table 4). Aubry *et al*[28] and Slane *et al*[29] also demonstrated that the elastic modulus of the Achilles tendon increases with a gradual increase in the degree of dorsiflexion of the ankle joint, and that dorsiflexion of the ankle joint can give traction to the Achilles tendon, which has a greater effect on the medial side of the Achilles tendon. Such an unbalanced distribution is likely the key reason for Achilles tendon injuries. Dorsiflexion is frequently involved in various activities of the ankle joint. Therefore, older adults who walk, run, or jump often are more prone to Achilles tendon injuries than their less active counterparts. Older adults who love sports should be taught how best to prevent Achilles tendon injuries and evaluate its health so that disorders can be prevented before they occur. Here, when the Achilles tendon was in a relaxed state, the

difference in elastic modulus was statistically significant among the three segments (Table 5). Moreover, the hardness of the Achilles tendon gradually decreased from near to far. Some foreign scholars compared Achilles tendon elastography with histological diagnosis, which showed that elastography could accurately evaluate the degree of Achilles tendon degeneration[30]. The hardness value of mild degeneration was reduced, while that of severe degeneration increased due to the presence of calcification. Although no pathological changes were detectable by ultrasound in the middle and distal parts of the Achilles tendon, the histology is very likely to show slight degeneration and tendency to injury, inflammation, and other related problems.

The incidences of chronic Achilles tendon disorders and rupture are increasing in older adults. Achilles tendon rupture treatment aims to fully restore the physiological length, integrity, and toughness of the tendon, plantar flexion force of the triceps of the lower limbs, and function of the ankle joint. Ultrasound SWE is a new imaging technology and a research hotspot which has emerged in recent years. It provides hardness information by detecting the Young's modulus value of a given tissue, and gradually demonstrates its unique application value in clinical practice. The change in Young's modulus of elasticity is an important indicator for determining health of the Achilles tendon, and can help clinically evaluate the condition of the tendon, formulate treatment plans based on that condition, and help patients recover better.

The findings of this study have the potential to provide clinicians with a non-invasive and quantitative method for assessing Achilles tendon stiffness in older adults. This information is crucial for early detection of tendon degeneration, monitoring disease progression, and evaluating the effectiveness of treatment interventions. Real-time SWE offers a direct measurement of tissue elasticity, which can complement traditional imaging modalities and subjective clinical assessments, leading to more accurate and objective evaluations of tendon health. Moreover, by focusing on older adults, this study addresses a population that is particularly susceptible to tendon injuries and degenerative changes. Understanding age-related alterations in Achilles tendon hardness can help in identifying individuals at higher risk of tendon pathologies and implementing preventive strategies to maintain tendon health in the aging population. In the broader context of musculoskeletal imaging research, this study contributes to the growing body of knowledge surrounding the utility of real-time SWE in assessing tendon properties. By demonstrating the feasibility and potential clinical value of this imaging technique in older adults with Achilles tendon concerns, our findings expand the application of elastography in musculoskeletal imaging and pave the way for further research in this area.

Overall, the implications of this study lie in its potential to advance the field of musculoskeletal imaging by providing a novel approach for evaluating Achilles tendon hardness in older adults. The insights gained from this research can inform clinical decision-making, improve patient care, and stimulate further investigations into the use of real-time SWE for assessing tendon health in diverse populations.

CONCLUSION

In summary, the application of real-time SWE to assess Achilles tendon stiffness in older adults can provide quantitative clinical indicators of Achilles tendon health and guide rehabilitation treatment.

FOOTNOTES

Author contributions: He X was the guarantor and designed the study; He X, Wei X, Hou J participated in the acquisition, analysis, and interpretation of the data, and drafted the initial manuscript; He X, Wei X, Hou J, Tan W, Luo P revised the article critically for important intellectual content.

Supported by Sichuan Orthopaedic Hospital Research Project, No. 2019MS02.

Institutional review board statement: The study was reviewed and approved by the Science and Research Office of Sichuan Province Orthopedic Hospital.

Informed consent statement: All study participants, or their legal guardian, provided informed written consent prior to study enrollment.

Conflict-of-interest statement: There are no conflicts of interest to report.

Data sharing statement: No additional data are available.

STROBE statement: The authors have read the STROBE Statement—checklist of items, and the manuscript was prepared and revised according to the STROBE Statement—checklist of items.

Country of origin: China

ORCID number: Jia Hou 0009-0006-8495-008X.

S-Editor: Lin C
L-Editor: A
P-Editor: Cai YX

REFERENCES

1 **Chen XM**, Wang R, Yuan SF, Bai L, Liu L. [Evaluation of ultrasonic shear wave elastography after surgical repair of Achilles tendon rupture]. *Hanshaojibing Zazhi* 2023; **30**: 69-71 [DOI: 10.3969/j.issn.1009-3257.2023.03.031]
2 **Cheng J**, Zhou L. [The effect of real-time ultrasound elastography measurement training mode on the biomechanical properties of Achilles tendon]. *Yixue Qianyan* 2018; **8**: 378-379
3 **Zhang ZF**, Wu JQ, Kong DW, Ma ZX, Li GC, Gao X, Ming LB. [Clinical experience in repairing old Achilles tendon rupture with flexor longus transposition combined with gastrocnemius tendon flipping and bridging]. *Zuhuai Waike Dianzi Zazhi* 2023; **10**: 33-36, 50
4 **Shen LM**, Yan RR. [External dynamic characteristics, causes and exercise intervention of Achilles tendon rupture]. *Hubei Shifandaxue Xuebao (Zirankexueban)* 2022; **42**: 74-79, 86
5 **Feng YH**, Cui JT, Zhou XK, Wang SB. [Comparative study of surgical and non-surgical treatment of acute Achilles tendon rupture]. *Zhongguo Xiangdai Yisheng* 2020; **58**: 85-88, 92
6 **Qiao XH**, Xing JF. [The principle and clinical application status of shear wave ultrasound elastography]. *Zhongguo Jieru Yingxiangyuzhiliaoxue* 2015; **12**: 512-515
7 **Zhou J**, Yan F, Xu J, Lu Q, Zhu X, Gao B, Zhang H, Yang R, Luo Y. Diagnosis of steatohepatitis and fibrosis in biopsy-proven nonalcoholic fatty liver diseases: including two-dimension real-time shear wave elastography and noninvasive fibrotic biomarker scores. *Quant Imaging Med Surg* 2022; **12**: 1800-1814 [PMID: 35284290 DOI: 10.21037/qims-21-700]
8 **Parikh P**, Ryan JD, Tsochatzis EA. Fibrosis assessment in patients with chronic hepatitis B virus (HBV) infection. *Ann Transl Med* 2017; **5**: 40 [PMID: 28251119 DOI: 10.21037/atm.2017.01.28]
9 **Xu Q**, Jin YH, Ding TY. [Application value of high-frequency ultrasound combined with ultrasound elastography in the diagnosis of papillary thyroid carcinoma]. *Linchuangheshiyanyixue Zazhi* 2023; **22**: 883-886 [DOI: 10.3969/j.issn.1671-4695.2023.08.026]
10 **Che DD**, He TJ, Lou XF, Sui Q. [Clinical application of the combination of ultrasound elastography and magnetic resonance imaging in benign and malignant breast tumors]. *Jinzhou Yikedaxue Xuebao* 2023; **44**: 49-53
11 **Niu Y**, Yue Y, Zheng Y, Long C, Li Q, Chen Y, Chen Z, Ma X. SWE (mean) of Quadriceps, a Potential Index of Complication Evaluation to Patients with Chronic Obstructive Pulmonary Disease. *Int J Chron Obstruct Pulmon Dis* 2022; **17**: 1921-1928 [PMID: 36039167 DOI: 10.2147/COPD.S374945]
12 **Li JR**, Wang ZT, Liu N, Liu YG, Shi L. [Application of real-time shear wave elastography and contrast-enhanced ultrasonography in evaluating the efficacy of radiofrequency ablation in the treatment of papillary thyroid microcarcinoma]. *Jiating Yiyao* 2018; **000**
13 **Wang X**, Zhu J, Liu Y, Li W, Chen S, Zhang H. Assessment of ultrasound shear wave elastography: An animal ex-vivo study. *J Appl Clin Med Phys* 2023; **24**: e13924 [PMID: 36729737 DOI: 10.1002/acm2.13924]
14 **Chen X**, Chen S, Zhang F, Zhu Y, Yi D, Xu H, Tang J, Zhang Q, Wang Y. Ultrasonic shear wave elastography predicts the quality of the residual tendon before the rotator cuff repair. *Insights Imaging* 2024; **15**: 72 [PMID: 38483642 DOI: 10.1186/s13244-024-01642-7]
15 **Pelea MA**, Serban O, Badarinza M, Gutiu R, Fodor D. Shear-Wave Elastography of the Achilles tendon: reliability analysis and impact of parameters modulating elasticity values. *J Ultrasound* 2024 [PMID: 38613661 DOI: 10.1007/s40477-024-00877-w]
16 **Chen Z**, Wang Y, Ying MTC, Su Z, Han X, Gunda ST. Association of renal elasticity evaluated by real-time shear wave elastography with renal fibrosis in patients with chronic kidney disease. *Br J Radiol* 2024; **97**: 392-398 [PMID: 38308024 DOI: 10.1093/bjr/tqad030]
17 **Sun B**, Sejati PA, Yao JF. [Study on the Electrical Characteristics of Human Calf Muscle Physiological Response to Exercise Training]. *Shengwuhuaxue Yu Shengwuwuli Jinzhan* 2023; **50**: 595-605 [DOI: 10.16476/j.pibb.2022.0211]
18 **Gennisson JL**, Cornu C, Catheline S, Fink M, Portero P. Human muscle hardness assessment during incremental isometric contraction using transient elastography. *J Biomech* 2005; **38**: 1543-1550 [PMID: 15922766 DOI: 10.1016/j.jbiomech.2004.07.013]
19 **Allum JH**, Mauritz KH. Compensation for intrinsic muscle stiffness by short-latency reflexes in human triceps surae muscles. *J Neurophysiol* 1984; **52**: 797-818 [PMID: 6512589 DOI: 10.1152/jn.1984.52.5.797]
20 **Hug F**, Tucker K, Gennisson JL, Tanter M, Nordez A. Elastography for Muscle Biomechanics: Toward the Estimation of Individual Muscle Force. *Exerc Sport Sci Rev* 2015; **43**: 125-133 [PMID: 25906424 DOI: 10.1249/JES.0000000000000049]
21 **Li S**, Guo RJ. [Real-time shear wave elastography in the assessment of acute blunt injury of the Achilles tendon]. *Zhongguo Yixueyingxiang Jishu* 2019; **35**: 1155-1158 [DOI: 10.13929/j.1003-3289.201903015]
22 **Du B**, Lu Q, Mao LL, Yan JF, Chen FH. [The significance of real-time shear wave elastography in measuring the stiffness of erector spinae in ultrasound practitioners]. *Zhejiang Linchuang Yixue* 2022; **24**
23 **Tan XX**, Liu MH, Liu XM, Liu Y, Lan Y, Yang ZR. [Acoustic palpation tissue quantitative imaging evaluation of changes in muscle stiffness after injection of botulinum toxin type A in the treatment of forearm pronator spasticity after stroke]. *Zhongguo Yixueyingxiang Jishu* 2019; **35**: 256-259 [DOI: 10.13929/j.1003-3289.201807087]
24 **Yan M**, Dai L, Wu R. [The diagnostic value of shear wave elastography in benign and malignant thyroid nodules]. *Zhongguo Zhongxiyijiehe Yingxinagxue Zazhi* 2021; **19**: 131-134, 139 [DOI: 10.3969/j.issn.1672-0512.2021.02.009]
25 **Zhou N**, Zhang HR, Jiang Y, Liang L. [The value of shear wave elastography in evaluating renal cortical stiffness in patients with normal renal function in type 2 diabetes]. *Yixueyanjiu Zazhi* 2020; **49**: 118-121 [DOI: 10.11969/j.issn.1673-548X.2020.12.028]
26 **Bai C**, Wang LQ, Zhang PF, Li Q, Chen R, Li SY, Zhu Y. [Preliminary study on the evaluation of puborectalis muscle in healthy adults with ultrasonic shear wave elastography]. *Zhongguo Chaoshengyixue Zazhi* 2022; **38**: 566-569 [DOI: 10.3969/j.issn.1002-0101.2022.05.024]
27 **Liu CL**, Xu K, Zhang ZJ, Yu J. [Research on the reliability of muscle state detection system in evaluating muscle tension in stroke patients]. *Zhongguo Kangfu* 2014; **29**: 99-100

28 **Aubry S**, Risson JR, Kastler A, Barbier-Brion B, Siliman G, Runge M, Kastler B. Biomechanical properties of the calcaneal tendon in vivo assessed by transient shear wave elastography. *Skeletal Radiol* 2013; **42**: 1143-1150 [PMID: 23708047 DOI: 10.1007/s00256-013-1649-9]

29 **Slane LC**, DeWall R, Martin J, Lee K, Thelen DG. Middle-aged adults exhibit altered spatial variations in Achilles tendon wave speed. *Physiol Meas* 2015; **36**: 1485-1496 [PMID: 26020294 DOI: 10.1088/0967-3334/36/7/1485]

30 **Barfod KW**, Riecke AF, Boesen A, Hansen P, Maier JF, Døssing S, Troelsen A. Validation of a novel ultrasound measurement of achilles tendon length. *Knee Surg Sports Traumatol Arthrosc* 2015; **23**: 3398-3406 [PMID: 25038882 DOI: 10.1007/s00167-014-3175-2]

World Journal of Clinical Cases

Submit a Manuscript: https://www.f6publishing.com

World J Clin Cases 2024 September 16; 12(26): 5930-5936

DOI: 10.12998/wjcc.v12.i26.5930

ISSN 2307-8960 (online)

ORIGINAL ARTICLE

Randomized Controlled Trial

Study of the intensive care unit activity scale in the early rehabilitation of patients after direct cardiac surgery

Li Wang, Jing-Ya Lu, Xiao-Xiao Ma, Lan-Ou Ma

Specialty type: Nursing

Provenance and peer review: Unsolicited article; Externally peer reviewed.

Peer-review model: Single blind

Peer-review report's classification

Scientific Quality: Grade C
Novelty: Grade C
Creativity or Innovation: Grade B
Scientific Significance: Grade B

P-Reviewer: Hayashi T

Received: May 18, 2024
Revised: June 29, 2024
Accepted: July 10, 2024
Published online: September 16, 2024
Processing time: 65 Days and 14.2 Hours

Li Wang, Jing-Ya Lu, Lan-Ou Ma, Intensive Care Unit, Dongyang People's Hospital, Jinhua 322100, Zhejiang Province, China

Xiao-Xiao Ma, Department of Rehabilitation Medicine, Dongyang People's Hospital, Jinhua 322100, Zhejiang Province, China

Corresponding author: Li Wang, MNurs, Nurse, Intensive Care Unit, Dongyang People's Hospital, No. 60 Wuning West Road, Dongyang City, Jinhua 322100, Zhejiang Province, China. dyyykhjjjj@163.com

Abstract

BACKGROUND

Direct cardiac surgery often necessitates intensive post-operative care, and the intensive care unit (ICU) activity scale represents a crucial metric in assessing and guiding early rehabilitation efforts to enhance patient recovery.

AIM

To clarify the clinical application value of the ICU activity scale in the early recovery of patients after cardiac surgery.

METHODS

One hundred and twenty patients who underwent cardiac surgery between September 2020 and October 2021 were selected and divided into two groups using the random number table method. The observation group was rated using the ICU activity scale and the corresponding graded rehabilitation interventions were conducted based on the ICU activity scale. The control group was assessed in accordance with the routine rehabilitation activities, and the postoperative rehabilitation indexes of the patients in both groups were compared (time of tracheal intubation, time of ICU admission, occurrence of complications, and activity scores before ICU transfer). The two groups were compared according to postoperative rehabilitation indicators (time of tracheal intubation, length of ICU stay, and occurrence of complications) and activity scores before ICU transfer.

RESULTS

In the observation group, tracheal intubation time lasted for 18.30 ± 3.28 h and ICU admission time was 4.04 ± 0.83 d, which were significantly shorter than the control group (t-values: 2.97 and 2.038, respectively, $P < 0.05$). The observation group also had a significantly lower number of complications and adverse events

compared to the control group ($P < 0.05$). Before ICU transfer, the observation group (6.7%) had few complications and adverse events than the control group (30.0 %), and this difference was statistically significant ($P < 0.05$). Additionally, the activity score was significantly higher in the observation (26.89 ± 0.97) compared to the control groups (22.63 ± 1.12 points) (*t*-value; -17.83, $P < 0.05$).

CONCLUSION
Implementation of early goal-directed activities in patients who underwent cardiac surgery using the ICU activity scale can promote the recovery of cardiac function.

Key Words: Early recovery activities; Goal orientated; ICU mobility scale; Intensive care unit; Cardiac surgery

Core Tip: Intensive care unit (ICU) activity scale-guided graded rehabilitation interventions significantly shortened the tracheal intubation time and ICU stay, lower complication rates, and improved the activity scores of patients undergoing cardiac surgery. This suggests that the ICU Activity Scale has a positive clinical application value in promoting early recovery after cardiac surgery.

Citation: Wang L, Lu JY, Ma XX, Ma LO. Study of the intensive care unit activity scale in the early rehabilitation of patients after direct cardiac surgery. *World J Clin Cases* 2024; 12(26): 5930-5936
URL: https://www.wjgnet.com/2307-8960/full/v12/i26/5930.htm
DOI: https://dx.doi.org/10.12998/wjcc.v12.i26.5930

INTRODUCTION

Direct-vision intracardiac surgery involves correcting defects or removing lesions, installing valves, vascular bypass, and other operations performed by opening the patient's heart in case of cardiac arrest or non-stop beating[1]. Various complications, such as pulmonary infection, neuromuscular atrophy, lower extremity venous thrombosis, and intensive care unit (ICU)-acquired debilitation, often occur in patients after direct cardiac surgery, which can easily affect the recovery of body function and increase the patient's economic burden. Recently, early rehabilitation activities have been considered effective and safe. With the in-depth study of early rehabilitation activities, they have become an important part of postoperative cardiac surgery care[2]. Studies have shown that the current early rehabilitation activities do not result in the highest level of patient mobility while ensuring safety, and there are no standardized criteria for the optimal mode, intensity, and duration of activities[3]. Early goal-directed activities are needed for ICU patients who require early rehabilitation activities. The team (physicians, nurses, and physiotherapists) sets a goal based on progressive, feasible, and safe activities and proceeds according to the goal, so that the patient's mobility can reach the highest level[4] and the patient can receive precise and individualized rehabilitation treatment. Based on multidisciplinary teamwork, ICU activity scale ratings were performed on patients who underwent direct cardiac surgery, early rehabilitation activity interventions were performed based on ICU activity scale ratings using goal orientation, and their effects on postoperative cardiac rehabilitation were observed. The remainder of this paper is organized as follows.

MATERIALS AND METHODS

Information and methods

General information: Postoperative cardiac surgery patients admitted to the ICU between September 2020 and October 2021 were selected and divided into two groups using the random number table method. Sample size estimation used the formula $N1 = N2 = 2[(t\alpha/2 + t\beta/2)S/\delta]2$ to estimate the mean of two samples in the experimental study, combined with the pre-test results of the tracheal intubation time to obtain $\delta = 15.58$, $S = 20.36$, bilateral $\alpha = 0.05$, $\beta = 0.1$, and examined the table to obtain $t\alpha/2 = 1.96$, $t\beta/2 = 1.282$, and substituting into the formula to obtain the samples needed in each of the two groups. Considering sample shedding, the sample size was expanded by 20%, that is, at least 48 cases were needed in each of the two groups. Both groups included 60 cases. Inclusion criteria: (1) Age ≥ 18 years; (2) Coronary artery bypass grafting, aortic replacement, and valve replacement surgery; (3) Postoperative hemodynamic stability, no angina attack, no acute myocarditis or pericarditis, no peripheral vascular thrombosis or embolism, no cerebrovascular accidents, good glycemic control, and no new electrocardiographic ischemic changes; (4) Basic verbal communication skills; and (5) The patients and their family members signed an informed consent form. Exclusion criteria: (1) Mental, cognitive, and consciousness disorders; (2) Lower limb mobility disorders or self-care ability defects; (3) Combined serious respiratory, hepatic, renal and systemic diseases; and (4) Combined with chest trauma or tumor. This study was approved by the Ethics Committee of Dongyang People's Hospital.

Table 1 Intensive care unit mobility scale rating scale

IMS	Activity content
Grade 0	Perform the first step, physical activity (goal; twice daily), including PROM at least 10 times daily, and train and encourage family members to perform PROM on the patient for 15–30 min, if the patient can tolerate it
Grade 1	Perform step 2 and step 3. If not tolerated, perform step 3 first and step 2 again. Step 2, elevate the head of the bed > 45° for > 1 h (goal: Twice daily). Step 3, adjust the bed to a chair position, elevate the head of the bed > 60° for > 1 h, and repeat every 2 h if tolerated by the patient
Grade 2	Perform step 4, adjusting the bed into a heart failure chair position for > 1 h, and if the patient tolerates it, repeat the above every 2 h for > 4 h at a time. Steps 2 to 4 require checking the patient's tolerance level at least twice every 30 min
Grade 3	Perform step 5, sit at the edge of the bed (target; 20 min) or help the patient to sit at the edge of the bed with minimal assistance, this step requires at least one staff member to help the patient sit and assist the patient to move their lower limbs
Grade 4	Perform step 6, stand at the edge of the bed for > 2 min (goal; twice daily). If possible, try to walk at the edge of the bed for 10 s
Grades 5–6	Perform step 7, move the patient to sit on a chair for > 60 min (goal; 2–3 times daily) and adjust the patient's sitting position every 1 h, if the patient is unstable during this process, support the patient to the chair with assistance and do not continue to step 8
Grades 7–10	Perform step 8, walking tolerance training (goal; 2-3 times daily), recording the distance the patient walks and assistive devices used

IMS: Intensive care unit mobility scale; PROM: Passive physical activity.

Research tool: In 2014, the ICU mobility scale (IMS) was developed by Australian researchers Hodgson *et al*[5] to assess the optimal level of activity of ICU patients, which is divided into 11 grades, of which inactivity is grade 0, and active activity in bed to independent walking is divided into 10 grades, with a reliability of 0.69–0.83. Liu *et al*[6] conducted Chinese translation and reliability and validity tests of the IMS, resulting in a weighted Kappa value of 0.84 and validity of 0.872. In the reliability and validity test, the results of the IMS had good reliability and internal consistency; the weighted Kappa value was 0.84 and validity was 0.872.

Perme *et al*[7] developed the Perme Critical Patient Mobility Score (The Perme Intensive Care Unit Mobility Score, Perme score) in 2014 at Houston Hospital, United States, and is suitable for assessing critically ill patients with any diagnosis. Wilches Luna *et al*[8] developed a Chinese version of the Perme Score and conducted a reliability analysis, with a Cronbach's α coefficient of 0.853, the scale has 13 entries in four dimensions, with a score of 30. The higher the score, the better the patient's mobility.

Research methods: (1) Observation group; After the MDT discussion based on the IMS rating of post-cardiac surgery patients, the patients were instructed to perform corresponding early activities; and (2) The control group included patients who underwent routine early activities.

Evaluation indexes

Postoperative recovery indices of the two patient groups: (1) The responsible nurse recorded the time of tracheal intubation, time of ICU admission, and related complications (Table 1); and (2) Revised Pelme Critical Patient Activity Score.

Statistical analysis

The researcher established a database based on the collected information and two-person entry ensured entry accuracy. SPSS 22.0 statistical analysis software was used for the analysis and processing. Measurement data were expressed as mean ± SD, *t*-test was used to measure normally distributed data, and rank-sum test was used to measure non-normally distributed data; count data were expressed as frequency and rate and compared using the χ^2 test for comparison. Statistical significance was defined as $P < 0.05$ indicated significant differences.

RESULTS

Comparison of general demographic data of patients in both groups

There were no statistically significant differences between the two groups concerning general demographic data, such as sex, age, occupation, acute physiology and chronic health status score II (APACHE-II), diagnosis, and operative style ($P > 0.05$) (Table 2).

Comparison of activity scores of critically ill patients in both groups

The activity scores of the observation group were significantly higher than that of the control group, and the difference was statistically significant ($P < 0.05$, Table 3).

Table 2 Comparison of general demographic and clinical data of post cardiac surgery patients in the two groups

Factors	Observation, *n* = 60	Control, *n* = 60	χ^2	*P* value
Sex				
Men	40	31	2.794	0.095
Women	20	29		
Age				
18–30	0	1	2.588	0.662
31–50	11	11		
51–60	23	17		
61–70	16	21		
70 above	10	10		
Occupation				
Farmer	54	54	1.612	0.816
Laborer	1	3		
Retired	2	1		
Other	3	2		
APACHE-II				
1–10	16	19	3.088	0.244
11–20	37	39		
21–30	7	2		
Diagnosis				
Heart valve disease	34	34	0	1
Coronary heart disease	18	18		
Aortic dissection	8	8		
Surgical procedure				
Heart valve replacement + plasty	21	26	2.037	0.361
Coronary bypass	18	20		
Aortic replacement + plasty	21	14		

APACHE-II scores: Acute Physiology and Chronic Health Status Score II.

Table 3 Comparison of the revised pelme critical patient activity score between the two groups of postoperative cardiac patients

Group	Cases	PermeScore	Of them			
			Activity upon request	Impaired mobility	Bed mobility	Underbed mobility
Observation	60	25.98 ± 0.97	7	1.1	5.8	12.1
Control	60	22.63 ± 1.08	7	1	5.35	9.2
t	-17.83					
P value	$P < 0.005$					

PermeScore: The Perme Intensive Care Unit Mobility Score.

Table 4 Comparison of rehabilitation indexes between two groups of postoperative cardiac patients (mean ± SD)

Group	Cases	Duration of mechanical ventilation (h)	Length of ICU stay (d)
Observation	60	18.30 ± 3.28	4.04 ± 0.83
Control	60	21.59 ± 7.93	4.66 ± 2.19
t		2.97	2.038
P value		$P < 0.05$	$P < 0.05$

ICU: Intensive care unit.

Table 5 Comparison of the incidence of complications or adverse events between the two groups of postoperative cardiac patients (cases), *n* (%)

Group	Cases	Number of cases	pulmonary atelectasis	arrhythmia	Poor incision healing	Pipe Slip	Total
Observation	60	2	1	1	0	0	4 (6.7)
Control	60	9	4	3	1	1	18 (30.0)
χ^2	4.904						
P value	$P < 0.05$						

Comparison of routine rehabilitation indicators between both groups

The mechanical ventilation time and ICU hospitalization time of the observation group were significantly better than those of the control group, with statistically significant differences ($P < 0.05$, Table 4), and the incidence of complications or adverse reactions was lower than that of the control group, with statistically significant differences ($P < 0.05$, Table 5).

DISCUSSION

Some foreign experts[4] used the IMS ratings to guide patients in performing early rehabilitation activities of different intensities, such as turning, sitting, standing, and walking, increasing exercise duration and physical mobility[8]. This study showed that early activities guided by IMS ratings for postoperative cardiac patients were beneficial for early rehabilitation, shortened the duration of tracheal intubation retention and ICU admission time, and reduced the occurrence of related complications. Consistent with the results of Gaweda *et al*[9], this study was better than ours regarding the index of tracheal intubation retention time in post-cardiac surgery patients. To analyze the reasons, because of the complexity and high risk of cardiac surgery, patients have more postoperative complications[10], and to reduce the work of the heart, postoperative cardiac patients mostly need ventilator-assisted respiration, which may cause Ventilator-associated pneumonia, ventilator-associated diaphragmatic insufficiency, and respiratory muscle wasting atrophy[11]. In this study, the IMS was used to assess the patient's mobility, and the corresponding early rehabilitation activities were implemented according to the grades assessed, so that the patient's physical mobility could reach the highest level under the premise of ensuring safety, while the time of tracheal intubation retention, ICU admission time, and related complications were significantly less in the observation group than in the control group.

Early rehabilitation activities guided by IMS ratings for postoperative cardiac patients are conducive to improving patient mobility, shortening ICU admission time, reducing hospitalization costs, and reducing hospitalization burden. This study showed that goal-directed activities after implementation of IMS ratings for postoperative cardiac patients can improve physical mobility, and the observation group was better than the control group by comparing the Revised Pelme Critical Patient Activity Score. This finding is consistent with the results of a large-sample study by Schaller *et al*[12]. For analysis, postoperative cardiac patients often suffer from various complications, which may affect the recovery of body functions and prolong hospital stay[13]. Early rehabilitation interventions are considered safe and beneficial to improve patients' muscle strength and physical function and reduce complications; thus, improving their care outcomes and reducing healthcare costs and ICU stay[14,15].

While the results of this study indicate that ICU activity-guided graded rehabilitation interventions can promote early recovery after cardiac surgery, several limitations should be acknowledged. Firstly, the study was conducted at a single center, limiting the generalizability of the findings across institutions with varying patient populations and surgical protocols. Second, the sample size of 120 patients may not have been sufficient to capture all potential variations in patient outcomes. Larger multicenter studies are required to provide more robust evidence. Additionally, the long-term effects of ICU activity scale-guided rehabilitation on patient outcomes, such as quality of life or mortality rates, were not assessed. Therefore, future studies should consider including these longer-term outcomes to fully evaluate the clinical value of this approach. Finally, the observational nature of the study did not account for the potential impact of other factors, such as patient comorbidities or surgical complexity, on the outcomes. Further research is required to investigate

the optimal ICU activity scale for different patient populations.

CONCLUSION

Overall, early rehabilitation activities guided by the IMS ratings for postoperative cardiac patients shortened the time of tracheal intubation retention and ICU admission, reduced the occurrence of related complications, and allowed patients to reach the highest level of physical activity they could tolerate. This study provides a scientific and targeted activity program for postoperative cardiac patients with team assistance. One hospital was selected for this study because of time and geographical constraints. A multicenter, large-sample trial will be conducted subsequently to further explore the effectiveness of this program for post-cardiac surgery patients.

FOOTNOTES

Author contributions: Wang L designed the research study; Wang L, Lu JY, Ma XX, and Ma LO performed the primary literature review and data extraction; Wang L, Lu JY, Ma XX, and Ma LO analyzed the data and wrote the manuscript; Wang Lwere responsible for revising the manuscript for important intellectual content; and all authors read and approved the final version.

Supported by Zhejiang Provincial Medical and Health Technology Plan, No. 2019KY762.

Institutional review board statement: This study was reviewed and approved by the Institutional Review Committee of Dongyang People's Hospital.

Clinical trial registration statement: This study was registered at the Clinical Trial Registry.

Informed consent statement: All study participants, or their legal guardian, provided informed written consent prior to study enrollment.

Conflict-of-interest statement: All authors declare no potential conflicting interests related to this paper.

Data sharing statement: No additional data are available.

CONSORT 2010 statement: The authors have read the CONSORT 2010 statement, and the manuscript was prepared and revised according to the CONSORT 2010 statement.

Country of origin: China

ORCID number: Li Wang 0009-0004-8506-1335.

S-Editor: Liu JH
L-Editor: A
P-Editor: Chen YX

REFERENCES

1 **Straily A**, Dahlgren FS, Peterson A, Paddock CD. Surveillance for Q Fever Endocarditis in the United States, 1999-2015. *Clin Infect Dis* 2017; **65**: 1872-1877 [PMID: 29140515 DOI: 10.1093/cid/cix702]
2 **Freeman R**, Maley K. Mobilization of intensive care cardiac surgery patients on mechanical circulatory support. *Crit Care Nurs Q* 2013; **36**: 73-88 [PMID: 23221444 DOI: 10.1097/CNQ.0b013e31827532c3]
3 **Westerdahl E**, Möller M. Physiotherapy-supervised mobilization and exercise following cardiac surgery: a national questionnaire survey in Sweden. *J Cardiothorac Surg* 2010; **5**: 67 [PMID: 20738852 DOI: 10.1186/1749-8090-5-67]
4 **Hodgson CL**, Bailey M, Bellomo R, Berney S, Buhr H, Denehy L, Gabbe B, Harrold M, Higgins A, Iwashyna TJ, Papworth R, Parke R, Patman S, Presneill J, Saxena M, Skinner E, Tipping C, Young P, Webb S; Trial of Early Activity and Mobilization Study Investigators. A Binational Multicenter Pilot Feasibility Randomized Controlled Trial of Early Goal-Directed Mobilization in the ICU. *Crit Care Med* 2016; **44**: 1145-1152 [PMID: 26968024 DOI: 10.1097/CCM.0000000000001643]
5 **Hodgson C**, Needham D, Haines K, Bailey M, Ward A, Harrold M, Young P, Zanni J, Buhr H, Higgins A, Presneill J, Berney S. Feasibility and inter-rater reliability of the ICU Mobility Scale. *Heart Lung* 2014; **43**: 19-24 [PMID: 24373338 DOI: 10.1016/j.hrtlng.2013.11.003]
6 **Liu Y**, Wang X, Li C, Yu D, Tian B, Li W, Sun Z. Research progress on the chemical components and pharmacological effects of Physalis alkekengi L. var. franchetii (Mast.) Makino. *Heliyon* 2023; **9**: e20030 [PMID: 38125457 DOI: 10.1016/j.heliyon.2023.e20030]

7 **Perme C**, Nawa RK, Winkelman C, Masud F. A tool to assess mobility status in critically ill patients: the Perme Intensive Care Unit Mobility Score. *Methodist Debakey Cardiovasc J* 2014; **10**: 41-49 [PMID: 24932363 DOI: 10.14797/mdcj-10-1-41]

8 **Wilches Luna EC**, de Oliveira AS, Perme C, Gastaldi AC. Spanish version of the Perme Intensive Care Unit Mobility Score: Minimal detectable change and responsiveness. *Physiother Res Int* 2021; **26**: e1875 [PMID: 32926503 DOI: 10.1002/pri.1875]

9 **Gaweda AE**, Muezzinoglu MK, Aronoff GR, Jacobs AA, Zurada JM, Brier ME. Using clinical information in goal-oriented learning. *IEEE Eng Med Biol Mag* 2007; **26**: 27-36 [PMID: 17441606 DOI: 10.1109/memb.2007.335580]

10 **Galluccio C**, Pazzaglia C, Spaccatrosi S, Giovannini S, Castelli L, Padua L. Focal vibration in dysphagia: A technological treatment for severe acquired brain injury rehabilitation. *J Oral Rehabil* 2023; **50**: 679-686 [PMID: 37067067 DOI: 10.1111/joor.13465]

11 **Gao F**, Yang LH, He HR, Ma XC, Lu J, Zhai YJ, Guo LT, Wang X, Zheng J. The effect of reintubation on ventilator-associated pneumonia and mortality among mechanically ventilated patients with intubation: A systematic review and meta-analysis. *Heart Lung* 2016; **45**: 363-371 [PMID: 27377334 DOI: 10.1016/j.hrtlng.2016.04.006]

12 **Schaller SJ**, Anstey M, Blobner M, Edrich T, Grabitz SD, Gradwohl-Matis I, Heim M, Houle T, Kurth T, Latronico N, Lee J, Meyer MJ, Peponis T, Talmor D, Velmahos GC, Waak K, Walz JM, Zafonte R, Eikermann M; International Early SOMS-guided Mobilization Research Initiative. Early, goal-directed mobilisation in the surgical intensive care unit: a randomised controlled trial. *Lancet* 2016; **388**: 1377-1388 [PMID: 27707496 DOI: 10.1016/S0140-6736(16)31637-3]

13 **Castelino T**, Fiore JF Jr, Niculiseanu P, Landry T, Augustin B, Feldman LS. The effect of early mobilization protocols on postoperative outcomes following abdominal and thoracic surgery: A systematic review. *Surgery* 2016; **159**: 991-1003 [PMID: 26804821 DOI: 10.1016/j.surg.2015.11.029]

14 **Vegh LA**, Blunt AM, Wishart LR, Gane EM, Paratz JD. Managing deteriorating patients with a physiotherapy critical care outreach service: A mixed-methods study. *Aust Crit Care* 2023; **36**: 223-231 [PMID: 35341669 DOI: 10.1016/j.aucc.2022.01.005]

15 **Klein K**, Mulkey M, Bena JF, Albert NM. Clinical and psychological effects of early mobilization in patients treated in a neurologic ICU: a comparative study. *Crit Care Med* 2015; **43**: 865-873 [PMID: 25517476 DOI: 10.1097/CCM.0000000000000787]

World Journal of Clinical Cases

Submit a Manuscript: https://www.f6publishing.com

World J Clin Cases 2024 September 16; 12(26): 5937-5945

DOI: 10.12998/wjcc.v12.i26.5937

ISSN 2307-8960 (online)

ORIGINAL ARTICLE

Clinical and Translational Research

Modifiable factors mediating the effects of educational attainment on gestational diabetes mellitus: A two-step Mendelian randomization study

Ming-Yue Ma, Ya-Song Zhao

Specialty type: Medicine, research and experimental

Provenance and peer review: Unsolicited article; Externally peer reviewed.

Peer-review model: Single blind

Peer-review report's classification

Scientific Quality: Grade C, Grade C, Grade C

Novelty: Grade B, Grade B, Grade B

Creativity or Innovation: Grade B, Grade B, Grade B

Scientific Significance: Grade B, Grade B, Grade B

P-Reviewer: Arumugam VA; Mogulkoc R

Received: April 24, 2024

Revised: July 1, 2024

Accepted: July 10, 2024

Published online: September 16, 2024

Processing time: 89 Days and 24 Hours

Ming-Yue Ma, Ya-Song Zhao, Department of Nursing, Shengjing Hospital of China Medical University, Shenyang 110004, Liaoning Province, China

Corresponding author: Ya-Song Zhao, PhD, Researcher, Department of Nursing, Shengjing Hospital of China Medical University, No. 36 Sanhao Street, Heping District, Shenyang 110004, Liaoning Province, China. zys18940252012@163.com

Abstract

BACKGROUND

Although there is currently a wealth of evidence to indicate that maternal educational attainment is associated with gestational diabetes mellitus (GDM), the specific modifiable risk factors that mediate the causal relationship between these two variables have yet to be identified.

AIM

To identify the specific modifiable risk factors that mediate the causal relationship between the level of maternal education and GDM.

METHODS

Mendelian randomization (MR) was conducted using data from genome-wide association studies of European populations. We initially performed a two-sample MR analysis using data on genetic variants associated with the duration of education as instruments, and subsequently adopted a two-step MR approach using metabolic and lifestyle factors as mediators to examine the mechanisms underlying the relationship between the level of maternal education and risk of developing GDM. In addition, we calculated the proportions of total causal effects mediated by identified metabolic and lifestyle factors.

RESULTS

A genetically predicted higher educational attainment was found to be associated with a lower risk of developing GDM (OR: 0.71, 95%CI: 0.60-0.84). Among the metabolic factors assessed, four emerged as potential mediators of the education-GDM association, which, ranked by mediated proportions, were as follows: Waist-to-hip-ratio (31.56%, 95%CI: 12.38%-50.70%), body mass index (19.20%, 95%CI: 12.03%-26.42%), high-density lipoprotein cholesterol (12.81%, 95%CI: 8.65%-17.05%), and apolipoprotein A-1 (7.70%, 95%CI: 4.32%-11.05%). These

findings proved to be robust to sensitivity analyses.

CONCLUSION
Our findings indicate a causal relationship between lower levels of maternal education and the risk of developing GDM can be partly explained by adverse metabolic profiles.

Key Words: Educational status; Gestational diabetes mellitus; Metabolism; Lifestyle factors; Mendelian randomization analysis

Core Tip: Studies have shown that the level of maternal education is associated with the risk of developing gestational diabetes mellitus (GDM). In this study, we sought to identify the specific modifiable risk factors that mediate the causal relationship between the level of maternal education and the likelihood of developing GDM. We performed Mendelian randomization analyses based on publicly available data obtained in a number of genome-wide association studies of European populations. Our findings indicate that a genetically predicted higher level of maternal education is associated with a lower GDM risk and that four modifiable metabolic factors contribute to mediating this association, namely, waist-to-hip ratio, body mass index, and the contents of high-density lipoprotein cholesterol and apolipoprotein A-1.

Citation: Ma MY, Zhao YS. Modifiable factors mediating the effects of educational attainment on gestational diabetes mellitus: A two-step Mendelian randomization study. *World J Clin Cases* 2024; 12(26): 5937-5945
URL: https://www.wjgnet.com/2307-8960/full/v12/i26/5937.htm
DOI: https://dx.doi.org/10.12998/wjcc.v12.i26.5937

INTRODUCTION

Gestational diabetes mellitus (GDM) is defined as a type of glucose intolerance that is initially detected during pregnancy [1]. It is a disorder of substantial public health significance worldwide, with prevalence estimates as high as 14%[2]. Moreover, the prevalence of GDM tends to be characterized by marked inter-population variance due to differences in associated risk factors and approaches to screening and diagnosis. GDM is associated with a higher risk of short- and long-term adverse health outcomes in both mothers and their offspring. Specifically, mothers diagnosed with GDM have been established to be more susceptible to the subsequent development of type 2 diabetes[3], metabolic syndrome[4], and cardiovascular disease[5]. Among the offspring of affected mothers, exposure to GDM in utero tends to increase the predisposition to adverse outcomes, not only in the perinatal period but also in later life. These include, although are not limited to, pre-term birth[6], excessive fetal growth[7], neonatal hypoglycemia[8], autism spectrum disorder[9], obesity [10], and cardiometabolic dysfunction[11].

Educational attainment is a robust predictor of socioeconomic achievement and has extensive implications for lifestyle behaviors and health resource utilization throughout life[12,13]. A robust and compelling body of epidemiological evidence indicates that women with a lower level of educational attainment are disproportionately affected by GDM[14]. An accumulating body of epidemiological research supports the potential advantages of mitigating modifiable risk factors, primarily metabolic factors and lifestyle behaviors, for the prevention and management of GDM[15]. However, whether education independently influences the risk of developing GDM and the degree to which modifiable factors mediate such effects remain unknown. Accordingly, elucidating the mediatory pathways linking educational attainment and GDM could enable the identification of targets for public health policies and interventions aimed at reducing the excess GDM risk arising from socioeconomic disadvantage.

Mendelian randomization (MR) has become an important epidemiological method for assessing causal relationships between exposures and outcomes. MR uses genetic variants, typically single-nucleotide polymorphisms (SNPs) identified from genome-wide association studies (GWASs), as instrumental variables (IVs) to better evaluate exposure-outcome associations[16]. Compared with conventional observational studies, the MR approach is potentially less susceptible to residual confounding, as genetic variants are randomly assigned at meiosis and conception[17]. Hence, MR can substantially enhance the validity and reliability of causal inferences. Additionally, MR minimizes the reverse causation bias as germline genotypes cannot be altered by disease onset or progression[18]. The successful application of MR is dependent on three key assumptions. First, the selected instrumental genetic variables should be strongly associated with the exposure of interest; second, these genetic variables should not be associated with any potential confounders of the exposure-outcome relationship; and third, the genetic variables exclusively influence outcomes *via* exposure[19]. When these assumptions are fulfilled, MR can provide compelling evidence for the causal relationship between exposure and outcome.

In this study, we adopted a two-sample MR approach to assess the causal relationship between maternal educational attainment and the risk of developing GDM. In addition, to guide clinical practice, we conducted MR mediation analyses to examine the extent to which metabolic and lifestyle factors may mediate the effects of educational attainment.

MATERIALS AND METHODS

Study design

We initially performed univariable MR (UVMR) analysis to assess the causal relationship between educational attainment and the risk of developing GDM, in which we conducted a comprehensive screening for potential factors that might mediate this relationship. Subsequently, we employed a two-step MR approach to estimate the mediatory effects of these factors. All data used in this study were derived from publicly available data obtained from studies that had appropriate participant consent and ethical approval. Moreover, the study was conducted in accordance with the Strengthening the Reporting of Observational Studies in Epidemiology guidelines for MR studies[20].

Data sources

Education attainment: Genetic variants for educational attainment were extracted from a GWAS of years of schooling encompassing 1131881 individuals of European descent performed by the Social Science Genetic Association Consortium. Summary statistics were accessible for 766345 of these participants upon the exclusion of those from 23andMe (Table 1).

Metabolic and lifestyle factors: Thirty-two modifiable factors (20 metabolic and 12 lifestyle factors) that we hypothesized might mediate the relationship between education and GDM were selected, and genetic variants for these mediators were extracted from the GWAS data (Table 1). Candidate mediators of the effects of education on GDM were selected according to certain prerequisites. First, the causal relationship between education and a mediator must be unidirectional, given that bi-directionality could compromise the validity of the mediation analyses. Second, the causal association between the mediator and GDM should persist irrespective of whether it is adjusted for education. Third, extant evidence dictates that the relationship between education and a mediator, and that between the mediator and GDM, should be in opposite directions. Ultimately, we identified four metabolic mediators that satisfied all stipulations and these were incorporated into the analyses to assess their mediating influence on the causal relationship between the level of maternal education and the risk of developing GDM.

GDM: Summary statistics for GDM were extracted from the Release 8 data of the GWAS performed by the FinnGen consortium (Table 1), which encompassed 190879 Finnish women, comprising 11279 cases and 179600 controls. GDM cases were defined by code O24.4 in the International Classification of Diseases-9th and 10th revisions.

To avoid biases from population stratification, in the main analysis, summary statistics for exposures, mediators, and outcomes were extracted from the GWAS data conducted predominantly on subjects of European ancestry.

Selection of IVs: To ensure the validity and accuracy of the inferences from this MR study, stringent quality control procedures were employed to select the optimal IVs for exposure, mediators, and outcomes. To obtain powerful IVs, we initially extracted SNPs from the GWAS dataset at a genome-wide significance threshold of $P < 5 \times 10^{-8}$. However, given the extremely limited number of qualified IVs obtained for total, early, and late gestational weight gain (GWG) at this threshold, we subsequently applied a relatively less stringent threshold ($P < 5 \times 10^{-5}$) to obtain a sufficiently large dataset. For genetic variants of interest, we selected a minor allele frequency threshold of 0.01. A fundamental principle of the MR approach is the absence of linkage disequilibrium (LD) between the included IVs, as substantial LD could yield biased results. We accordingly selected genetic variants that achieved independence at LD ($r^2 = 0.001$) and a distance of 10000 kb from the European 1000 Genome Reference Panel. Furthermore, to avoid accidental bias during harmonization, we removed palindromic SNPs, and to avoid the potential influence of horizontal pleiotropy on the MR estimates, we used PhenoScanner to identify and remove SNPs associated with other potential confounders affecting the outcome[21]. Finally, to evaluate the strength of the IVs, we generated *F*-statistics for each SNP, and to minimize potential weak instrument bias, SNPs with *F* values < 10 were deleted[22].

Statistical analysis

UVMR: The UVMR method was used to assess the total impact of the exposure (educational attainment) on the outcomes (GDM and the selected mediators). The primary method of analysis used in this MR study was inverse variance weighted (IVW), which combines Wald ratios *via* a random-effects meta-analysis[23].

Mediation MR analyses

We conducted a two-stage MR analysis to investigate whether any modifiable factors mediated the causal relationship between educational attainment and the risk of GDM. In the initial stage, we employed IVW as the primary approach to estimate the causal effects of educational attainment on each potential mediator (β1), and in the second stage, we assessed the causal effects of each mediator on GDM risk after adjusting for the genetic influence of the IVs on education (β2) using regression-based multivariable MR (MVMR)[24]. The individual mediatory effect of each mediator was then calculated by multiplying the results from the two stages (β1 × β2)[25]. The proportion of the total effect of educational attainment on the risk of GDM mediated by each mediator was estimated by dividing the indirect effect by the total effect. Standard errors were derived using the delta method, based on the effect estimates obtained from the two-sample MR analysis[26].

Sensitivity analyses: To validate the robustness of the IVW results in UVMR analyses, we employed MR-Egger[27], weighted median[28], and MR-pleiotropic residual sum and outliers (MR-PRESSO) methods[29]. In addition, we used MVMR Egger sensitivity to validate the robustness of the IVW results in the MVMR analyses. Each approach is dependent on different hypothetical models to evaluate the causal effects. The MR-Egger method provides estimates adjusted for pleiotropy[27], whereas the weighted median approach allows for causal effect estimation when 50% of the

Table 1 Summary of the genome-wide association study data used in the mendelian randomization analyses

Phenotype	Datatype	Sample size	Population	Consortium/cohort
Exposure				
Education	Continuous	766345	European	SSGAC
Outcome				
GDM	Binary	190879	European	FinnGen
Metabolic factors				
BMI[1]	Continuous	681275	European	GIANT
BF%	Continuous	65831	European	Meta
Waist circumference	Continuous	231353	European	GIANT
WHR[1]	Continuous	212244	European	GIANT
Total GWG	Continuous	10555	European	EGG
Early GWG	Continuous	7704	European	EGG
Late GWG	Continuous	7681	European	EGG
Hypertension	Binary	342439	European	FinnGen
Systolic blood pressure	Continuous	757601	European	UK Biobank
Diastolic blood pressure	Continuous	757601	European	UK Biobank
LDL-C	Continuous	440546	European	UK Biobank
HDL-C[a]	Continuous	403943	European	UK Biobank
Triglyceride	Continuous	441016	European	UK Biobank
Apolipoprotein A-1[1]	Continuous	393193	European	UK Biobank
Apolipoprotein B	Continuous	439214	European	UK Biobank
Serum urate	Continuous	110347	European	GUGC
Serum iron	Continuous	23986	European	GISC
Ferritin	Continuous	23986	European	GISC
Transferrin	Continuous	23986	European	GISC
Transferrin saturation	Continuous	23986	European	GISC
Lifestyle factors				
Strenuous sports or other exercises	Continuous	350492	European	UK Biobank
Moderate to vigorous physical activity	Continuous	377234	European	UK Biobank
Sedentary behavior	Continuous	91105	European	UK Biobank
Smoking initiation	Binary	1232091	European	GSCAN
Smoking cessation	Binary	547219	European	GSCAN
Smoking heaviness	Continuous	337334	European	GSCAN
Alcohol drinking	Continuous	941280	European	GSCAN
Coffee consumption	Continuous	375833	European	UK Biobank
Insomnia	Binary	1331010	European	UK Biobank
Sleep duration	Continuous	446118	European	UK Biobank
Long sleep duration	Binary	339926	European	UK Biobank
Short sleep duration	Binary	446118	European	UK Biobank

[1]Candidate mediators met all criteria of mediator selection.

GDM: Gestational diabetes mellitus; BMI: Body mass index; BF: Body fat; WHR: Waist-to-hip ratio; GWG: Gestational weight gain; LDL-C: Low-density lipoprotein cholesterol; HDL-C: High-density lipoprotein cholesterol; SSGAC: Social Science Genetic Association Consortium; GIANT: Genetic Investigation of Anthropometric Traits; EGG: Early Growth Genetics Consortium; GUGC: Global Urate Genetics Consortium; GISC: Genetics of Iron Status Consortium; GSCAN: GWAS & Sequencing Consortium of Alcohol and Nicotine use.

SNPs are invalid[28], and the MR-PRESSO technique is used to detect and correct outliers, thereby yielding MR estimates that are robust to heterogeneity after removing the identified outliers[29]. We performed MR-Egger regression intercept analysis to assess horizontal pleiotropy, and also assessed heterogeneity using the IVW and MRI-Egger methods based on Cochran's Q statistic.

All MR analyses were conducted using the TwoSampleMR, MRPRESSO, MR, and MVMR packages in R (version 4.1.3). To account for multiple testing in the UVMR analyses, we applied a Bonferroni corrected significance level of P value < 1.52×10^{-3} (= 0.05/33). For MVMR analysis, we set the statistical significance at a P value < 0.05.

RESULTS

Effects of education on GDM

In the UVMR analyses, the results of IVW revealed that a genetically predicted higher level of maternal education attainment (OR: 0.71, 95%CI: 0.60-0.84) was associated with a lower risk of GDM (Table 2). MR-Egger and MR-PRESSO sensitivity analyses confirmed the robustness of the IVW results. There was adequate instrument strength (F-statistics > 10) among the genetic variants assessed for educational attainment (Table 2). The IVs selected based on educational attainment were characterized by sustained heterogeneity and no pleiotropy (Supplementary Tables 1 and 2).

Effects of education on different mediators

We identified four candidate mediators for inclusion in the mediation MR analyses, namely, waist-to-hip ratio (WHR), body mass index (BMI), high-density lipoprotein cholesterol (HDL-C), and apolipoprotein A-1 (Table 1). In UVMR analyses, each genetically predicted single standard deviation increase in years of schooling was associated with lower levels of WHR (β: -0.22, 95%CI: -0.29 to -0.16) and BMI (β: -0.16, 95%CI: -0.21 to -0.11) and higher levels of HDL-C (β: 0.18, 95%CI: 0.15-0.21) and apolipoprotein A-1 (β: 0.13, 95%CI: 0.10-0.16). At least two or three sensitivity analyses confirmed the IVW estimates (Table 2). Genetic IVs for educational attainment exhibited sustained heterogeneity and no pleiotropy (Supplementary Tables 1 and 2). The F-statistics of the IVs were greater than 10, thereby tending to indicate an absence of any substantial weak instrument bias (Table 2). In the reverse MR analyses, we found that there was a causal association between BMI (β: -0.12, 95%CI: -0.14 to -0.10) and HDL-C (β: 0.02, 95%CI: 0.01-0.03) and educational attainment, which were largely driven by horizontal pleiotropy (Supplementary Table 3).

Effects of different mediators on GDM with adjustment for education

In the MVMR results, a higher WHR (OR: 2.31, 95%CI: 1.65-3.23) and BMI (OR: 1.53, 95%CI: 1.32-1.76) were found to be associated with an increased GDM risk after adjustment for education (Table 3). In contrast, higher levels of HDL-C (OR: 0.76, 95%CI: 0.70-0.82) and apolipoprotein A-1 (OR: 0.81, 95%CI: 0.74-0.89) were shown to be associated with a reduced GDM risk having adjusted for education (Table 3). MVMR sensitivity analyses validated the sustained heterogeneity and absence of pleiotropy across the selected genetic variants (Supplementary Table 4).

Mediating effects of mediators in the association between education and GDM

Figure 1 depicts the proportions of the effects of educational attainment on GDM risk explained by each of the four identified mediators. WHR accounted for 31.56% (95%CI: 12.38%-50.70%) of the total influence of educational attainment on the risk of GDM, whereas BMI explained 19.20% (95%CI: 12.03%-26.42%) of the total effect, an HDL-C and apolipoprotein A-1 mediated 12.81% (95%CI: 8.65%-17.05%) and 7.70% (95%CI: 4.32%-11.05%) of the total effect, respectively.

DISCUSSION

This MR study provides compelling novel evidence of the causal protective effect of educational attainment on GDM susceptibility. To elucidate the factors associated with this effect, we further assessed potential intermediaries in the path from education to GDM and identified four modifiable risk factors as causal mediators, which, ranked in terms of proportional mediation in the association between education and GDM, were WHR (31.56%), BMI (19.20%), HDL-C (12.81%), and apolipoprotein A-1 (7.70%). Our findings accordingly highlight the causal protective role of education and the substantial mediatory influence of several prevalent metabolic factors on the pathogenesis of GDM.

These findings build on previous work by providing further evidence to indicate that attainment of a higher level of education is a protective factor against the likelihood of developing GDM. Accumulating evidence from observational and MR studies indicates that a higher level of education is protective against hyperglycemia[14,30]. Educational attainment represents a modifiable and malleable factor with an enduring influence on financial status, access to social

Table 2 Univariable mendelian randomization estimating the causal effect of education on candidate mediators and gestational diabetes mellitus

Phenotype	Method	nSNPs	*F*-statistics	Beta	95%CI	*P* value
Outcome						
GDM	IVW	294	49.21	-0.34	-0.51 to -0.18	3.80E-05
	MR Egger	294		-0.41	-1.04 to 0.22	0.21
	Weighted Median	294		-0.38	-0.59 to -0.16	5.47E-04
	MR-PRESSO	294		-0.34	-0.51 to -0.18	4.95E-05
Mediators						
WHR	IVW	145	47.46	-0.22	-0.29 to -0.16	2.76E-12
	MR Egger	145		-0.36	-0.63 to -0.08	0.01
	Weighted Median	145		-0.23	-0.32 to -0.15	1.16E-07
	MR-PRESSO	145		-0.22	-0.29 to -0.16	9.50E-11
BMI	IVW	106	44.47	-0.16	-0.21 to -0.11	1.97E-10
	MR Egger	106		-0.17	-0.43 to 0.09	0.19
	Weighted Median	106		-0.15	-0.19 to -0.10	7.27E-09
	MR-PRESSO	106		-0.16	-0.21 to -0.11	5.26E-09
HDL-C	IVW	245	46.18	0.18	0.15 to 0.21	1.75E-34
	MR Egger	245		0.15	0.03 to 0.27	0.02
	Weighted Median	245		0.17	0.13 to 0.21	2.81E-20
	MR-PRESSO	245		0.18	0.15 to 0.21	3.38E-27
Apolipoprotein A-1	IVW	266	48.41	0.13	0.10 to 0.16	8.03E-19
	MR Egger	266		0.05	-0.06 to 0.17	0.34
	Weighted Median	266		0.11	0.08 to 0.15	3.07E-10
	MR-PRESSO	266		0.13	0.10 to 0.16	1.19E-16

nSNPs: Number of single-nucleotide polymorphisms; GDM: Gestational diabetes mellitus; WHR: Waist-to-hip ratio; BMI: Body mass index; HDL-C: High density lipoprotein cholesterol; IVW: Inverse variance weighted; MR-PRESSO: Mendelian randomization-pleiotropic residual sum and outliers.

Table 3 Multivariable mendelian randomization assessing the causal association between each mediator and gestational diabetes mellitus with adjustment for education from inverse variance weighted results

Mediators	nSNPs	Beta	SE	OR	95%CI	*P* value
WHR	154	0.84	0.17	2.31	1.65 to 3.23	1.00E-06
BMI	420	0.42	0.07	1.53	1.32 to 1.76	5.59E-09
HDL-C	381	-0.28	0.04	0.76	0.70 to 0.82	1.59E-10
Apolipoprotein A-1	358	-0.21	0.05	0.81	0.74 to 0.89	6.08E-06

nSNPs: Number of single-nucleotide polymorphisms; WHR: Waist-to-hip ratio; BMI: Body mass index; HDL-C: High density lipoprotein cholesterol.

capital, and the adoption of healthy lifestyles over the course of an individual's lifespan[31]. Moreover, although formal education typically concludes in early adulthood, adopting a lifelong learning perspective provides opportunities to continually acquire knowledge and contributes to enhancing cognitive abilities and promoting long-term health throughout adult life[31]. Thus, our findings offer key insights into prioritizing educational policies and reducing educational inequities as effective precautionary measures against GDM and its related disease burden.

A further salient finding of this study was our identification and quantification of the mediatory roles of certain metabolic factors in the relationship between education and GDM. On the basis of the application of stringent criteria, we identified four causal mediators, among which BMI and WHR appeared to be the principal mediators of the effects of

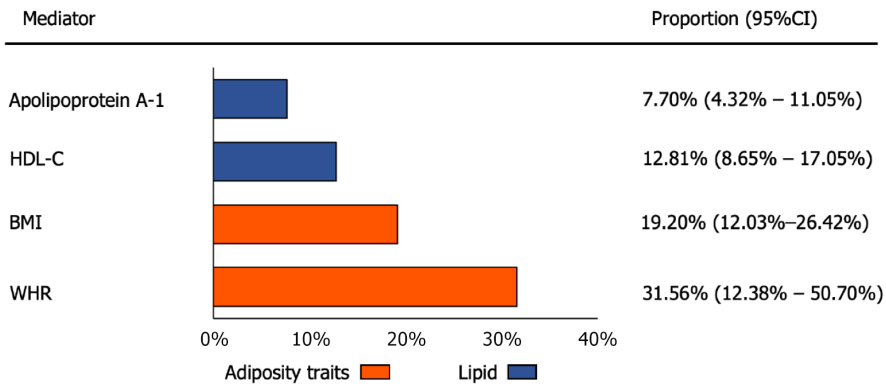

Figure 1 Mendelian randomization estimates of proportional mediation by candidate mediators in the causal relationship between educational attainment and gestational diabetes mellitus. HDL-C: High-density lipoprotein cholesterol; BMI: Body mass index; WHR: Waist-to-hip ratio.

education on the risk of developing GDM. These findings are consistent with previous epidemiological and MR evidence indicating that obesity, measured primarily *via* BMI and WHR, is strongly associated with GDM, thereby indicating that interventions targeting obesity may have the desired effects in low-education scenarios[32,33]. Of the other two identified mediators, HDL-C and apolipoprotein A-1 were shown to be associated with 12.81% and 7.70% of the causal effect of education on the risk of GDM, respectively. Notably, obesity and dyslipidemia are major public health issues that often co-occur and have common biological underpinnings, including immune inflammation and abnormal neuroendocrine regulation and energy metabolism[12,34]. Thus, given the inter-relationships among these four mediators, we suspect that there may be a certain degree of overlap in the proportional mediatory effects of these factors.

Our MR findings of no causal links between genetically predicted GDM and several metabolic and lifestyle factors would tend to indicate that significant relationships detected in observational studies may partly stem from residual confounding or a reverse causation bias, including adiposity traits (body fat percentage, waist circumference[33], total, early, and late GWG[35]), lipids (low-density lipoprotein cholesterol[36], and apolipoprotein B[37]), physical activity and sedentary behaviors[38] (moderate to vigorous physical activity levels and sedentary behavior), sleep-related traits[39,40] (insomnia, sleep duration, long sleep duration, and short sleep duration), and smoking and dietary behaviors[41] (smoking initiation, smoking cessation, smoking heaviness, alcohol consumption[42], and coffee consumption[43]).

To the best of our knowledge, this MR study is the first to establish the causal effects of education on the likelihood of developing GDM, and to identify causal intermediaries in the path between education and GDM. The study has several notable strengths. First, it uses SNPs as genetic instruments to mitigate confounding and reverse causation. Second, the robustness of the IVW estimates was demonstrated by performing multiple MR sensitivity analyses under different assumptions regarding genetic pleiotropy[44]. Third, our application of stringent criteria for mediator selection minimized the reverse causation of mediators on education, thereby ensuring the credibility and rationale of our proposed model explaining the mediating influence. However, despite these strengths, the study does have certain limitations. First, the heterogeneity of the SNPs may have introduced bias and influenced the robustness of our MR findings. Second, the GWAS data used for analyses were obtained from a European population, limiting the generalizability of our results to other ethnicities pending further study. Finally, sample overlap between GWASs may have biased the MR estimates toward observational association estimates[45].

CONCLUSION

In this MR study, we succeeded in elucidating the causal protective influence of educational attainment on the risk of developing GDM and identified four causal mediators underlying the impact of education, namely, WHR, BMI, HDL-C, and apolipoprotein A-1. Our findings in this study provide novel insights into the mechanisms underlying the association between educational attainment and GDM susceptibility.

ACKNOWLEDGEMENTS

We thank the participants of the UK Biobank study and the genome-wide association study consortiums who made their summary statistics publicly available for this study.

FOOTNOTES

Author contributions: Ma MY provide an idea, find data, data analysis, and manuscript checking; Zhao YS write the first draft and data visualization; all authors have read and agreed to publish the manuscript; all authors participated in data interpretation, revisions, and

approved the final version submitted for publication.

Conflict-of-interest statement: All authors declare no conflicts of interest.

Country of origin: China

ORCID number: Ya-Song Zhao 0009-0007-3866-6413.

S-Editor: Lin C
L-Editor: A
P-Editor: Zhang XD

REFERENCES

1 **Ye W**, Luo C, Huang J, Li C, Liu Z, Liu F. Gestational diabetes mellitus and adverse pregnancy outcomes: systematic review and meta-analysis. *BMJ* 2022; **377**: e067946 [PMID: 35613728 DOI: 10.1136/bmj-2021-067946]
2 **Sweeting A**, Hannah W, Backman H, Catalano P, Feghali M, Herman WH, Hivert MF, Immanuel J, Meek C, Oppermann ML, Nolan CJ, Ram U, Schmidt MI, Simmons D, Chivese T, Benhalima K. Epidemiology and management of gestational diabetes. *Lancet* 2024 [PMID: 38909620 DOI: 10.1016/S0140-6736(24)00825-0]
3 **Bellamy L**, Casas JP, Hingorani AD, Williams D. Type 2 diabetes mellitus after gestational diabetes: a systematic review and meta-analysis. *Lancet* 2009; **373**: 1773-1779 [PMID: 19465232 DOI: 10.1016/S0140-6736(09)60731-5]
4 **Lauenborg J**, Mathiesen E, Hansen T, Glümer C, Jørgensen T, Borch-Johnsen K, Hornnes P, Pedersen O, Damm P. The prevalence of the metabolic syndrome in a danish population of women with previous gestational diabetes mellitus is three-fold higher than in the general population. *J Clin Endocrinol Metab* 2005; **90**: 4004-4010 [PMID: 15840755 DOI: 10.1210/jc.2004-1713]
5 **Kramer CK**, Campbell S, Retnakaran R. Gestational diabetes and the risk of cardiovascular disease in women: a systematic review and meta-analysis. *Diabetologia* 2019; **62**: 905-914 [PMID: 30843102 DOI: 10.1007/s00125-019-4840-2]
6 **Hedderson MM**, Ferrara A, Sacks DA. Gestational diabetes mellitus and lesser degrees of pregnancy hyperglycemia: association with increased risk of spontaneous preterm birth. *Obstet Gynecol* 2003; **102**: 850-856 [PMID: 14551018 DOI: 10.1016/s0029-7844(03)00661-6]
7 **Kim SY**, Sharma AJ, Sappenfield W, Wilson HG, Salihu HM. Association of maternal body mass index, excessive weight gain, and gestational diabetes mellitus with large-for-gestational-age births. *Obstet Gynecol* 2014; **123**: 737-744 [PMID: 24785599 DOI: 10.1097/AOG.0000000000000177]
8 **Voormolen DN**, de Wit L, van Rijn BB, DeVries JH, Heringa MP, Franx A, Groenendaal F, Lamain-de Ruiter M. Neonatal Hypoglycemia Following Diet-Controlled and Insulin-Treated Gestational Diabetes Mellitus. *Diabetes Care* 2018; **41**: 1385-1390 [PMID: 29654142 DOI: 10.2337/dc18-0048]
9 **Xiang AH**, Wang X, Martinez MP, Walthall JC, Curry ES, Page K, Buchanan TA, Coleman KJ, Getahun D. Association of maternal diabetes with autism in offspring. *JAMA* 2015; **313**: 1425-1434 [PMID: 25871668 DOI: 10.1001/jama.2015.2707]
10 **Furse S**, Koulman A, Ozanne SE, Poston L, White SL, Meek CL. Altered Lipid Metabolism in Obese Women With Gestational Diabetes and Associations With Offspring Adiposity. *J Clin Endocrinol Metab* 2022; **107**: e2825-e2832 [PMID: 35359001 DOI: 10.1210/clinem/dgac206]
11 **Tam WH**, Ma RC, Yang X, Li AM, Ko GT, Kong AP, Lao TT, Chan MH, Lam CW, Chan JC. Glucose intolerance and cardiometabolic risk in adolescents exposed to maternal gestational diabetes: a 15-year follow-up study. *Diabetes Care* 2010; **33**: 1382-1384 [PMID: 20215448 DOI: 10.2337/dc09-2343]
12 **Wang Y**, Ye C, Kong L, Zheng J, Xu M, Xu Y, Li M, Zhao Z, Lu J, Chen Y, Wang W, Ning G, Bi Y, Wang T. Independent Associations of Education, Intelligence, and Cognition With Hypertension and the Mediating Effects of Cardiometabolic Risk Factors: A Mendelian Randomization Study. *Hypertension* 2023; **80**: 192-203 [PMID: 36353998 DOI: 10.1161/HYPERTENSIONAHA.122.20286]
13 **Lövdén M**, Fratiglioni L, Glymour MM, Lindenberger U, Tucker-Drob EM. Education and Cognitive Functioning Across the Life Span. *Psychol Sci Public Interest* 2020; **21**: 6-41 [PMID: 32772803 DOI: 10.1177/1529100620920576]
14 **Swaminathan G**, Swaminathan A, Corsi DJ. Prevalence of Gestational Diabetes in India by Individual Socioeconomic, Demographic, and Clinical Factors. *JAMA Netw Open* 2020; **3**: e2025074 [PMID: 33165611 DOI: 10.1001/jamanetworkopen.2020.25074]
15 **Brown J**, Alwan NA, West J, Brown S, McKinlay CJ, Farrar D, Crowther CA. Lifestyle interventions for the treatment of women with gestational diabetes. *Cochrane Database Syst Rev* 2017; **5**: CD011970 [PMID: 28472859 DOI: 10.1002/14651858.CD011970.pub2]
16 **Lin J**, Zhou J, Xu Y. Potential drug targets for multiple sclerosis identified through Mendelian randomization analysis. *Brain* 2023; **146**: 3364-3372 [PMID: 36864689 DOI: 10.1093/brain/awad070]
17 **Smith GD**. Mendelian Randomization for Strengthening Causal Inference in Observational Studies: Application to Gene × Environment Interactions. *Perspect Psychol Sci* 2010; **5**: 527-545 [PMID: 26162196 DOI: 10.1177/1745691610383505]
18 **Pingault JB**, O'Reilly PF, Schoeler T, Ploubidis GB, Rijsdijk F, Dudbridge F. Using genetic data to strengthen causal inference in observational research. *Nat Rev Genet* 2018; **19**: 566-580 [PMID: 29872216 DOI: 10.1038/s41576-018-0020-3]
19 **Lawlor DA**, Harbord RM, Sterne JA, Timpson N, Davey Smith G. Mendelian randomization: using genes as instruments for making causal inferences in epidemiology. *Stat Med* 2008; **27**: 1133-1163 [PMID: 17886233 DOI: 10.1002/sim.3034]
20 **Skrivankova VW**, Richmond RC, Woolf BAR, Yarmolinsky J, Davies NM, Swanson SA, VanderWeele TJ, Higgins JPT, Timpson NJ, Dimou N, Langenberg C, Golub RM, Loder EW, Gallo V, Tybjaerg-Hansen A, Davey Smith G, Egger M, Richards JB. Strengthening the Reporting of Observational Studies in Epidemiology Using Mendelian Randomization: The STROBE-MR Statement. *JAMA* 2021; **326**: 1614-1621 [PMID:

34698778 DOI: 10.1001/jama.2021.18236]
21 **Kamat MA**, Blackshaw JA, Young R, Surendran P, Burgess S, Danesh J, Butterworth AS, Staley JR. PhenoScanner V2: an expanded tool for searching human genotype-phenotype associations. *Bioinformatics* 2019; **35**: 4851-4853 [PMID: 31233103 DOI: 10.1093/bioinformatics/btz469]
22 **Burgess S**, Thompson SG. Bias in causal estimates from Mendelian randomization studies with weak instruments. *Stat Med* 2011; **30**: 1312-1323 [PMID: 21432888 DOI: 10.1002/sim.4197]
23 **Burgess S**, Butterworth A, Thompson SG. Mendelian randomization analysis with multiple genetic variants using summarized data. *Genet Epidemiol* 2013; **37**: 658-665 [PMID: 24114802 DOI: 10.1002/gepi.21758]
24 **Burgess S**, Thompson SG. Multivariable Mendelian randomization: the use of pleiotropic genetic variants to estimate causal effects. *Am J Epidemiol* 2015; **181**: 251-260 [PMID: 25632051 DOI: 10.1093/aje/kwu283]
25 **VanderWeele TJ**. Mediation Analysis: A Practitioner's Guide. *Annu Rev Public Health* 2016; **37**: 17-32 [PMID: 26653405 DOI: 10.1146/annurev-publhealth-032315-021402]
26 **MacKinnon DP**, Fairchild AJ, Fritz MS. Mediation analysis. *Annu Rev Psychol* 2007; **58**: 593-614 [PMID: 16968208 DOI: 10.1146/annurev.psych.58.110405.085542]
27 **Bowden J**, Davey Smith G, Burgess S. Mendelian randomization with invalid instruments: effect estimation and bias detection through Egger regression. *Int J Epidemiol* 2015; **44**: 512-525 [PMID: 26050253 DOI: 10.1093/ije/dyv080]
28 **Bowden J**, Davey Smith G, Haycock PC, Burgess S. Consistent Estimation in Mendelian Randomization with Some Invalid Instruments Using a Weighted Median Estimator. *Genet Epidemiol* 2016; **40**: 304-314 [PMID: 27061298 DOI: 10.1002/gepi.21965]
29 **Verbanck M**, Chen CY, Neale B, Do R. Detection of widespread horizontal pleiotropy in causal relationships inferred from Mendelian randomization between complex traits and diseases. *Nat Genet* 2018; **50**: 693-698 [PMID: 29686387 DOI: 10.1038/s41588-018-0099-7]
30 **Zhang J**, Chen Z, Pärna K, van Zon SKR, Snieder H, Thio CHL. Mediators of the association between educational attainment and type 2 diabetes mellitus: a two-step multivariable Mendelian randomisation study. *Diabetologia* 2022; **65**: 1364-1374 [PMID: 35482055 DOI: 10.1007/s00125-022-05705-6]
31 **Lawrence EM**. Why Do College Graduates Behave More Healthfully than Those Who Are Less Educated? *J Health Soc Behav* 2017; **58**: 291-306 [PMID: 28845056 DOI: 10.1177/0022146517715671]
32 **Wang Y**, Wu P, Huang Y, Ye Y, Yang X, Sun F, Ye YX, Lai Y, Ouyang J, Wu L, Li Y, Li Y, Zhao B, Wang Y, Liu G, Pan XF, Chen D, Pan A. BMI and lipidomic biomarkers with risk of gestational diabetes in pregnant women. *Obesity (Silver Spring)* 2022; **30**: 2044-2054 [PMID: 36046944 DOI: 10.1002/oby.23517]
33 **Song X**, Wang C, Wang T, Zhang S, Qin J. Obesity and risk of gestational diabetes mellitus: A two-sample Mendelian randomization study. *Diabetes Res Clin Pract* 2023; **197**: 110561 [PMID: 36738839 DOI: 10.1016/j.diabres.2023.110561]
34 **Vekic J**, Zeljkovic A, Stefanovic A, Jelic-Ivanovic Z, Spasojevic-Kalimanovska V. Obesity and dyslipidemia. *Metabolism* 2019; **92**: 71-81 [PMID: 30447223 DOI: 10.1016/j.metabol.2018.11.005]
35 **LifeCycle Project-Maternal Obesity and Childhood Outcomes Study Group**, Voerman E, Santos S, Inskip H, Amiano P, Barros H, Charles MA, Chatzi L, Chrousos GP, Corpeleijn E, Crozier S, Doyon M, Eggesbø M, Fantini MP, Farchi S, Forastiere F, Georgiu V, Gori D, Hanke W, Hertz-Picciotto I, Heude B, Hivert MF, Hryhorczuk D, Iñiguez C, Karvonen AM, Küpers LK, Lagström H, Lawlor DA, Lehmann I, Magnus P, Majewska R, Mäkelä J, Manios Y, Mommers M, Morgen CS, Moschonis G, Nohr EA, Nybo Andersen AM, Oken E, Pac A, Papadopoulou E, Pekkanen J, Pizzi C, Polanska K, Porta D, Richiardi L, Rifas-Shiman SL, Roeleveld N, Ronfani L, Santos AC, Standl M, Stigum H, Stoltenberg C, Thiering E, Thijs C, Torrent M, Trnovec T, van Gelder MMHJ, van Rossem L, von Berg A, Vrijheid M, Wijga A, Zvinchuk O, Sørensen TIA, Godfrey K, Jaddoe VWV, Gaillard R. Association of Gestational Weight Gain With Adverse Maternal and Infant Outcomes. *JAMA* 2019; **321**: 1702-1715 [PMID: 31063572 DOI: 10.1001/jama.2019.3820]
36 **Paradisi G**, Ianniello F, Tomei C, Bracaglia M, Carducci B, Gualano MR, La Torre G, Banci M, Caruso A. Longitudinal changes of adiponectin, carbohydrate and lipid metabolism in pregnant women at high risk for gestational diabetes. *Gynecol Endocrinol* 2010; **26**: 539-545 [PMID: 20170346 DOI: 10.3109/09513591003632084]
37 **Zheng S**, Han T, Xu H, Zhou H, Ren X, Wu P, Zheng J, Wang L, Zhang M, Jiang Y, Chen Y, Qiu H, Liu W, Hu Y. Associations of apolipoprotein B/apolipoprotein A-I ratio with pre-diabetes and diabetes risks: a cross-sectional study in Chinese adults. *BMJ Open* 2017; **7**: e014038 [PMID: 28110289 DOI: 10.1136/bmjopen-2016-014038]
38 **Mijatovic-Vukas J**, Capling L, Cheng S, Stamatakis E, Louie J, Cheung NW, Markovic T, Ross G, Senior A, Brand-Miller JC, Flood VM. Associations of Diet and Physical Activity with Risk for Gestational Diabetes Mellitus: A Systematic Review and Meta-Analysis. *Nutrients* 2018; **10** [PMID: 29849003 DOI: 10.3390/nu10060698]
39 **Xu YH**, Shi L, Bao YP, Chen SJ, Shi J, Zhang RL, Lu L. Association between sleep duration during pregnancy and gestational diabetes mellitus: a meta-analysis. *Sleep Med* 2018; **52**: 67-74 [PMID: 30286382 DOI: 10.1016/j.sleep.2018.07.021]
40 **Reutrakul S**, Anothaisintawee T, Herring SJ, Balserak BI, Marc I, Thakkinstian A. Short sleep duration and hyperglycemia in pregnancy: Aggregate and individual patient data meta-analysis. *Sleep Med Rev* 2018; **40**: 31-42 [PMID: 29103944 DOI: 10.1016/j.smrv.2017.09.003]
41 **Bar-Zeev Y**, Haile ZT, Chertok IA. Association Between Prenatal Smoking and Gestational Diabetes Mellitus. *Obstet Gynecol* 2020; **135**: 91-99 [PMID: 31809434 DOI: 10.1097/AOG.0000000000003602]
42 **Hayes L**, McParlin C, Azevedo LB, Jones D, Newham J, Olajide J, McCleman L, Heslehurst N. The Effectiveness of Smoking Cessation, Alcohol Reduction, Diet and Physical Activity Interventions in Improving Maternal and Infant Health Outcomes: A Systematic Review of Meta-Analyses. *Nutrients* 2021; **13** [PMID: 33806997 DOI: 10.3390/nu13031036]
43 **Hinkle SN**, Gleason JL, Yisahak SF, Zhao SK, Mumford SL, Sundaram R, Grewal J, Grantz KL, Zhang C. Assessment of Caffeine Consumption and Maternal Cardiometabolic Pregnancy Complications. *JAMA Netw Open* 2021; **4**: e2133401 [PMID: 34748005 DOI: 10.1001/jamanetworkopen.2021.33401]
44 **Burgess S**, Thompson SG. Interpreting findings from Mendelian randomization using the MR-Egger method. *Eur J Epidemiol* 2017; **32**: 377-389 [PMID: 28527048 DOI: 10.1007/s10654-017-0255-x]
45 **Burgess S**, Davies NM, Thompson SG. Bias due to participant overlap in two-sample Mendelian randomization. *Genet Epidemiol* 2016; **40**: 597-608 [PMID: 27625185 DOI: 10.1002/gepi.21998]

World Journal of Clinical Cases

Submit a Manuscript: https://www.f6publishing.com

World J Clin Cases 2024 September 16; 12(26): 5946-5951

DOI: 10.12998/wjcc.v12.i26.5946

ISSN 2307-8960 (online)

CASE REPORT

Periorbital purpura can be the only initial symptom of primary light chain amyloidosis: A case report

Xiu-Feng Wang, Ting Li, Man Yang, Yan Huang

Specialty type: Hematology

Provenance and peer review: Unsolicited article; Externally peer reviewed.

Peer-review model: Single blind

Peer-review report's classification

Scientific Quality: Grade C
Novelty: Grade C
Creativity or Innovation: Grade C
Scientific Significance: Grade C

P-Reviewer: Attallah HS

Received: February 6, 2024
Revised: June 20, 2024
Accepted: June 27, 2024
Published online: September 16, 2024
Processing time: 167 Days and 14.8 Hours

Xiu-Feng Wang, Man Yang, Yan Huang, Department of Hematology, The First Affiliated Hospital of Xinxiang Medical University, Xinxiang 453100, Henan Province, China

Ting Li, Department of Blood Purification, The First Affiliated Hospital of Xinxiang Medical University, Xinxiang 453100, Henan Province, China

Co-corresponding authors: Xiu-Feng Wang and Yan Huang.

Corresponding author: Xiu-Feng Wang, PhD, Doctor, Department of Hematology, The First Affiliated Hospital of Xinxiang Medical University, No. 88 Jiangkang Road, Xinxiang 453100, Henan Province, China. 81848616@qq.com

Abstract

BACKGROUND

Primary light chain amyloidosis is a rare and complex disease with complex clinical features and is highly susceptible to misdiagnosis and underdiagnosis in the early stages.

CASE SUMMARY

We report a case of a 47-year-old female patient whose only initial symptom was periorbital purpura, which was not taken seriously enough. As the disease progressed, pleural effusion gradually appeared, and after systematic diagnosis and treatment, she was diagnosed with "primary light chain amyloidosis". She achieved rapid hematological remission after treatment with a daratumumab + bortezomib + cyclophosphamide + dexamethasone regimen.

CONCLUSION

Periorbital purpura can be the only initial symptom of primary light chain amyloidosis; we should pay attention to the cases where the initial clinical symptoms are only periorbital purpura.

Key Words: Primary light chain amyloidosis; Periorbital purpura; Initial symptom; Literature review; Case report

Core Tip: Amyloidosis is a rare and difficult to diagnose disease. Periorbital purpura can be the only initial symptom of primary light chain amyloidosis, and we should pay attention to these cases.

Citation: Wang XF, Li T, Yang M, Huang Y. Periorbital purpura can be the only initial symptom of primary light chain amyloidosis: A case report. *World J Clin Cases* 2024; 12(26): 5946-5951
URL: https://www.wjgnet.com/2307-8960/full/v12/i26/5946.htm
DOI: https://dx.doi.org/10.12998/wjcc.v12.i26.5946

INTRODUCTION

Amyloidosis is a rare disease that is difficult to diagnose, which is a collective term for clinical disorders that occur due to localized or systemic accumulation of amyloid. Amyloid protein misfolds into β-fold and deposits in human tissues and organs, leading to organ dysfunction[1]. In 1923, Bennhold found Congo red stained amyloid deposits with typical apple green birefringence under polarized light microscopy, becoming the gold standard for the pathology of amyloidosis. More than thirty types of amyloidosis have been identified, the most common being the light chain (AL) type of amyloidosis due to deposition of immunoglobulin light chains secreted by aberrant clonal plasma cells, as well as the transthyretin (ATTR) type, serum amyloid (AA) type, and others[2].

Owing to the rarity and complexity of amyloidosis, many clinicians do not recognize it and it is easily misdiagnosed and underdiagnosed in its early stage. Here, we report the case of a patient with periorbital purpura as the initial symptom that was not effectively diagnosed, progressed to pleural effusion, and was finally diagnosed with primary light-chain amyloidosis.

CASE PRESENTATION

Chief complaints

A 47-year-old female patient with petechiae formed when she rubbed her eyelids lightly for half a year, without any other bleeding symptoms such as epistaxis, vomiting blood, black stools, *etc*, as well as any systemic symptom.

History of present illness

The patient was treated at several hospitals as allergies or bleeding; however, the treatment was ineffective. One week prior, she had shortness of breath after activity and was admitted to our hospital after ultrasonography revealed pleural effusion at a local hospital.

History of past illness

The patient had no significant previous medical history.

Personal and family history

The patient denied any family history of malignancy.

Physical examination

During the physical examination upon admission, periorbital purpura were seen (Figure 1), and the right lower lung was hypopneic, with turbid tones on percussion, and no dry or wet rales.

Laboratory examinations

Admission routine blood and coagulation function tests did not show any abnormality, denied long-term oral antiplatelet aggregation drugs, the nature of the pleural fluid was leakage fluid, cardiac ultrasound showed that the interventricular septum was 12 mm, left ventricular ejection fractions was 62%; two-dimensional speckle tracking strain and strain rate imaging of the myocardium with significant reduction in overall longitudinal strain of the left ventricle and visible apical exemption phenomenon (Figure 2); Brain natriuretic peptide: 3400 pg/mL, further immunofixation electrophoresis showed that the IgA-L was positive, the median value of difference between involved and uninvolved serum immunoglobulin free light chain levels (dFLC) was 320 ng/mL, and bone marrow cytology showed 12% plasma cells; abdominal fat biopsy showed amyloid deposition in collagen fibers of the dermis and positive Congo red staining (Figure 3).

FINAL DIAGNOSIS

Primary light chain amyloidosis (cardiac and soft tissue involvement).

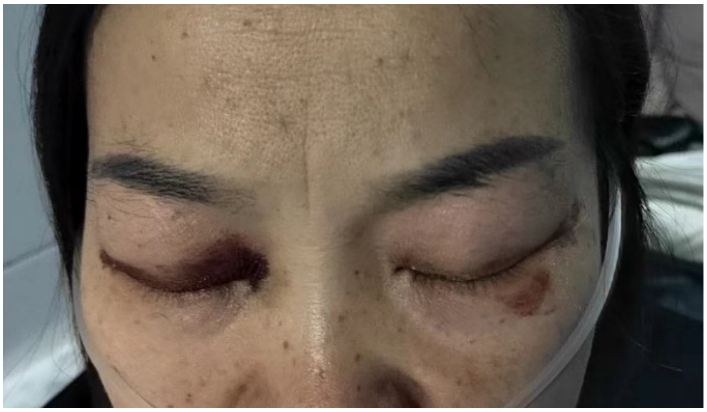

Figure 1 Periorbital purpura was visible.

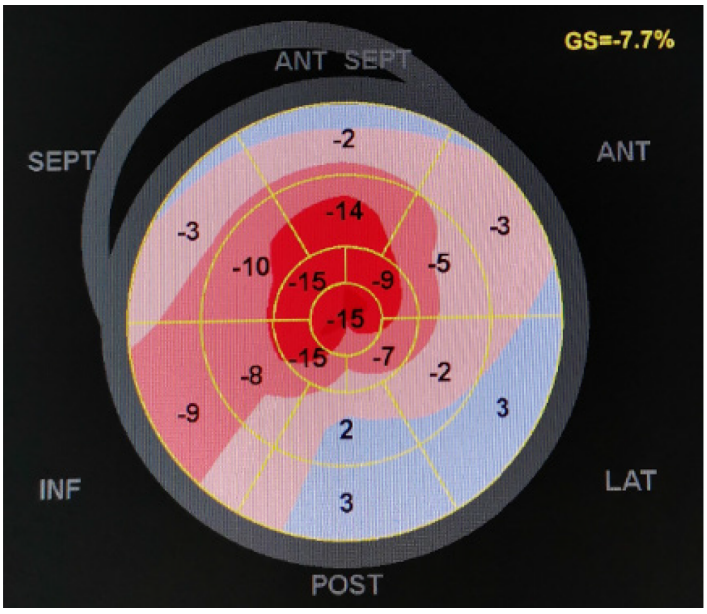

Figure 2 Two-dimensional speckle tracking strain and strain rate imaging of the myocardium: Visible apical exemption phenomenon is visible. ANT: Anterior; GS: Global strain; INF: Inferior; LAT: Anterolateral; POST: Inferolateral; SEPT: Posterior septum.

TREATMENT

The patient was treated with a daratumumab + bortezomib + cyclophosphamide + dexamethasone (D-VCD) regimen.

OUTCOME AND FOLLOW-UP

The patient achieved a stringent complete response in one cycle and is now undergoing regular treatment.

DISCUSSION

Primary light chain amyloidosis (AL type) is a rare hematologic disorder primarily associated with abnormal proliferation of clonal plasma cells and, to a lesser extent, with lymphoproliferative disorders[3]. Currently, according to statistical data in Europe and the United States, the incidence of the disease is about 9-14 per million person-years. AL amyloidosis is most commonly seen in the elderly, with a median age at diagnosis of about 60 years, and the proportion of male patients is slightly higher than that of females[4]. Currently, the majority of AL patients are not recognized and diagnosed early, and even in referral centers it takes a median of 10 months to diagnose patients with pre-existing plasma cell malignancy[4], yet even a few months of delay can irreversibly result in the loss of the opportunity for patients to benefit from effective treatments. Therefore, early recognition and diagnosis of AL is a pressing concern.

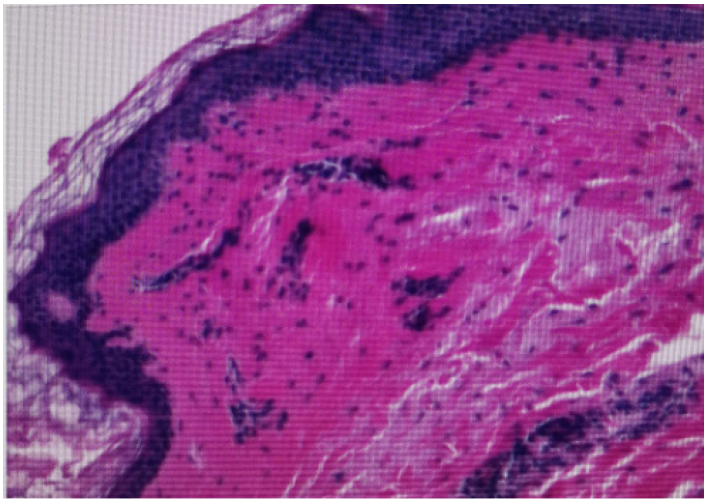

Figure 3 Amyloid deposition in collagen fibers of the dermis and positive Congo red staining.

In our case, the initial symptom was periorbital purpura without other systemic symptoms. The patient was seen in the dermatology department of several hospitals, but the etiology had not been recognized. As the disease progressed, the patient gradually developed pleural effusion, which on detailed examination revealed ventricular septal hyperplasia, ejection fraction preserved heart failure, positive monoclonal immunoglobulin, plasma cell hyperplasia in the bone marrow, and positive Congo red staining of an abdominal fat biopsy. Therefore, she was diagnosed with "primary light chain amyloidosis (cardiac and soft tissue involvement)".

In this case, periorbital purpura was the only initial symptom of primary light chain amyloidosis. The European Society of Cardiology statement also indicates that unexplained skin bruising may be a red flag for amyloidosis, especially in combination with heart failure with preserved ejection fraction[5]. Although periorbital purpura is pathognomonic for AL amyloidosis, it is rare, occurring in 1%-10% of cases, especially in patients whose initial symptom is only periorbital purpura. Primary light chain amyloidosis may also present with other cutaneous and mucosal manifestations, such as waxing and thickening, petechiae, and subcutaneous nodules or plaques, which need to be differentiated from the cutaneous manifestations of xanthomatosis, progressive necrotizing yellow granuloma, dermatomyositis, and senile purpura[6]. The cause of periorbital purpura may be related to amyloid deposition within the vessel wall, leading to increased vascular fragility, and when large amounts of amyloid are deposited in the skin, papules, plaques, and even nodules with bleeding manifestations may appear[5,6].

We suggest that patients with unexplained periorbital purpura should be examined in detail and be aware of the presence of comorbid systemic symptoms such as edema, proteinuria, hypotension, peripheral neuropathy, *etc*. If there is such a condition, then there is a need to be vigilant against systemic amyloidosis, which requires further blood/urine immunoprotein electrophoresis, free light chain and other tests, and, if necessary, a biopsy of the affected tissues and bone marrow or abdominal wall fat to make a definitive diagnosis.

The current diagnosis of AL-type amyloidosis requires the following[7]: Clinical manifestations of typical organ involvement + evidence of M protein (for M protein detection, serum free light chain, serum immunofixation electrophoresis combined with urine immunofixation electrophoresis is recommended, and the combination of all three can achieve a positive rate of up to 98.4%[8]) + positive Congo red staining of the tissue biopsy (the highest positivity is detected in the involved organs, and abdominal wall fat and bone marrow can also be part of the available biopsy[9]) + deposited amyloid material identified as immunoglobulin light chains.

All patients with AL amyloidosis should begin treatment for the primary disease as soon as possible after diagnosis. The primary goal is to achieve rapid and deep hematologic remission, with a greater proportion of organ remission achieved as hematologic remission deepens (from very good partial response to microscopic residual disease-negative), although organ remission tends to lag behind hematologic remission by several months[10]. Current therapeutic options target plasma cells. Daltolizumab is a humanized IgG-κ monoclonal antibody targeting the CD38 antigen on the surface of plasma cells, and a prospective randomized controlled study published in the July 2021 issue of the New England Journal of Medicine explored the value of chemotherapy in combination with or without daltolizumab in patients with primary AL-type amyloidosis, showing that combination of daratumumab with a regimen of bortezomib + cyclophosphamide + dexamethasone significantly improved hematologic complete remission. Monoclonal antibody significantly increased the rates of hematologic complete remission (53.3% *vs* 18.1%) and cardiac remission (41.5% *vs* 22.2%), and prolonged the progression-free survival of patients[11]. Therefore, daratumumab was included in the first-line treatment. Our patient was also treated with the D-VCD regimen, which led to a rapid hematologic remission. It is believed that organ remission will slowly appear with time.

Progress in anti-amyloid therapy has been relatively slow. Ward *et al*[12] found that oral doxycycline reduced amyloid deposition in the stomachs of mice with AL-type amyloidosis, while a European retrospective cohort study found that the combination of doxycycline on the basis of chemotherapy improved the rate of cardiac remission and survival time[13]. As a result, doxycycline has been included in the NCCN guidelines as a treatment option for AL-type amyloidosis, but a multicenter randomized controlled study led by Peking Union Medical College Hospital showed that chemotherapy-

based combination of doxycycline did not prolong progression-free survival and cardiac remission rate in patients[14]. CAEL-101 is a monoclonal antibody targeting misfolded light chains that promotes phagocytosis and clearance of amyloid. The results of a phase 1 a/b study showed that 63% of CAEL-101-treated patients achieved organ remission, with a median time to remission of only 3 weeks[15]. However, there is still a large gap in the application of new anti-amyloid substances in the clinic.

CONCLUSION

Periorbital purpura may be the only initial symptom of primary light chain amyloidosis. We suggest that when seeing a patient with periorbital purpura, we should be aware of the possibility of amyloidosis. The earlier the diagnosis, the faster treatment can begin, thus delaying or avoiding the progression of irreversible disease such as renal failure and cardiomyopathy.

FOOTNOTES

Author contributions: Wang XF and Huang Y contributed equally to this work as co-corresponding authors; Wang XF contributed to writing; Li T and Yang M contributed to conceptualization and data collection; Huang Y contributed to project administration; All authors have read and approved the final manuscript.

Supported by the Henan Province Medical Science and Technology Research Plan Joint Construction Project, No. LHGJ20210533; and Xinxiang Science and Technology Research Project, No. GG2020029.

Informed consent statement: Informed written consent was obtained from the patients for the publication of this report and any accompanying images.

Conflict-of-interest statement: The authors declare that they have no conflict of interest to disclose.

CARE Checklist (2016) statement: The authors have read the CARE Checklist (2016), and the manuscript was prepared and revised according to the CARE Checklist (2016).

Country of origin: China

ORCID number: Xiu-Feng Wang 0009-0006-8432-197X.

S-Editor: Chen YL
L-Editor: Filipodia
P-Editor: Wang WB

REFERENCES

1 **Chiti F**, Dobson CM. Protein Misfolding, Amyloid Formation, and Human Disease: A Summary of Progress Over the Last Decade. *Annu Rev Biochem* 2017; **86**: 27-68 [PMID: 28498720 DOI: 10.1146/annurev-biochem-061516-045115]
2 **Dogan A**. Amyloidosis: Insights from Proteomics. *Annu Rev Pathol* 2017; **12**: 277-304 [PMID: 27959636 DOI: 10.1146/annurev-pathol-052016-100200]
3 **Wechalekar AD**, Gillmore JD, Hawkins PN. Systemic amyloidosis. *Lancet* 2016; **387**: 2641-2654 [PMID: 26719234 DOI: 10.1016/S0140-6736(15)01274-X]
4 **Quock TP**, Yan T, Chang E, Guthrie S, Broder MS. Epidemiology of AL amyloidosis: a real-world study using US claims data. *Blood Adv* 2018; **2**: 1046-1053 [PMID: 29748430 DOI: 10.1182/bloodadvances.2018016402]
5 **Gertz MA**, Dispenzieri A. Systemic Amyloidosis Recognition, Prognosis, and Therapy: A Systematic Review. *JAMA* 2020; **324**: 79-89 [PMID: 32633805 DOI: 10.1001/jama.2020.5493]
6 **Merlini G**, Seldin DC, Gertz MA. Amyloidosis: pathogenesis and new therapeutic options. *J Clin Oncol* 2011; **29**: 1924-1933 [PMID: 21483018 DOI: 10.1200/JCO.2010.32.2271]
7 **Chen-Xu M**, Achilleos K. Periorbital purpura of AL amyloidosis. *Rheumatology (Oxford)* 2021; **60**: 1165 [PMID: 32944781 DOI: 10.1093/rheumatology/keaa545]
8 **Zhang CL**, Feng J, Shen KN, Su W, Zhang CL, Huang XF, Cao XX, Zhang L, Zhou DB, Li J. [The diagnostic and prognostic values of serum free light chain in patients with primary light chain amyloidosis]. *Zhonghua Xue Ye Xue Za Zhi* 2016; **37**: 942-945 [PMID: 27995877 DOI: 10.3760/cma.j.issn.0253-2727.2016.11.003]
9 **Gertz MA**. Immunoglobulin light chain amyloidosis: 2016 update on diagnosis, prognosis, and treatment. *Am J Hematol* 2016; **91**: 947-956

[PMID: 27527836 DOI: 10.1002/ajh.24433]

10 **Manwani R**, Cohen O, Sharpley F, Mahmood S, Sachchithanantham S, Foard D, Lachmann HJ, Quarta C, Fontana M, Gillmore JD, Whelan C, Hawkins PN, Wechalekar AD. A prospective observational study of 915 patients with systemic AL amyloidosis treated with upfront bortezomib. *Blood* 2019; **134**: 2271-2280 [PMID: 31578202 DOI: 10.1182/blood.2019000834]

11 **Kastritis E**, Palladini G, Minnema MC, Wechalekar AD, Jaccard A, Lee HC, Sanchorawala V, Gibbs S, Mollee P, Venner CP, Lu J, Schönland S, Gatt ME, Suzuki K, Kim K, Cibeira MT, Beksac M, Libby E, Valent J, Hungria V, Wong SW, Rosenzweig M, Bumma N, Huart A, Dimopoulos MA, Bhutani D, Waxman AJ, Goodman SA, Zonder JA, Lam S, Song K, Hansen T, Manier S, Roeloffzen W, Jamroziak K, Kwok F, Shimazaki C, Kim JS, Crusoe E, Ahmadi T, Tran N, Qin X, Vasey SY, Tromp B, Schecter JM, Weiss BM, Zhuang SH, Vermeulen J, Merlini G, Comenzo RL; ANDROMEDA Trial Investigators. Daratumumab-Based Treatment for Immunoglobulin Light-Chain Amyloidosis. *N Engl J Med* 2021; **385**: 46-58 [PMID: 34192431 DOI: 10.1056/NEJMoa2028631]

12 **Ward JE**, Ren R, Toraldo G, Soohoo P, Guan J, O'Hara C, Jasuja R, Trinkaus-Randall V, Liao R, Connors LH, Seldin DC. Doxycycline reduces fibril formation in a transgenic mouse model of AL amyloidosis. *Blood* 2011; **118**: 6610-6617 [PMID: 21998211 DOI: 10.1182/blood-2011-04-351643]

13 **Wechalekar AD**, Whelan C. Encouraging impact of doxycycline on early mortality in cardiac light chain (AL) amyloidosis. *Blood Cancer J* 2017; **7**: e546 [PMID: 28338670 DOI: 10.1038/bcj.2017.26]

14 **Shen KN**, Fu WJ, Wu Y, Dong YJ, Huang ZX, Wei YQ, Li CR, Sun CY, Chen Y, Miao HL, Zhang YL, Cao XX, Zhou DB, Li J. Doxycycline Combined With Bortezomib-Cyclophosphamide-Dexamethasone Chemotherapy for Newly Diagnosed Cardiac Light-Chain Amyloidosis: A Multicenter Randomized Controlled Trial. *Circulation* 2022; **145**: 8-17 [PMID: 34503349 DOI: 10.1161/CIRCULATIONAHA.121.055953]

15 **Edwards CV**, Rao N, Bhutani D, Mapara M, Radhakrishnan J, Shames S, Maurer MS, Leng S, Solomon A, Lentzsch S, Eisenberger A. Phase 1a/b study of monoclonal antibody CAEL-101 (11-1F4) in patients with AL amyloidosis. *Blood* 2021; **138**: 2632-2641 [PMID: 34521113 DOI: 10.1182/blood.2020009039]

World Journal of Clinical Cases

Submit a Manuscript: https://www.f6publishing.com

World J Clin Cases 2024 September 16; 12(26): 5952-5959

DOI: 10.12998/wjcc.v12.i26.5952

ISSN 2307-8960 (online)

CASE REPORT

Concurrent occurrence of adenocarcinoma and urothelial carcinoma of the prostate gland: A case report

Jhe Yuan Hsu, Yi Sheng Lin, Li Hua Huang, Tang Yi Tsao, Chao Yu Hsu, Yen Chuan Ou, Min Che Tung

Specialty type: Medicine, research and experimental

Provenance and peer review: Unsolicited article; Externally peer reviewed.

Peer-review model: Single blind

Peer-review report's classification

Scientific Quality: Grade C, Grade C

Novelty: Grade B, Grade B

Creativity or Innovation: Grade B, Grade C

Scientific Significance: Grade B, Grade B

P-Reviewer: Yan B

Received: February 25, 2024

Revised: June 15, 2024

Accepted: July 15, 2024

Published online: September 16, 2024

Processing time: 148 Days and 16.4 Hours

Jhe Yuan Hsu, Yi Sheng Lin, Li Hua Huang, Chao Yu Hsu, Yen Chuan Ou, Min Che Tung, Division of Urology, Department of Surgery, Tungs' Taichung MetroHarbor Hospital, Taichung 435403, Taiwan

Tang Yi Tsao, Department of Pathology, Tungs' Taichung MetroHarbor Hospital, Taichung 435403, Taiwan

Corresponding author: Yi Sheng Lin, MD, Chief Doctor, Division of Urology, Department of Surgery, Tungs' Taichung MetroHarbor Hospital, No. 699 Section 8, Taiwan Boulevard, Wuqi District, Taichung 435403, Taiwan. tung12197@gmail.com

Abstract

BACKGROUND

Adenocarcinoma is the most common subtype of prostate cancer. Prostatic urothelial carcinoma (UC) typically originates from the prostatic urethra. The concurrent occurrence of adenocarcinoma and UC of the prostate gland is uncommon.

CASE SUMMARY

We present the case of an 82-year-old male patient with simultaneous adenocarcinoma and UC of the prostate gland. The patient underwent a transrectal ultrasound-guided biopsy, and the pathology test revealed UC. Subsequently, transurethral laser prostatectomy was performed, and the pathology test indicated adenocarcinoma of the prostate with a Gleason score of 3 + 4 and high-grade UC. Therefore, the patient was treated with androgen deprivation therapy, systemic chemotherapy, and immunotherapy. Magnetic resonance imaging performed during follow-up revealed a prostate tumor classified as cT2cN1M0, stage IVA. Therefore, the patient underwent robotic-assisted radical prostatectomy and bilateral pelvic lymph node dissection. The final pathology test of the prostate gland revealed acinar-type adenocarcinoma, Gleason pattern 4 + 3, pT2N0M0, and high-grade UC. The patient regularly presented to the clinic for postoperative follow-up evaluations. He did not experience any urinary discomfort.

CONCLUSION

According to our literature review, this is the first reported case of coexisting adenocarcinoma and UC of the prostate gland.

Key Words: Adenocarcinoma; Urothelial carcinoma; Prostate; Coexist; Case report

Core Tip: This report of synchronous adenocarcinoma and urothelial carcinoma (UC) of the prostate gland describes the unique prostate cancer manifestations in a male patient as well as the clinical journey from his initial symptoms of urinary retention and gross hematuria to the final treatment comprising robotic-assisted radical prostatectomy and bilateral pelvic lymph nodes dissection. This rare co-occurrence of two distinct cancer subtypes of the prostate gland without a history of UC of the urinary bladder and evident recurrence after treatment emphasizes the need for heightened diagnostic awareness and suggests novel oncogenic pathways and genetic predispositions.

Citation: Hsu JY, Lin YS, Huang LH, Tsao TY, Hsu CY, Ou YC, Tung MC. Concurrent occurrence of adenocarcinoma and urothelial carcinoma of the prostate gland: A case report. *World J Clin Cases* 2024; 12(26): 5952-5959
URL: https://www.wjgnet.com/2307-8960/full/v12/i26/5952.htm
DOI: https://dx.doi.org/10.12998/wjcc.v12.i26.5952

INTRODUCTION

Prostate cancer is the second most common cancer among men worldwide, and its incidence increases with age. The predominant subtype of carcinoma of the prostate is adenocarcinoma. Adenocarcinoma is graded using the Gleason scoring system. Prostate urothelial carcinoma (UC) is a subtype that usually develops from the urothelium lining the prostatic urethra and the proximal sections of the prostatic ducts[1]. As far as we are aware, this is the first documented report of adenocarcinoma and UC co-occurring in the prostate gland.

CASE PRESENTATION

Chief complaints

An 82-year-old male patient presented to the urology clinic with a 5-day history of acute urinary retention and gross hematuria.

History of present illness

The patient experienced gross hematuria and intermittent acute urinary retention for 5 days before presentation.

History of past illness

The patient was initially evaluated at another hospital because he experienced acute urinary retention and gross hematuria. A digital rectal examination (DRE) revealed firm prostate nodules and an increased prostate-specific antigen (PSA) level of 53 ng/mL. In October 2020, the patient underwent a transrectal ultrasound-guided biopsy that revealed UC. Subsequently, he underwent transurethral laser prostatectomy. The pathology test indicated prostatic adenocarcinoma with a Gleason score of 3 + 4 and high-grade UC. Cystoscopy revealed no papillary tumors in the prostatic urethra or urinary bladder. No evidence of bone metastasis was observed during a bone scan. Therefore, the patient was treated with androgen deprivation therapy (ADT) with leuprorelin and bicalutamide in December 2020. In January and February 2021, the patient was treated with systemic chemotherapy with gemcitabine and cisplatin. In February 2021, the patient was treated with immunotherapy with nivolumab at another hospital (Figure 1).

Personal and family history

The patient had a history of hypertension and arrhythmia that were controlled with medication. He did not have a family history of malignant tumors.

Physical examination

During the physical examination, the external genitalia appeared normal. The DRE revealed a firm prostate with an estimated volume of 25 cm^3.

Laboratory examinations

The preoperative blood test revealed a white blood cell count of 8.2 × 10^3/μL, hemoglobin level of 12.3 g/dL, platelet count of 263 × 10^3/μL, glutamic oxaloacetic transaminase level of 21 IU/L, blood urea nitrogen level of 21 mg/dL, creatinine level of 1.01 mg/dL, estimated glomerular filtration rate of 75, and PSA level of 8.877 ng/dL. The urinalysis results were within normal ranges.

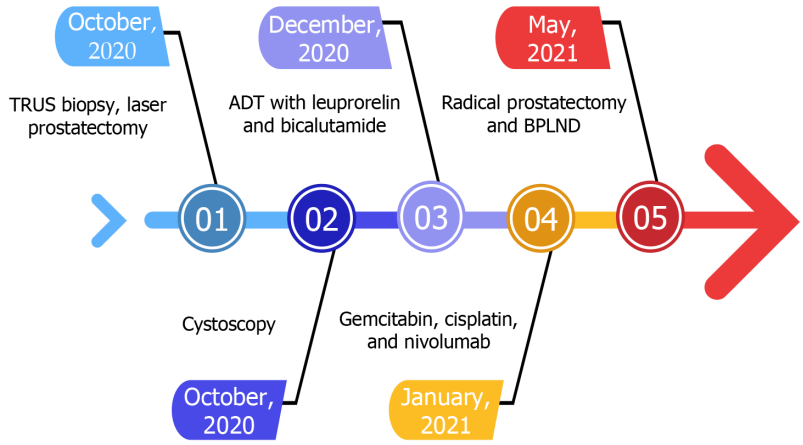

Figure 1 Fishbone diagram of treatment. ADT: Androgen deprivation therapy; BPLND: Bilateral pelvic lymph node dissection; TRUS: Transrectal ultrasound.

Imaging examinations

Ultrasonography was performed to estimate the volume of the prostate gland (25 cm^3). The postvoid volume was 29 mL. Magnetic resonance imaging was performed during follow-up and revealed a prostate tumor classified as cT2cN1M0, stage IVA (Figure 2).

MULTIDISCIPLINARY EXPERT CONSULTATION

A technetium-99 m methylene diphosphonate whole-body bone scan revealed no evidence of bone metastasis (Figure 3). An 18F-fluorodeoxyglucose positron emission tomography examination revealed no evidence of metastasis (Figure 4). Cystoscopy revealed no papillary tumors in the urinary bladder or urethra.

FINAL DIAGNOSIS

The final diagnosis was adenocarcinoma and high-grade UC of the prostate classified as cT2cN1M0, stage IVA.

TREATMENT

The patient presented to our hospital for a second opinion regarding the diagnosis. Radical cystoprostatectomy was suggested; however, the patient refused this procedure. Therefore, he underwent robotic-assisted radical prostatectomy (RaRP) and bilateral pelvic lymph node dissection (BPLND) on May 11, 2021 (Figure 5).

OUTCOME AND FOLLOW-UP

The results of the final pathology test of the prostate gland indicated acinar-type adenocarcinoma, gleason pattern 4 + 3 (grade group 3), pT2N0M0, and high-grade UC (Figure 6). The surgical margins were clear, and extraprostatic extension was not observed. The immunohistochemical staining results were as follows: Negative CK5; Positive α-methylacyl coenzyme A racemase; Positive synaptophysin (20%); and Positive GATA binding protein 3 (GATA3). These findings indicated concurrent adenocarcinoma and UC of the prostate gland. The patient was discharged 6 days postoperatively. He experienced good recovery and did not report any major complications. Outpatient evaluations comprising PSA monitoring and cystoscopy were performed every 3 months. The PSA levels remained less than 0.008 ng/dL. Urinary discomfort and signs of recurrence were not observed during the most recent clinical evaluation. The patient expressed that he was highly satisfied with the surgical outcome and that his quality of life had significantly improved with treatment.

DISCUSSION

To our knowledge, this is the first reported case of simultaneous adenocarcinoma and UC of the prostate gland in Taiwan. Typically, prostate cancer manifests as adenocarcinoma. Although there have been case reports of adenocar-

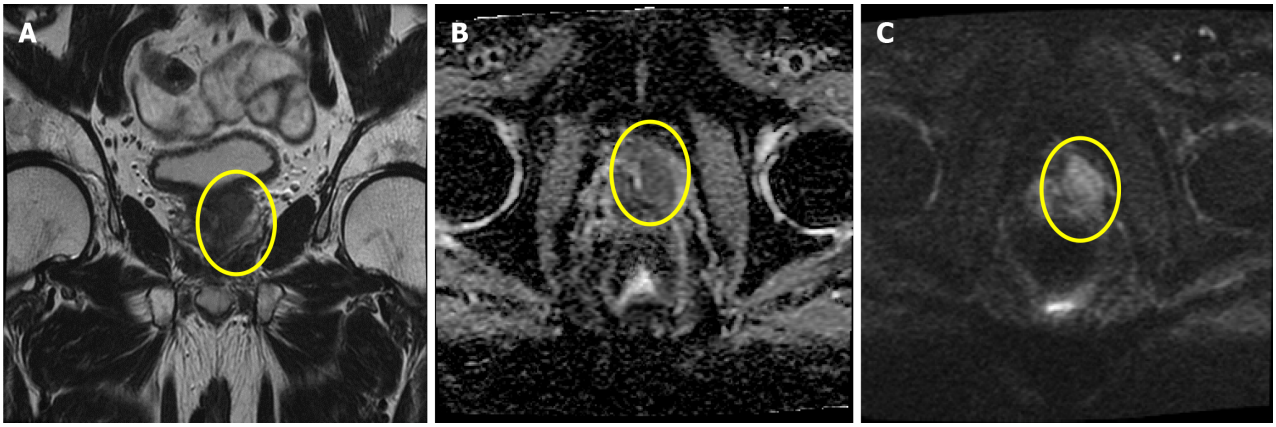

Figure 2 Image of the pelvis obtained during follow-up with magnetic resonance imaging. A: A 2.4-cm lesion with low T2 signal is observed in the posterolateral portion of the left transitional zone; B: Apparent diffusion coefficient of the lesion with low signal; C: Increased diffusion tensor imaging signals are observed.

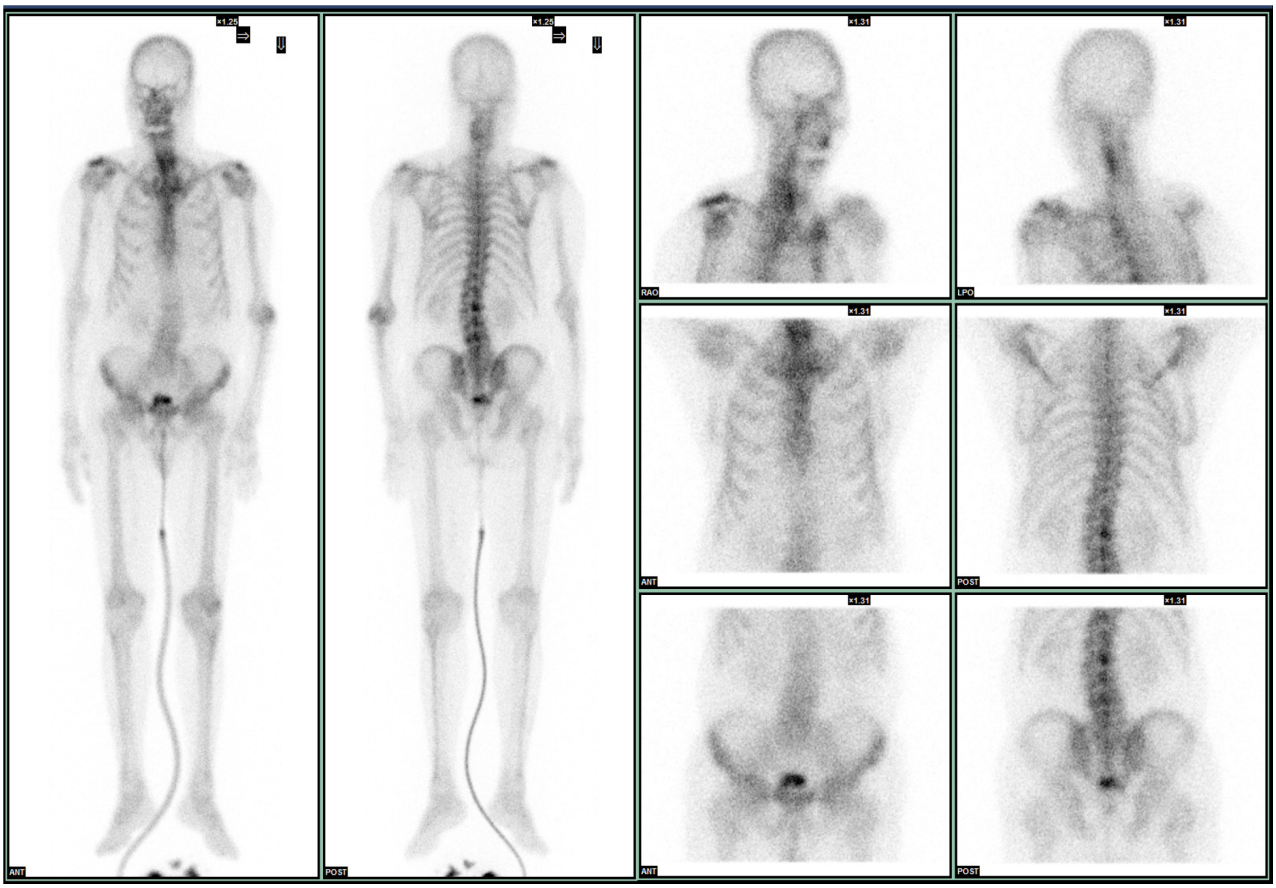

Figure 3 Technetium-99m methylene diphosphonate whole-body bone scan. Focal areas of increased radioactivity uptake are noted in the lumbar spine at levels L1/2, L3/4, and L4/5, as well as in the left elbow and bilateral acromioclavicular joints. These findings suggest a benign etiology.

cinoma and tubulovillous adenoma of the urinary bladder, UC predominantly occurs in the urinary bladder or ureter[2, 3]. One of the primary objectives of this study was to stimulate further research into the mechanisms underlying the coexistence of these conditions.

According to the World Health Organization GLOBOCAN database, prostate cancer is a significant medical concern because of its prevalence, impact on the quality of life, and mortality. Risk factors include age, ethnicity, genetics, diet, hormones, obesity, and others[4-8]. Patients are often asymptomatic initially. Bone pain is a common clinical presentation among patients with metastatic prostate cancer at the time of diagnosis because the bones are the predominant sites of dissemination[9].

Prostate cancer is typically suspected when increased PSA levels or abnormal DRE findings are observed. There is no single threshold for abnormal PSA levels. However, age-specific reference PSA levels, which increase faster in older men,

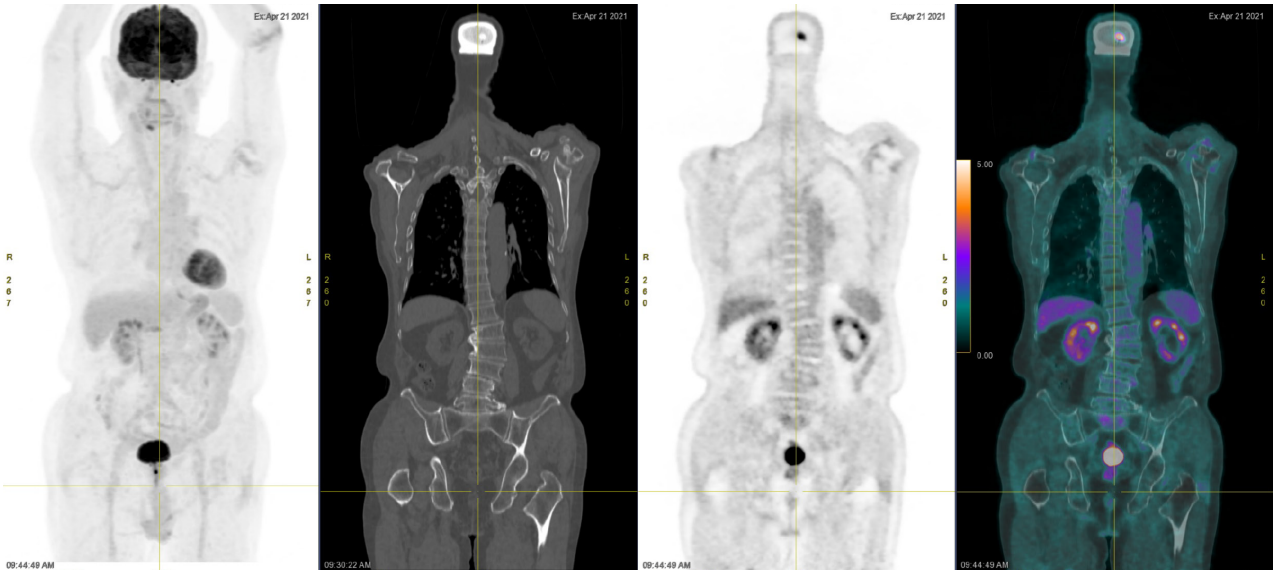

Figure 4 Images obtained during an 18F-fluorodeoxyglucose positron emission tomography evaluation of the region comprising the head to the upper thigh. From left to right: Ill-defined fluorodeoxyglucose (FDG) avidity is observed in the prostate; No FDG-avid regional or distant lymph nodes are apparent; Ill-defined FDG avidity is noted in the right buccal region after the dental prosthesis; and Ill-defined FDG avidity in the right T1, T4, T8, T12, and left upper ilia with sclerotic changes, suggesting a benign etiology.

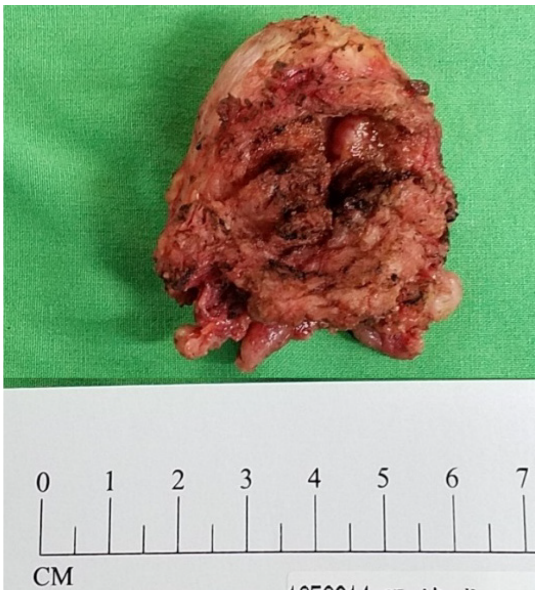

Figure 5 Gross examination of the prostate tumor after robotic-assisted radical prostatectomy. 4 cm × 3 cm × 4 cm prostate gland with a volume of 24.96 mL and weight of 29 g; The 19 cm × 1.3 cm × 0.7 cm adenocarcinoma is located in the left anterior lateral lobe and, specifically, in the middle area transitioning to the peripheral zone. The 1 cm × 0.6 cm × 0.6 cm carcinoma of the urethra is observed in the right posterior lobe, middle area, and near the periurethra.

and the velocity of increase in the PSA level, which often has a cutoff of more than 0.75 ng/dL within 1 year, are considered significant findings[10].

A definitive diagnosis requires the evaluation of tissue samples obtained during a transrectal or transperineal biopsy [11]. Most malignant prostatic neoplasms are carcinomas that originate from and are differentiated from epithelial tissue. Adenocarcinoma, which accounts for more than 95% of all cases, is characterized by its glandular structure, absence of basal cells, and distinct nuclear characteristics of the glandular epithelial cells[12]. Compared to benign glands, malignant glands present more frequently with intraluminal crystalloids, amorphous secretions, or blue-tinged mucin. Adenocarcinomas are mostly acinar; the ductal types are less common[13]. UC, which is another less common subtype, typically occurs concurrently with bladder carcinoma; however, it can arise as the primary disease. Immunohistochemical findings that differentiate UC from adenocarcinoma of the prostate include thrombomodulin, GATA3, p63, and high-molecular-weight cytokeratins[14].

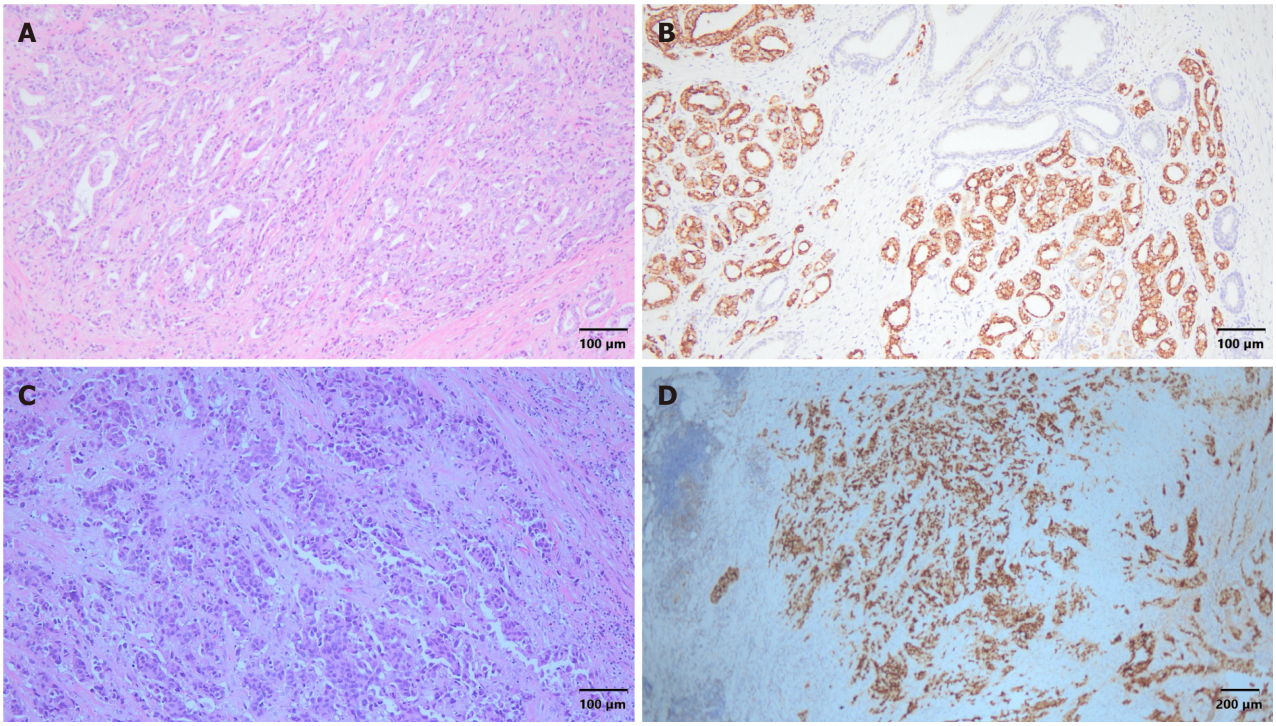

Figure 6 Histopathological analysis and immunohistochemical examination of the resected specimen. A: Adenocarcinoma of the prostate (hematoxylin and eosin staining × 100); B: Positive immunohistochemical (IHC) staining for α-methylacyl coenzyme A racemase (× 200); C: Prostate urothelial carcinoma (hematoxylin and eosin staining × 100); D: Positive IHC staining for GATA binding protein 3 (× 40).

The staging and evaluation of adenocarcinoma of the prostate as well as its treatment strategies are based on its risk stratification determined by the DRE results, serum PSA levels, pathology results of the prostate biopsy sample, and imaging results. Treatment options for very low-risk disease include active surveillance and, if necessary, definitive local therapy such as radiation therapy (RT) and radical prostatectomy[15]. Definitive treatment options for patients with low-risk prostate cancer and a life expectancy of more than 10 years include RT, radical prostatectomy, and active surveillance [16]. Intermediate-risk disease can be treated with RT and radical prostatectomy. Clinically localized high-risk prostate cancer is typically managed with external beam RT combined with brachytherapy, ADT, or radical prostatectomy[15]. Treatments for locally advanced and very high-risk prostate cancer include external beam RT with or without brachytherapy, long-term ADT, and radical prostatectomy[17]. The outcomes of these treatments depend on the disease stage and patient compliance.

A review of the literature indicated that most patients with UC of the prostate had a history of UC of the urinary bladder[18]. Additionally, concurrent UC of the urinary bladder and prostate was diagnosed incidentally after cystoprostatectomy[19,20]. In this case, UC was not observed in the urinary bladder. However, the coexistence of UC and adenocarcinoma of the prostate was incidentally discovered after the prostate biopsy. According to previous research of the different immunohistochemical findings that distinguish prostate carcinoma from UC, the sensitivities of prostatic markers of prostate adenocarcinoma were as follows: 100% for PSA; 83.8% for prostate-specific membrane antigen; 91.9% for prostate acid phosphatase; 93.7% for P501s; 88.3% for NKX 3.1; and 66.7% for α-methylacyl coenzyme a racemase. In contrast, the sensitivities of urothelial markers of UC were 75.4% for CK34βE12, 73.9% for p63, 45.7% for thrombomodulin, 22.5% for S100P, and 84.8% for GATA3[21]. The immunohistochemical staining results of the prostate samples from our patient were positive for both α-methylacyl coenzyme A racemase and GATA3; therefore, the coexistence of adenocarcinoma and UC was strongly suggested.

We proposed three hypotheses regarding the potential mechanisms of synchronous adenocarcinoma and UC of the prostate. First, metaplastic transformation may result in this phenomenon. Metaplastic transformation involves the conversion of one differentiated cell type to another. In this context, some glandular cells within the prostate may have undergone metaplastic transformation to urothelial cells, potentially driven by chronic inflammation or other local environmental factors[22]. Second, the presence of multipotent stem cells within the prostate could explain the coexistence of adenocarcinoma and UC. Multipotent stem cells can differentiate into various cell types, including glandular and urothelial cells. This pluripotency may lead to the simultaneous emergence of adenocarcinoma and UC in the same tissue[23,24]. Third, the intraluminal spread of UC cells from an occult site within the urinary tract to the prostate could cause this uncommon disease occurrence. Intraluminal spread can occur without a documented history of primary UC, particularly if the primary site is very small or has regressed[25]. Although these hypotheses provide various potential explanations for the simultaneous presence of adenocarcinoma and UC of the prostate, they have not been confirmed.

Our patient initially underwent ADT for adenocarcinoma of the prostate because he preferred nonsurgical intervention. Consequently, leuprorelin and bicalutamide were administered for several months. Although the PSA level of

our patient decreased to 8.78 ng/mL after 4 months of treatment, he sought a second opinion at our hospital. Because the tumor was restricted to the prostate stroma without involvement of the prostatic urethra, as confirmed by cystoscopy and magnetic resonance imaging, and because the patient's Eastern Cooperative Oncology Group performance status was good, radical cystoprostatectomy was recommended. However, after a thorough discussion and explanation, the patient chose RaRP and BPLND as bladder-sparing surgery. Additionally, four cycles of systemic chemotherapy with gemcitabine and cisplatin for UC of the prostate were initially administered at another hospital by a physician with clinical experience with UC of the prostate with stromal invasion. Subsequently, second-line systemic immunotherapy with Nivolumab was administered.

Despite the absence of a history of UC in the urinary bladder, cystoscopy revealed no recurrence following ADT, chemotherapy, and immunotherapy. Two years after RaRP and BPLND, the patient was recurrence-free. No reports of synchronous adenocarcinoma and UC of the prostate gland were found during our literature review.

CONCLUSION

To the best of our knowledge, this is the first reported case of synchronous adenocarcinoma and UC of the prostate gland. Although a correlation between adenocarcinoma and UC of the prostate gland has not been proven, this case highlights the potential for the coexistence of these two cancer subtypes in the prostate gland and suggests the need for further genetic studies and case reports to improve the understanding of the causes and mechanisms of their coexistence.

ACKNOWLEDGEMENTS

We extend our heartfelt appreciation to the patient for consenting to the publication of this case. We also express our special thanks to the staff of Tungs' Taichung MetroHarbor Hospital for their exemplary care and dedication to patient service.

FOOTNOTES

Author contributions: Hsu JY, Lin YS, Huang LH, and Tsao TY contributed to patient care, data collection, and manuscript writing and editing; Hsu CY, Ou YC, and Tung MC contributed to conceptualization and supervision; All authors have read and approved the final manuscript.

Informed consent statement: Written informed consent was obtained from the patient for the publication of this report and any accompanying images.

Conflict-of-interest statement: The authors declare that they have no conflict of interest.

CARE Checklist (2016) statement: The authors have read the CARE Checklist (2016), and the manuscript was prepared and revised according to the CARE Checklist (2016).

Country of origin: Taiwan

ORCID number: Jhe Yuan Hsu 0000-0001-5006-0149; Yi Sheng Lin 0000-0003-0592-0036; Li Hua Huang 0000-0003-4337-7230; Chao Yu Hsu 0000-0001-9809-7442; Yen Chuan Ou 0000-0002-6080-7231; Min Che Tung 0000-0002-4136-7613.

S-Editor: Fan M
L-Editor: A
P-Editor: Che XX

REFERENCES

1 **Liedberg F**, Chebil G, Månsson W. Urothelial carcinoma in the prostatic urethra and prostate: current controversies. *Expert Rev Anticancer Ther* 2007; **7**: 383-390 [PMID: 17338657 DOI: 10.1586/14737140.7.3.383]
2 **Tsai PH**, Chiang HC, Chen PH. Adenocarcinoma of urinary bladder– A case report. *Urol Sci* 2015; **26**: 298 [DOI: 10.1016/j.urols.2015.11.052]
3 **Chen I**, Chien C, Yu C, Wu T, Huang J. Primary tubulovillous adenoma of the urinary bladder: Case report and literature review. *Urol Sci* 2014; **25**: 139-142 [DOI: 10.1016/j.urols.2013.08.003]

4 **Parker PM**, Rice KR, Sterbis JR, Chen Y, Cullen J, McLeod DG, Brassell SA. Prostate cancer in men less than the age of 50: a comparison of race and outcomes. *Urology* 2011; **78**: 110-115 [PMID: 21397300 DOI: 10.1016/j.urology.2010.12.046]

5 **Barber L**, Gerke T, Markt SC, Peisch SF, Wilson KM, Ahearn T, Giovannucci E, Parmigiani G, Mucci LA. Family History of Breast or Prostate Cancer and Prostate Cancer Risk. *Clin Cancer Res* 2018; **24**: 5910-5917 [PMID: 30082473 DOI: 10.1158/1078-0432.CCR-18-0370]

6 **Chan JM**, Gann PH, Giovannucci EL. Role of diet in prostate cancer development and progression. *J Clin Oncol* 2005; **23**: 8152-8160 [PMID: 16278466 DOI: 10.1200/JCO.2005.03.1492]

7 **Endogenous Hormones and Prostate Cancer Collaborative Group**, Roddam AW, Allen NE, Appleby P, Key TJ. Endogenous sex hormones and prostate cancer: a collaborative analysis of 18 prospective studies. *J Natl Cancer Inst* 2008; **100**: 170-183 [PMID: 18230794 DOI: 10.1093/jnci/djm323]

8 **Allott EH**, Masko EM, Freedland SJ. Obesity and prostate cancer: weighing the evidence. *Eur Urol* 2013; **63**: 800-809 [PMID: 23219374 DOI: 10.1016/j.eururo.2012.11.013]

9 **Collin SM**, Metcalfe C, Donovan JL, Athene Lane J, Davis M, Neal DE, Hamdy FC, Martin RM. Associations of sexual dysfunction symptoms with PSA-detected localised and advanced prostate cancer: a case-control study nested within the UK population-based ProtecT (Prostate testing for cancer and Treatment) study. *Eur J Cancer* 2009; **45**: 3254-3261 [PMID: 19541477 DOI: 10.1016/j.ejca.2009.05.021]

10 **Oesterling JE**, Jacobsen SJ, Chute CG, Guess HA, Girman CJ, Panser LA, Lieber MM. Serum prostate-specific antigen in a community-based population of healthy men. Establishment of age-specific reference ranges. *JAMA* 1993; **270**: 860-864 [PMID: 7688054]

11 **Lin H**, Huang C, Chang C, Chiu Y, Hsueh TY, Lu S, Chiu AW. The efficacy of transrectal prostate needle biopsy in older men. *Urol Sci* 2016; **27**: S34-S35 [DOI: 10.1016/j.urols.2016.05.054]

12 **Humphrey PA**. Histopathology of Prostate Cancer. *Cold Spring Harb Perspect Med* 2017; **7** [PMID: 28389514 DOI: 10.1101/cshperspect.a030411]

13 **Chow K**, Bedő J, Ryan A, Agarwal D, Bolton D, Chan Y, Dundee P, Frydenberg M, Furrer MA, Goad J, Gyomber D, Hanegbi U, Harewood L, King D, Lamb AD, Lawrentschuk N, Liodakis P, Moon D, Murphy DG, Peters JS, Ruljancich P, Verrill CL, Webb D, Wong LM, Zargar H, Costello AJ, Papenfuss AT, Hovens CM, Corcoran NM. Ductal variant prostate carcinoma is associated with a significantly shorter metastasis-free survival. *Eur J Cancer* 2021; **148**: 440-450 [PMID: 33678516 DOI: 10.1016/j.ejca.2020.12.030]

14 **Paner GP**, Annaiah C, Gulmann C, Rao P, Ro JY, Hansel DE, Shen SS, Lopez-Beltran A, Aron M, Luthringer DJ, De Peralta-Venturina M, Cho Y, Amin MB. Immunohistochemical evaluation of novel and traditional markers associated with urothelial differentiation in a spectrum of variants of urothelial carcinoma of the urinary bladder. *Hum Pathol* 2014; **45**: 1473-1482 [PMID: 24780825 DOI: 10.1016/j.humpath.2014.02.024]

15 **Bekelman JE**, Rumble RB, Chen RC, Pisansky TM, Finelli A, Feifer A, Nguyen PL, Loblaw DA, Tagawa ST, Gillessen S, Morgan TM, Liu G, Vapiwala N, Haluschak JJ, Stephenson A, Touijer K, Kungel T, Freedland SJ. Clinically Localized Prostate Cancer: ASCO Clinical Practice Guideline Endorsement of an American Urological Association/American Society for Radiation Oncology/Society of Urologic Oncology Guideline. *J Clin Oncol* 2018; **36**: 3251-3258 [PMID: 30183466 DOI: 10.1200/JCO.18.00606]

16 **Donovan JL**, Hamdy FC, Lane JA, Mason M, Metcalfe C, Walsh E, Blazeby JM, Peters TJ, Holding P, Bonnington S, Lennon T, Bradshaw L, Cooper D, Herbert P, Howson J, Jones A, Lyons N, Salter E, Thompson P, Tidball S, Blaikie J, Gray C, Bollina P, Catto J, Doble A, Doherty A, Gillatt D, Kockelbergh R, Kynaston H, Paul A, Powell P, Prescott S, Rosario DJ, Rowe E, Davis M, Turner EL, Martin RM, Neal DE; ProtecT Study Group*. Patient-Reported Outcomes after Monitoring, Surgery, or Radiotherapy for Prostate Cancer. *N Engl J Med* 2016; **375**: 1425-1437 [PMID: 27626365 DOI: 10.1056/NEJMoa1606221]

17 **Tsao CK**, Gray KP, Nakabayashi M, Evan C, Kantoff PW, Huang J, Galsky MD, Pomerantz M, Oh WK. Patients with Biopsy Gleason 9 and 10 Prostate Cancer Have Significantly Worse Outcomes Compared to Patients with Gleason 8 Disease. *J Urol* 2015; **194**: 91-97 [PMID: 25623747 DOI: 10.1016/j.juro.2015.01.078]

18 **Pawar D**, Arif D, Raghunath A, Rehman S. Urothelial carcinoma with mandibular metastasis and synchronous prostate cancer. *BMJ Case Rep* 2022; **15** [PMID: 35288430 DOI: 10.1136/bcr-2021-247419]

19 **Dell'Atti L**. Relevance of prostate cancer in patients with synchronous invasive bladder urothelial carcinoma: a monocentric retrospective analysis. *Arch Ital Urol Androl* 2015; **87**: 76-79 [PMID: 25847902 DOI: 10.4081/aiua.2015.1.76]

20 **Sivalingam S**, Drachenberg D. The incidence of prostate cancer and urothelial cancer in the prostate in cystoprostatectomy specimens in a tertiary care Canadian centre. *Can Urol Assoc J* 2013; **7**: 35-38 [PMID: 23671490 DOI: 10.5489/cuaj.212]

21 **Oh WJ**, Chung AM, Kim JS, Han JH, Hong SH, Lee JY, Choi YJ. Differential Immunohistochemical Profiles for Distinguishing Prostate Carcinoma and Urothelial Carcinoma. *J Pathol Transl Med* 2016; **50**: 345-354 [PMID: 27498545 DOI: 10.4132/jptm.2016.06.14]

22 **Humphrey PA**. Histological variants of prostatic carcinoma and their significance. *Histopathology* 2012; **60**: 59-74 [PMID: 22212078 DOI: 10.1111/j.1365-2559.2011.04039.x]

23 **Lawson DA**, Xin L, Lukacs R, Xu Q, Cheng D, Witte ON. Prostate stem cells and prostate cancer. *Cold Spring Harb Symp Quant Biol* 2005; **70**: 187-196 [PMID: 16869753 DOI: 10.1101/sqb.2005.70.003]

24 **Shen MM**, Abate-Shen C. Molecular genetics of prostate cancer: new prospects for old challenges. *Genes Dev* 2010; **24**: 1967-2000 [PMID: 20844012 DOI: 10.1101/gad.1965810]

25 **Cohen RJ**, Shannon BA, Weinstein SL. Intraductal carcinoma of the prostate gland with transmucosal spread to the seminal vesicle: a lesion distinct from high-grade prostatic intraepithelial neoplasia. *Arch Pathol Lab Med* 2007; **131**: 1122-1125 [PMID: 17617002 DOI: 10.5858/2007-131-1122-ICOTPG]

World Journal of Clinical Cases

Submit a Manuscript: https://www.f6publishing.com

World J Clin Cases 2024 September 16; 12(26): 5960-5967

DOI: 10.12998/wjcc.v12.i26.5960

ISSN 2307-8960 (online)

CASE REPORT

Stage IV non-small cell lung cancer with multiple metastases to the small intestine leading to intussusception: A case report

Qi-Guang Niu, Min-Hao Huang, Wei-Qi Kong, Yang Yu

Specialty type: Medicine, research and experimental

Provenance and peer review: Unsolicited article; Externally peer reviewed.

Peer-review model: Single blind

Peer-review report's classification

Scientific Quality: Grade C, Grade C

Novelty: Grade B, Grade B

Creativity or Innovation: Grade A, Grade B

Scientific Significance: Grade B, Grade B

P-Reviewer: Casu C; Lomeli SM

Received: March 26, 2024

Revised: June 19, 2024

Accepted: July 2, 2024

Published online: September 16, 2024

Processing time: 118 Days and 13.6 Hours

Qi-Guang Niu, Department of General Surgery, Tong Ren Hospital, Shanghai Jiao Tong University School of Medicine, Shanghai 200336, China

Min-Hao Huang, Wei-Qi Kong, Yang Yu, Department of General Surgery, Tong Ren Hospital, Shanghai Jiao Tong University School of Medicine, Shanghai 200050, China

Corresponding author: Qi-Guang Niu, Doctor, Attending Doctor, Department of General Surgery, Tong Ren Hospital, Shanghai Jiao Tong University School of Medicine, No. 1111 Xian Xia Road, Changning District, Shanghai 200336, China. 1594792830@qq.com

Abstract

BACKGROUND

Gastrointestinal tract metastasis from lung cancer is rare and compared to small cell lung cancer (SCLC), non-SCLC (NSCLC) is even less likely to metastasize in this manner. Additionally, small intestinal tumors can also present with diverse complications, some of which require urgent intervention.

CASE SUMMARY

In this report, we detail a unique case of stage IV lung cancer, where the presence of small intestine tumors led to intussusception. Subsequent to a small intestine resection, pathology confirmed that all three tumors within the small intestine were metastases from adenocarcinoma of the lung. The postoperative follow-up period extended beyond 14 mo.

CONCLUSION

In patients with stage IV NSCLC, local tumor control can be achieved with various treatments. However, if small intestinal metastasis occurs, surgical intervention remains necessary, as it may improve survival.

Key Words: Non-small cell lung cancer; Brain metastases ablation; Small bowel metastases; Small bowel resection; Case report

Core Tip: Small bowel metastases may occur in advanced lung cancer, leading to gastrointestinal obstruction and requiring aggressive surgical intervention. In such patients, survival may be improved if the gastrointestinal obstruction is relieved and the primary lung lesion can be controlled.

Citation: Niu QG, Huang MH, Kong WQ, Yu Y. Stage IV non-small cell lung cancer with multiple metastases to the small intestine leading to intussusception: A case report. *World J Clin Cases* 2024; 12(26): 5960-5967
URL: https://www.wjgnet.com/2307-8960/full/v12/i26/5960.htm
DOI: https://dx.doi.org/10.12998/wjcc.v12.i26.5960

INTRODUCTION

Lung cancer is one of the leading causes of mortality among malignant diseases in humans and is characterized by high incidence and mortality rates, with the majority of deaths resulting from metastasis. Based on histopathological characteristics, lung cancer is primarily classified into non-small cell lung cancer (NSCLC) and SCLC. NSCLC accounts for approximately 80%-85% of all lung cancer cases[1]. Metastasis in lung cancer involves the spread of primary malignant tumors of the lung from their origin to distant sites through various mechanisms. The most common sites of metastasis include the brain, bones, lymph nodes, and liver[1,2], among which metastasis to the bone is the most frequent site, occurring in about 20%–40% of lung cancer patients[2,3]. NSCLC with brain metastases has the worst prognosis, with a 2-year overall survival rate of no more than 10%-20%[3,4]. Compared to SCLC, the occurrence of multiple metastases in NSCLC is significantly rarer. In NSCLC, cases of metastasis to soft tissue and organs such as the kidneys, pancreas, spleen, peritoneal cavity, intestines, bone marrow, eyes, ovaries, thyroid, heart, breasts, tonsils, and nasal cavity have been reported and found to be associated with a poor prognosis[5,6]. An analysis of 17431 deceased lung cancer patients diagnosed from 2002 to 2010 from the nationwide Swedish Cancer Registry revealed that the most frequent metastatic sites were the nervous system, bone, liver, respiratory system, and adrenal gland. Liver (35%) and nervous system (47%) metastases were common in patients with metastases from SCLC, and bone (39%) and respiratory system (22%) metastases in adenocarcinoma[7]. Skin metastases were revealed to be relatively infrequent in lung cancer, with a rate of only 2.8% in patients with advanced lung cancer[8]. In this retrospective cohort study, all patients diagnosed with stage IV NSCLC from 2014 to 2016 at two tertiary metropolitan health centers were assessed, and it was found that of the 893 patients analyzed, 457 (51%) had single organ metastasis, while 436 (49%) had multiple organ metastases at initial diagnosis. Among NSCLC patients with single organ metastasis, the most common sites of metastasis were the brain (26%), lung (23%), and bone (22%)[9]. The data of patients with newly diagnosed metastatic or unresectable NSCLC and treated with pembrolizumab-based therapy at two tertiary metropolitan health centers in Victoria, Australia from 2018 to April 2021 were retrieved and assessed. They were identified through pharmacy records of immunotherapy administration and other eligibility criteria. The most common sites of metastasis were found to be the liver (14.9%), brain (21.3%), bone (38.3%), and subdiaphragmatic regions (25.2%)[10]. The occurrence of gastrointestinal tract metastasis was relatively uncommon, reported at only 1.77%[11]. A retrospective analysis of 366 patients with gastrointestinal metastases of lung cancer showed that more than half of them died within 3 mo of diagnosis, with a median overall survival of 2.8 mo[12].

The incidence of gastrointestinal metastases from lung cancer is extremely low, and among sites, metastasis to the gastrointestinal tract is exceedingly rare, accounting for only 0.19% to 0.26% of all cases[13]. Among these, small intestinal metastasis is even rarer, reported in 11.9% of gastrointestinal cases, but has been found to substantially shorten the survival of lung cancer patients[14]. The occurrence of multiple metastases in NSCLC is also rarer compared to SCLC. In this case report, we present a rare case of NSCLC with multiple metastases to the small intestine. And we describe all treatment procedures and postoperative follow-ups.

CASE PRESENTATION

Chief complaints

Nausea and vomiting for one day with fever.

History of present illness

A 62-year-old female patient presented with sudden onset diarrhea, which began one day prior without an identifiable trigger. Her symptoms included watery stools with frequent episodes, accompanied by abdominal distension and an absence of flatus. The patient also reported nausea and vomiting, with vomitus comprising gastric contents. She developed a fever, peaking at 38 °C (100.4 °F). Due to persistent symptoms, she was admitted to the general surgery department on September 7, 2022.

History of past illness

The patient was diagnosed with NSCLC in September 2021 at Zhongshan Hospital affiliated with Fudan University

(Shanghai, China). An enhanced chest computed tomography (CT) scan at that time revealed a lobulated soft tissue mass adjacent to the right pulmonary hilum, measuring 3.9 cm in diameter, with irregular margins and uneven internal density, accompanied by enhancement. Biopsy pathology indicated poorly differentiated NSCLC, with the specific pathological type not further clarified. A cranial CT scan suggested possible intracranial metastasis. The patient did not undergo surgery but began oral targeted therapy with osimertinib (AZD-9291). Subsequently, the patient developed neurological symptoms, including headaches and seizures. Due to brain metastasis from lung cancer, the patient underwent two intracranial tumor ablation surgeries in December 2021 and June 2022 at another hospital, followed by a lung tumor ablation surgery in July 2022.

Personal and family history

The patient reported no remarkable personal and family history.

Physical examination

Upon admission, physical examination revealed a flat and soft abdomen with scattered epigastric tenderness, without rebound pain or muscle tensing. The patient's vital signs were: Body temperature, 37.3 °C (90.14 °F); heart rate, 100 beats/min; respiration rate: 18 breaths/min; blood pressure, 12.13/7.33 kPa.

Laboratory examinations

The patient's laboratory testing results were: White blood cell count, 10.65 × 10^9/L; C-reactive protein, 61.87 mg/L; neutrophil percentage, 87.4%; haemoglobin, 87 g/L; platelet count: 210 × 10^9/L.

Imaging examinations

A pre-admission plain CT scan indicated partial small intestinal obstruction and a possible intra-abdominal hernia. A subsequent chest CT scan was also conducted upon admission (Figure 1). After oral contrast administration, an enhanced CT scan (Figure 2) suggested nodular thickening of the small intestinal wall in the left abdomen. A segment of the small intestine in the pelvic region was found to exhibit a circular intussusception structure, with localized wall thickening and uneven enhancement post-contrast, and was accompanied by significant dilation of the upstream small intestine, accumulation of gas and fluid with fluid levels, and the presence of gas within the wall, indicating a high likelihood of strangulation.

FINAL DIAGNOSIS

Based on the patient's history, the clinical diagnosis was as follows: Small intestine tumor with intussusception, small intestinal obstruction, post-lung cancer ablation status, post-brain tumor ablation status, and anemia.

TREATMENT

After consultations with the patient and her family, an exploratory laparotomy was performed. During the surgery, approximately 200 mL of brownish-yellow ascites was found in her abdominal cavity. An intussusception of the small intestine was identified about 100 cm from the Treitz ligament, with the intussuscepted segment measuring approximately 40 cm in length and showing significant local edema. The proximal small intestine was slightly dilated, and at the site of intussusception, three small intestinal tumors were identified. They were palpable and firm in consistency, with the largest being 6 cm and the smallest 1 cm in diameter. A segment of the small intestine, approximately 50 cm in length, including the tumors and the intussuscepted portion, was resected 5 cm away from the tumors, followed by a side-to-side anastomosis using a linear cutting stapler. No significant lymph node enlargement was observed at the root of the mesentery. The resected specimen was visually examined, as shown in Figure 3.

OUTCOME AND FOLLOW-UP

On the fifth postoperative day, the patient's surgical wound showed satisfactory healing. She tolerated a semi-liquid diet without discomfort and was discharged after the normal resumption of gas and bowel movements. The postoperative pathology report indicated a malignant tumor in the small intestine, consistent with metastatic poorly differentiated adenocarcinoma from the lung (Figure 4). The tumor infiltrated up to the serosal layer, exhibited vascular invasion, and had clear resection margins. There was no evidence of nerve invasion. Immunohistochemistry results were as follows: CK7 (+), Napsin A (+), Ki67 (80%+), ALK (-), AE1/AE3 (+), TTF-1 (+), P40 (-), CK20 (-), Syn (-), Villin (-), CD34 (-), CD117 (-), Dog-1 (-), and D2-40 (+). Special staining for AB-PAS was also performed.

The patient was followed for over 14 mo after discharge. The timeline of the patient's disease diagnosis and treatment is shown in Figure 5. At the most recent successful follow-up conducted by telephone in April 2024, she was continuing her medication regimen, but her quality of life was declining. Regrettably, the patient is currently lost to follow-up, suggesting that she might have either passed away or sought treatment at another hospital.

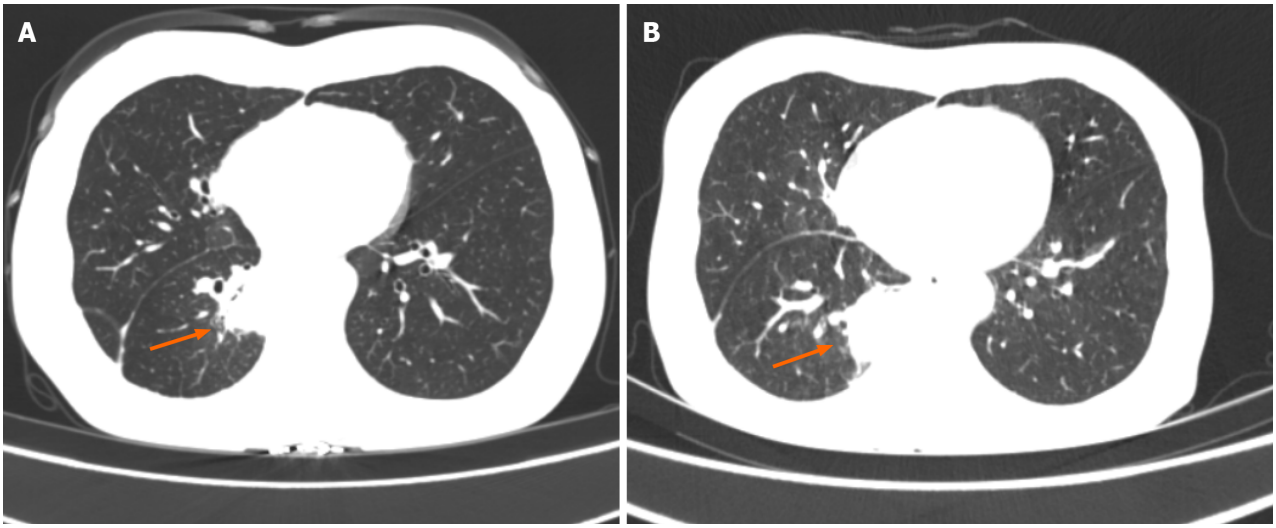

Figure 1 Lung cancer after ablation treatment. Arrows show the primary lesion. A: Primary site of lung cancer; B: Imaging manifestations after ablative therapy for lung cancer.

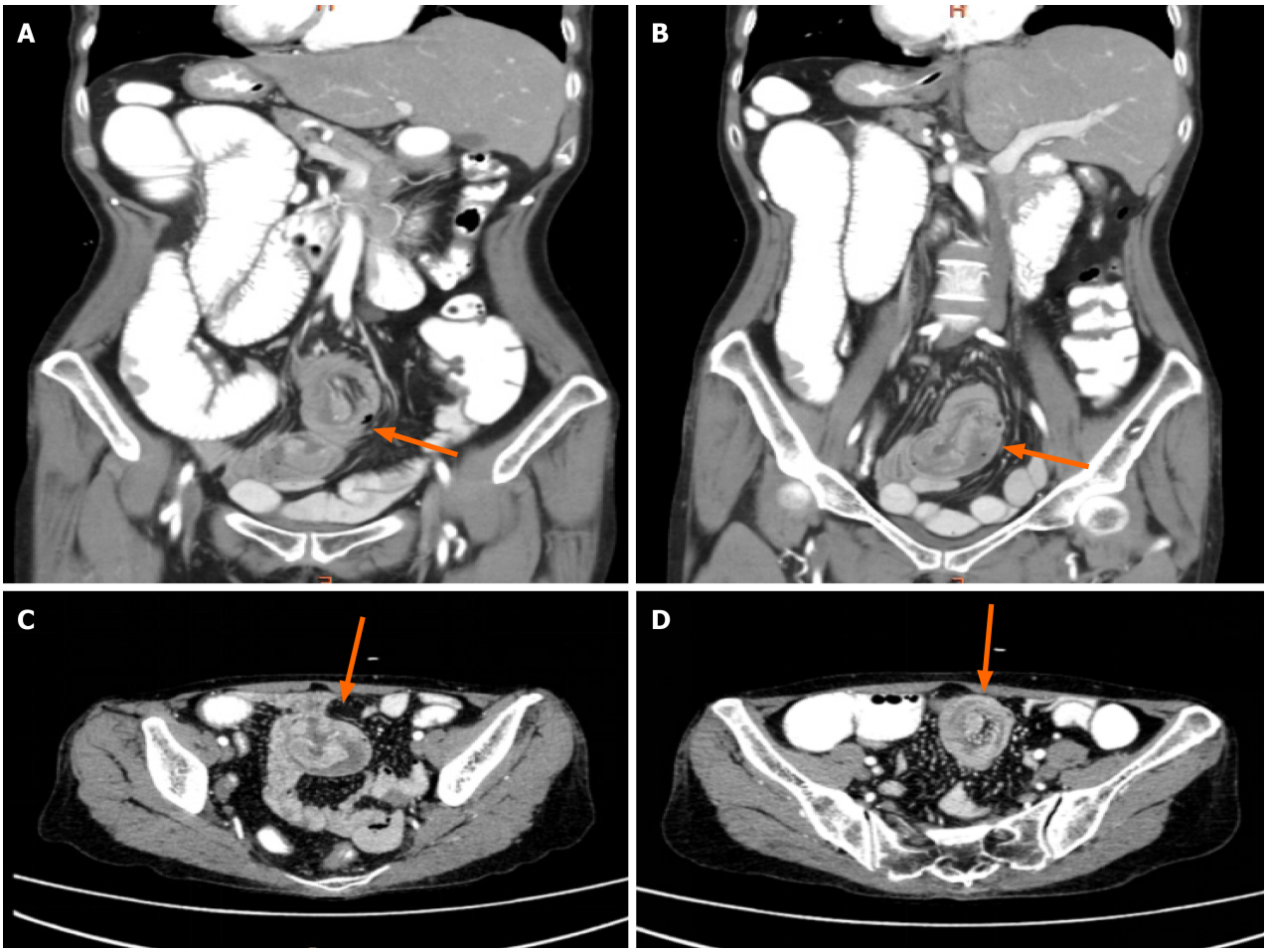

Figure 2 Location of the small bowel intussusception. Arrows show the location of the small bowel intussusception. A, C, and D: Imaging manifestations of small bowel tumors; B: Location where small bowel obstruction occurred.

DISCUSSION

This case report describes a patient who developed multiple small bowel metastases from advanced lung cancer with multiple metastases. The patient had undergone various non-radical therapies, including targeted agents and ablative therapy, and was receiving oral osimertinib. Osimertinib is a third-generation, irreversible, oral epidermal growth factor

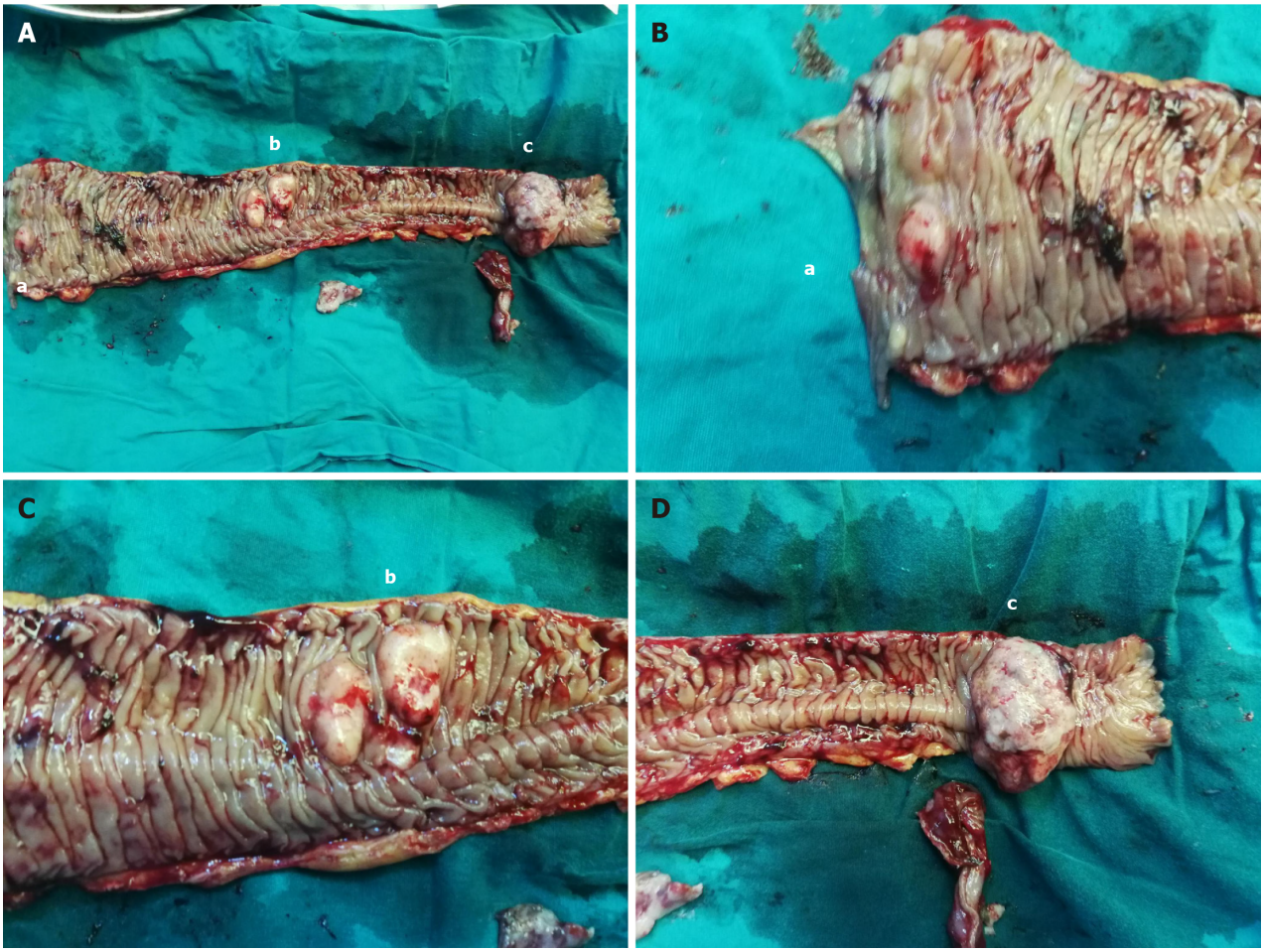

Figure 3 Small bowel tumor. A: Overall view of the resected small bowel segment that includes three tumors (a, b, and c); B: The smallest small bowel tumor is about 1 cm (a); C: The second largest small bowel tumor (b); D: The largest small bowel tumor was about 6 cm (c).

receptor (EGFR)-tyrosine kinase inhibitor that potently and selectively inhibits both EGFR-sensitizing mutations and the T790M mutation. It has shown a 71% objective response rate with a median progression-free survival of 8.5 mo[15]. After the discovery of brain metastases, the patient underwent intracranial tumor ablation. Brain metastases are the most common intracranial tumors, occurring ten times more frequently than primary brain tumors[16]. To address inoperable cases, minimally invasive techniques like magnetic resonance imaging-guided laser interstitial thermotherapy (LITT) have been explored. In this regard, LITT delivers precise heat in a controlled manner, aiming to minimize collateral damage[17-19]. The patient's lung tumor was also ablated. Microwave ablation (MWA) is an important alternative therapy to conventional surgery for the treatment of lung cancer. In addition to eliminating local tumors, MWA may promote antitumor immunological responses, such as abscopal effects in distant lesions[20], and for inoperable early-stage and metastatic lung cancer, MWA is usually performed[21]. It causes water molecules within tumor tissue to vibrate and collide in microwave electromagnetic fields, resulting in high temperatures and a coagulative necrotic zone in which local tumor cells are killed[22]. For local treatment, MWA is precise, with minimal invasiveness and few complications. In our case, the patient also required a small bowel resection for intussusception, and follow-up after surgery showed that the patient was still undergoing treatment. We report this case not only due to its clinical rarity but also to illustrate a potential treatment strategy for similar cases. Comprehensive evaluations, targeted surgical interventions, and systemic therapies tailored to individual patients - conducted through multidisciplinary team discussions - can enhance survival rates and quality of life[23,24]. The primary goal of surgery is to alleviate symptoms while minimizing the tumor burden. Early detection, accurate diagnosis, and prompt treatment are essential for improving patient outcomes.

Gastrointestinal metastasis from lung cancer is caused by haematogenous spread and usually occurs in the end stage of lung cancer. Symptoms always present with clinical complications, including gastrointestinal perforation, haemorrhage, and obstruction. Our case suggested that aggressive management of complications has the potential to improve patient survival. Xie *et al*[25] reported on two male patients in their 60s with primary poorly differentiated NSCLC with initially undetectable distant metastases. Both cases presented with abdominal pain and distension, and immunohistochemistry of small bowel biopsy samples obtained by endoscopy confirmed lung cancer metastasis. The biopsies were then subjected to second-generation sequencing, which identified mutations in the genes *TP53*, *LRP1B*, and *FGFR2*, which are associated with the onset and progression of poorly differentiated NSCLC and its small bowel metastasis. Because digestive tract metastasis of lung cancer is often insidious, studying the genetic profile of NSCLC small bowel metastasis by second-generation sequencing is crucial for early detection and prevention[25]. Recent studies have observed that estrogen

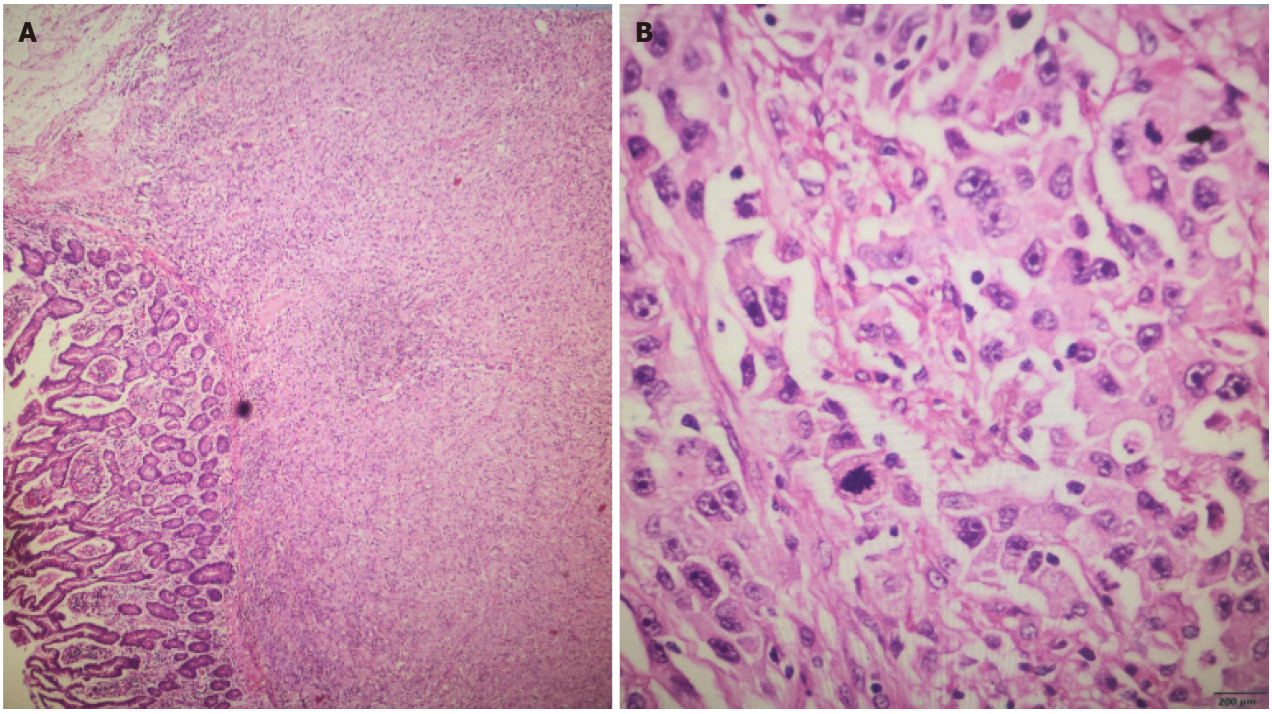

Figure 4 Hematoxylin-eosin staining of tumors of the small intestine. A: Tumor infiltration to the serosa layer; B: Lung adenocarcinoma metastasis.

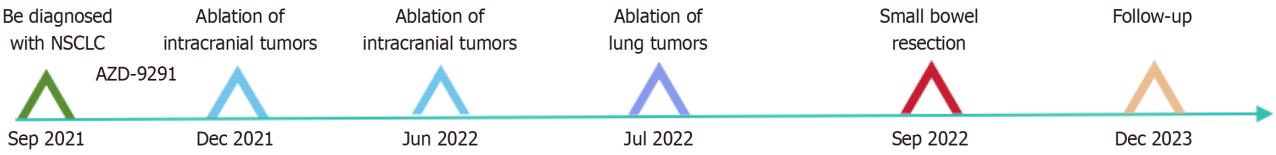

Figure 5 Timeline of diagnosis and treatment. NSCLC: Non-small cell lung cancer.

promotes (NSCLC) metastasis by facilitating the formation of invasive pseudopods in NSCLC cells *via* estrogen receptor beta[26].

Therefore, if occult metastases from advanced lung cancer can be recognized as early as possible so that early intervention can be carried out, it may improve the patient's prognosis considerably. This will also broaden new ideas on treatment strategies for other patients with advanced NSCLC.

CONCLUSION

In conclusion, patients diagnosed with stage IV NSCLC and small bowel metastases could be recommended to undergo prompt surgical intervention, provided that their condition allows, to alleviate obstruction, and may continue pharmacological therapy postoperatively. This approach outlines a potential treatment strategy for metastatic lesions, emphasizing the reduction of tumor burden through feasible surgical or ablative methods, with ongoing pharmacological management of the primary lung lesion aiming to enhance patient survival.

FOOTNOTES

Author contributions: Niu QG and Huang MH contributed to manuscript writing and editing, and data collection; Kong WQ contributed to data analysis; Niu QG and Yu Y contributed to conceptualization and supervision; all authors have read and approved the final manuscript.

Informed consent statement: Informed written consent was obtained from the patient for the publication of this case report.

Conflict-of-interest statement: The authors declare that the research was conducted in the absence of any commercial or financial relationships that could be construed as a potential conflict of interest.

CARE Checklist (2016) statement: The authors have read the CARE Checklist (2016), and the manuscript was prepared and revised

according to the CARE Checklist (2016).

Country of origin: China

ORCID number: Qi-Guang Niu 0009-0009-2733-9024.

S-Editor: Liu H
L-Editor: Wang TQ
P-Editor: Zhao YQ

REFERENCES

1 **Tamura T**, Kurishima K, Nakazawa K, Kagohashi K, Ishikawa H, Satoh H, Hizawa N. Specific organ metastases and survival in metastatic non-small-cell lung cancer. *Mol Clin Oncol* 2015; **3**: 217-221 [PMID: 25469298 DOI: 10.3892/mco.2014.410]
2 **Zhou Q**, Zu L, Li L, Chen X, Chen X, Li Y, Liu H, Sun Z. [Screening and establishment of human lung cancer cell lines with organ-specific metastasis potential]. *Zhongguo Fei Ai Za Zhi* 2014; **17**: 175-182 [PMID: 24667252 DOI: 10.3779/j.issn.1009-3419.2014.03.20]
3 **D'Antonio C**, Passaro A, Gori B, Del Signore E, Migliorino MR, Ricciardi S, Fulvi A, de Marinis F. Bone and brain metastasis in lung cancer: recent advances in therapeutic strategies. *Ther Adv Med Oncol* 2014; **6**: 101-114 [PMID: 24790650 DOI: 10.1177/1758834014521110]
4 **Dodson C**, Richards TJ, Smith DA, Ramaiya NH. Tyrosine Kinase Inhibitor Therapy for Brain Metastases in Non-Small-Cell Lung Cancer: A Primer for Radiologists. *AJNR Am J Neuroradiol* 2020; **41**: 738-750 [PMID: 32217548 DOI: 10.3174/ajnr.A6477]
5 **Lin L**, Wang X, Tang C, Liang J. Clinical Characteristics and Prognosis of Gastrointestinal Metastases in Solid Tumor Patients: A Retrospective Study and Review of Literatures. *Anal Cell Pathol (Amst)* 2019; **2019**: 4508756 [PMID: 31929965 DOI: 10.1155/2019/4508756]
6 **Niu FY**, Zhou Q, Yang JJ, Zhong WZ, Chen ZH, Deng W, He YY, Chen HJ, Zeng Z, Ke EE, Zhao N, Zhang N, Sun HW, Zhang QY, Xie Z, Zhang XC, Wu YL. Distribution and prognosis of uncommon metastases from non-small cell lung cancer. *BMC Cancer* 2016; **16**: 149 [PMID: 26911831 DOI: 10.1186/s12885-016-2169-5]
7 **Gunev V**. [Prenatal diagnosis of hereditary diseases]. *Akush Ginekol (Sofiia)* 1975; **14**: 322-329 [PMID: 130083 DOI: 10.1016/j.lungcan.2014.07.020]
8 **Song Z**, Lin B, Shao L, Zhang Y. Cutaneous metastasis as a initial presentation in advanced non-small cell lung cancer and its poor survival prognosis. *J Cancer Res Clin Oncol* 2012; **138**: 1613-1617 [PMID: 22581263 DOI: 10.1007/s00432-012-1239-6]
9 **Li Y**, Wong M, Zhan L, Corke L, Brown MC, Cheng S, Khan K, Balatnaram K, Chowdhury M, Sabouhanian A, Herman J, Walia P, Strom E, Patel D, García-Pardo M, Schmid S, Eng L, Sacher AG, Leighl N, Bradbury PA, Shepherd FA, Shultz D, Liu G. Single organ metastatic sites in non-small cell lung cancer: Patient characteristics, treatment patterns and outcomes from a large retrospective Canadian cohort. *Lung Cancer* 2024; **192**: 107823 [PMID: 38763103 DOI: 10.1016/j.lungcan.2024.107823]
10 **Smith S**, Kao S, Boyer M, Franco M, Moore M. Treatment selection and real-world analysis of immunotherapy with or without chemotherapy in PD-L1-high metastatic non-small cell lung cancer. *Intern Med J* 2024 [PMID: 38622825 DOI: 10.1111/imj.16389]
11 **Siegel RL**, Miller KD, Jemal A. Cancer statistics, 2020. *CA Cancer J Clin* 2020; **70**: 7-30 [PMID: 31912902 DOI: 10.3322/caac.21590]
12 **Hu Y**, Feit N, Huang Y, Xu W, Zheng S, Li X. Gastrointestinal metastasis of primary lung cancer: An analysis of 366 cases. *Oncol Lett* 2018; **15**: 9766-9776 [PMID: 29928351 DOI: 10.3892/ol.2018.8575]
13 **Wang M**, Chen G, Luo J, Fan Z, Liu Y, Xie C, Gong Y. Case Report: Genetic profiling of small intestine metastasis from poorly differentiated non-small cell lung cancer: report of 2 cases and literature review of the past 5 years. *Front Oncol* 2023; **13**: 1265749 [PMID: 38074661 DOI: 10.3389/fonc.2023.1265749]
14 **Yoshimoto A**, Kasahara K, Kawashima A. Gastrointestinal metastases from primary lung cancer. *Eur J Cancer* 2006; **42**: 3157-3160 [PMID: 17079136 DOI: 10.1016/j.ejca.2006.08.030]
15 **Soria JC**, Ohe Y, Vansteenkiste J, Reungwetwattana T, Chewaskulyong B, Lee KH, Dechaphunkul A, Imamura F, Nogami N, Kurata T, Okamoto I, Zhou C, Cho BC, Cheng Y, Cho EK, Voon PJ, Planchard D, Su WC, Gray JE, Lee SM, Hodge R, Marotti M, Rukazenkov Y, Ramalingam SS; FLAURA Investigators. Osimertinib in Untreated EGFR-Mutated Advanced Non-Small-Cell Lung Cancer. *N Engl J Med* 2018; **378**: 113-125 [PMID: 29151359 DOI: 10.1056/NEJMoa1713137]
16 **Siegel RL**, Miller KD, Wagle NS, Jemal A. Cancer statistics, 2023. *CA Cancer J Clin* 2023; **73**: 17-48 [PMID: 36633525 DOI: 10.3322/caac.21763]
17 **Jethwa PR**, Barrese JC, Gowda A, Shetty A, Danish SF. Magnetic resonance thermometry-guided laser-induced thermal therapy for intracranial neoplasms: initial experience. *Neurosurgery* 2012; **71**: 133-44; 144 [PMID: 22653396 DOI: 10.1227/NEU.0b013e31826101d4]
18 **Salem U**, Kumar VA, Madewell JE, Schomer DF, de Almeida Bastos DC, Zinn PO, Weinberg JS, Rao G, Prabhu SS, Colen RR. Neurosurgical applications of MRI guided laser interstitial thermal therapy (LITT). *Cancer Imaging* 2019; **19**: 65 [PMID: 31615562 DOI: 10.1186/s40644-019-0250-4]
19 **Shah AH**, Semonche A, Eichberg DG, Borowy V, Luther E, Sarkiss CA, Morell A, Mahavadi AK, Ivan ME, Komotar RJ. The Role of Laser Interstitial Thermal Therapy in Surgical Neuro-Oncology: Series of 100 Consecutive Patients. *Neurosurgery* 2020; **87**: 266-275 [PMID: 31742351 DOI: 10.1093/neuros/nyz424]
20 **Liu Y**, Dong Y, Kong L, Shi F, Zhu H, Yu J. Abscopal effect of radiotherapy combined with immune checkpoint inhibitors. *J Hematol Oncol* 2018; **11**: 104 [PMID: 30115069 DOI: 10.1186/s13045-018-0647-8]
21 **Ma F**, Lin Y, Ni Z, Wang S, Zhang M, Wang X, Zhang Z, Luo X, Miao X. Microwave ablation enhances the systemic immune response in

patients with lung cancer. *Oncol Lett* 2024; **27**: 106 [PMID: 38298427 DOI: 10.3892/ol.2024.14239]

22 **Ni Y**, Xu H, Ye X. Image-guided percutaneous microwave ablation of early-stage non-small cell lung cancer. *Asia Pac J Clin Oncol* 2020; **16**: 320-325 [PMID: 32969192 DOI: 10.1111/ajco.13419]

23 **Guo Z**, Han B, Wang Y. [The status of diagnosis and therapy for gastrointestinal metastasis from primary lung cancer]. *Zhongguo Fei Ai Za Zhi* 2011; **14**: 69-71 [PMID: 21219836 DOI: 10.3779/j.issn.1009-3419.2011.01.14]

24 **Kini S**, Kapadia RM, Amarapurkar A. Intussusception due to intestinal metastasis from lung cancer. *Indian J Pathol Microbiol* 2010; **53**: 141-143 [PMID: 20090247 DOI: 10.4103/0377-4929.59208]

25 **Xie S**, Wu Z, Qi Y, Wu B, Zhu X. The metastasizing mechanisms of lung cancer: Recent advances and therapeutic challenges. *Biomed Pharmacother* 2021; **138**: 111450 [PMID: 33690088 DOI: 10.1016/j.biopha.2021.111450]

26 **Wang Y**, Qiu W, Chen J, Meng W, Zhao R, Lin W, Mei P, Diao M, Xiao H, Liao Y. ERβ promoted invadopodia formation-mediated non-small cell lung cancer metastasis *via* the ICAM1/p-Src/p-Cortactin signaling pathway. *Int J Cancer* 2023; **153**: 1287-1299 [PMID: 37212571 DOI: 10.1002/ijc.34563]

World Journal of Clinical Cases

Submit a Manuscript: https://www.f6publishing.com

World J Clin Cases 2024 September 16; 12(26): 5968-5973

DOI: 10.12998/wjcc.v12.i26.5968

ISSN 2307-8960 (online)

CASE REPORT

Uterine artery pseudoaneurysm caused by hysteroscopic surgery: A case report

Kaoru Kakinuma, Toshiyuki Kakinuma, Kyouhei Ueyama, Rora Okamoto, Kaoru Yanagida, Nobuhiro Takeshima, Michitaka Ohwada

Specialty type: Medicine, research and experimental

Provenance and peer review: Unsolicited article; Externally peer reviewed.

Peer-review model: Single blind

Peer-review report's classification

Scientific Quality: Grade C

Novelty: Grade B

Creativity or Innovation: Grade C

Scientific Significance: Grade C

P-Reviewer: Tsibouris P

Received: March 26, 2024

Revised: June 19, 2024

Accepted: July 5, 2024

Published online: September 16, 2024

Processing time: 118 Days and 17.8 Hours

Kaoru Kakinuma, Toshiyuki Kakinuma, Kyouhei Ueyama, Rora Okamoto, Kaoru Yanagida, Nobuhiro Takeshima, Michitaka Ohwada, Department of Obstetrics and Gynecology, International University of Health and Welfare Hospital, 537-3 Iguchi, Nasushiobara, Tochigi 329-2763, Japan

Corresponding author: Toshiyuki Kakinuma, MD, PhD, Doctor, Professor, Department of Obstetrics and Gynecology, International University of Health and Welfare Hospital, 537-3 Iguchi, Nasushiobara, Tochigi 329-2763, Japan. tokakinuma@gmail.com

Abstract

BACKGROUND

We report a case of uterine artery pseudoaneurysm (UAP) occurrence during hysteroscopic endometrial polypectomy and its treatment *via* uterine artery embolization (UAE).

CASE SUMMARY

A 48-year-old primigravid, primiparous patient was incidentally found to have an endometrial polyp during a health checkup, and underwent a hysteroscopic polypectomy at another hospital. Her cervix was dilated with a Laminken-R® device. After the Laminken-R® was withdrawn, a large amount of genital bleeding was observed. This bleeding persisted after the hysteroscopic polypectomy, and, as hemostasis became impossible, the patient was transferred to our hospital by ambulance. On arrival, transvaginal ultrasonography revealed a 3-cm hypoechoic mass with a swirling internal pulse on the right side of the uterus, and color Doppler ultrasonography showed feeder vessels penetrating the mass. Pelvic contrast-enhanced computed tomography (CT) confirmed the presence of a mass at this site, and vascular proliferation was observed within the uterine cavity. Consequently, UAP was diagnosed, and UAE was performed. The patient's postoperative course was uneventful, and 6 mo post-UAE, no recurrence of blood flow to the UAP was observed.

CONCLUSION

When abnormal genital bleeding occurs during hysteroscopic surgery, ultrasonography and contrast-enhanced CT can assist in the detection of early UAPs.

Key Words: Cervical dilation; Hysteroscopic surgery; Uterine artery pseudoaneurysm; Uterine artery embolization; Case report

Core Tip: When abnormal uterine bleeding occurs after hysteroscopic surgery, the possibility of uterine artery pseudoaneurysm (UAP) must be considered. Confirmed UAP must be managed promptly and appropriately.

Citation: Kakinuma K, Kakinuma T, Ueyama K, Okamoto R, Yanagida K, Takeshima N, Ohwada M. Uterine artery pseudoaneurysm caused by hysteroscopic surgery: A case report. *World J Clin Cases* 2024; 12(26): 5968-5973
URL: https://www.wjgnet.com/2307-8960/full/v12/i26/5968.htm
DOI: https://dx.doi.org/10.12998/wjcc.v12.i26.5968

INTRODUCTION

Uterine artery pseudoaneurysm (UAP) is an acquired condition in which the wall of the uterine artery collapses, and the arterial wall layers engulf the blood that has leaked from the vessel[1]. UAPs generally occur after delivery or miscarriage and often cause massive hemorrhage, but cases of its occurrence unrelated to pregnancy, such as during myomectomies, have also been reported. Although UAP is rare, it is a potentially life-threatening condition that can cause massive hemorrhage when it ruptures[2]. We report our experience of uterine artery embolization (UAE) to treat a patient who developed a UAP during hysteroscopic surgery.

CASE PRESENTATION

Chief complaints

A 48-year-old primigravid, primiparous patient (vaginal delivery) was transferred to our clinic for persistent genital bleeding after hysteroscopic polypectomy.

History of present illness

An endometrial polyp was incidentally identified during a health checkup, and a hysteroscopic polypectomy was conducted at another hospital. The cervix was dilated with a 5-mm Laminken-R® device (Ken Medical Company Ltd., Hyogo, Japan). After the Laminken-R® was withdrawn, a large amount of genital bleeding was observed, but transcervical resection was nevertheless performed. A rigid OLYMPUS hystero-resectoscope (OES Pro Resectoscope, Olympus Medical Systems Corporation, Japan) was used with 3% D-sorbitol (UromaticS®, Baxter Ltd., United States) as the perfusion solution. Although the procedure only took 15 min, the genital bleeding persisted even after the hysteroscopic polypectomy. As hemostasis proved impossible, the patient was brought to our hospital by ambulance for further investigation and treatment.

History of past illness

Nothing of note.

Personal and family history

Nothing of note.

Physical examination

On examination upon arrival, her vital signs were as follows: Blood pressure, 108/72 mmHg; heart rate, 72 beats/min; and body temperature, 36.8 ºC.

Laboratory examinations

Colposcopy revealed persistent bleeding from the external uterine orifice. Blood test results revealed anemia, with a hemoglobin level of 8.3 g/dL, but all other test results were unremarkable.

Imaging examinations

Transvaginal ultrasonography: A 3-cm hypoechoic mass with a swirling internal pulse was apparent in the right wall of the uterus (Figure 1A), and color Doppler revealed abundant turbulent blood flow into the mass (Figure 1B).

FINAL DIAGNOSIS

Pelvic contrast-enhanced computed tomography (CT) showed the presence of a contrast-enhanced mass at the site

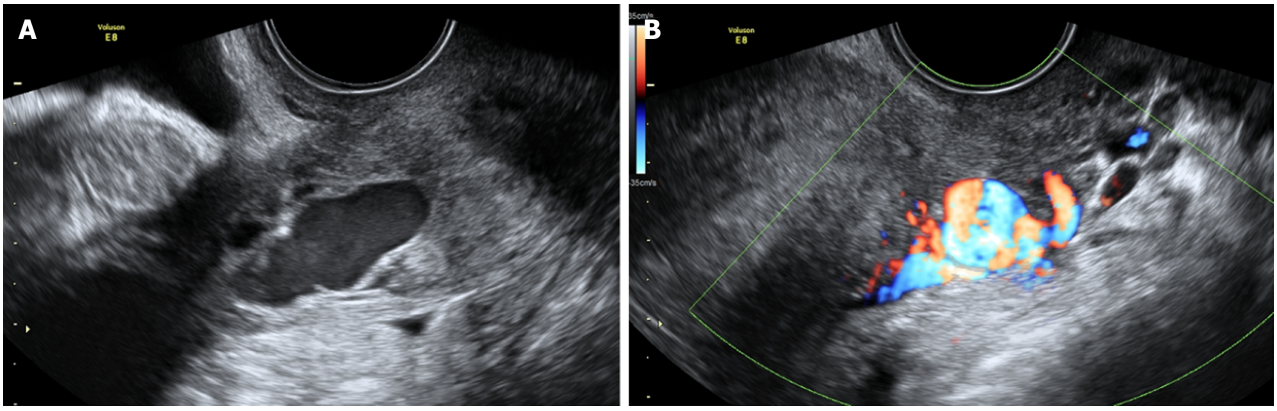

Figure 1 Transvaginal ultrasonography. A: A 3-cm echo-free space is evident in the right wall of the uterus; B: Color Doppler reveals abundant blood flow at the same site.

identified on ultrasonography (Figure 2A). Three-dimensional image reconstruction showed that the aneurysm was continuous with the right uterine artery. A UAP in the right uterine artery trunk was diagnosed (Figure 2B).

TREATMENT

Because of the risk of bleeding, UAE was chosen as the treatment method. Angiography showed the formation of a 3-cm UAP in the descending branch of the right uterine artery (Figure 3A). There was no sign of extravasation. Since the blood flow to the UAP was observed, and this patient did not want to have a baby and wanted to ensure hemostasis, the feeder artery was subjected to coil embolization (Figure 3B). The patient's post-treatment course was uneventful, and, after color Doppler ultrasonography confirmed that there was no recurrence of blood flow to the uterine pseudoaneurysm, she was discharged on postoperative day 4.

OUTCOME AND FOLLOW-UP

Presently, 6 mo post-UAE, her course has been uneventful, with no recurrence of blood flow to the UAP.

DISCUSSION

UAP is a condition in which the wall of a uterine blood vessel collapses due to some invasive event, and the resulting leaked blood is engulfed by soft tissue, forming a cavity that is in communication with the vessel. The walls of the cavity are fragile and break down easily, frequently causing massive hemorrhage[1]. UAPs frequently develop during the puerperal period or after a miscarriage and reportedly occur in 0.2–0.3% of all pregnancies[2,3]. The most reported cause unrelated to pregnancy is myomectomy[4]. In rare cases, it is caused by adeno myomectomy, cervical conization, abdominal total hysterectomy, transvaginal simple total hysterectomy, and robot-assisted total hysterectomy[5-9].

Ultrasonography is regarded as a helpful modality in diagnosing UAPs[10]. On transvaginal ultrasonography, a UAP can be visualized as an area of low brightness, and on color Doppler ultrasonography, pulsatile spiral blood flow, known as "swirling blood flow" is evident at the same site. Dynamic CT is another useful imaging modality[11] that enables the visualization of not only UAP as an area of early enhancement continuous with a blood vessel, but also of the responsible vessel, thus enabling timely diagnosis. Whether or not the UAP has ruptured can easily be determined from the presence or absence of extravasation, making this an essential modality to decide on the management and treatment strategy for UAPs.

The treatment method used in this case, UAE, is used in almost all cases of genital bleeding, and it is reportedly effective[12-14]. Regarding the incidence of complications of UAE, those associated with vascular contrast procedures account for approximately 6%–9% of total complications. The most common complication is post-UAE fever, and other symptoms, including pain, endometritis, intrauterine adhesions, uterine necrosis, pelvic infections, and reduced ovarian function, may also occur[15-18]. Although post-UAE fertility is believed to be comparatively good, some studies have reported significant increases in the rates of miscarriage, postpartum hemorrhage, premature birth, and abnormal fetal presentation following UAE, as well as cases of intrauterine fetal growth restriction. Thus, women who become pregnant after UAE require careful perinatal management[1,19].

In cases where the UAP is asymptomatic, there is no consensus on whether UAE should be conducted prophylactically or whether the watch-and-wait strategy should be adopted. Although some asymptomatic UAPs resolve spontaneously, others rupture and cause massive bleeding; currently, it is difficult to predict whether a UAP will rupture. The treatment

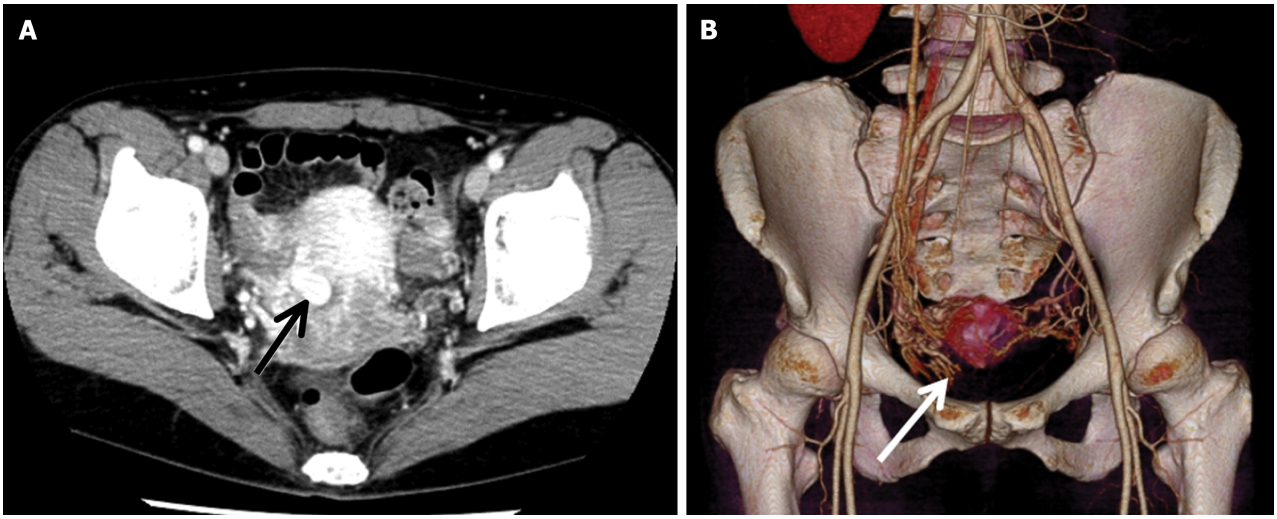

Figure 2 Pelvic contrast-enhanced computed tomography. A: A contrast-enhanced mass (arrow) is evident in the arterial phase; a uterine artery pseudoaneurysm was diagnosed (dynamic imaging); B: Three-dimensional image reconstruction shows the uterine artery and the uterine artery pseudoaneurysm (arrow) continuous with it.

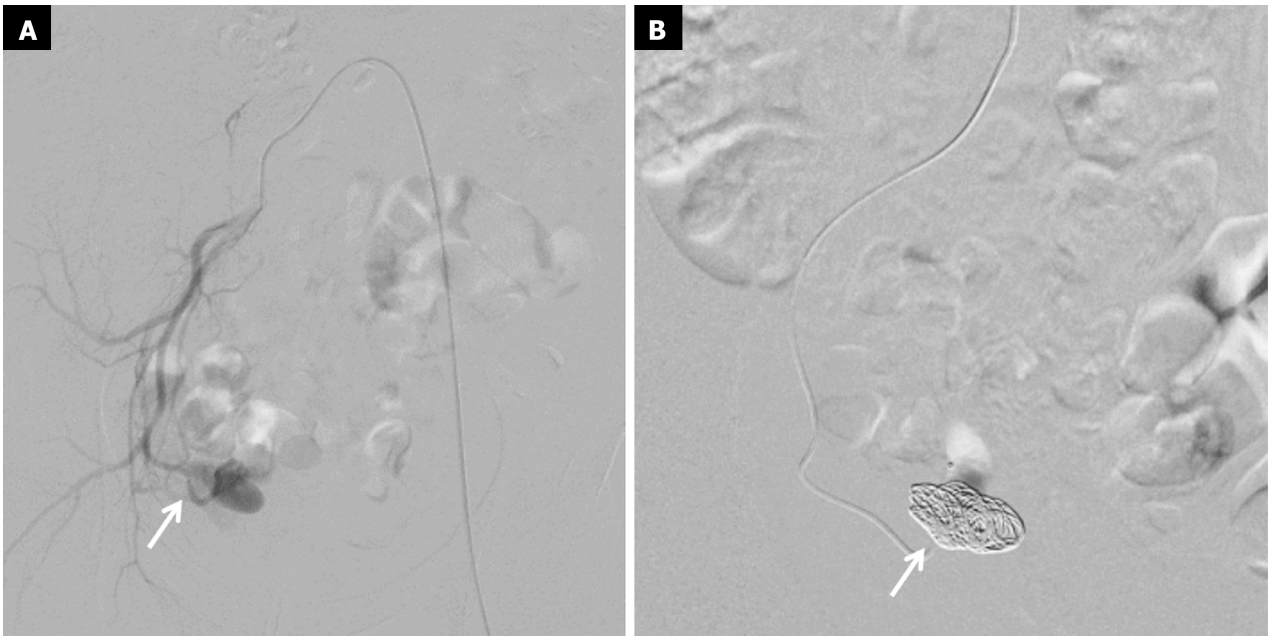

Figure 3 Pelvic angiography. A: Selective contrast in the right uterine artery allows visualization of the contrast-enhanced uterine artery pseudoaneurysm (arrow); B: As blood flow from the right uterine artery to the uterine artery pseudoaneurysm was evident, coil embolization (arrow) was conducted.

strategy for an unruptured UAP merits further investigation. At this stage, indications for treatment must be determined according to individual patient factors, such as changes in the size of the UAP and treatment resources available at specific institutions, including the feasibility of emergency UAE when bleeding occurs.

In the present case, a UAP that had not been evident on preoperative imaging was observed after hysteroscopic surgery, suggesting that the surgery may have induced the UAP. Cervical dilation is not always necessary for small-diameter hysteroscopic surgery. However, in our patient, the procedure was conducted with a conventional rigid hysteroscope, and the cervix was therefore dilated preoperatively with a 5-mm Laminken-R® before performing the hysteroscopic polypectomy. The profuse genital bleeding observed after the Laminken-R® was withdrawn suggests that the UAP was caused either by direct injury from the Laminken-R® or due to over-dilation. The perfusion solution used during hysteroscopic surgery increases the intrauterine pressure, and this could also have led to the collapse of the vascular wall. Laminken-R® insertion involves blunt manipulation and must be conducted with caution since it is an invasive device. When inserting the Laminken-R®, the direction of the uterine cavity should be checked, and a uterine probe must be used to measure its length. Furthermore, the Laminken-R® comes in a range of sizes, and observing the cervix before dilation is important for choosing the correct size. In addition, the appropriate flow rate for the perfusion solution used during hysteroscopy may vary between individuals, depending on factors such as the volume of the uterine cavity and the

flexibility of the myometrium, and attention must also be paid to this flow rate to avoid an excessive increase in intrauterine pressure.

CONCLUSION

In the event of abnormal uterine bleeding after hysteroscopic surgery, the possibility of a UAP must be considered; transvaginal ultrasonography and tomography using color Doppler ultrasonography and dynamic CT must be conducted to ensure prompt and appropriate management.

FOOTNOTES

Author contributions: Kakinuma K and Kakinuma T contributed to conceptualization, methodology, software, validation, original draft preparation, manuscript review and editing, visualization, supervision, and project administration; Ueyama K, Okamoto R, Yanagida K, Takeshima N, Ohwada M contributed to the formal analysis, investigation, resources, and data curation; All authors have read and agreed to the published version of the manuscript.

Informed consent statement: Informed written consent was obtained from the patient for publication of this report and any accompanying images.

Conflict-of-interest statement: The authors declare that they have no conflict of interest to disclose.

CARE Checklist (2016) statement: The authors have read the CARE Checklist (2016), and the manuscript was prepared and revised according to the CARE Checklist (2016).

Country of origin: Japan

ORCID number: Kaoru Kakinuma 0000-0003-4647-9582; Toshiyuki Kakinuma 0000-0001-7853-4860; Kyouhei Ueyama 0009-0001-8212-9945; Rora Okamoto 0009-0006-7846-3402; Kaoru Yanagida 0000-0002-5348-3603; Nobuhiro Takeshima 0000-0001-9500-9427; Michitaka Ohwada 0000-0002-0396-6228.

S-Editor: Liu H
L-Editor: Filipodia
P-Editor: Cai YX

REFERENCES

1 **Goldberg J**, Pereira L, Berghella V. Pregnancy after uterine artery embolization. *Obstet Gynecol* 2002; **100**: 869-872 [PMID: 12423843 DOI: 10.1016/s0029-7844(02)02347-5]
2 **Matsubara S**, Kuwata T, Usui R, Ohkuchi A. Uterine artery pseudoaneurysm: a master of deception. *Arch Gynecol Obstet* 2014; **289**: 469-470 [PMID: 23934243 DOI: 10.1007/s00404-013-2992-8]
3 **Baba Y**, Matsubara S, Kuwata T, Ohkuchi A, Usui R, Saruyama M, Nakata M, Suzuki M. Uterine artery pseudoaneurysm: not a rare condition occurring after non-traumatic delivery or non-traumatic abortion. *Arch Gynecol Obstet* 2014; **290**: 435-440 [PMID: 24691826 DOI: 10.1007/s00404-014-3226-4]
4 **Takeda A**, Kato K, Mori M, Sakai K, Mitsui T, Nakamura H. Late massive uterine hemorrhage caused by ruptured uterine artery pseudoaneurysm after laparoscopic-assisted myomectomy. *J Minim Invasive Gynecol* 2008; **15**: 212-216 [PMID: 18312994 DOI: 10.1016/j.jmig.2007.09.006]
5 **Matsubara S**, Usui R, Sato T, Kuwata T, Ohkuchi A, Nakata M. Adenomyomectomy, curettage, and then uterine artery pseudoaneurysm occupying the entire uterine cavity. *J Obstet Gynaecol Res* 2013; **39**: 1103-1106 [PMID: 23551573 DOI: 10.1111/jog.12021]
6 **Moon G**, Jeon S, Nam KH, Choi S, Sunwoo J, Ryu A. Pseudoaneurysm of uterine artery causing intra-abdominal and vaginal bleeding after cervical conization. *Obstet Gynecol Sci* 2015; **58**: 256-259 [PMID: 26023677 DOI: 10.5468/ogs.2015.58.3.256]
7 **Lee WK**, Roche CJ, Duddalwar VA, Buckley AR, Morris DC. Pseudoaneurysm of the uterine artery after abdominal hysterectomy: radiologic diagnosis and management. *Am J Obstet Gynecol* 2001; **185**: 1269-1272 [PMID: 11717672 DOI: 10.1067/mob.2001.117974]
8 **Langer JE**, Cope C. Ultrasonographic diagnosis of uterine artery pseudoaneurysm after hysterectomy. *J Ultrasound Med* 1999; **18**: 711-714 [PMID: 10511305 DOI: 10.7863/jum.1999.18.10.711]
9 **Gerardi MA**, Díaz-Montes TP. Late onset hemorrhage caused by ruptured uterine artery pseudoaneurysm after robotic-assisted total hysterectomy. *J Robot Surg* 2011; **5**: 295-298 [PMID: 27628121 DOI: 10.1007/s11701-011-0265-8]
10 **Matsubara S**. Pseudoaneurysm: a chameleon in obstetrical emergency practice. *Arch Gynecol Obstet* 2011; **283**: 669-670 [PMID: 20549507 DOI: 10.1007/s00404-010-1551-9]

11 **Isono W**, Tsutsumi R, Wada-Hiraike O, Fujimoto A, Osuga Y, Yano T, Taketani Y. Uterine artery pseudoaneurysm after cesarean section: case report and literature review. *J Minim Invasive Gynecol* 2010; **17**: 687-691 [PMID: 20656567 DOI: 10.1016/j.jmig.2010.06.004]

12 **Wan AY**, Shin JH, Yoon HK, Ko GY, Park S, Seong NJ, Yoon CJ. Post-operative hemorrhage after myomectomy: safety and efficacy of transcatheter uterine artery embolization. *Korean J Radiol* 2014; **15**: 356-363 [PMID: 24843240 DOI: 10.3348/kjr.2014.15.3.356]

13 **Takeda A**, Koike W, Imoto S, Nakamura H. Conservative management of uterine artery pseudoaneurysm after laparoscopic-assisted myomectomy and subsequent pregnancy outcome: case series and review of the literature. *Eur J Obstet Gynecol Reprod Biol* 2014; **182**: 146-153 [PMID: 25277771 DOI: 10.1016/j.ejogrb.2014.09.020]

14 **Ito N**, Natimatsu Y, Tsukada J, Sato A, Hasegawa I, Lin BL. Two cases of postmyomectomy pseudoaneurysm treated by transarterial embolization. *Cardiovasc Intervent Radiol* 2013; **36**: 1681-1685 [PMID: 23354964 DOI: 10.1007/s00270-013-0551-0]

15 **Badawy SZ**, Etman A, Singh M, Murphy K, Mayelli T, Philadelphia M. Uterine artery embolization: the role in obstetrics and gynecology. *Clin Imaging* 2001; **25**: 288-295 [PMID: 11566093 DOI: 10.1016/s0899-7071(01)00307-2]

16 **Vegas G**, Illescas T, Muñoz M, Pérez-Piñar A. Selective pelvic arterial embolization in the management of obstetric hemorrhage. *Eur J Obstet Gynecol Reprod Biol* 2006; **127**: 68-72 [PMID: 16229935 DOI: 10.1016/j.ejogrb.2005.09.008]

17 **Hong TM**, Tseng HS, Lee RC, Wang JH, Chang CY. Uterine artery embolization: an effective treatment for intractable obstetric haemorrhage. *Clin Radiol* 2004; **59**: 96-101 [PMID: 14697382 DOI: 10.1016/j.crad.2003.08.007]

18 **Kirby JM**, Kachura JR, Rajan DK, Sniderman KW, Simons ME, Windrim RC, Kingdom JC. Arterial embolization for primary postpartum hemorrhage. *J Vasc Interv Radiol* 2009; **20**: 1036-1045 [PMID: 19647182 DOI: 10.1016/j.jvir.2009.04.070]

19 **Inoue S**, Masuyama H, Hiramatsu Y; Multi-Institutional Study Group of Transarterial Embolization for Massive Obstetric Haemorrhage in Chugoku & Shikoku Area Society of Obstetrics and Gynecology. Efficacy of transarterial embolisation in the management of post-partum haemorrhage and its impact on subsequent pregnancies. *Aust N Z J Obstet Gynaecol* 2014; **54**: 541-545 [PMID: 25350565 DOI: 10.1111/ajo.12228]

World Journal of Clinical Cases

Submit a Manuscript: https://www.f6publishing.com

World J Clin Cases 2024 September 16; 12(26): 5974-5982

DOI: 10.12998/wjcc.v12.i26.5974

ISSN 2307-8960 (online)

CASE REPORT

Organizing pneumonia secondary to pulmonary tuberculosis: A case report

Min Liu, Xi-Yang Dong, Zhi-Xiang Ding, Qing-Hai Wang, De-Hui Li

Specialty type: Medicine, research and experimental

Provenance and peer review: Unsolicited article; Externally peer reviewed.

Peer-review model: Single blind

Peer-review report's classification

Scientific Quality: Grade B

Novelty: Grade B

Creativity or Innovation: Grade B

Scientific Significance: Grade B

P-Reviewer: Agarwal A

Received: March 27, 2024

Revised: June 7, 2024

Accepted: July 10, 2024

Published online: September 16, 2024

Processing time: 117 Days and 17.1 Hours

Min Liu, Xi-Yang Dong, Zhi-Xiang Ding, Qing-Hai Wang, De-Hui Li, Department of Infectious Diseases, Changde Hospital, Xiangya School of Medicine, Central South University (The First People's Hospital of Changde City), Changde 415000, Hunan Province, China

Corresponding author: De-Hui Li, BM, Chief Doctor, Department of Infectious Diseases, Changde Hospital, Xiangya School of Medicine, Central South University (The First People's Hospital of Changde City), No. 818 Renmin Road, Wuling District, Changde 41500, Hunan Province, China. cdyygrk@163.com

Abstract

BACKGROUND

Organizing pneumonia secondary to pulmonary tuberculosis is rare. Moreover, the temporal boundary between pulmonary tuberculosis and secondary organizing pneumonia has not been defined. We report a case of secondary organizing pneumonia associated with pulmonary tuberculosis occurring after nine months of antituberculosis treatment.

CASE SUMMARY

A 54 years old man, previously diagnosed with pulmonary tuberculosis and tuberculous pleurisy, underwent nine months of antituberculosis treatment. Follow-up lung computed tomography revealed multiple new subpleural ground-glass opacities in both lungs, and a lung biopsy confirmed organizing pneumonia. Treatment continued with anti-tuberculosis agents and hormone therapy, and subsequent dynamic pulmonary computed tomography exams demonstrated improvement in lesion absorption. No disease recurrence was observed after corticosteroid therapy discontinuation.

CONCLUSION

When treating patients with active pulmonary tuberculosis, if an increase in lesions is observed during anti-tuberculosis treatment, it is necessary to consider the possibility of tuberculosis-related secondary organizing pneumonia, timely lung biopsy is essential for early intervention.

Key Words: Pulmonary tuberculosis; Antituberculosis treatment; Lung biopsy; Organizing pneumonia; Corticoids; Case report

Core Tip: We report a case of secondary organizing pneumonia associated with pulmonary tuberculosis occurring after nine months of antituberculosis treatment. So when treating patients with active pulmonary tuberculosis, if an increase in lesions is observed during antituberculosis treatment, it is necessary to consider the possibility of tuberculosis-related secondary organizing pneumonia, and timely lung biopsy is essential for early intervention.

Citation: Liu M, Dong XY, Ding ZX, Wang QH, Li DH. Organizing pneumonia secondary to pulmonary tuberculosis: A case report. *World J Clin Cases* 2024; 12(26): 5974-5982
URL: https://www.wjgnet.com/2307-8960/full/v12/i26/5974.htm
DOI: https://dx.doi.org/10.12998/wjcc.v12.i26.5974

INTRODUCTION

Organizing pneumonia (OP) is a form of lung tissue repair following injury, characterized pathologically by the infiltration of inflammatory fragments into the alveoli, spreading to the alveolar ducts and terminal bronchioles, accompanied by the typical intraluminal granulation tissue, forming Masson bodies[1]. OP is categorized into secondary OP (SOP) and cryptogenic OP (COP). COP is a form of idiopathic interstitial pneumonia that results from the pulmonary reactions to various unidentified injuries[2]. SOP, differing from COP, is attributed to specific causes including connective tissue disease, infections, tumors and drugs[3]. Among these, SOP caused by infections presents diagnostic challenges and there are limited reports both domestically and internationally on SOP caused by Mycobacterium tuberculosis (MTB) infection. Herein, we report a case of pulmonary tuberculosis with subsequent SOP treated in our department of tuberculosis, and review the relevant literatures.

CASE PRESENTATION

Chief complaints

Intermittent chest pain and fever for one month.

History of present illness

He experienced paroxysmal and pinprick right-sided chest pain a month earlier without any obvious triggers that worsened with physical activity. He also experienced fever, which was more pronounced at night and in the afternoon, with a maximum temperature of 39 °C, accompanied by dizziness and fatigue. He self-administered cephalosporin antibiotics orally for five days, but his symptoms did not significantly improve. A chest radiograph taken at a local hospital showed right-sided pleural effusion and chronic bronchitis changes. Routine blood analysis revealed a slightly increased white blood cell count mainly composed of neutrophils. Additional lung computed tomography (CT) imaging performed at our hospital revealed multiple bilateral nodules and cavitary lesions, which were considered infectious lesions caused by tuberculosis.

History of past illness

The patient has exhibited a history of robust health, he had no history of respiratory, heart, liver or kidney diseases.

Personal and family history

The patient has no history of smoking or drinking; no cases of similar diseases have been reported in the patient's family.

Physical examination

Physical examination revealed decreased breathing sounds in the lower right lung and dullness on percussion.

Laboratory examinations

(1) Blood tests analysis (A local hospital): Indicated a slight increase in white blood cell count, predominantly neutrophils; (2) An adenosine deaminase level of the pleural fluid was 35.0 U/L; An erythrocyte sedimentation rate of 78 mm/hour; (3) The levels of tumor markers, myocardial enzymes, electrolytes, blood glucose, lipids, and bicarbonate were normal; (4) Two sputum specimens positive for acid-fast bacillus confirmed mycobacterial growth; and (5) The lung biopsy of new lesions showed alveolar atrophy, interstitial fibrosis, scattered inflammatory cell infiltration, and focal organizing pneumonia changes (Figure 1). Special staining, including acid-fast, periodic acid shiff, and hexamine-silver, did not detect pathogenic bacteria (Figure 2).

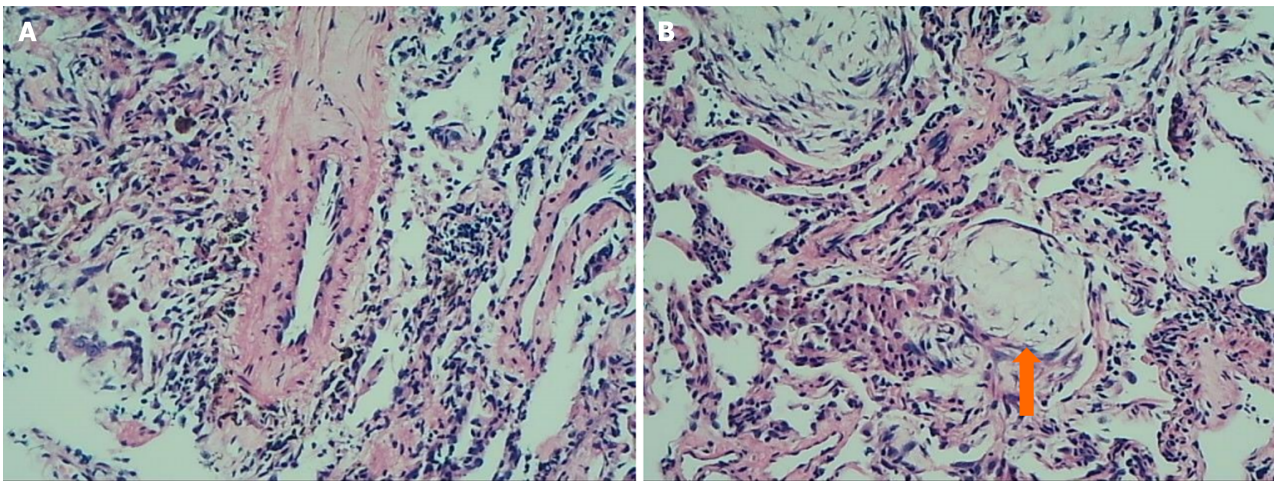

Figure 1 The lung biopsy showed alveolar atrophy, interstitial fibrosis, scattered inflammatory cell infiltration, and focal organizing pneumonia changes, and focal presence of Masson's bodies (indicated by arrows) (Hematoxylin-eosin staining × 100 magnification).

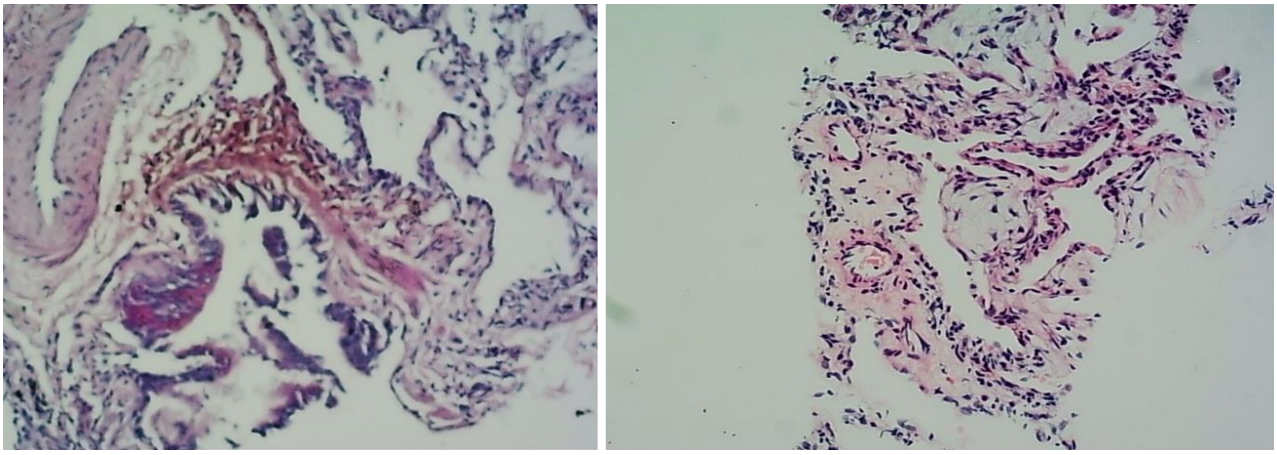

Figure 2 Special staining, including acid-fast, periodic acid shiff, and hexamine-silver, did not detect pathogenic bacteria (Hematoxylin-eosin staining × 100 magnification).

Imaging examinations

(1) A local hospital's chest radiograph showed right-sided pleural effusion and chronic bronchitis changes; (2) Lung CT imaging at our hospital (September 10, 2018): Showed multiple bilateral nodules and cavitary lesions, suggesting infection particularly due to tuberculosis (Figure 3); (3) Following a 5-month course of anti-tuberculosis treatment, the subsequent CT scan revealed complete closure of the cavity in the right upper lung, absorbtion of pleural effusion in the right hemithorax, and significant reduction in size of the cavity in the lower left lung (Figure 4); (4) A follow-up lung CT scan in June 2019 revealed new multifocal subpleural ground-glass opacities in both lungs (Figure 5); (5) Another lung CT reexamination on August 16, 2019, indicated a significant increase in ground-glass opacities in both lungs (Figure 6); (6) On August 21, 2019, bronchoscopy and bronchoalveolar lavage (BAL) of the upper lobes of both lungs were performed and no significant abnormalities were observed; (7) On September 16, 2019, after undergoing hormone therapy, subsequent dynamic pulmonary CT exams showed improvement in lesion absorption and gradual closure of the cavity (Figure 7); and (8) On July 22, 2020, A one-year follow-up lung CT scan showed no new lesions (Figure 8).

MULTIDISCIPLINARY EXPERT CONSULTATION

Our patient developed new bilateral pulmonary lesions after 9 months of antituberculosis treatment and the possible causes were as follows: (1) Development of resistance after antituberculosis treatment; (2) Secondary bacterial or fungal infection; and (3) Pulmonary manifestations of connective tissue disease. Subsequent lung biopsy revealed typical OP, but acid fast bacilus (AFB) staining results were negative. The low positive rate of AFB staining and the rapid appearance of new lesions in the right lower lung did not support a diagnosis of tuberculosis, but the persistent cavity lesions in the left

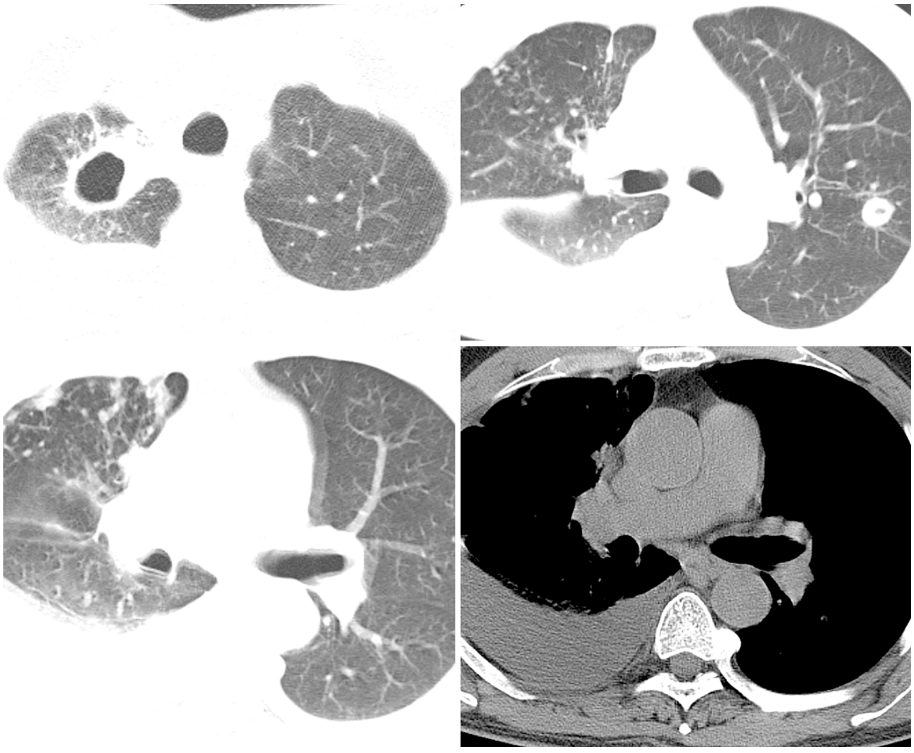

Figure 3 After admission, the computed tomography scan unveiled multiple nodules and cavities in both lungs, suggesting infection, particularly tuberculosis. Right pleurisy and pleural effusion were noted.

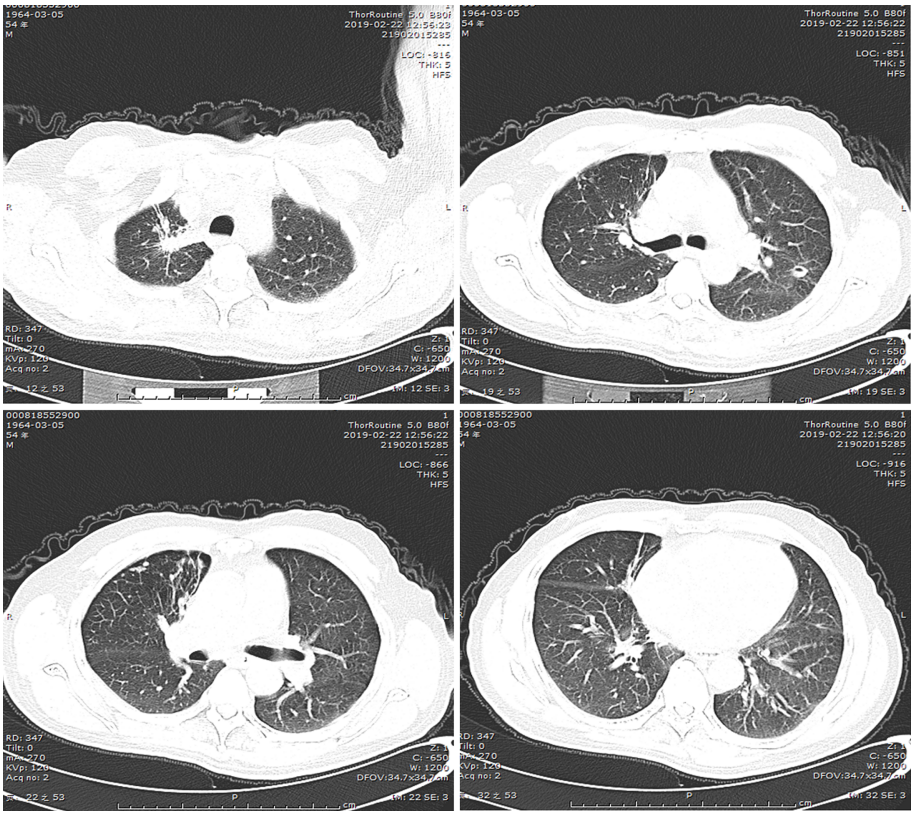

Figure 4 Following a 5-month course of anti-tuberculosis treatment, the subsequent computed tomography scan revealed complete closure of the cavity in the right upper lung, absorbtion of pleural effusion in the right hemithorax, and significant reduction in size of the cavity in the lower left lung.

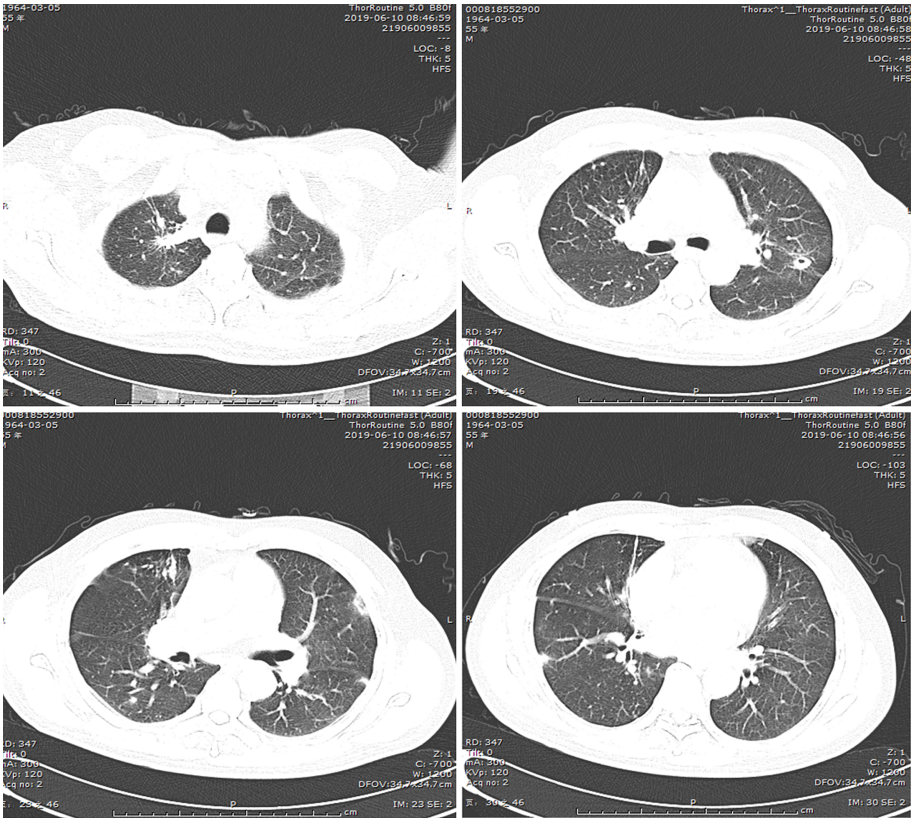

Figure 5 A follow-up lung computed tomography scan in June 2019 revealed new multifocal subpleural ground-glass opacities in both lungs.

lower lung were considered to indicate tuberculosis infection. Since corticosteroid therapy alone carries the risk of tuberculosis dissemination, we administered both antituberculosis and corticosteroid treatments after diagnosing OP. Over time, the newly developed subpleural lesions gradually absorbed and subsided, and cavity lesions in the lower left lung also closed. Therefore, we concluded that the OP was secondary to tuberculosis infection, not related to anti-tuberculosis medication or other factors.

FINAL DIAGNOSIS

(1) Pulmonary tuberculosis; (2) Tuberculous pleurisy; (3) Drug-induced dermatitis; and (4) Secondary organizing pneumonia.

TREATMENT

(1) Treatment began with isoniazid (0.3 g/day), ethambutol (0.75 g/day), pyrazinamide (1.5 g/day), and rifampicin (0.6 g/day). One week after the treatment, the patient developed a rash on the trunk, accompanied by fever, suggesting an allergic reaction to anti-tuberculosis drugs. The anti-tuberculosis treatment was temporarily halted, and anti-allergy treatment was initiated. After the rash subsided, the regimen was adjusted to rifampicin, ethambutol, pyrazinamide, and levofloxacin; and (2) After the organizing pneumonia was confirmed, treatment was initiated with 40 mg methylprednisolone once daily. The steroid was gradually tapered off and discontinued after a total course of six months. Anti-tuberculosis medication was also discontinued at the same time.

OUTCOME AND FOLLOW-UP

Follow-up lung CT scan showed improvement in lesion absorption and gradual closure of the cavity, a one-year follow-up lung CT scan showed no new lesions.

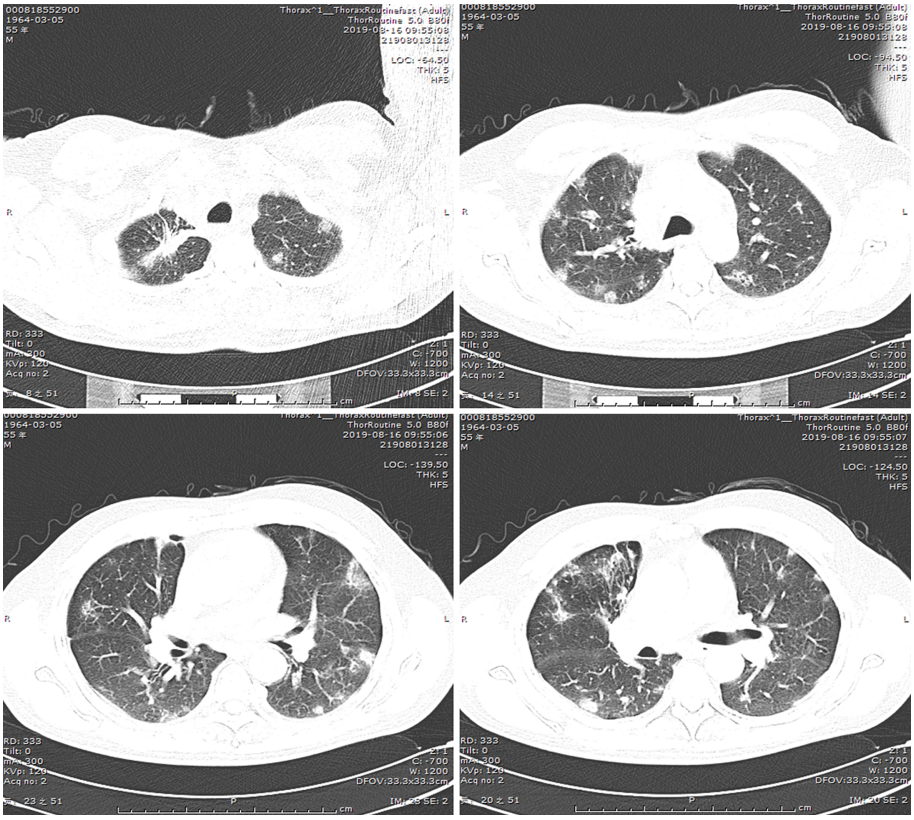

Figure 6 On August 16, 2019, another lung computed tomography reexamination indicated a significant increase in ground-glass opacities in both lungs.

DISCUSSION

The epidemiology of OP is not well understood currently. An early retrospective study suggests an incidence rate of 1.97 to 7 per 100000 individuals, with the median age of onset between 50 and 60 years[4]. The clinical manifestations of OP are nonspecific, which always delayed diagnosis by 6 to 12 weeks. Common symptoms include dry cough, flu-like symptoms, and respiratory distress, while hemoptysis is rare and acute respiratory distress syndrome is uncommon. Breath crackles are often observed in OP patients, yet around 25% of patients have normal lung auscultation findings. There are no specific laboratory tests for diagnosing OP. About 50% of patients may have leukocytosis, along with elevated c-reactive protein and erythrocyte sedimentation rate. Pulmonary function tests generally show mild-to-moderate diffusion dysfunction, and some smokers may exhibit obstructive ventilation dysfunction[5].

In clinical practice, once OP is diagnosed through tissue biopsy, it should not be readily categorized as COP. It is crucial to differentiate the etiology and actively rule out SOP. In contrast to COP with no determined causes, SOP could be specifically triggered by infection, connective tissue disease, drug damage, inflammatory bowel disease, hematologic malignancies, organ transplantations, and radiation therapy[3]. Histopathological presence of epithelioid cell granulomas or giant multinucleated cells suggests infection-related OP[6], with viruses and fungi as primary causes[7-9]. However, OP secondary to tuberculosis is rarely reported, possibly due to the low incidence of OP itself and the low positive detection rate of both AFB staining and tuberculosis cultures. A previous study analyzed 11 global cases of tuberculosis complicated with OP and found that the positive rate of sputum AFB staining was only 18%, while the positive rate of MTB DNA detection in sputum or bronchoalveolar lavage fliud (BALF) reached 87.5%[10]. Therefore, MTB DNA detection in sputum or BALF should be recommended for early diagnosis of tuberculosis.

Currently, the mechanism of tuberculosis infection leading to OP remains unclear. A previous research suggests that MTB may first enter the alveolar epithelial cells before being phagocytosed. The MTB infection-mediated immune response causes damage to the alveolar epithelial cells. Subsequently, neutrophils and lymphocytes are triggered, becoming activated and aggregated, and release inflammatory mediators and cytokines. Concurrently, fibroblasts are also activated. During alveolar damage, leakage of coagulation proteins occurs, leading to the accumulation of fibrin. The activity of fibrinolysis decreases, eventually resulting in fibrosis and granuloma formation[11]. This process is reversible in its early stages; early diagnosis and glucocorticoid use can prevent irreversible pulmonary fibrosis and impaired gas exchange function.

The imaging features of OP are vary with over 70% of patients showing subpleural ground-glass opacities and/or peribronchovascular consolidation. These lesions are usually bilateral and asymmetric; single or multiple nodules are uncommon, and in some instances, the lesions may exhibit migratory changes. Unlike those in COP and other SOPs, the lesions in infection-associated SOP cases are mostly fixed due to the relatively fixed location of the infection[12]. Previously reported cases of tuberculosis complicated with OP mostly involved localized consolidation or nodular

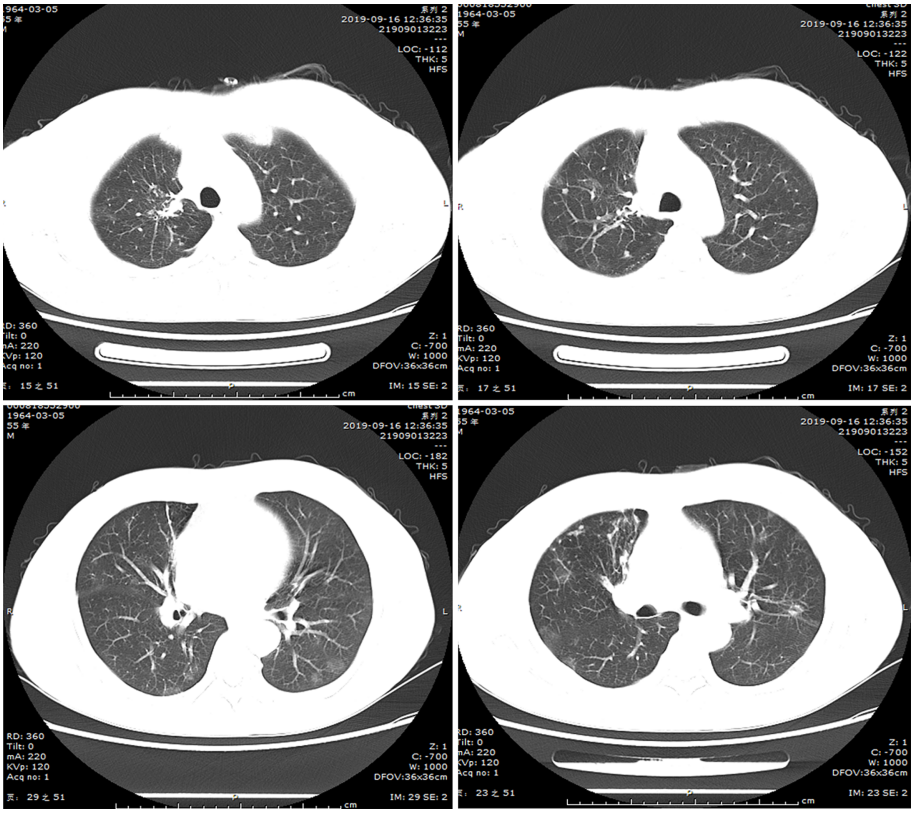

Figure 7 After undergoing hormone therapy, the follow-up examination revealed a significant improvement in the subpleural ground-glass opacities observed in both lungs.

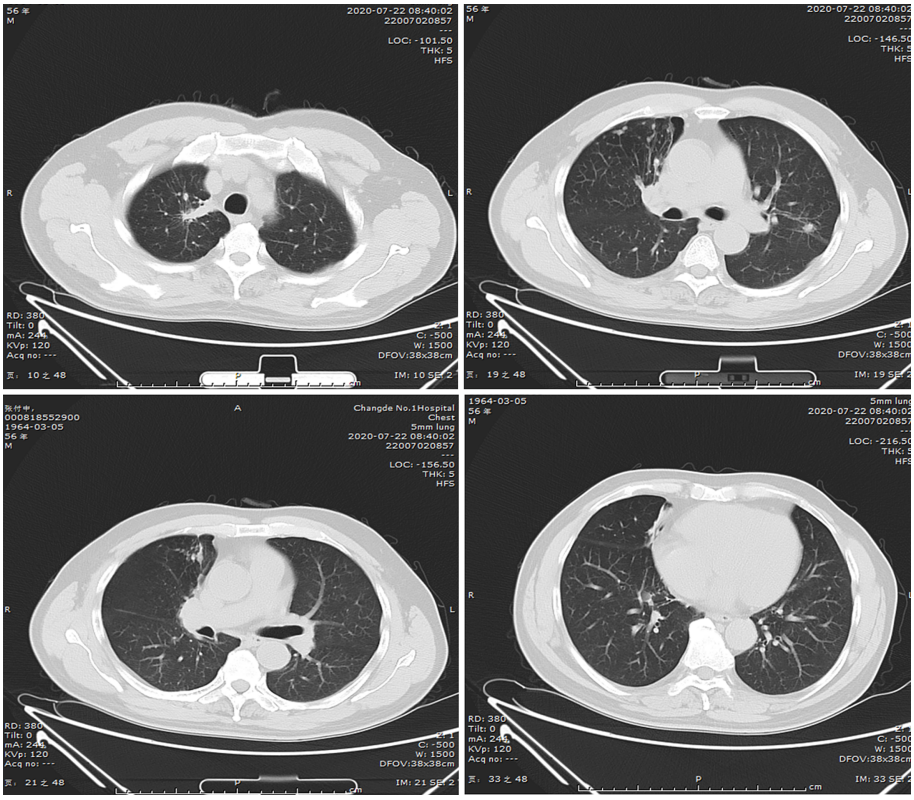

Figure 8 No new lesions were detected on computed tomography follow-up one year after treatment discontinuation.

lesions, often presenting as focal OP[10,13,14]. Huang *et al*[15] reported a patient with multiple migratory ground-glass opacities distributed bilaterally in the subpleural region of the lungs. Uniquely, in the current study, the patient with tuberculosis-induced OP showed scattered bilateral ground-glass opacities, predominantly in the lower lungs, without migratory changes. Furthermore, in previous studies, radiological signs of disseminated tuberculosis, such as cavities and tree-in-bud signs, were seldom observed in patients with pulmonary tuberculosis-related SOP.

The temporal boundary between infection and the occurrence of SOP is unclear. In some patients, infection and OP coexist, whereas in others, the inflammatory response persists even after the infection has been resolved, leading to the development of OP caused by an excessive inflammatory response[16,17]. In all previous domestic and international reports of tuberculosis complicated with OP, the two conditions have coexisted. In this study, our patient developed new bilateral pulmonary lesions after 9 months of antituberculosis treatment and the possible causes were as follows: (1) Development of resistance after antituberculosis treatment; (2) Secondary bacterial or fungal infection; and (3) Pulmonary manifestations of connective tissue disease. To clarify the aetiology, further bronchoscopy and BAL, in addition to tests for drug-resistant tuberculosis and connective tissue disease, were performed, and the results of all tests were negative. Subsequent lung biopsy revealed typical OP, but AFB staining results were negative. The low positive rate of AFB staining and the rapid appearance of new lesions in the right lower lung did not support a diagnosis of tuberculosis, but the persistent cavity lesions in the left lower lung were considered to indicate tuberculosis infection. Since corticosteroid therapy alone carries the risk of tuberculosis dissemination, we administered both antituberculosis and corticosteroid treatments after diagnosing OP. Over time, the newly developed subpleural lesions gradually absorbed and subsided, and cavity lesions in the lower left lung also closed. Therefore, we concluded that the OP was secondary to tuberculosis infection, not related to anti-tuberculosis medication or other factors.

CONCLUSION

In summary, pulmonary tuberculosis complicated with OP is rare in clinical setting. Its diagnosis requires a comprehensive evaluation of the patient's medical history, symptoms, radiological findings, and histopathological examination. In treating patients with active pulmonary tuberculosis, if an increase in lesions is observed during anti-tuberculosis treatment, it is necessary to consider the possibility of tuberculosis-related SOP, apart from excluding factors like drug resistance. Specifically, timely lung biopsy is essential for early intervention. In some cases, anti-tuberculosis treatment alone may suffice, but if glucocorticoids are used, enhanced anti-tuberculosis treatment is necessary to prevent tuberculosis dissemination.

ACKNOWLEDGEMENTS

We thank Rui P for assisting in preparation of this manuscript.

FOOTNOTES

Author contributions: Liu M contributed to the diagnosis of this case, drafting the article; Dong XY and Ding ZX contributed to the diagnosis of this case; Wang QH contributed to histological diagnosis; Li DH conceived the idea of the manuscript, responsible for the patient's follow-up, critical revision of the article and final approval of the version to be published; All authors read and approved the final manuscript.

Supported by The Science and Technology Innovation Program of Changde City.

Informed consent statement: Study participant provided informed written consent prior to study enrollment.

Conflict-of-interest statement: The authors declare that they have no competing interests.

CARE Checklist (2016) statement: The authors have read the CARE Checklist (2016), and the manuscript was prepared and revised according to the CARE Checklist (2016).

Country of origin: China

ORCID number: De-Hui Li 0009-0004-6636-5835.

S-Editor: Fan M
L-Editor: A

P-Editor: Cai YX

REFERENCES

1 **Baque-Juston M**, Pellegrin A, Leroy S, Marquette CH, Padovani B. Organizing pneumonia: what is it? A conceptual approach and pictorial review. *Diagn Interv Imaging* 2014; **95**: 771-777 [PMID: 24559802 DOI: 10.1016/j.diii.2014.01.004]

2 **Raghu G**, Meyer KC. Cryptogenic organising pneumonia: current understanding of an enigmatic lung disease. *Eur Respir Rev* 2021; **30** [PMID: 34407978 DOI: 10.1183/16000617.0094-2021]

3 **Krupar R**, Kümpers C, Haenel A, Perner S, Stellmacher F. [Cryptogenic organizing pneumonia versus secondary organizing pneumonia]. *Pathologe* 2021; **42**: 55-63 [PMID: 33462627 DOI: 10.1007/s00292-020-00903-8]

4 **Gudmundsson G**, Sveinsson O, Isaksson HJ, Jonsson S, Frodadottir H, Aspelund T. Epidemiology of organising pneumonia in Iceland. *Thorax* 2006; **61**: 805-808 [PMID: 16809413 DOI: 10.1136/thx.2006.059469]

5 **Cherian SV**, Patel D, Machnicki S, Naidich D, Stover D, Travis WD, Brown KK, Naidich JJ, Mahajan A, Esposito M, Mina B, Lakticova V, Cohen SL, Muller NL, Schulner J, Shah R, Raoof S. Algorithmic Approach to the Diagnosis of Organizing Pneumonia: A Correlation of Clinical, Radiologic, and Pathologic Features. *Chest* 2022; **162**: 156-178 [PMID: 35038455 DOI: 10.1016/j.chest.2021.12.659]

6 **Sander R**, Gómez C, Borderías L. Organizing pneumonia and pulmonary tuberculosis: Coexistent or associated diseases. *Arch Bronconeumol* 2016; **52**: 570-571 [PMID: 27156206 DOI: 10.1016/j.arbres.2016.03.009]

7 **Asai N**, Yokoi T, Nishiyama N, Koizumi Y, Sakanashi D, Kato H, Hagihara M, Suematsu H, Yamagishi Y, Mikamo H. Secondary organizing pneumonia following viral pneumonia caused by severe influenza B: a case report and literature reviews. *BMC Infect Dis* 2017; **17**: 572 [PMID: 28810835 DOI: 10.1186/s12879-017-2677-1]

8 **Sakurai A**, Yanai H, Ishida T, Kuwata H, Kamei K, Izumi S. Possible relationship between organizing pneumonia and chronic pulmonary aspergillosis: A case report and literature review. *Respir Investig* 2017; **55**: 74-78 [PMID: 28012499 DOI: 10.1016/j.resinv.2016.07.004]

9 **Ketchersid K**. A review of organizing pneumonia. *JAAPA* 2023; **36**: 16-19 [PMID: 36749158 DOI: 10.1097/01.JAA.0000918776.59717.eb]

10 **Kim EJ**, Kim KC. Pulmonary tuberculosis presenting secondary organizing pneumonia with organized polypoid granulation tissue: case series and review of the literature. *BMC Pulm Med* 2020; **20**: 252 [PMID: 32962688 DOI: 10.1186/s12890-020-01292-7]

11 **Kligerman SJ**, Franks TJ, Galvin JR. From the radiologic pathology archives: organization and fibrosis as a response to lung injury in diffuse alveolar damage, organizing pneumonia, and acute fibrinous and organizing pneumonia. *Radiographics* 2013; **33**: 1951-1975 [PMID: 24224590 DOI: 10.1148/rg.337130057]

12 **Arenas-Jiménez JJ**, García-Garrigós E, Ureña Vacas A, Sirera Matilla M, Feliu Rey E. Organizing pneumonia. *Radiologia (Engl Ed)* 2022; **64** Suppl 3: 240-249 [PMID: 36737163 DOI: 10.1016/j.rxeng.2022.08.002]

13 **Yoon HS**, Lee EJ, Lee JY, Chon GR, Lee SH, Kim SJ. Organizing pneumonia associated with M ycobacterium tuberculosis infection. *Respirol Case Rep* 2015; **3**: 128-131 [PMID: 26835126 DOI: 10.1002/rcr2.135]

14 **Hsieh MH**, Lin CY. Pulmonary tuberculosis presenting as organizing pneumonia. *Am J Respir Crit Care Med* 2014; **189**: e63 [PMID: 24787075 DOI: 10.1164/rccm.201304-0722IM]

15 **Huang LL**, Wang C, Liu Y, Gu XY, Wang WX, Chen W, Hu CM. Resolution of an insidious and migratory Mycobacterium tuberculosis-associated secondary organizing pneumonia: a case report and literature review. *BMC Infect Dis* 2023; **23**: 372 [PMID: 37264312 DOI: 10.1186/s12879-023-08334-5]

16 **Huo Z**, Feng R, Tian X, Zhang H, Huo L, Liu H. Clinicopathological findings of focal organizing pneumonia: a retrospective study of 37 cases. *Int J Clin Exp Pathol* 2015; **8**: 511-516 [PMID: 25755741]

17 **Zhou H**, Gu W, Li C. Post-Infectious Organizing Pneumonia: an Indistinguishable and Easily Misdiagnosed Organizing Pneumonia. *Clin Lab* 2015; **61**: 1755-1761 [PMID: 26732002 DOI: 10.7754/clin.lab.2015.150234]

World Journal of Clinical Cases

Submit a Manuscript: https://www.f6publishing.com

World J Clin Cases 2024 September 16; 12(26): 5983-5989

DOI: 10.12998/wjcc.v12.i26.5983

ISSN 2307-8960 (online)

CASE REPORT

Sclerosing epithelioid fibrosarcoma of the pancreas: A case report

Meng-Qing Sun, Li-Na Guo, Yan You, Yan-Yu Qiu, Xiao-Dong He, Xian-Lin Han

Specialty type: Medicine, research and experimental

Provenance and peer review: Unsolicited article; Externally peer reviewed.

Peer-review model: Single blind

Peer-review report's classification

Scientific Quality: Grade C
Novelty: Grade B
Creativity or Innovation: Grade B
Scientific Significance: Grade B

P-Reviewer: Kitamura K

Received: March 29, 2024
Revised: July 2, 2024
Accepted: July 10, 2024
Published online: September 16, 2024
Processing time: 115 Days and 23.7 Hours

Meng-Qing Sun, Yan-Yu Qiu, Xiao-Dong He, Xian-Lin Han, Department of General Surgery, Peking Union Medical College Hospital, Chinese Academy of Medical Sciences, Beijing 100730, China

Li-Na Guo, Yan You, Department of Pathology, Peking Union Medical College Hospital, Chinese Academy of Medical Sciences, Beijing 100730, China

Corresponding author: Xian-Lin Han, MD, Professor, Department of General surgery, Peking Union Medical College Hospital, Chinese Academy of Medical Sciences, No. 1 Shuai Fu Yuan, Dongcheng District, Beijing 100730, China. hanxianlin@pumch.cn

Abstract

BACKGROUND

A sclerosing epithelioid fibrosarcoma (SEF) is a rare malignant fibroblastic soft tissue tumor that rarely occurs in intra-abdominal organs. A case of a SEF in the pancreatic head is reported herein, including its clinical manifestations, pre-operative imaging features, gross specimen and pathological findings.

CASE SUMMARY

A 33-year-old male patient was admitted to Peking Union Medical College Hospital in December 2023 due to a one-year history of intermittent upper abdominal pain and the discovery of a pancreatic mass. The patient underwent an enhanced computed tomography scan of the abdomen, which revealed a well-defined, round mass with clear borders and calcifications in the pancreatic head. The mass exhibited progressive, uneven mild enhancement, measuring approximately 6.6 cm × 6.3 cm. The patient underwent laparoscopic pylorus-preserving pancreaticoduodenectomy. Postoperative pathological examination revealed that the lesion was consistent with a SEF. At the 3-month postoperative follow-up, the patient did not report any short-term complications, and there were no signs of tumor recurrence.

CONCLUSION

SEFs are rare malignant fibrous soft tissue tumors. SEFs rarely develop in the pancreas, and its preoperative diagnosis depends on imaging findings, with confirmation depending on pathological examination and immunohistochemistry. Currently, only four cases of pancreatic SEF have been reported in studies written in English. This case is the first reported case of a pancreatic SEF by a clinical physician.

Key Words: Sclerosing epithelioid fibrosarcoma of the pancreas; Abdominal malignant

fibroblastic soft tissue tumor; Abdominal enhanced computed tomography; Laparoscopic pancreaticoduodenectomy; Case report

Core Tip: Sclerosing epithelioid fibrosarcoma (SEF) is a rare malignant fibroblastic soft tissue tumor, which is extremely rare in intra-abdominal organs. This article reports a case of SEF in the pancreatic head, presenting its clinical manifestations, preoperative imaging, gross specimen and pathological findings.

Citation: Sun MQ, Guo LN, You Y, Qiu YY, He XD, Han XL. Sclerosing epithelioid fibrosarcoma of the pancreas: A case report. *World J Clin Cases* 2024; 12(26): 5983-5989
URL: https://www.wjgnet.com/2307-8960/full/v12/i26/5983.htm
DOI: https://dx.doi.org/10.12998/wjcc.v12.i26.5983

INTRODUCTION

Sclerosing epithelioid fibrosarcoma (SEF) is a malignant fibrous soft tissue tumor that was first reported by Meis-Kindblom *et al*[1]. This disease is primarily diagnosed *via* pathological examination and immunohistochemical (IHC) staining. SEF is generally considered a low-grade malignant tumor, but some have proposed a more aggressive clinical course. The tumor can develop at any time during the life course in males and females alike. SEFs most commonly occur in the soft tissues of the limbs, followed by the trunk and head and neck. SEFs are extremely rare in intra-abdominal organs, with only a few cases reported in the pancreas. A case of SEF in the pancreatic head, including its clinical manifestations, preoperative imaging features, gross specimen and pathological findings, are presented herein.

CASE PRESENTATION

Chief complaints

A 33-year-old male patient was admitted to Peking Union Medical College Hospital in December 2023 due to a one-year history of intermittent upper abdominal pain and the discovery of a pancreatic mass.

History of present illness

The patient had been experiencing unexplained upper abdominal pain without fever, abdominal distension, diarrhea, nausea, or vomiting. A previous abdominal ultrasound at a local hospital revealed a mass in the pancreatic head, and the patient was given oral ibuprofen for symptomatic relief. An abdominal magnetic resonance imaging (MRI) in October 2022 revealed a round mass in the pancreatic head area measuring approximately 6.4 cm × 6.1 cm × 6.6 cm (no images available). The patient experienced episodic abdominal pain every three months and responded to symptomatic treatment. A repeat abdominal ultrasound at our hospital revealed a hypoechoic mass in the pancreatic head area measuring approximately 6.6 cm × 5.6 cm × 5.7 cm, with somewhat regular morphology and uneven internal echoes. The patient was admitted for surgical treatment of a suspected pancreatic head mass.

History of past illness

There was no significant medical history, personal history, or family history.

Personal and family history

See above.

Physical examination

On admission, physical examination did not reveal any significant positive signs, and no obvious mass was palpated in the abdomen.

Laboratory examinations

Preoperative tumor marker examination revealed a carbohydrate antigen 19-9 level of 5.0 U/mL and a carcinoembryonic antigen level of 1.3 ng/mL.

Imaging examinations

Following admission, the patient underwent an enhanced computed tomography (CT) scan of the abdomen, which revealed a well-defined, round mass with clear borders and calcifications in the pancreatic head. The mass exhibited

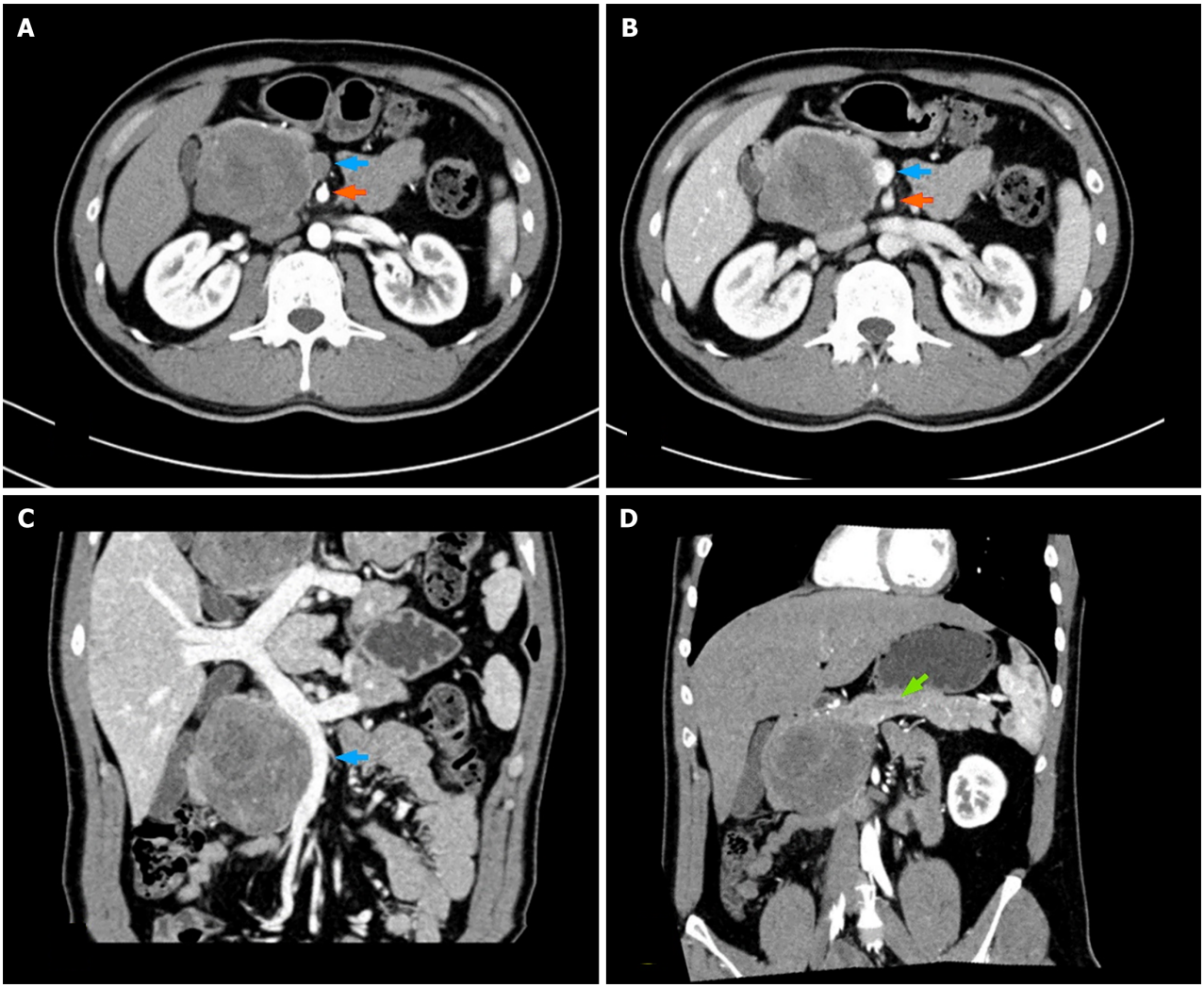

Figure 1 An enhanced computed tomography image of the abdomen revealed a mass in the head of the pancreas. A: Arterial phase; B: Portal phase; C: Portal venous system reconstruction; D: Coronal reconstruction. Blue arrow: Superior mesenteric vein; Orange arrow: Superior mesenteric artery; Green arrow: Main pancreatic duct.

progressive, uneven mild enhancement, measuring approximately 6.6 cm × 6.3 cm. Additionally, compression and displacement were observed in the distal duodenum, gallbladder, lower segment of the inferior vena cava, and proximal segment of the superior mesenteric vein. These imaging findings suggest a potential diagnosis of a solid pseudopapillary tumor (SPT) of the pancreas. Notably, the size and morphology of the body and tail of the pancreas appeared normal, with clear margins and homogeneous parenchymal density. No significant dilation of the pancreatic duct was evident (Figure 1).

TREATMENT

The patient subsequently underwent laparoscopic pylorus-preserving pancreaticoduodenectomy. Upon resection, the tumor exhibited solid characteristics, with a gray-white cut surface, hard texture, and well-defined borders, measuring 8 cm × 8 cm × 6 cm (Figure 2). Postoperatively, the patient had a smooth recovery, resumed an oral liquid diet on postoperative day (POD) 5, had all the abdominal drainage tubes removed on POD 7, and was discharged on POD 9.

FINAL DIAGNOSIS

Postoperative pathological examination revealed that the lesion was consistent with a SEF, invading peripancreatic adipose tissue but not involving the duodenal muscular layer, common bile duct, or major duodenal papilla. The margins of the small intestine, bile duct, portal vein groove, and retroperitoneum were unremarkable, and no lymph node metastasis was observed. IHC analysis revealed positive staining for *MUC4*, vimentin, *ATRX*, *SMARCA4*, sporadic S-100 protein, occasional *SATB2*, β-catenin, partial cluster of differentiation (CD) 99, and vascular CD34 and negative staining

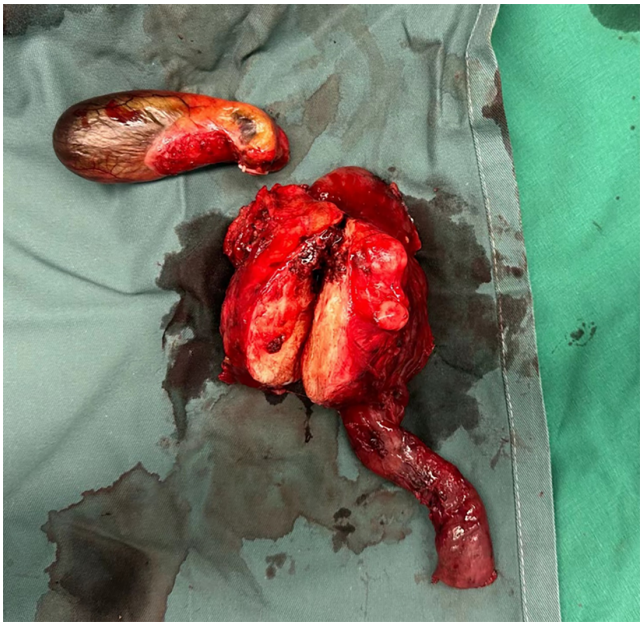

Figure 2 Macroscopic photographs of the resected specimen. The tumor was solid, gray-white, hard in texture, and had roughly clear borders.

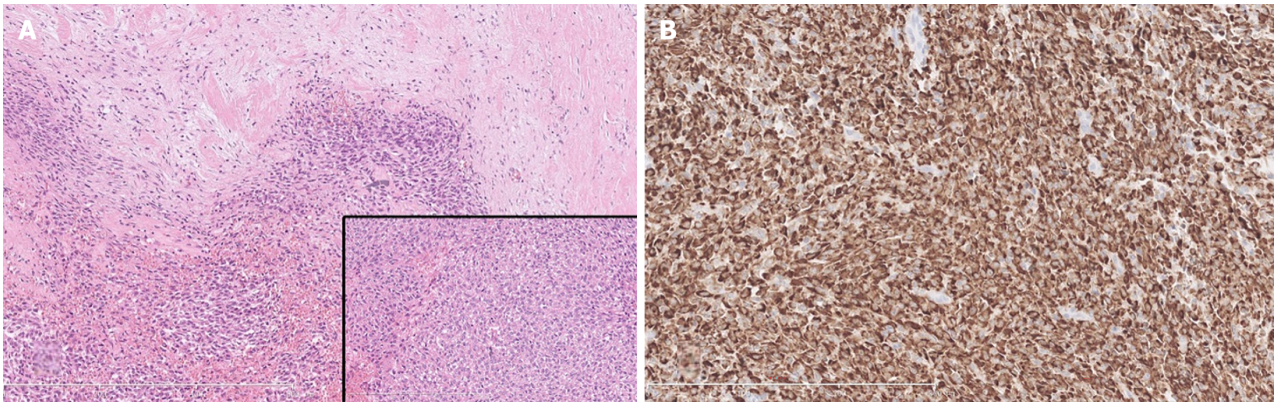

Figure 3 Histopathological sections of the resected specimen. A: Low × 10 and medium × 20 (inserted) magnification H and E stains demonstrating that the tumor cells are epithelioid and that mitosis is easily observed; B: Mucin 4 stain demonstrating strong and diffuse staining of the tumor cells.

for Cytokeratin AE1/AE3, CD10, chromogranin A, synaptophysin, B-cell lymphoma 10, tumor protein P53, *SOX10*, CD117, *DOG-1*, smooth muscle actin, desmin, Myo-D1, Myogenin, and P63, with a Ki-67 index of 30% in hot spots (Figure 3).

OUTCOME AND FOLLOW-UP

At the 3-month postoperative follow-up, the patient did not report any short-term complications, and there were no signs of tumor recurrence.

DISCUSSION

A SEF is a rare malignant fibroblastic soft tissue tumor that can at any age. The average age at onset, as reported in various studies, is approximately 38-55 years, with an equal incidence in both men and women[1-3]. A SEF can occur in almost any soft tissue, typically affecting the limbs or trunk, followed by the intra-abdominal organs such as the liver, gastrointestinal tract, ovaries, and kidneys[4-6]. The tumor tends to grow slowly, but the average size at the time of diagnosis is 7-8 cm, and it can metastasize to the lungs, bones, and other sites[2,3,7]. SEFs rarely develop in the pancreas, with only four cases reported in studies written in English to date[8-11]. These cases were reported by departments of radiology or pathology, and this case represents the first reported case of pancreatic SEF by clinicians. A summary of the reported cases of pancreatic SEF is presented in Table 1.

Table 1 Summary of clinical data on reported pancreatic sclerosing epithelioid fibrosarcoma in the literature

No.	Year	Ref.	Gender	Age	Location	Size (cm)	Clinical presentation	Surgical procedure	IHC	Ki-67 index	Follow up (m)	Recurrence
1	2013	Bai *et al*[8]	M	67	Body	1	None	DP and splenectomy	Vimentin (+), EMA (-), SMA (-), S-100 protein (-)	< 5%	NM	NM
2	2014	Luo *et al*[11]	M	42	Head	2.9	Upper abdominal pain	PD	Vimentin (+), SMA (-), S-100 protein (-), *bcl-2* (-)	15%	16	None
3	2020	Xia *et al*[10]	M	64	Tail	2	None	DP and splenectomy	Vimentin (+), *bcl-2* (+), EMA (+), SMA (+), CD34 (-), S-100 protein (-)	8% (+)	12	None
4	2020	Kramer *et al*[9]	M	58	Head	6	None	PPPD	*MUC4* (+)	NM	3	None
5	2024	Present case	M	33	Head	8	Upper abdominal pain	Laparoscopic PPPD	*MUC4* (+), Vimentin (+), SMA (-), S-100 protein (scattered +), CD34 (vessel +)	30%	2	None

IHC: Immunohistochemistry; DP: Distal pancreatectomy; CD: Cluster of differentiation; PD: pancreaticoduodenectomy; PPPD: Pylorus-preserving pancreaticoduodenectomy; NM: Not mentioned; EMA: Epithelial membrane antigen; SMA: Smooth muscle actin.

All 5 patients were male, with a median age of 58 years (range: 33-67). Two patients presented with nonspecific abdominal symptoms, such as upper abdominal pain, while the remaining patients did not report any tumor-related discomfort. SEFs can be found in the head, body, or tail of the pancreas, ranging from 1 to 8 cm in size at the time of discovery. None of the patients were diagnosed with a SEF preoperatively. In two patients with small tumors, the preoperative diagnosis was pancreatic neuroendocrine tumors[8,10], whereas in this case, the preoperative diagnosis was SPT of the pancreas. The preoperative diagnoses for the remaining two patients were not mentioned. All 5 patients underwent radical surgery (pancreaticoduodenectomy or distal pancreatectomy with splenectomy), and during the reported follow-up period, no tumor recurrence or metastasis was observed. However, one patient underwent right buttock soft tissue tumor resection 6 years prior, and upon reviewing the histological slides of the tumor, it was also considered to be a SEF. Therefore, the pancreatic lesion in this patient was considered to be a metastatic SEF[11].

SEFs are mainly diagnosed *via* imaging, especially enhanced CT and MRI. Imaging can provide information on the location, size, and borders of the tumor, as well as the tumor's relationship with blood vessels, bile ducts, and the main pancreatic duct and the presence of lymph node or distant metastases. On enhanced CT, SEFs appear as solid masses in the pancreas, with larger SEFs possibly showing uneven density. The enhancement pattern is characterized by gradual centripetal and nonuniform enhancement toward the center of the lesion[10]. Previously reported pancreatic SEFs often exhibit expansive growth, causing compressive and space-occupying changes to adjacent organ tissues, with direct invasion being less common. Apart from one patient with pancreatic duct dilation, the remaining patients did not show any signs of vascular invasion or pancreatic duct or bile duct dilation[11]. In this case, the large tumor caused displacement of the descending duodenum, gallbladder, lower segment of the inferior vena cava, and proximal segment of the superior mesenteric vein, as observed on preoperative images. However, intraoperative findings and postoperative pathological examination confirmed that the abovementioned organ structures were not invaded by the tumor. Notably, the typical imaging characteristics of SPTs are similar to those described above. However, SPTs predominantly develop in premenopausal women, which differs from the typical demographic characteristics of this disease. Owing to the rarity of

pancreatic SEF, preoperative imaging can easily lead to misdiagnosis as primitive neurotodermal tumor, SPT, or other solid pancreatic tumors. Positron emission tomography-CT may be helpful in preoperative diagnosis, but the fludeoxyglucose (FDG) uptake of SEFs shows some heterogeneity, with different lesions exhibiting varying FDG uptake, possibly related to their different levels of invasiveness[11].

There are no studies on the value of preoperative biopsy. In this case, the patient did not undergo preoperative biopsy, mainly because the diagnosis of the pancreatic head mass was relatively clear, with preoperative images showing a SPT clearly indicated for surgical intervention. Preoperative biopsy does not alter the surgical approach and carries risks of bleeding, pancreatitis, and other complications. Pancreatic SEFs are extremely rare; thus, is it necessary to perform preoperative biopsy for differentiation? We believe that the answer to this question is complex.

The gross appearance of SEFs is typically nodular or lobulated, with a gray-white cut surface, firm or elastic consistency, and potential cystic changes and calcifications. Histologically, it is characterized by epithelioid tumor cells arranged in nests or cords that are uniformly embedded in a dense collagenous stroma. However, its tissue morphology can be easily confused with that of primary or metastatic sarcomas, SPTs of the pancreas, and other tumors. Therefore, it is typically diagnosed *via* immunohistochemistry. IHC staining for SEFs typically shows strong positivity for *MUC4* and vimentin, whereas epithelial membrane antigen, CD34, *S100* protein, and *bcl-2* are weakly positive or negative[7,12]. Most cases (75%) exhibit *EWSR1* gene rearrangement[7,13]. In this case, the gross specimen had a hard, gray-white cut surface, and histological examination showed epithelioid tumor cells arranged in nests and cords, with visible nuclear division. Immunohistochemistry revealed *MUC4* (+), vimentin (+), S-100 (scattered +), and CD34 (vascular +), which is consistent with the above characteristics of this disease.

Although a SEF is a low-grade tumor, it typically presents aggressiveness, with a risk of local recurrence and distant metastasis. These recurrences and metastases often occur several years after initial treatment. While some patients with SEFs undergo postoperative chemotherapy, existing radiotherapy and chemotherapy have shown poor efficacy for this disease[7]. There have been reports exploring molecular targeted therapy, immunotherapy, and other potential future treatment approaches[14,15]. At present, the patient in this report has been followed for a relatively short period and has not shown signs of recurrence or metastasis, but the long-term prognosis requires further assessment. In conclusion, pancreatic SEFs are rare malignant soft tissue tumors of the pancreas with nonspecific clinical manifestations. Preoperative diagnosis is primarily based on imaging, with confirmation depending on the results of pathological examination and immunohistochemistry. Radical surgical resection is currently the main treatment method.

CONCLUSION

In conclusion, pancreatic SEFs are rare malignant soft tissue tumors of the pancreas with nonspecific clinical manifestations. Preoperative diagnosis is primarily based on imaging, with confirmation depending on the results of pathological examination and immunohistochemistry. Radical surgical resection is currently the main treatment method.

FOOTNOTES

Author contributions: Sun MQ is responsible for collecting case data, creating illustrations, and writing the manuscript; Guo LN and You Y are responsible for interpreting and analyzing the pathological results; Qiu YY is responsible for manuscript editing; He XD provides technical support and guidance for case management; Han XL provides the case, performs the surgery, and is fully responsible for case management throughout.

Supported by National High Level Hospital Clinical Research Funding, No. 2022-PUMCH-B-003; National Multidisciplinary Cooperative Diagnosis and Treatment Capacity Building Project for Major Diseases.

Informed consent statement: Informed written consent for the treatment was obtained from the patients.

Conflict-of-interest statement: The authors declare that they have no conflict of interest.

CARE Checklist (2016) statement: The authors have read the CARE Checklist (2016), and the manuscript was prepared and revised according to the CARE Checklist (2016).

Country of origin: China

ORCID number: Yan You 0000-0003-4971-7830; Xiao-Dong He 0000-0002-6682-2926; Xian-Lin Han 0000-0003-4083-3640.

S-Editor: Fan M
L-Editor: A
P-Editor: Chen YX

REFERENCES

1 **Meis-Kindblom JM**, Kindblom LG, Enzinger FM. Sclerosing epithelioid fibrosarcoma. A variant of fibrosarcoma simulating carcinoma. *Am J Surg Pathol* 1995; **19**: 979-993 [PMID: 7661286 DOI: 10.1097/00000478-199509000-00001]

2 **Blay JY**, Tlemsani C, Toulmonde M, Italiano A, Rios M, Bompas E, Valentin T, Duffaud F, Le Nail LR, Watson S, Firmin N, Dubray-Longeras P, Ropars M, Perrin C, Hervieu A, Lebbe C, Saada-Bouzid E, Soibinet P, Fiorenza F, Bertucci F, Boudou P, Vaz G, Bonvalot S, Honoré C, Marec-Berard P, Minard V, Cleirec M, Biau D, Meeus P, Babinet A, Dumaine V, Carriere S, Fau M, Decanter G, Gouin F, Ngo C, Le Loarer F, Karanian M, Meurgey A, Dufresne A, Brahmi M, Chemin-Airiau C, Ducimetiere F, Penel N, Le Cesne A; NETSARC/REPPS/RESOS and French Sarcoma Group- Groupe d'Etude des Tumeurs Osseuses (GSF-GETO) networks. Sclerosing Epithelioid Fibrosarcoma (SEF) versus Low Grade Fibromyxoid Sarcoma (LGFMS): Presentation and outcome in the nationwide NETSARC+ series of 330 patients over 13 years. *Eur J Cancer* 2024; **196**: 113454 [PMID: 38008029 DOI: 10.1016/j.ejca.2023.113454]

3 **Peng Y**, Zhang D, Lei T, Xie J, Wu C, Wang H, Shi Y, Li Q, Wang J. The clinicopathological spectrum of sclerosing epithelioid fibrosarcoma: report of an additional series with review of the literature. *Pathology* 2023; **55**: 355-361 [PMID: 36690575 DOI: 10.1016/j.pathol.2022.10.005]

4 **Wu KH**, Huang YS, Li CC. Primary sclerosing epithelioid fibrosarcoma of the kidney: A rare case report. *Urol Case Rep* 2024; **53**: 102657 [PMID: 38304065 DOI: 10.1016/j.eucr.2024.102657]

5 **Armstrong A**, Boulos F, Kulkarni S, Stoll J, Doyle MBM, Khan A, He M. Sclerosing Epithelioid Fibrosarcoma of the Liver in a Pediatric Patient. *Pediatr Dev Pathol* 2023; **26**: 153-160 [PMID: 36748108 DOI: 10.1177/10935266221146378]

6 **Pathak N**, Kakkar A, Kaushal S, Batra A. Sclerosing epithelioid fibrosarcoma of the kidney. *BMJ Case Rep* 2023; **16** [PMID: 37295814 DOI: 10.1136/bcr-2022-253447]

7 **Warmke LM**, Yu W, Meis JM. Sclerosing Epithelioid Fibrosarcoma. *Surg Pathol Clin* 2024; **17**: 119-139 [PMID: 38278601 DOI: 10.1016/j.path.2023.06.009]

8 **Bai S**, Jhala N, Adsay NV, Wei S. Sclerosing epithelioid fibrosarcoma of the pancreas. *Ann Diagn Pathol* 2013; **17**: 214-216 [PMID: 22056035 DOI: 10.1016/j.anndiagpath.2011.06.006]

9 **Kramer SP**, Bowman CJ, Wang ZJ, Sheahon KM, Nakakura EK, Cho SJ, Umetsu SE, Behr SC. Hybrid Low-Grade Fibromyxoid Sarcoma and Sclerosing Epithelioid Fibrosarcoma of the Pancreas. *J Gastrointest Cancer* 2020; **51**: 1025-1029 [PMID: 32034641 DOI: 10.1007/s12029-020-00369-0]

10 **Xia W**, Yang Y, Huang Y. Imaging Features of Sclerosing Epithelioid Fibrosarcoma of the Pancreas: A Case Report. *Front Oncol* 2020; **10**: 901 [PMID: 32626655 DOI: 10.3389/fonc.2020.00901]

11 **Luo Y**, Hu W, Wu H, Xue H, Huo L, Li F, Zhao Y, Dai M. ^{18}F-fluorodeoxyglucose PET/CT features and correlations with histopathologic characteristics in sclerosing epithelioid fibrosarcoma. *Int J Clin Exp Pathol* 2014; **7**: 7278-7285 [PMID: 25400826]

12 **Hassan U**, Saeed SM Sr, Mushtaq S, Hussain M, Hameed M. The Expression of Mucin-4 (MUC4) in Sarcomas Apart From Sclerosing Epithelioid Fibrosarcoma and Low-Grade Fibromyxoid Sarcoma. *Cureus* 2023; **15**: e49546 [PMID: 38156143 DOI: 10.7759/cureus.49546]

13 **Zhang M**, Yu Y, Guan X, Yao X, Jia C, Hong E, Guo Y, He L. A group of sclerosing epithelioid fibrosarcomas with low-level amplified EWSR1-CREB3L1 fusion gene in children. *Pathol Res Pract* 2022; **230**: 153754 [PMID: 34990868 DOI: 10.1016/j.prp.2021.153754]

14 **Koerner AS**, Zhou M, Brook A, Yoon SS, Ganjoo KN. Response to Immunotherapy in Sclerosing Epithelioid Fibrosarcoma: Case Report and Literature Review. *Cureus* 2023; **15**: e50967 [PMID: 38259411 DOI: 10.7759/cureus.50967]

15 **Badran A**, Steele C, Alquaydheb H, Ba Theeb A, Bawazir A, Elshenawy MA, Atallah JP. The Use of Crizotinib in Sclerosing Epithelioid Fibrosarcoma with ALK Mutation: A Case Report. *Case Rep Oncol* 2023; **16**: 746-752 [PMID: 37900840 DOI: 10.1159/000532099]

World Journal of Clinical Cases

Submit a Manuscript: https://www.f6publishing.com

World J Clin Cases 2024 September 16; 12(26): 5990-5997

DOI: 10.12998/wjcc.v12.i26.5990

ISSN 2307-8960 (online)

CASE REPORT

Extragastrointestinal stromal tumors with diffuse membranous distribution with bleeding: A case report

Jian-Duo Xu, Zheng Wang, Qian Zhou, Ning Meng, Shu-Mei Zhang, Nan Liu

Specialty type: Medicine, research and experimental

Provenance and peer review: Unsolicited article; Externally peer reviewed.

Peer-review model: Single blind

Peer-review report's classification

Scientific Quality: Grade B

Novelty: Grade B

Creativity or Innovation: Grade B

Scientific Significance: Grade B

P-Reviewer: Puleo S

Received: April 18, 2024

Revised: June 8, 2024

Accepted: July 3, 2024

Published online: September 16, 2024

Processing time: 95 Days and 11.6 Hours

Jian-Duo Xu, Department of Gastrointestinal Surgery, Shijiazhuang People's Hospital, Shijiazhuang 050000, Hebei Province, China

Zheng Wang, Shu-Mei Zhang, Nan Liu, Department of Gastroenterology, Shijiazhuang People's Hospital, Shijiazhuang 050000, Hebei Province, China

Qian Zhou, Ning Meng, Department of General Surgery, Shijiazhuang People's Hospital, Shijiazhuang 050000, Hebei Province, China

Corresponding author: Zheng Wang, MD, Associate Chief Physician, Department of Gastroenterology, Shijiazhuang People's Hospital, No. 9 Fangbei Street, Shijiazhuang 050000, Hebei Province, China. wzcelia1983@163.com

Abstract

BACKGROUND

Extragastrointestinal stromal tumors (EGIST) and gastrointestinal stromal tumors are of similar pathological type and form. Here we report a rare case of EGIST diffusely distributed in membranous tissue in abdominal cavity, the feature of which included diffuse tumors at membranous tissue in entire abdominal cavity and spontaneous bleeding of the tumors.

CASE SUMMARY

The patient was a 71-year man and hospitalized due to continuous pain at lower abdomen for more than 10 days. Upon physical examination, the patient had flat and tough abdomen with mild pressing pain at lower abdomen, no obvious abdominal mass was touchable, and shifting dullness was positive. Positron emission tomography-computed tomography (CT) showed that in his peritoneal cavity, there were multiple nodules of various sizes, seroperitoneum, multiple enlarged lymph nodes in abdominal/pelvic cavity and right external ilium as well as pulmonary nodules. Plain CT scanning at epigastrium/hypogastrium/pelvic cavity + enhanced three-dimensional reconstruction revealed multiple soft tissue nodules in abdominal/pelvic cavity, peritoneum and right groin. Tumor marker of carbohydrate antigen 125 was 808 U/mL, diffuse tuberous tumor was seen in abdominal/pelvic cavity during operation with hematocelia, and postoperative pathological examination confirmed EGIST. Imatinib was administered with better therapeutic effect.

CONCLUSION

Gene testing showed *breast cancer susceptibility gene 1 interacting protein C-terminal*

helicase 1 and *KIT* genovariation, and the patient was treated with imatinib follow-up visit found that his clinical symptoms disappeared and the tumor load alleviated obviously *via* imageological examination.

Key Words: Diffuse tumor in abdominal cavity; Extragastrointestinal stromal tumors; Gastrointestinal stromal tumors; Malignant extragastrointestinal stromal tumors; Diffusely membranous metastasis

Core Tip: Extragastrointestinal stromal tumors (EGIST) are less common in comparison with gastrointestinal stromal tumors. EGIST tumors in the membranous tissue are rare and tumors independently developing in membrane tissues such as greater omentum, mesentery or peritoneum are occasionally reported. Diffuse membranous tumor in entire abdominal cavity is extremely rare worldwide. We report a case of EGIST with the tumors like cobblestone being diffusely distributed in entire abdominal cavity accompanied by spontaneous bleeding. The tumors may not be fully resected by surgery, hence we made biopsy, pathological examination and gene detection to determine the therapy. Treatment with imatinib achieved better outcome.

Citation: Xu JD, Wang Z, Zhou Q, Meng N, Zhang SM, Liu N. Extragastrointestinal stromal tumors with diffuse membranous distribution with bleeding: A case report. *World J Clin Cases* 2024; 12(26): 5990-5997
URL: https://www.wjgnet.com/2307-8960/full/v12/i26/5990.htm
DOI: https://dx.doi.org/10.12998/wjcc.v12.i26.5990

INTRODUCTION

Extragastrointestinal stromal tumors (EGIST) are less common compared with gastrointestinal stromal tumors (GIST). The tumor developing in membranous tissue is rare and independently developing in membrane tissues such as greater omentum, mesentery or peritoneum has been occasionally reported. Diffuse membranous tumor in entire abdominal cavity is extremely rare worldwide. We here report a case of EGIST with the tumors like cobblestone being diffusely distributed in entire abdominal cavity accompanied by spontaneous bleeding. The tumors may not be fully resected by surgery, hence we made biopsy, pathological examination and gene detection to determine the treatment strategy. The patient was treated with imatinib, and achieved better outcome.

CASE PRESENTATION

Chief complaints

The patient was a 71-year man, with hypertensive disease for 6 months, the highest pressure being 200/110 mmHg, and he has been taking felodipine orally to control blood pressure.

History of present illness

The patient had continuous mild pain at lower abdomen about 10 days prior to hospitalization, with regular bowel movement, and loss of appetite and weight for 5 kg.

History of past illness

He had a history of smoking for 50 years, 60 cigarettes/day, without drinking or exposing to radioactive substance.

Personal and family history

His family history was unremarkable.

Physical examination

Upon physical examination, the patient had normal abdominal appearance, tough abdomen with mild pressing pain at lower abdomen, no rebound tenderness or muscular tension, no obvious abdominal mass was touchable, shifting dullness was positive, with normal bowel sound.

Laboratory examinations

Tumor marker of carbohydrate antigen 125 was 808 U/mL. Gene detection showed *breast cancer susceptibility gene 1 interacting protein C-terminal helicase 1 (BRIP1)* and *KIT* genovariation, and the patient was thus sensitive to imatinib. Immunohistochemical analysis resulted in the following results: Calretinin (-), D2-40 (-), CK5/6 (-), WT-1 (+), CD117 (+), Dog-1 (+), SHA (diffused weakly +), Desmin (-), S-100 (-), SOX-10 (-), P16 (-), CD34 (-), and Ki-67 (30% approximately).

Imaging examinations

Plain CT scanning at epigastrium/hypogastrium/pelvic cavity + enhanced three-dimensional reconstruction revealed multiple soft tissue nodules in abdominal/pelvic cavity, peritoneum and right groin (Figure 1). Positron emission tomography-computed tomography showed thickened peritoneum with abnormal hypermetabolism, multiple mass or nodular soft tissue density images in abdominal/pelvic cavity and peritoneum (Figure 2). On enhanced scanning, the lesion was enhanced at a mild to moderate level; multiple hypermetabolic lymph nodes in abdominal/pelvic cavity and right external ilium; and seroperitoneum were observed.

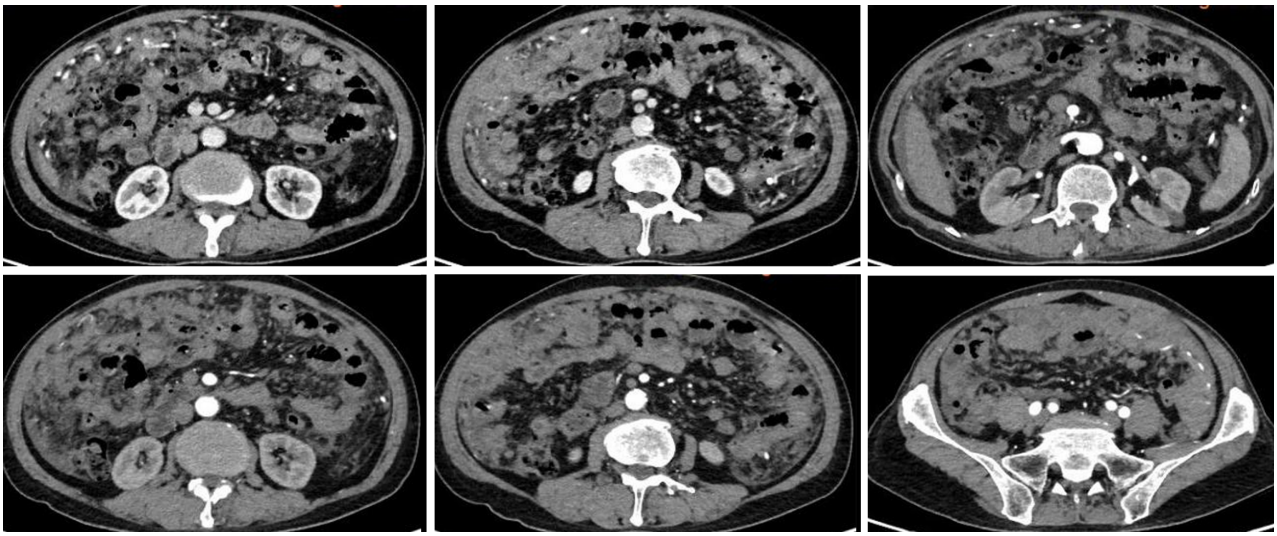

Figure 1 Abdominal computed tomography scanning. It shows that the tumor is of heavy load and diffused in the abdominal cavity.

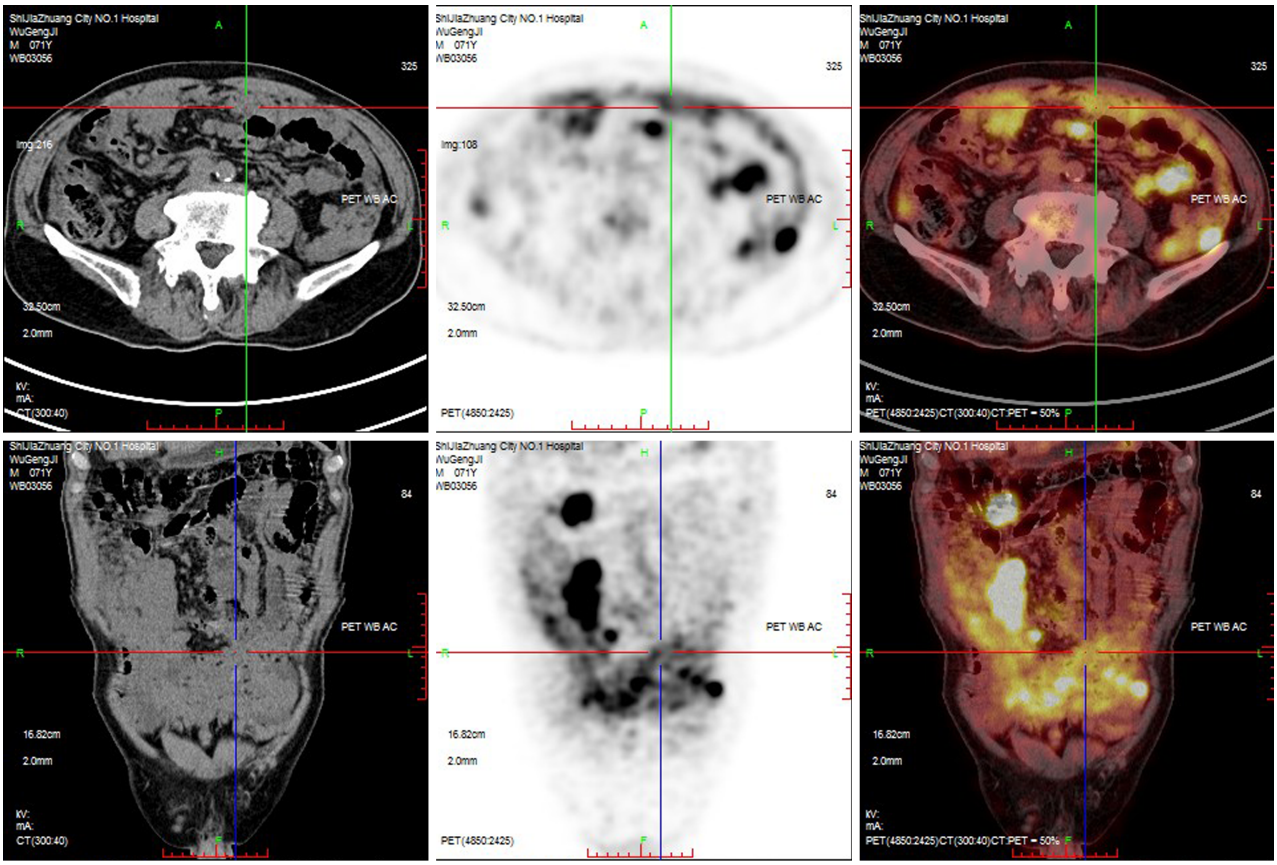

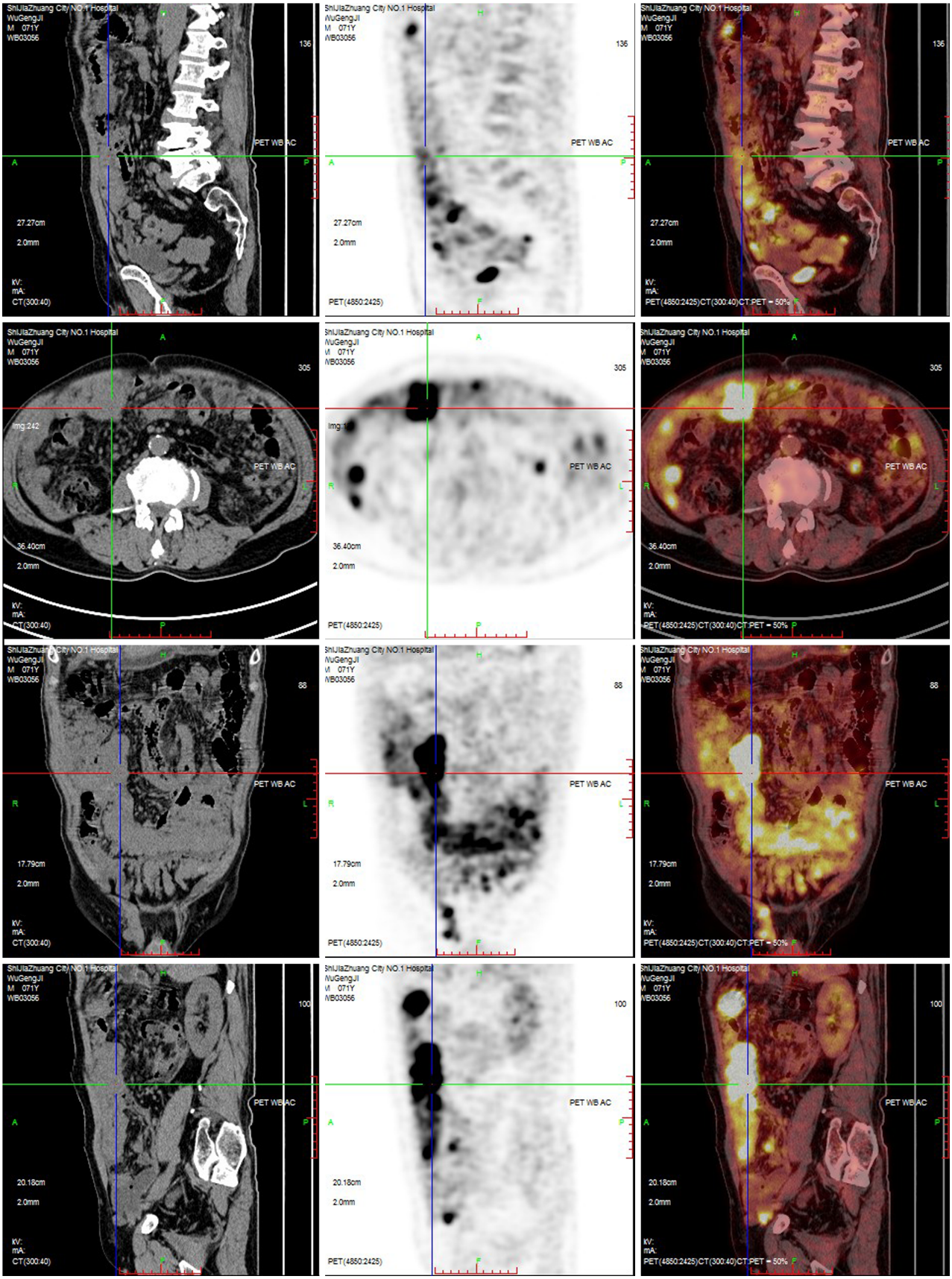

Figure 2 Positron emission tomography-computed tomography. It shows that the peritoneum is thickened with abnormal hypermetabolism, multiple mass or nodular soft tissue density images in abdominal/pelvic cavity and peritoneum; *via* enhancement scanning, the lesion is enhanced in mild to moderate level; multiple hypermetabolic lymph nodes in abdominal/pelvic cavity and right external ilium; and seroperitoneum.

FINAL DIAGNOSIS

Based on pathological examination, a diagnosis of EGIST was considered (Figure 3).

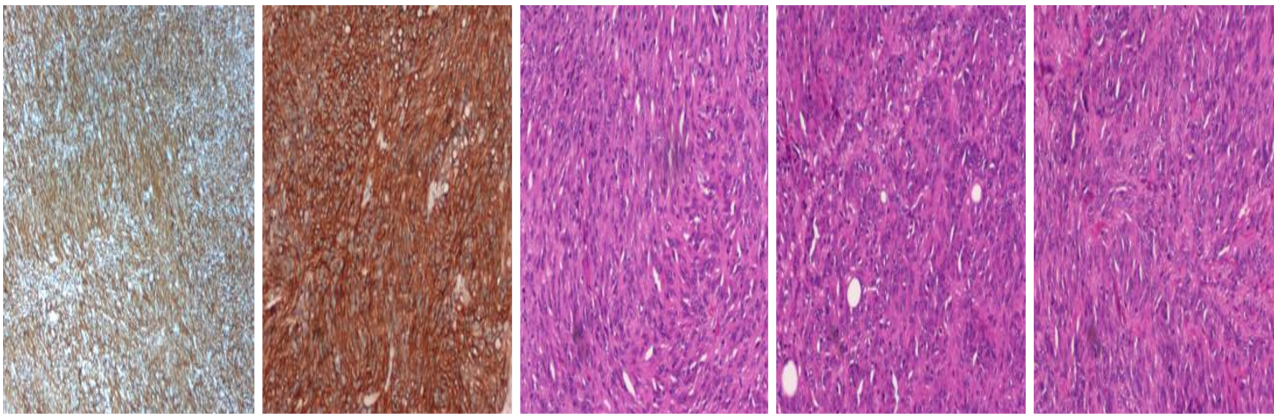

Figure 3 Pathological examination. Based on pathological examination, extragastrointestinal stromal tumors of high risk was considered.

TREATMENT

Based on gene detection results, the patient was treated with imatinib.

OUTCOME AND FOLLOW-UP

Follow-up visit found that his clinical symptoms disappeared and the tumor load alleviated obviously *via* imageological examination (Figure 4).

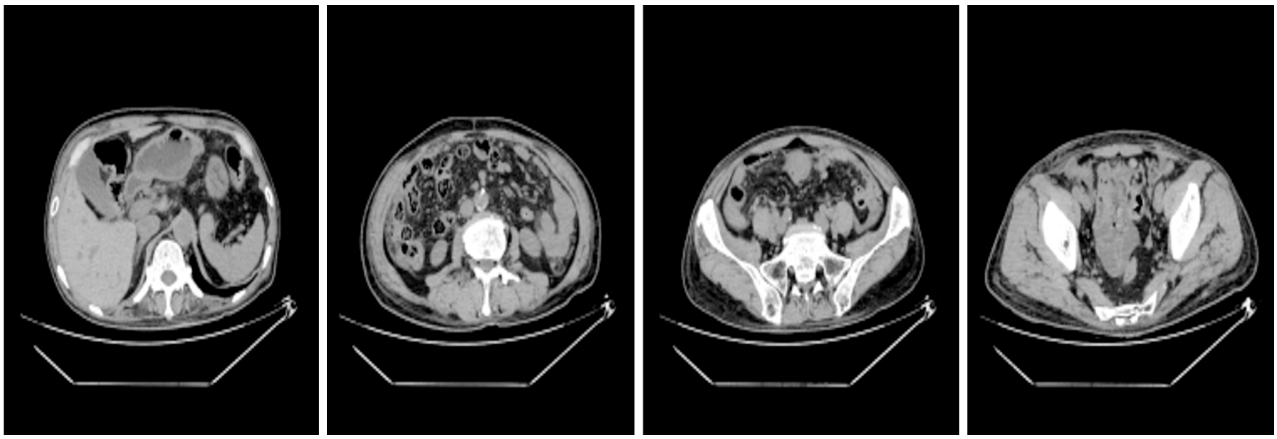

Figure 4 Abdominal computed tomography after treatment. It shows the tumor load is alleviated obviously with good therapeutic effect.

DISCUSSION

EGIST is rarer in comparison with GIST. GIST is diagnosed due to bleeding and obstruction while EGIST usually presents pain and palpable lump. In this case, the patient was hospitalized due to abdominal pain; upon physical examination, the entire abdomen was tough without solitary lump, but accompanied with spontaneous bleeding in abdominal cavity (Figure 5). The patient had symptoms of both GIST and EGIST. EGIST is commonly seen at vulva[1,2], vagina[3,4], retroperitoneum[5], ovary, posterior gastric, testis[6], greater omentum[7,8], pancreas[9,10], prostate[11-13], bladder[14], mesentery[15,16], liver[17], rectum[18,19], rectosacral space[20], esophagus[21], *etc*. But this case is rare where diffuse membranous tissue tumors existed in abdominal cavity. In addition, EGIST may have spontaneous rupture[22], just as this case, as shown in Figure 6 for tumor rupture and bleeding. Some EGIST cases are characterized by strong invasion and have unfavorable prognosis[23]. Uzunoglu and Tosun[24] have reported 135 EGIST cases between 2007 and 2020 and showed that elderly or female patients had worse prognosis. In our case, the patient was an old man with strong tumor

invasiveness; however, conservative medicating treatment showed a better treatment effect.

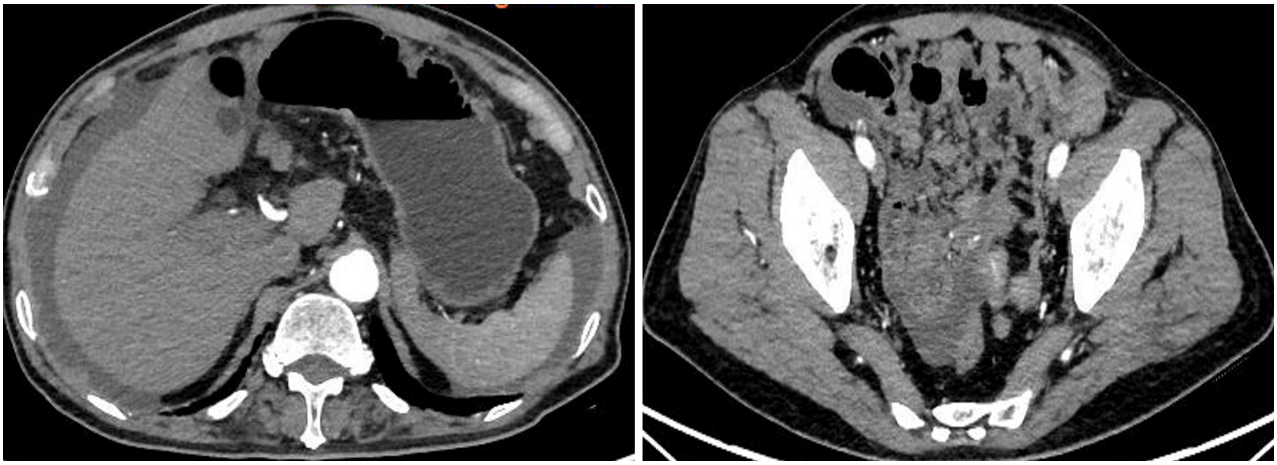

Figure 5 Preoperative abdominal computed tomography. Surgical exploration shows that the masses in abdominal cavity had spontaneous necrosis and bleeding.

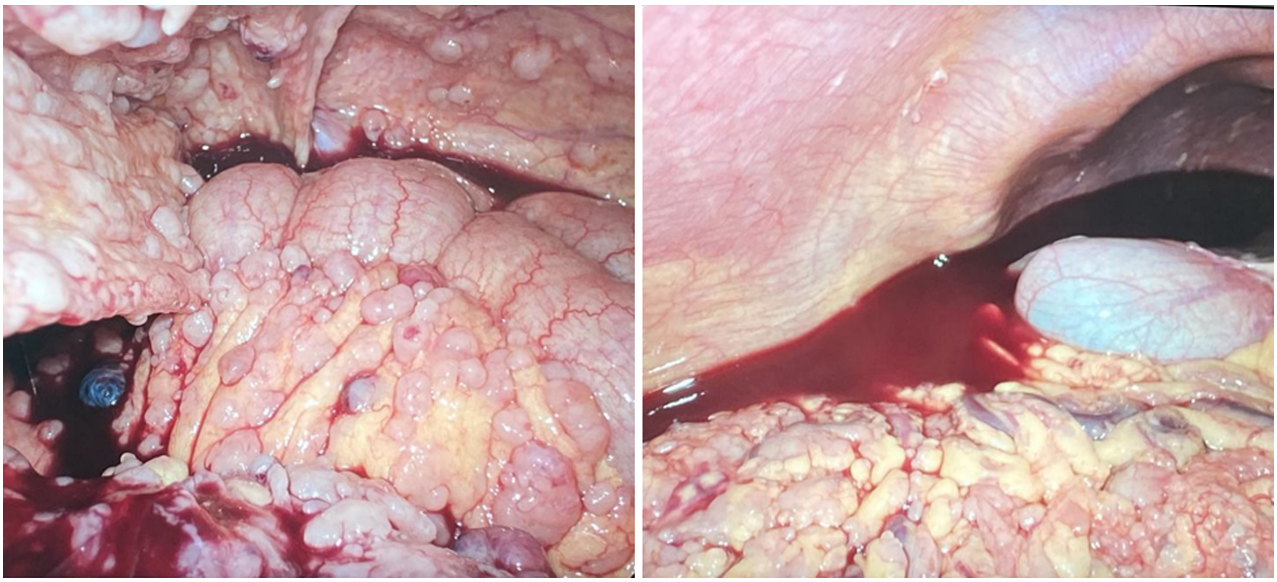

Figure 6 Tumor rupture and bleeding. During operation, diffuse nodules like cobblestone in abdominal cavity with hematocelia were seen. The nodules were in various sizes, approximately 0.5-1.5 cm, diffusely distributed in membrane tissues such as peritoneum, greater omentum and mesentery. The first picture on the left showed purple black nodules bleeding and bright red blood not coagulated.

Compared with GIST, EGIST has negative c-KIT mutation and positive PDGFRA in histopathological examination and immunohistochemical analysis. Whatever the tumor location is, DOG1 remains a preferred biomarker and CN34 and CD117 are deemed as auxiliary examination[25]. The gene detection for this case showed *BRIP1* and *KIT* genovariation, *BRIP1* (point mutation, exon11; nucleotide variation c.1567A > G; amino acid variation p.T523A; abundance 34.45%), *KIT* (insertion/deletion variation, exon11; nucleotide variation c.1672_1677del; amino acid variation p.K558_V559del; abundance 34.94%). The detection showed that the patient was sensitive to imatinib. After treatment with imatinib, his clinical symptoms disappeared gradually and the abdominal CT reexamination showed that the imageological indexes had obviously improved. This case is different from previous ones in clinical symptoms, imageological manifestations and gene detection results, which have indicated that EGIST has various manifestations, thus comprehensive diagnostics should be performed.

CONCLUSION

This case of EGIST is rarely seen in clinical practice. The patient was a 71-year man with continuous hypogastralgia. During laparoscopic surgery, several botryoid nodules of various sizes were found in the abdominal cavity. Surgical

treatment was impossible. The patient underwent tumor biopsy, and histopathological examination, which showed positive CD117, and gene detection showed *BRIP1* and *KIT* genovariation. After treatment with imatinib, his clinical symptoms disappeared and the abdominal CT reexamination showed that the imageological indexes had obviously improved. In this case, we made an overall evaluation on tumor characteristics in the aspects of imageological examination, gene detection, immunohistochemical analysis and pathological feature, and clinical manifestation difference, which verifies that imatinib treatment for EGIST with diffuse membranous distribution has better therapeutic effect than surgical treatment.

FOOTNOTES

Author contributions: Xu JD designed the research; Wang Z performed the research; Meng N, Zhou Q, Zhang SM, and Liu N analyzed the data and wrote the manuscript; all authors have read and approved the final manuscript.

Informed consent statement: All patients and healthy volunteers provided written informed consent prior to their inclusion in the study.

Conflict-of-interest statement: The authors declare no competing interests.

CARE Checklist (2016) statement: The authors have read the CARE Checklist (2016), and the manuscript was prepared and revised according to the CARE Checklist (2016).

Country of origin: China

ORCID number: Zheng Wang 0000-0001-9501-2933.

S-Editor: Luo ML
L-Editor: A
P-Editor: Cai YX

REFERENCES

1 **Mohamed N**, Khan M, Hosler G, Tumminello K. Primary vulvar extragastrointestinal stromal tumor in a 77-year-old woman. *J Cutan Pathol* 2023; **50**: 723-729 [PMID: 37127848 DOI: 10.1111/cup.14432]
2 **Asada Y**, Kuroda K, Shirasaka D, Era Y, Ikegawa T, Arai Y, Nakahara A, Kawano M, Kadowaki Y, Okino T. [A case of rectovaginal metastasis 6 years after initial resection of extra-gastrointestinal stromal tumor of vulvar origin]. *Nihon Shokakibyo Gakkai Zasshi* 2022; **119**: 946-953 [PMID: 36216545 DOI: 10.11405/nisshoshi.119.946]
3 **Liu S**, Pan P, Han B, Wang J, Sun M, Sun Y. Extragastrointestinal Stromal Tumor Presenting as a Recurrent Vaginal Mass: Case Report. *Onco Targets Ther* 2021; **14**: 959-965 [PMID: 33603400 DOI: 10.2147/OTT.S284101]
4 **Addley S**, Alazzam M, Johnson C, Soleymani Majd H. Rectovaginal extragastrointestinal stromal tumour (EGIST): an additional entity to be considered in the differential diagnosis of tumours of the rectovaginal septum. *BMJ Case Rep* 2021; **14**: e237669 [PMID: 33685909 DOI: 10.1136/bcr-2020-237669]
5 **Lin J**, Liao W, Wang J, Li W, Tang X, Li H, Yi X, Lu X, Chen Z, Zhu B, Feng X, Diao D. Primary extra-gastrointestinal stromal tumor of retroperitoneum: Clinicopathologic characteristics and prognosis of six cases. *Front Oncol* 2023; **13**: 1033598 [PMID: 36895492 DOI: 10.3389/fonc.2023.1033598]
6 **El Charif MH**, Amro S, Boulos F, Khalife M, Shamseddine A, Assi H, Sbaity E. Extra-gastrointestinal stromal tumors (EGISTs): A case report for a mischief entity. *Medicine (Baltimore)* 2023; **102**: e33394 [PMID: 37000068 DOI: 10.1097/MD.0000000000033394]
7 **Almeida M**, Sousa F, Resende F, Devesa V, Ferrão A, Carneiro S, Canão P, Barbosa E, Barbosa J. Primary EGIST of the greater omentum - a rare presentation. *Acta Chir Belg* 2024; **124**: 137-142 [PMID: 37027318 DOI: 10.1080/00015458.2023.2201084]
8 **Kataoka M**, Saitoh T, Kawashima K, Yazaki T, Sonoyama H, Okimoto E, Oka A, Mishima Y, Mishiro T, Oshima N, Shibagaki K, Tobita H, Moriyama I, Ishimura N, Nagase M, Hirahara N, Tajima Y, Ishihara S. Primary Extragastrointestinal Stromal Tumor of Greater Omentum with Intraperitoneal Bleeding. *Intern Med* 2021; **60**: 3413-3419 [PMID: 34024850 DOI: 10.2169/internalmedicine.6519-20]
9 **Zackria R**, Jayaraman V. The Gastrointestinal Stromal Tumor (GIST) of a Pancreatic Cyst. *Cureus* 2022; **14**: e26197 [PMID: 35891821 DOI: 10.7759/cureus.26197]
10 **Ene D**, Florescu LM, Ene R, Popescu B, Gheonea IA. An extremely uncommon case of pancreatic extragastrointestinal stromal tumor in a 53-year-old female patient. *Rom J Morphol Embryol* 2021; **62**: 569-573 [PMID: 35024746 DOI: 10.47162/RJME.62.2.24]
11 **Yang Y**, Sun D, Tang K. Primary extragastrointestinal stromal tumors of the prostate: A case report and literature review. *Front Oncol* 2022; **12**: 1038853 [PMID: 36425555 DOI: 10.3389/fonc.2022.1038853]
12 **Lu L**, Qu H, Wang J, Yao B, Ma B, Qiu JG, Wang ZY, Ren DL. Whole-exome sequencing for high-risk primary prostatic extra-gastrointestinal stromal tumor: A case report. *Mol Clin Oncol* 2021; **15**: 249 [PMID: 34671468 DOI: 10.3892/mco.2021.2411]
13 **Li L**, Hu ZQ, Yang CG, Gan JH, Tian JH, Ke CJ, Zeng X. Current knowledge of primary prostatic extra-gastrointestinal stromal tumor: a case report and review of the literature. *J Int Med Res* 2021; **49**: 3000605211013172 [PMID: 33983064 DOI: 10.1177/03000605211013172]

14 **Tripathy S**, Arun Raj ST, Prakash S, Thanaignathan T, Shamim SA. Response Assessment of Recurrent Extragastrointestinal Stromal Tumor of the Urinary Bladder to Imatinib: Findings on Serial (18)F-Fluorodeoxyglucose Positron Emission Tomography-Computed Tomography Scans. *Indian J Nucl Med* 2020; **35**: 350-352 [PMID: 33642766 DOI: 10.4103/ijnm.IJNM_68_20]

15 **Sajjanar AB**, Katole NT, Vagha SJ. KIT (CD117) Positive Huge Primary Malignant Extra Gastrointestinal Stromal Tumors (EGISTs) Arising From Jejunal Mesentery: A Rare Case Report. *Cureus* 2022; **14**: e33168 [PMID: 36742272 DOI: 10.7759/cureus.33168]

16 **Kadel D**, Bhuju S, Thapa BR, Chalise S, Kumar Sah S. Curative intent treatment of late presented extragastrointestinal stromal tumor: two identical case reports with literature review. *J Surg Case Rep* 2021; **2021**: rjab220 [PMID: 34104404 DOI: 10.1093/jscr/rjab220]

17 **Lian J**, Feng M, Zhang S, Lu H. Case report: 10-year survival of a patient with a primary hepatic gastrointestinal stromal tumor. *Front Oncol* 2022; **12**: 1035824 [PMID: 36530972 DOI: 10.3389/fonc.2022.1035824]

18 **Harouachi A**, Harhar M, Mhand M, Atmani A, Elamrani A, Kharkhach A, Bouhout T, Serji B, Harroudi TE. Extra gastrointestinal stromal tumor EGIST in the recto-vesical pouch: A case report and literature review. *Ann Med Surg (Lond)* 2022; **74**: 103283 [PMID: 35127068 DOI: 10.1016/j.amsu.2022.103283]

19 **Elagami MM**, Khalid A, Kumar V, Singhal M, Grossman MA. Perirectal Extragastrointestinal Stromal Tumor: An Unusual Presentation. *Cureus* 2021; **13**: e15529 [PMID: 34268049 DOI: 10.7759/cureus.15529]

20 **El-Helou E**, Chamma L, Mazraani HB, Sebaaly D, Chamma OG, Naccour J, Haddad MM, Lichaa D, Alam H. Extra-Gastrointestinal Stromal Tumor (EGIST) in the Pelvis Mimicking Retroperitoneal Sarcoma. *Surg J (N Y)* 2022; **8**: e266-e269 [PMID: 36172533 DOI: 10.1055/s-0042-1757335]

21 **Fujiwara N**, Sato H, Miyawaki Y, Ito M, Aoyama J, Ito S, Oya S, Watanabe K, Sugita H, Yasuda M, Sakuramoto S. The hybrid procedure of thoracoscopic and hand-assisted laparoscopic resection of an esophageal gastrointestinal stromal tumor: A case report. *Asian J Endosc Surg* 2021; **14**: 286-289 [PMID: 32812354 DOI: 10.1111/ases.12853]

22 **Murata T**, Ishimori T, Naitou W, Igrashi Y, Suno Y, Kawachi J. Laparoscopic resection for spontaneously ruptured primary extragastrointestinal stromal tumor of the greater omentum: A case report. *Int J Surg Case Rep* 2022; **99**: 107567 [PMID: 36096080 DOI: 10.1016/j.ijscr.2022.107567]

23 **Abidoye O**, Johnson A. Extremely Aggressive Mesenteric Extragastrointestinal Stromal Tumor: A Case Report and Literature Review. *Cureus* 2022; **14**: e23108 [PMID: 35464497 DOI: 10.7759/cureus.23108]

24 **Uzunoglu H**, Tosun Y. Primary extra gastrointestinal stromal tumors of the abdomen. *North Clin Istanb* 2021; **8**: 464-471 [PMID: 34909584 DOI: 10.14744/nci.2021.46794]

25 **Moldovan VT**, Pătraşcu OM, Ali L, Costache M, Sajin M. Morphological and immunohistochemical diagnostic of extragastrointestinal stromal tumors - a 51 case series analysis. *Rom J Morphol Embryol* 2021; **62**: 1011-1016 [PMID: 35673820 DOI: 10.47162/RJME.62.4.13]

World Journal of Clinical Cases

Submit a Manuscript: https://www.f6publishing.com

World J Clin Cases 2024 September 16; 12(26): 5998-6000

DOI: 10.12998/wjcc.v12.i26.5998

ISSN 2307-8960 (online)

LETTER TO THE EDITOR

Fragile hearts: Unveiling the crucial layers of frailty in elderly patients undergoing percutaneous coronary interventions

Andreas Mitsis, Michael Myrianthefs

Specialty type: Medicine, research and experimental

Provenance and peer review: Unsolicited article; Externally peer reviewed.

Peer-review model: Single blind

Peer-review report's classification

Scientific Quality: Grade B, Grade C, Grade E

Novelty: Grade B, Grade B, Grade D

Creativity or Innovation: Grade B, Grade B, Grade D

Scientific Significance: Grade B, Grade B, Grade D

P-Reviewer: Barik R; Kapritsou M; Shao JK

Received: January 30, 2024

Revised: June 22, 2024

Accepted: July 10, 2024

Published online: September 16, 2024

Processing time: 174 Days and 17.5 Hours

Andreas Mitsis, Michael Myrianthefs, Department of Cardiology, Nicosia General Hospital, Nicosia 2026, Cyprus

Corresponding author: Andreas Mitsis, MD, MSc, Academic Research, Consultant Physician-Scientist, Department of Cardiology, Nicosia General Hospital, 215 Old Road Nicosia-Limassol, Nicosia 2026, Cyprus. andymits7@gmail.com

Abstract

Wang and Liu's systematic review of frailty among elderly patients undergoing percutaneous coronary intervention (PCI) revealed that patients with frailty have significantly higher risks of all-cause and in-hospital death, major undesirable cardiovascular events, and major haemorrhage. Frailty is associated with adverse events, prolonged hospital stays, increased complications, and elevated mortality risk due to diminished physiological reserves. Integrating frailty into risk assessment tools is crucial, and gait speed has emerged as a key predictor of frailty. Recognizing the impact of frailty leads to personalized and informed decision-making, and frailty assessments should be performed. This holistic approach can inform tailored interventions, thereby optimizing outcomes for this vulnerable population undergoing PCI.

Key Words: Frailty; Elderly; Percutaneous coronary intervention; Outcomes; Risk assessment tools

Core Tip: Elderly frail patients undergoing percutaneous coronary intervention (PCI) have increased risks of mortality and adverse cardiovascular events. It is important to integrate frailty into risk assessment tools. Therefore, this study underscores the importance of comprehensive frailty evaluations to enable informed decision-making in PCIs. The findings suggest that tailored interventions should be implemented to optimize outcomes and enhance care quality for this vulnerable population.

Citation: Mitsis A, Myrianthefs M. Fragile hearts: Unveiling the crucial layers of frailty in elderly patients undergoing percutaneous coronary interventions. *World J Clin Cases* 2024; 12(26): 5998-6000
URL: https://www.wjgnet.com/2307-8960/full/v12/i26/5998.htm
DOI: https://dx.doi.org/10.12998/wjcc.v12.i26.5998

TO THE EDITOR

We read with great interest the systematic review by Wang and Liu[1] that examined the influence of frailty on the outcomes of elderly individuals undergoing percutaneous coronary intervention (PCI). The authors conducted a systematic meta-analysis in accordance with PRISMA guidelines, and the study included 739693 elderly patients undergoing PCI. Compared with non-frail patients, frail patients faced considerably elevated risks of in-hospital death [95% confidence interval (95%CI): 1.90-6.25], all-cause mortality [hazard ratio (HR): 2.08, 95%CI: 1.78-2.43], major adverse cardiovascular events (HR: 2.92, 95%CI: 1.85-4.60), and major haemorrhages (HR: 4.60, 95%CI: 2.89-7.32).

Frailty can significantly impact the outcomes of elderly patients undergoing PCI. Compared with non-frail individuals, frail individuals may experience higher rates of adverse events, longer hospital stays, and increased postoperative complications as well as a higher risk of mortality[2,3]. Frailty is associated with decreased physiological reserves, thus making elderly patients more susceptible to the stresses of PCI and less likely to recover quickly[4,5].

The impact of frailty on PCI outcomes is underscored by the utility of risk assessment tools[6-8]. These tools, which incorporate frailty as a crucial component, aid in estimating the likelihood of adverse outcomes in elderly patients undergoing PCI. Gait speed, a key aspect of frailty assessment, has emerged as an incremental predictor of mortality and major morbidity in the context of cardiac procedures, including PCI[8]. This underlines the importance of adopting a comprehensive approach to frailty assessment that extends beyond chronological age, thus providing a more accurate understanding of vulnerability among patients with frailty.

In current clinical practice, the recognition of frailty's substantial influence on PCI outcomes prompts a shift towards more personalized and informed decision-making. The incorporation of frailty assessment tools into routine practice allows health care professionals to better anticipate and manage the unique challenges faced by elderly patients undergoing PCI[9]. This holistic understanding of frailty contributes to the development of tailored intervention strategies aimed at optimizing outcomes and enhancing the overall quality of care for this vulnerable population[10].

Recognizing the substantial impact of frailty on the outcomes of elderly patients undergoing PCI provides valuable insights for optimizing care in this vulnerable population. A stepwise approach is essential (Table 1), starting with a preprocedural assessment that prioritizes a comprehensive evaluation of physical, cognitive, and psychosocial frailty components. Therefore, risk stratification becomes crucial, and frailty status should be incorporated into models for more accurate outcome predictions and informed decision-making during PCI. The development of tailored treatment plans is pivotal and requires adjustments to procedural and postprocedural care strategies based on individual frailty components to optimize patient outcomes.

Table 1 Stepwise assessment of the elderly frail patient

Steps	Proposed approach
Step 1	Pre-procedural assessment
Step 2	Risk stratification
Step 3	Tailored treatment plan
Step 4	Multidisciplinary approach
Step 5	Informed decision-making
Step 6	Post-procedure care
Step 7	Comprehensive geriatric assessment
Step 8	Education and awareness
Step 9	Quality improvement initiatives

The multidisciplinary approach is paramount because it emphasizes collaboration among geriatricians, cardiologists, and other specialists to address the complex needs of frail elderly patients, thus enhancing overall patient care and support. Informed decision-making, which is guided by shared discussions with patients and families, becomes central; this process provides clear expectations and considers frailty as a key factor in exploring alternative treatment options. Integrating a comprehensive geriatric assessment with a preprocedural evaluation further aids in understanding the holistic health, functional status, and social support of patients.

Postprocedural care is equally vital, as it focuses on tailored rehabilitation programs to meet the specific needs of frail patients, emphasizing functional recovery and strategies to mitigate frailty-related complications. Education and quality improvement initiatives play a crucial role in raising awareness among health care professionals about the impact of frailty on PCI outcomes. Providing education and training enhances the recognition and management of frailty in the cardiology setting, with ongoing assessment and refinement of protocols based on experience.

In conclusion, understanding the significance of frailty in elderly PCI patients is pivotal for advancing patient care. Integrating this knowledge into practice and research enables the development of tailored strategies, thereby leading to improvements in care outcomes. Encouraging and participating in research focused on frailty and PCI outcomes is essential, thus paving the way for interventions specifically addressing frailty in cardiovascular procedures and enhancing overall patient care.

FOOTNOTES

Author contributions: Mitsis A and Myrianthefs M designed the research study, performed the research, analysed the data, and wrote the manuscript; Mitsis A and Myrianthefs M have read and approved the final manuscript.

Conflict-of-interest statement: The authors have no conflicts of interest to declare.

Country of origin: Cyprus

ORCID number: Andreas Mitsis 0000-0002-0286-7762.

S-Editor: Qu XL
L-Editor: A
P-Editor: Cai YX

REFERENCES

1 **Wang SS**, Liu WH. Impact of frailty on outcomes of elderly patients undergoing percutaneous coronary intervention: A systematic review and meta-analysis. *World J Clin Cases* 2024; **12**: 107-118 [PMID: 38292628 DOI: 10.12998/wjcc.v12.i1.107]

2 **Heaton J**, Singh S, Nanavaty D, Okoh AK, Kesanakurthy S, Tayal R. Impact of frailty on outcomes in acute ST-elevated myocardial infarctions undergoing percutaneous coronary intervention. *Catheter Cardiovasc Interv* 2023; **101**: 773-786 [PMID: 36806859 DOI: 10.1002/ccd.30595]

3 **Kwok CS**, Achenbach S, Curzen N, Fischman DL, Savage M, Bagur R, Kontopantelis E, Martin GP, Steg PG, Mamas MA. Relation of Frailty to Outcomes in Percutaneous Coronary Intervention. *Cardiovasc Revasc Med* 2020; **21**: 811-818 [PMID: 31761641 DOI: 10.1016/j.carrev.2019.11.009]

4 **Uchmanowicz I**, Lisiak M, Wleklik M, Gurowiec P, Kałużna-Oleksy M. The relationship between frailty syndrome and quality of life in older patients following acute coronary syndrome. *Clin Interv Aging* 2019; **14**: 805-816 [PMID: 31190767 DOI: 10.2147/CIA.S204121]

5 **Damluji AA**, Huang J, Bandeen-Roche K, Forman DE, Gerstenblith G, Moscucci M, Resar JR, Varadhan R, Walston JD, Segal JB. Frailty Among Older Adults With Acute Myocardial Infarction and Outcomes From Percutaneous Coronary Interventions. *J Am Heart Assoc* 2019; **8**: e013686 [PMID: 31475601 DOI: 10.1161/JAHA.119.013686]

6 **Afilalo J**. The Clinical Frailty Scale: Upgrade Your Eyeball Test. *Circulation* 2017; **135**: 2025-2027 [PMID: 28302750 DOI: 10.1161/CIRCULATIONAHA.116.025958]

7 **Singh M**, Rihal CS, Lennon RJ, Spertus J, Rumsfeld JS, Holmes DR Jr. Bedside estimation of risk from percutaneous coronary intervention: the new Mayo Clinic risk scores. *Mayo Clin Proc* 2007; **82**: 701-708 [PMID: 17550750 DOI: 10.4065/82.6.701]

8 **Afilalo J**, Eisenberg MJ, Morin JF, Bergman H, Monette J, Noiseux N, Perrault LP, Alexander KP, Langlois Y, Dendukuri N, Chamoun P, Kasparian G, Robichaud S, Gharacholou SM, Boivin JF. Gait speed as an incremental predictor of mortality and major morbidity in elderly patients undergoing cardiac surgery. *J Am Coll Cardiol* 2010; **56**: 1668-1676 [PMID: 21050978 DOI: 10.1016/j.jacc.2010.06.039]

9 **Walston J**, Buta B, Xue QL. Frailty Screening and Interventions: Considerations for Clinical Practice. *Clin Geriatr Med* 2018; **34**: 25-38 [PMID: 29129215 DOI: 10.1016/j.cger.2017.09.004]

10 **Yang CC**, Chen PH, Yang CH, Dai CY, Luo KH, Chen TH, Chuang HY, Kuo CH. Physical frailty identification using machine learning to explore the 5-item FRAIL scale, Cardiovascular Health Study index, and Study of Osteoporotic Fractures index. *Front Public Health* 2024; **12**: 1303958 [PMID: 38784574 DOI: 10.3389/fpubh.2024.1303958]

World Journal of Clinical Cases

Submit a Manuscript: https://www.f6publishing.com

World J Clin Cases 2024 September 16; 12(26): 6001-6003

DOI: 10.12998/wjcc.v12.i26.6001

ISSN 2307-8960 (online)

LETTER TO THE EDITOR

T lymphocyte proportion in Alzheimer's disease prognosis

Matthew Willman, Gopi Patel, Brandon Lucke-Wold

Specialty type: Medicine, general and internal

Provenance and peer review: Invited article; Externally peer reviewed.

Peer-review model: Single blind

Peer-review report's classification

Scientific Quality: Grade B
Novelty: Grade B
Creativity or Innovation: Grade B
Scientific Significance: Grade B

P-Reviewer: Bai H

Received: April 17, 2024
Revised: June 23, 2024
Accepted: July 15, 2024
Published online: September 16, 2024
Processing time: 96 Days and 6.5 Hours

Matthew Willman, Gopi Patel, College of Medicine, University of Florida, Gainesville, FL 32610, United States

Brandon Lucke-Wold, Department of Neurosurgery, University of Florida, Gainesville, FL 32611, United States

Co-corresponding authors: Matthew Willman and Brandon Lucke-Wold.

Corresponding author: Matthew Willman, College of Medicine, University of Florida, 1600 SW Archer Road, Gainesville, FL 32610, United States. matthewwillman@ufl.edu

Abstract

Bai *et al* investigate the predictive value of T lymphocyte proportion in Alzheimer's disease (AD) prognosis. Through a retrospective study involving 62 AD patients, they found that a decrease in T lymphocyte proportion correlated with a poorer prognosis, as indicated by higher modified Rankin scale scores. While the study highlights the potential of T lymphocyte proportion as a prognostic marker, it suggests the need for larger, multicenter studies to enhance generalizability and validity. Additionally, future research could use cognitive exams when evaluating prognosis and delve into immune mechanisms underlying AD progression. Despite limitations inherent in retrospective designs, Bai *et al*'s work contributes to understanding the immune system's role in AD prognosis, paving the way for further exploration in this under-researched area.

Key Words: Alzheimer's disease; T lymphocyte; T lymphocyte proportion; Alzheimer's disease prognosis; Modified rankin scale; Immune cell count; Electroencephalogram; Immune function

Core Tip: Bai *et al* propose a novel marker for Alzheimer's disease (AD) prognosis: The proportion of T lymphocytes. In their single-center retrospective study, they found that a decrease in T lymphocyte proportion correlated with a poorer prognosis, as measured by the modified Rankin scale. This suggests T lymphocytes could serve as a predictive biomarker for AD prognosis. The study underscores the need for larger, multicenter investigations to validate these findings and highlights the potential of immune system dysregulation in AD progression, opening avenues for further research in understanding AD pathology and prognosis.

Citation: Willman M, Patel G, Lucke-Wold B. T lymphocyte proportion in Alzheimer's disease prognosis. *World J Clin Cases* 2024; 12(26): 6001-6003
URL: https://www.wjgnet.com/2307-8960/full/v12/i26/6001.htm
DOI: https://dx.doi.org/10.12998/wjcc.v12.i26.6001

TO THE EDITOR

Bai *et al*[1] describes how a decrease in the proportion of T lymphocytes may predict poor prognosis in Alzheimer's disease (AD). In this single-center retrospective study, 62 patients with a clinical diagnosis of AD were ultimately enrolled after admission to the Third Affiliated Hospital of Guizhou Medical University[1]. As an assessment of neurologic function and prognosis, the modified Rankin scale (mRS) was recorded at admission, discharge, and follow-up[1]. In addition to blood immune cell flow cytometry for immune cell count, electroencephalogram, brain magnetic resonance imaging, and routine blood tests were recorded at admission[1]. Ultimately, Bai *et al*[1] determined that the proportion of T lymphocytes < 55% as determined on flow cytometry was predictive of a poor prognosis as determined by an elevated mRS score of 3-6 in AD patients.

DISCUSSION

While the mRS may allow for assessment of the functional status of a patient from the perspective of their ability to perform daily activities, further evaluation of the cognitive function of the patients when determining severity staging could be concluded from other exams such as the Mini-Mental State Examination, Montreal Cognitive Assessment Basic, and the Alzheimer's Disease Assessment Scale-Cognitive subscale[2,3]. The inclusion of these exams when determining the prognosis of the patients with AD may increase the validity of the study.

While there is clear evidence that chronic inflammation in the brain, a potential byproduct of immune dysregulation, is implicated in the progression of AD, the precise role of inflammation or immune dysregulation is not clearly understood in the setting of AD. Studies of systemic immune-mediated inflammatory diseases have been inconclusive in indicating systemic inflammation or immunosuppression as a potential risk for the development of AD, but may suggest that immune dysregulation is a downstream symptom of AD progression[4,5]. Whether a downstream product of AD progression or a preceding cause, the reduction in the proportion of T lymphocytes observed by Bai *et al*[1] may offer some insight into the prognosis of AD patients.

Future studies investigating the connection between T lymphocytes and AD prognosis would benefit from an increased sample size to increase the power of the study and reduce the risk of Type II errors. Additionally, studies that involve patients from multiple hospitals rather than single centers could increase the generalizability of the study to a broader population and enhance external validity.

As the study design was retrospective in nature, it is susceptible to common limitations of this approach, such as the presence of confounding variables. For instance, Bai *et al*[1] investigated T lymphocyte proportion, which can be altered in a wide range of clinical presentations. Factors such as age, comorbidities like diabetes or cardiovascular disease, and lifestyle factors may influence the relationship between the T lymphocyte proportion and AD prognosis.

Future research may also benefit from studies that focus on exploring the immune mechanisms involved with the interplay between the immune system and AD prognosis. Research that focuses on the molecular and cellular pathways involved in immune system function and AD pathology may be valuable in deciphering the role T lymphocytes play in AD prognosis.

CONCLUSION

Bai *et al*'s exploration of the connection between T lymphocytes and AD disease progression addresses an area of AD research that has been largely understudied[1,6]. Though the study has certain limitations expected in a preliminary retrospective study, this research represents vital progress towards unveiling the complex role of our immune system in AD and enhancing our understanding of the positive predictive value of T lymphocyte proportion in AD prognosis.

FOOTNOTES

Author contributions: Willman M was responsible for conception of original paper outline of content. He designed out format of the paper and drafted the paper including discussing the overview of the paper discussed and it's limitations. Willman M was responsible for all revisions and communication with the publisher; Patel G was responsible for drafting the paper including the section discussing the limitations of the paper being discussed; Lucke-wold B was responsible for conception of original paper content outline. He also overlooked the revision of the paper.

Conflict-of-interest statement: All the authors declare that they have no conflict of interest.

Country of origin: United States

ORCID number: Matthew Willman 0000-0002-0388-2964; Brandon Lucke-Wold 0000-0001-6577-4080.

S-Editor: Liu JH
L-Editor: A
P-Editor: Chen YX

REFERENCES

1 **Bai H**, Zeng HM, Zhang QF, Hu YZ, Deng FF. Correlative factors of poor prognosis and abnormal cellular immune function in patients with Alzheimer's disease. *World J Clin Cases* 2024; **12**: 1063-1075 [PMID: 38464932 DOI: 10.12998/wjcc.v12.i6.1063]
2 **Benoit JS**, Chan W, Piller L, Doody R. Longitudinal Sensitivity of Alzheimer's Disease Severity Staging. *Am J Alzheimers Dis Other Demen* 2020; **35**: 1533317520918719 [PMID: 32573256 DOI: 10.1177/1533317520918719]
3 **Huang L**, Chen KL, Lin BY, Tang L, Zhao QH, Lv YR, Guo QH. Chinese version of Montreal Cognitive Assessment Basic for discrimination among different severities of Alzheimer's disease. *Neuropsychiatr Dis Treat* 2018; **14**: 2133-2140 [PMID: 30174426 DOI: 10.2147/NDT.S174293]
4 **Booth MJ**, Kobayashi LC, Janevic MR, Clauw D, Piette JD. No increased risk of Alzheimer's disease among people with immune-mediated inflammatory diseases: findings from a longitudinal cohort study of U.S. older adults. *BMC Rheumatol* 2021; **5**: 48 [PMID: 34763722 DOI: 10.1186/s41927-021-00219-x]
5 **Yeung CHC**, Schooling CM. Systemic inflammatory regulators and risk of Alzheimer's disease: a bidirectional Mendelian-randomization study. *Int J Epidemiol* 2021; **50**: 829-840 [PMID: 33313759 DOI: 10.1093/ije/dyaa241]
6 **Lutshumba J**, Nikolajczyk BS, Bachstetter AD. Dysregulation of Systemic Immunity in Aging and Dementia. *Front Cell Neurosci* 2021; **15**: 652111 [PMID: 34239415 DOI: 10.3389/fncel.2021.652111]

Published by **Baishideng Publishing Group Inc**
7041 Koll Center Parkway, Suite 160, Pleasanton, CA 94566, USA
Telephone: +1-925-3991568
E-mail: office@baishideng.com
Help Desk: https://www.f6publishing.com/helpdesk
https://www.wjgnet.com